

# TEXTURED FLUIDS

by

Gerhard K. Guenther

Dissertation submitted to the Faculty of  
The Virginia Polytechnic Institute and State University  
in partial fulfillment of the degree of

DOCTOR OF PHILOSOPHY

in

Chemical Engineering

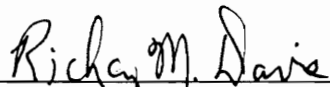
APPROVED:



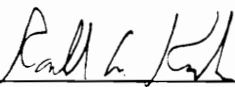
Dr. Donald G. Baird, Chairman



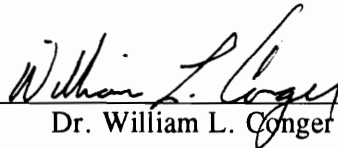
Dr. Eva Marand



Dr. Richey M. Davis



Dr. Ronald G. Kander



Dr. William L. Conger

February 1, 1995

Blacksburg, Virginia

C.2

LID

5655

V856

1995

5846

C.2



## **Textured Fluids**

By Gerhard K. Guenther

D. G. Baird (chairman)

### **(ABSTRACT)**

The rheology and development morphology of textured fluids have been investigated. The first fluid considered in this work was a liquid crystalline polymer consisting of isotropic and anisotropic solutions of poly-p-phenyleneterephthalamide (PPT) in sulfuric acid. The second textured fluid considered in this work was an immiscible polymer blend consisting of poly(ethylene terephthalate) (PET) and nylon 6,6

The role played by liquid crystalline order (LCO) and a polydomain texture on the rheology of PPT solutions was investigated. It was found that several of the rheological phenomena commonly attributed to liquid crystalline order in polymers (e.g., three region flow curve, negative steady state first normal stress difference, and oscillatory behavior at the start up of shear flow) were not observed in the solution in its anisotropic state. The solution in both its anisotropic and isotropic state exhibited a two region flow curve (Newtonian plateau and shear thinning region at rates ranging from  $10^{-4}$  to  $10^2 \text{ sec}^{-1}$ ), a positive steady state first normal stress difference which increased with shear rate, and a transient shear stress which displayed a single overshoot before reaching a steady state value.

The rheology of PET/nylon 6,6 blends was found to be a function of both polymer degradation and the two phase texture. An accelerated degradation rate was found for the blends relative to the neat polymers, and as a consequence, the values of the steady shear viscosity ( $\eta$ ), magnitude of the complex viscosity  $|\eta^*|$ , storage modulus ( $G'$ ) and steady state first normal stress difference ( $N_1$ ) for samples melt blended in an extruder were lower than those of the neat polymers. Blends prepared by dry blending followed by mixing in a cone and

plate device where the degradation occurring during extrusion was avoided were found to have a higher value of  $|\eta^*|$  and  $G'$  and enhanced transient behavior relative to those of the neat polymers. Scaling of the transient stress indicated there was no intrinsic time constant for these blends at shear rates lower than the longest relaxation time of the neat polymers

The theory developed by Doi and Ohta which describes the additional stresses arising as a consequence of interfacial tension in two phase systems was evaluated for its ability to model the rheology of the 25/75 w/w PET/nylon 6,6 blend. The Doi-Ohta theory was found to be capable of qualitatively predicting the extra stresses arising as a result of the interfacial tension as observed in the steady state viscosity and steady state first normal stress difference and the transient stresses at the start up of steady shear flow. While the overshoot and undershoot of the stresses observed during stepwise changes of shear rate were not predicted, the scaling relation for the transient stresses predicted by the theory were found to hold for the blend using stepwise changes of shear rate at a constant step ratio.

## Acknowledgments

It is a pleasure for the author to acknowledge the advice, help, and support of his major advisor, Dr. Donald G. Baird. This work would not have been completed except for his guidance and valuable suggestions. The author would also like to thank his advisory committee, Drs. E. Marand, R. M. Davis, R. G. Kander, and W. L. Conger.

The Author would also like to express his appreciation to the following:

- Dr. Tina Handlos for her assistance in all aspects of this dissertation as well as all the other *stuff* that went along with its completion.
- All the people in the lab including Ed Sabol, Dr. Paulo De Souza, and fairly soon to be Drs. Chris Roberts, Robert Young and Mike McCloud.
- Those in Dr. Wilkes' lab who helped me in many different ways including David Shelby, Srivatson 'Watson' Srinivas and Tau Hua, and Don Brandom.

## Original Contributions

The following is a list of original contributions made by the author during his study at Virginia Polytechnic Institute and State University.

- It was shown that a three region flow curve, a negative steady state first normal stress difference, and oscillatory behavior at the inception of steady shear flow are not characteristic of liquid crystalline polymers.
- Steady shear viscosity data was obtained for PPT/H<sub>2</sub>SO<sub>4</sub> solutions at shear rates as low as  $10^{-4} \text{ sec}^{-1}$  using a modified creep experiment.
- The role played by the two phase nature and degradation on the steady shear and transient shear rheological properties measured in simple shear flow were determined for an immiscible polymer blend system consisting of PET and nylon 6,6.
- The transient rheological response of PET and nylon 6,6 blends was found to scale in stress and strain using stepwise changes of shear rate when the time scale associated with the flow are removed.
- A method of determining the unknown parameter in the kinetic equation for the relaxation of the anisotropy in the Doi-Ohta theory was presented.
- The Doi-Ohta theory was shown to qualitatively predict the extra stresses associated with the two phase nature of an immiscible polymer blend consisting of PET and nylon 6,6 as measured by the viscosity and steady state first normal stress difference .
- The Doi-Ohta was shown to qualitatively predict the transient shear stress and first normal stress difference at the start-up of shear flow but was shown to be incapable of predicting the overshoot and undershoot observed using stepwise changes of shear rate for an immiscible polymer blend consisting of PET and nylon 6,6.

## **Format of Dissertation**

This dissertation is written in a journal format. Chapters 3 to 5 are self-contained papers that describe the experiments, results and conclusions particular to each chapter.

## Table of Contents

1.0 Introduction .....	1
1.1 Rheology.....	3
1.2 Polymer Liquid Crystalline Systems .....	9
1.3 Liquid Crystalline Polymer and Thermoplastic Blends .....	12
1.4 Models for Textured Materials .....	15
1.5 Research Objectives .....	18
2.0 Literature Review .....	25
2.1 Rheology of Liquid Crystalline Polymers .....	25
2.1.1 Viscosity Behavior of Liquid Crystalline Polymers .....	26
2.1.1.2 Yield Stress .....	29
2.1.1.3 Plateau Viscosity .....	33
2.1.1.4 Onset of Shear Thinning.....	37
2.1.2 Normal Stress Behavior .....	41
2.1.3 Comparison of Steady State and Dynamic Behavior.....	47
2.1.4 Shear History and Transient Behavior.....	52
2.2 Rheology of Polymer Blends .....	60
2.2.1 Blends of Isotropic Polymers.....	60
2.2.2 LCP/thermoplastic Blends .....	68
2.3 Rheology of Filled Polymers .....	82
2.3.1 Viscous Effects.....	85
2.3.2 Elastic Nature .....	87
2.4 Mathematical Models for Viscoelastic Behavior of Textured Fluids.....	90
2.4.1 Constitutive Equations for Textured Materials .....	92
2.4.1.1 Derivation of Doi Ohta Equation .....	92
2.4.1.2 Deformation by Macroscopic Flow.....	94
2.4.1.3 Relaxation by Interfacial Tension .....	97
2.4.1.4 Constitutive Equation .....	99
2.4.2 Scaling Property .....	100
2.4.3 Steady Shear Flow Predictions.....	101
2.4.4 Transient Shear Flow Predictions .....	103
2.4.5 Oscillatory Shear Flow Predictions .....	107
2.5 Research Objectives .....	109
3.0 Rheological Properties of Liquid Crystalline Polymers .....	123

3.1	Introduction .....	125
3.2	Experimental .....	129
3.2.1	Materials .....	129
3.2.2	Optical Measurements .....	130
3.2.3	Rheological Measurements.....	131
3.2.4	Preliminary Rheological Experiments .....	132
3.2.5	Creep Experiments .....	133
3.3	Results and Discussion.....	135
3.3.1	State of the Solution.....	136
3.3.2	Viscosity .....	136
3.3.3	Steady State First Normal Stress Difference and Storage Modulus.....	153
3.3.4	Start Up of Steady Shear Flow.....	155
3.4	Conclusions .....	162
3.5	Acknowledgments.....	164
3.6	References .....	165
4.0	Rheology of an Immiscible Polymer Blend .....	169
4.1	Introduction .....	171
4.2	Experimental .....	176
4.2.1	Materials and Sample Preparation.....	176
4.2.2	Rheological Measurements.....	178
4.2.3	Microscopy .....	178
4.3	Results.....	179
4.3.1	Viscosity .....	179
4.3.2	Steady State First Normal Stress Difference and Storage Modulus.....	196
4.3.3	Transient Shear Stress and First Normal Stress Difference .....	202
4.4	Conclusions .....	211
4.5	Acknowledgments.....	212
4.6	References .....	213
5.0	An Evaluation of the Doi-Ohta Theory .....	215
5.1	Introduction .....	217
5.2	Summary of the Doi-Ohta Theory .....	220
5.3	Experimental .....	227
5.3.1	Materials and Sample Preparation.....	227
5.3.2	Rheological Measurements.....	229

5.3.3 Microscopy .....	229
5.3.4 Interfacial Tension.....	229
5.4 Results.....	230
5.4.1 Parameters and Initial Conditions .....	230
5.4.2 Steady Shear Flow Predictions.....	240
5.4.3 Transient Shear Flow Predictions .....	246
5.5 Conclusions .....	255
5.6 Acknowledgments.....	256
5.7 References .....	257
6.0 Recommendations .....	259
Vita .....	262



## List of Figures

Figure 1.1	Schematic representation of texture in polymer blends and LCPs. ....	2
Figure 1.2	Material being sheared between two parallel planes. (a) Simple shear flow (b) Displacement profile for a solid. ....	5
Figure 1.3	Schematic representations of LCP structure. ....	10
Figure 1.4	Schematic representation of drop coalescence, deformation and breakup during shear flow. ....	17
Figure 2.1	Schematic of proposed three region flow curve [8]. ....	28
Figure 2.2	Viscosity vs. shear rate for various liquid crystal polymers [9]. ....	30
Figure 2.3	Viscosity vs. concentration for 50/50 copolymer of n-hexyl and n- propylisocyanate, molecular weight 41000, in toluene at 25°C [70]. ....	34
Figure 2.4	Viscosity jump at the isotropic-nematic transition [43]. ....	35
Figure 2.5	First normal-stress difference versus shear rate for isotropic solutions of PBG in m-cresol [19]. ....	42
Figure 2.6	The primary normal stress difference vs. the shear rate [19]. ....	44
Figure 2.7	Effect of preshear on the dynamic viscosity of a thermotropic LCP [80]. ....	53
Figure 2.8	Start-up of shear flow. Shear rate: (■) shear stress; (▲) first normal stress difference [26]. ....	56
Figure 2.9	The effect of varying the relaxation time $\tau_r$ for interrupted stress growth of 60HBA/PET at 275°C and [110]. ....	58
Figure 2.10	Composition dependence of the viscosity of polystyrene-polyethylene blends at various shear stresses ( $T=170^\circ\text{C}$ ): Shear stress ( $\text{dyn/cm}^2$ ) ( $\nabla$ ) $0.5 \times 10^5$ (○) $1 \times 10^5$ ; (□) $5 \times 10^5$ ; (Δ) $10 \times 10^5$ [120]. ....	63
Figure 2.11	Viscosity as a function of shear stress of polystyrene-polyethylene blends at $T=210^\circ\text{C}$ . (○) polystyrene (■) 90/10 PS/PE; (Δ) 50/50 PS/PE; (●) 30/70 PS/PE; (□) polyethylene [120]. ....	64
Figure 2.12	Comparison of the composition and temperature dependence of the viscosity and normal stress of blends of polystyrene and polyethylene at various shear stresses [121]. ....	65
Figure 2.13	Composition dependence of the viscosity of blends of CPA and POM as a function of shear stress: (curve 1) 1.27; (curve 2) 3.93; (curve 3) 5.44; (curve 4) 6.30; (curve 5) 12.59; (curve 6) 19.25; (curve 7) 31.62 ( $\times 10^{-5} \text{dyn/cm}^2$ ) [124] ....	67

Figure 2.14	Viscosity vs. shear rate for PC-PET/60HBA blends. The LCP content is $\Delta$ 0%; $\nabla$ 5%; $\diamond$ 10%; $\square$ 90%; and $\bigcirc$ 100% [128].	71
Figure 2.15	Viscosity vs. shear rate for PC-PET/60HBA blends [39].	72
Figure 2.16	Transient shear stress vs. strain a) TLCP ; b) PEI; c) PEI/TLCP 90/10 at 330°C [150].	76
Figure 2.17	Comparison between steady shear and complex viscosities. ( $\blacksquare$ ) $\eta$ ; ( $\blacktriangle$ ) $\eta^*$ [126].	78
Figure 2.18	Comparison of observed composition dependence with theoretical predictions at $T = 170^\circ\text{C}$ [126].	81
Figure 2.19	Shear viscosity vs. apparent shear rate, for HDPE suspensions at 170°C. The concentrations of fibers for the sets of data are, from top to bottom, 40%, 10%, 0% [187].	88
Figure 2.20	Extra shear viscosity and the normal viscosity for steady shear flow and $\eta_{\text{ex}}$ is defined by Eq. 2.41 [1].	102
Figure 2.21	Stepwise change of the shear rate [1].	104
Figure 2.22	Calculated shear stress for a step change in the shear rate. The parameter $\mu$ is chosen to be 0.9 [1].	105
Figure 2.23	Calculated shear stress when a shear flow of constant shear rate is started for an isotropic system at time $t = 0$ . The parameter $\mu$ is chosen to be 0.9 [1].	106
Figure 3.1	Intensity of transmitted polarized light as function of temperature for 12.6% PPT/H <sub>2</sub> SO <sub>4</sub> solution.	137
Figure 3.2	Increase in the magnitude of the complex viscosity of the 12.6% PPT/H <sub>2</sub> SO <sub>4</sub> solution at 60 °C as a function of time at frequencies of: ( $\Delta$ ) 0.3; ( $\bigcirc$ ) 0.5; ( $\square$ ) 1.0 rad/sec. The line is a statistical fit of the data using Eq. (1) where $\dot{\gamma} = 0.3, 0.5, \text{ and } 1.0 \text{ rad/sec}$ .	139
Figure 3.3	Increase in the time required to reach steady state in step-down experiments from an initial shear rate of $1 \text{ sec}^{-1}$ as a function of the final shear rate for 12.6% PPT/H <sub>2</sub> SO <sub>4</sub> solution. The line represents a statistical fit of the data using Eq. (2).	140
Figure 3.4	Flow curve for the 6.7% PPT/H <sub>2</sub> SO <sub>4</sub> solution at 60 °C: ( $\Delta$ ) magnitude of the complex viscosity; ( $\blacktriangle$ ) steady shear viscosity from steady shear experiments; and ( $\bullet$ ) steady shear viscosity from step-down creep	

experiments. The line represents linear regression analysis of the creep data.....	142
Figure 3.5 Flow curve for 12.6% PPT/H <sub>2</sub> SO <sub>4</sub> solution at 60 °C: (Δ) magnitude of the complex viscosity; (▲) steady shear viscosity from steady shear experiments; (●) steady shear viscosity from step-down creep experiments; and (○) creep data corrected for coagulation using Eq. (3). The line represents linear regression analysis of the corrected creep data.....	143
Figure 3.6 Magnitude of the complex viscosity versus frequency as a function of temperature for the 6.7% PPT/H <sub>2</sub> SO <sub>4</sub> solution: (□) 40 °C; (○) 60 °C; and (Δ) 75 °C. The lines represent a best fits using the Carreau-Yasuda model. ....	146
Figure 3.7 Magnitude of the complex viscosity versus frequency as a function of temperature for the 12.6% PPT/H <sub>2</sub> SO <sub>4</sub> solution: (□) 60 °C; (○) 75 °C; and (Δ) 90 °C. The lines represent best fits using the Carreau-Yasuda model. ....	147
Figure 3.8 Magnitude of the complex viscosity versus temperature for the 12.6% PPT/H <sub>2</sub> SO <sub>4</sub> solution. ....	148
Figure 3.9 Master curve for the magnitude of the complex viscosity as function of frequency shifted to a reference temperature of T <sub>0</sub> =60 °C for a 6.7% PPT/H <sub>2</sub> SO <sub>4</sub> solution where the values were taken at temperatures of (□) 40 °C, (○) 60 °C, and (Δ) 75 °C. ....	152
Figure 3.10 Dimensionless complex viscosity versus dimensionless shear rate for a 6.7% PPT/H <sub>2</sub> SO <sub>4</sub> solution at (■) 40 °C, (●) 60 °C, and (▲) 75 °C and a 12.6% PPT/H <sub>2</sub> SO <sub>4</sub> at (□) 60 °C, (○) 75 °C, and (Δ) 90 °C.....	154
Figure 3.11 First normal stress difference and 2G' as a function of shear rate and frequency, respectively, at 60 °C: N <sub>1</sub> (●) 6.7% PPT/H <sub>2</sub> SO <sub>4</sub> solution, (▲) 12.6% PPT/H <sub>2</sub> SO <sub>4</sub> solution; 2G', (○) 6.7% PPT/H <sub>2</sub> SO <sub>4</sub> solution, (Δ) 12.6% PPT/H <sub>2</sub> SO <sub>4</sub> solution. ....	156
Figure 3.12 Transient shear stress at a constant shear rate of 1 sec <sup>-1</sup> at the start up of steady shear flow versus strain at 40 °C, 60 °C, and 75 °C for the 6.7% PPT/H <sub>2</sub> SO <sub>4</sub> solution. ....	158
Figure 3.13 Transient shear stress at a constant shear rate of 1 sec <sup>-1</sup> at the start up of steady shear flow versus strain at 60 °C, 75 °C, and 90 °C for the 12.6% PPT/H <sub>2</sub> SO <sub>4</sub> solution. ....	159

Figure 3.14 Transient first normal stress difference at a constant shear rate of $1 \text{ sec}^{-1}$ at the start up of steady shear flow versus strain at $40^\circ\text{C}$ , $60^\circ\text{C}$ and $75^\circ\text{C}$ for the 6.7% PPT/ $\text{H}_2\text{SO}_4$ solution. ....	160
Figure 3.15 Transient first normal stress difference at a constant shear rate of $1 \text{ sec}^{-1}$ at the start up of steady shear flow versus strain at $60^\circ\text{C}$ , $75^\circ\text{C}$ and $90^\circ\text{C}$ for the 12.6% PPT/ $\text{H}_2\text{SO}_4$ solution. ....	161
Figure 4.1 Normalized magnitude of the complex viscosity as a function of time at a fixed frequency of $1 \text{ rad/sec}$ and a strain of 5% in air at (a) $290^\circ\text{C}$ and (b) $300^\circ\text{C}$ for melt blended PET/nylon 6,6 samples: (■) 100/0; (□) 75/25; (◇) 50/50; (○) 25/75; and (●) 0/100. The lines represent best fits using eq. (1).....	181
Figure 4.2 Logarithmic decrement of viscosity as a function of reciprocal temperature samples based on time sweep measurements for PET/nylon 6,6 samples: (■) 100/0; (□) 75/25; (◇) 50/50; (○) 25/75; and (●) 0/100 and estimated for PET/nylon 6,6 samples subject to extrusion: (■) 100/0; (□) 75/25; (◇) 50/50; (○) 25/75; and (●) 0/100 estimated for the extrusion process. The lines represent best fits using eq. (2).....	183
Figure 4.3 Normalized magnitude of the complex viscosity as a function of time at a fixed frequency of $1 \text{ rad/sec}$ and a strain of 5% in nitrogen for (a) melt blended and (b) dry blended PET/nylon 6,6 samples: (■) 100/0; (□) 75/25; (◇) 50/50; (○) 25/75; and (●) 0/100 at $290^\circ\text{C}$ . ....	186
Figure 4.4 Magnitude of the complex viscosity as a function of frequency at $290^\circ\text{C}$ for melt blended PET/nylon 6,6 samples: (■) 100/0; (□) 75/25; (◇) 50/50; (○) 25/75; and (●) 0/100. ....	189
Figure 4.5 Steady shear viscosity as a function of shear rate at $290^\circ\text{C}$ for melt blended PET/nylon 6,6 samples: (■) 100/0; (□) 75/25; (◇) 50/50; (○) 25/75; and (●) 0/100.....	191
Figure 4.6 Magnitude of the complex viscosity as a function of frequency at $290^\circ\text{C}$ for dry blended PET/nylon 6,6 samples: (■) 100/0; (□) 75/25; (◇) 50/50; (○) 25/75; and (●) 0/100. ....	192
Figure 4.7 Scanning electron micrographs of melt blended PET/nylon 6,6 samples: (a) 75/25; (b) 50/50; and (c) 25/75.....	194
Figure 4.8 Scanning electron micrographs of dry blended PET/nylon 6,6 samples: (a) 75/25; (b) 50/50; and (c) 25/75.....	195

Figure 4.9 Scanning electron micrographs of melt blended 25/75 PET/nylon 6,6 sample quenched after shear flow.....	197
Figure 4.10 Storage modulus as a function of frequency at 290 °C for melt blended PET/nylon 6,6 samples: (■) 100/0; (□) 75/25; (◇) 50/50; (○) 25/75; and (●) 0/100. ....	199
Figure 4.11 Steady state first normal stress difference as a function of shear rate at 290 °C for melt blended PET/nylon 6,6 samples: (■) 100/0; (□) 75/25; (◇) 50/50; (○) 25/75; and (●) 0/100. ....	200
Figure 4.12 Storage modulus as a function of frequency at 290 °C for dry blended PET/nylon 6,6 samples: (■) 100/0; (□) 75/25; (◇) 50/50; (○) 25/75; and (●) 0/100. ....	201
Figure 4.13 Transient shear stress at the start up of shear flow at 290 °C and a shear rate of 1 sec <sup>-1</sup> for melt blended PET/nylon 6,6 samples: (■) 100/0; (□) 75/25; (◇) 50/50; (○) 25/75; and (●) 0/100.....	203
Figure 4.14 Transient shear stress at the start up of shear flow at 290 °C and a shear rate of 1 sec <sup>-1</sup> for dry blended PET/nylon 6,6 samples: (■) 100/0; (□) 75/25; (◇) 50/50; (○) 25/75; and (●) 0/100.....	204
Figure 4.15 Transient first normal stress difference at the start up of shear flow at 290 °C and a shear rate of 1 sec <sup>-1</sup> for melt blended PET/nylon 6,6 samples: (■) 100/0; (□) 75/25; (◇) 50/50; (○) 25/75; and (●) 0/100. ....	206
Figure 4.16 Transient reduced shear stress $\sigma_r = \sigma^+(t, \dot{\gamma}_o) / \sigma(t)$ versus time using interrupted stress growth experiments as function of recovery time for the melt blended 25/75 PET/nylon 6,6 sample at 290 °C.....	207
Figure 4.17 Transient scaled shear stress $\sigma_s = [\sigma^+(t, \dot{\gamma}_1) - \sigma(\dot{\gamma}_0)] / [\sigma(\dot{\gamma}_1) - \sigma(\dot{\gamma}_0)]$ versus $\gamma_1$ where $(\dot{\gamma}_1 / \dot{\gamma}_0 = 3)$ and where $\dot{\gamma}_1$ is; (○) 0.5 sec <sup>-1</sup> ; and (●) 1.0 sec <sup>-1</sup> ; (■) 1.5 sec <sup>-1</sup> ; and (□) 3 sec <sup>-1</sup> for melt blended PET/nylon 6,6 samples: (a) 100/0; (b) 75/25; (c) 50/50; (d) 25/75; and (e) 0/100 at 290 °C .....	208
Figure 4.18 Transient scaled shear stress $\sigma_s = [\sigma^+(t, \dot{\gamma}_1) - \sigma(\dot{\gamma}_0)] / [\sigma(\dot{\gamma}_1) - \sigma(\dot{\gamma}_0)]$ versus $\gamma_1$ where $(\dot{\gamma}_0 / \dot{\gamma}_1 = 3)$ and where $\dot{\gamma}_1$ is; (○) 1 sec <sup>-1</sup> ; and (●) 0.5 sec <sup>-1</sup> for melt blended PET/nylon 6,6 samples: (a) 100/0; (b) 75/25; (c) 50/50; (d) 25/75; and (e) 0/100 at 290 °C. ....	209

Figure 5.1 Viscosity versus shear rate at 290 °C before and after extrusion: (□) PET; (○) nylon 6,6; (■) extruded PET; and (●) extruded nylon 6,6.....	232
Figure 5.2 Magnitude of the complex viscosity versus time at 290 °C for: (■) PET; (○) nylon; and (●) 25/75 PET/nylon 6,6 blend.. .....	234
Figure 5.3 Scanning electron micrograph of 25/75 PET/nylon 6,6 blend.....	236
Figure 5.4 Weighted relaxation time spectra for PET, nylon 6,6 and 25/75 PET/nylon 6,6 blend at 290 °C.. .....	239
Figure 5.5 Best fit for the parameter c in the Doi-Ohta theory using the transient shear stress at the start up of shear flow at 290 °C for 25/75 PET/nylon 6,6 blend: (●) experimental; and (—) model. ....	241
Figure 5.6 Best fit for the parameter c in the Doi-Ohta theory using the transient first normal stress difference at the start up of shear flow at 290 °C for 25/75 PET/nylon 6,6 blend: (●) experimental; and (—) model.. .....	242
Figure 5.7 Viscosity as a function of shear rate at 290 °C for 25/75 PET/nylon 6,6 blend: (○) experimental; (-----) predicted by the Doi-Ohta theory using $\eta_0(\text{constant})$ ; and (—) predicted by the Doi-Ohta theory using $\eta_0(\dot{\gamma})$ .. .....	244
Figure 5.8 First normal stress difference as a function of shear rate at 290 °C: (○) weighted average of PET and nylon 6,6; (●) experimental 25/75 PET/nylon 6,6 blend; (-----) predicted by Doi-Ohta theory; and (—) predicted using weighted average of neat polymers plus Doi-Ohta theory. ....	245
Figure 5.9 Transient shear stress versus time for at 290 °C: (○) PET; (Δ) nylon 6,6; (●) 25/75 PET/nylon 6,6 blend; (—) predicted by Doi-Ohta theory. ....	247
Figure 5.10 Transient first normal stress difference versus time for at 290 °C: (○) PET; (Δ) nylon 6,6; (●) 25/75 PET/nylon 6,6 blend; (—) predicted by Doi-Ohta theory. ....	248
Figure 5.11 Transient scaled shear stress $\sigma_s = [\sigma^+(t, \dot{\gamma}_1) - \sigma(\dot{\gamma}_0)] / [\sigma(\dot{\gamma}_1) - \sigma(\dot{\gamma}_0)]$ versus $\gamma_1$ where $(\dot{\gamma}_1 / \dot{\gamma}_0 = 3)$ and where $\dot{\gamma}_1$ is; (Δ) 1.5 sec <sup>-1</sup> ; (●) 3.0 sec <sup>-1</sup> ; and (□) 4.5 sec <sup>-1</sup> for 25/75 PET/nylon 6,6 blend at 290 °C.....	250
Figure 5.12 Transient scaled shear stress $\sigma_s = [\sigma^+(t, \dot{\gamma}_1) - \sigma(\dot{\gamma}_0)] / [\sigma(\dot{\gamma}_1) - \sigma(\dot{\gamma}_0)]$ versus $\gamma_1$ where $(\dot{\gamma}_0 / \dot{\gamma}_1 = 3)$ and where $\dot{\gamma}_1$ is; (Δ) 0.5 sec <sup>-1</sup> ; (●) 1.0 sec <sup>-1</sup> ; and (□) 1.5 sec <sup>-1</sup> for 25/75 PET/nylon 6,6 blend at 290 °C.....	251

Figure 5.13 Recovery of overshoot as a function of recovery time using interrupted stress growth experiments for the 25/75 PET/nylon 6,6 blend at 290 °C. ....	252
Figure 5.14 Predicted normalized interfacial area per unit volume using the Doi-Ohta theory as a function of time at the start up of shear flow, step-up of the shear rate and cessation of shear flow. ....	254

## List of Tables

Table 2.1 Rheology of Lyotropic and Thermotropic LCPs [51].	27
Table 2.2 Onset of Shear Rate Dependence of Viscosity of PBLG [9].	38
Table 2.3 Steady Shear versus Dynamic Properties [9].	49
Table 2.4 Viscosity of polymer blends [122].	62
Table 2.5 Viscosity behavior of TLCP/thermoplastic blends [126].	69
Table 2.6 Empirical Relations for Predictions of Blend Viscosity	79
Table 2.7 Summary of Particulate Filled Polymers [159]	83
Table 2.8 Summary of Fiber Filled Polymers [159].	84
Table 3.1 Carreau-Yasuda model parameters for the 6.7% and 12.6% PPT/H <sub>2</sub> SO <sub>4</sub> solutions fit to the magnitude of the complex viscosity versus angular frequency data.	150
Table 4.1 Logarithmic decrement of viscosity (D) and the apparent overall activation energy of degradation (ED) in air for PET/nylon 6,6 blends.	184
Table 4.2 Logarithmic decrement of viscosity (D) in nitrogen PET/nylon 6,6 blends.	187
Table 5.1 Model parameters and initial conditions for the 25/75 PET/nylon 6,6 blend.	231



## 1.0 Introduction

This research is concerned with the rheology and structure development during flow of polymeric fluids consisting of more than one phase. Two examples of these fluids include binary blends of immiscible polymers and liquid crystalline polymers (LCPs) with a polydomain structure. The texture of these two materials is shown schematically in Fig. 1.1. In the case of blends, one of the phases may consist of drops (see Figure 1.1a) which during flow, undergo deformation, breakup and coalescence (see Figure 1.1b). In the case of LCPs with a polydomain structure, domains containing highly oriented rodlike molecules are seen in the absence of flow (see Figure 1.1a) which during flow undergo deformation, breakup, and coalescence (see Figure 1.1b) much in the same way as for blend systems. Because a microstructure exists during flow, these materials are referred to as "textured fluids" [1]. Under an applied flow field textured fluids undergo complex structural changes and as a consequence may exhibit rheological properties which are a function of their texture and are not seen in the individual phases from which the texture is formed.

The rheological research which has been performed on textured materials consisting of LCPs and polymer blends has at this time not produced a fundamental understanding of their flow behavior. Although there is now agreement that LCPs contain a polydomain texture, most of the work to date has ignored this aspect and has treated LCPs as monodomain systems in which the rheology is related to changes in the orientation of the director. The director is a unit vector representing the average orientation of a collection of rodlike molecules. In the case of polymer blends, research has focused on the mechanical properties and texture in the final products, while the rheology and corresponding development of texture during flow in these systems has been largely ignored. At the present time, the rheology and development of texture during flow

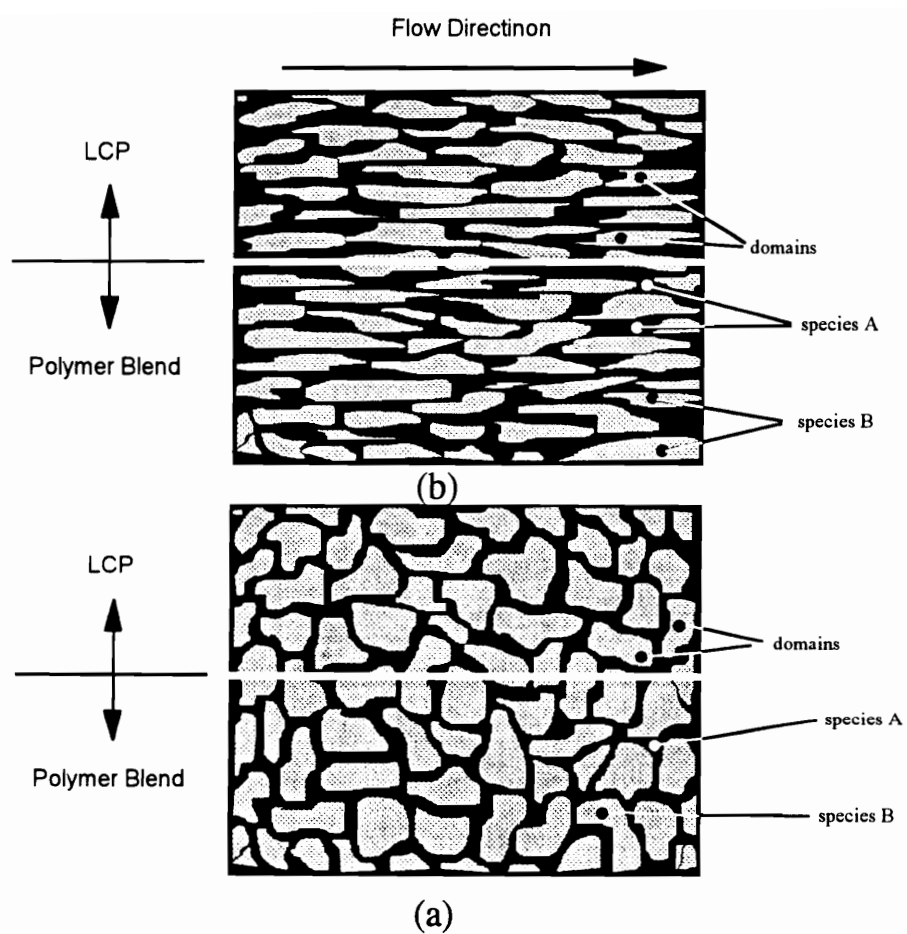


**Figure 1.1 Schematic representation of texture in polymer blends and LCPs.**

of LCPs and polymer blends are not well understood. As a consequence of the lack of a fundamental understanding of these systems, models capable of comprehensively predicting their rheological behavior do not exist at this time.

In this chapter the relevant research performed in the area textured fluids is reviewed. Chapter 1 will begin with a definition of rheology and an introduction to the viscometric functions used to describe the rheological properties of polymeric materials. In Sections 1.2 and 1.3 the general aspects of structure and rheology of LCPs and polymer blends will be discussed, respectively. This will be followed in Section 1.4 by a brief discussion of three constitutive equations which have been used to predict the behavior of some textured materials. Finally in Section 1.5 the research objectives intended to further the state of knowledge of the rheological behavior and development of texture during flow of LCPs and polymer blends will be presented.

## **1.1 Rheology**

The scope of the work proposed here involves the study of the rheological behavior of LCPs and polymer blends. This section will, therefore, introduce the reader to the concepts of rheology and will introduce the material functions which are required to describe the behavior of textured fluids.

The classical definition of rheology is "the science of deformation and flow of matter." The field of rheology is primarily concerned with those properties of matter which determine how it will flow when subjected to an external force or system of forces. The relationship between the applied stress and the resulting deformation is a function of the material, and it is this function which then defines the rheological properties of the material. In general, materials of rheological interest often include those which, because of their

nature or because of large deformations, display properties which do not obey either Newton's Law of viscosity or Hooke's Law of elasticity. Materials such as polymeric and textured fluids display rheological properties which do not obey Newton's or Hooke's laws but rather exhibit behavior which is both viscous and elastic in nature.

One of the aspects which determines the flow behavior of fluids (i.e., fluid response to a stress or deformation) is the fluids viscous properties. The viscous properties of a fluid can be described by considering the fluid's response to a fundamental deformation called simple shear flow. Simple shear flow will occur, for example, in a fluid constrained between two infinite parallel plates, where the lower plate is fixed and the upper plate moves with a constant velocity  $V$  (see Figure 1.2a). Consider a velocity field, where the velocity vector, with respect to a Cartesian coordinate system  $(x, y, z)$  fixed in space, has only one component,  $v_x$ , which is a linear function of  $y$ :

$$\begin{aligned} v_x &= v_x(y) \\ v_y &= v_z = 0 \end{aligned} \tag{1.1}$$

This type of deformation is distinguished by an imposed rate of deformation (tensor) which has two independent non-zero components and is uniform throughout the material. The rate of deformation tensor in simple shear flow takes on the following distinct form

$$\dot{\gamma}_{ij} = \dot{\gamma}(t) \begin{pmatrix} 0 & 1 & 0 \\ 1 & 0 & 0 \\ 0 & 0 & 0 \end{pmatrix} \tag{1.2}$$

where  $\dot{\gamma}(t)$  may be constant or a function of time. Simple shear flow is often used to study the rheology of fluids, but it represents only one type of flow experienced in practice or used in rheological experiments.

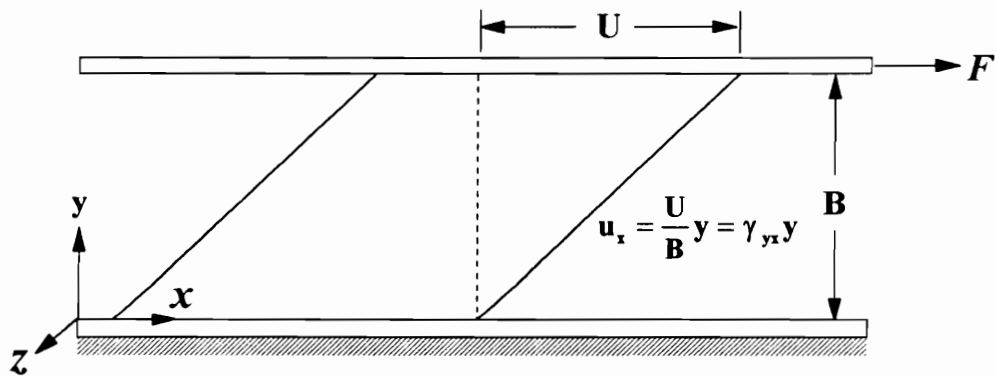
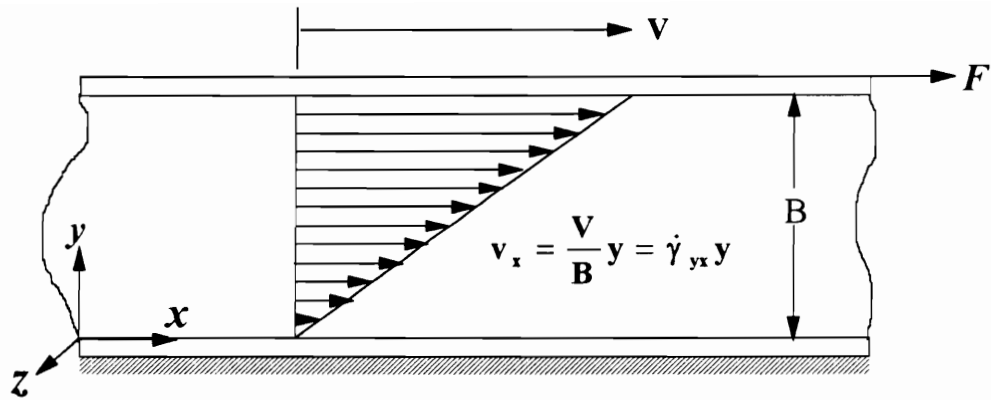


**Figure 1.2. Material being sheared between two parallel planes. (a) Simple shear flow (b) Displacement profile for a solid.**

For many fluids in simple shear flow, shear rate ( $\dot{\gamma}_{yx}$ ) which is the magnitude of the rate of deformation tensor and shear stress ( $\tau_{yx}$ ), prove to be proportional to each other

$$\tau_{yx} = -\mu \dot{\gamma}_{yx} \quad (1.3)$$

where the coefficient of proportionality,  $\mu$ , is a rheological property called viscosity. This equation states that the shear stress is proportional to the negative of the velocity gradient and is known as Newton's Law of viscosity. It can also be interpreted to signify that the momentum transfer takes place in the direction of decreasing velocity gradient and is analogous with the corresponding laws for diffusive mass and heat transfer (i.e., Fick's and Fourier laws, respectively). Materials which have a constant viscosity regardless of the magnitude of the shear stress or shear rate at a given temperature and pressure are defined as being Newtonian fluids. Additionally, Newtonian fluids are further required to have a viscosity which is independent of time and display no anisotropic normal stresses during flow. Examples of Newtonian fluids include gases, low molecular weight liquids, molten salts and metals. The rheological behavior of Newtonian fluids can be characterized solely by their density and viscosity.

While the rheology of some materials is adequately described by the relationship between shear rate and shear stress as described by Eq. 1.3, there are many fluids which deviate from this behavior. Examples of materials which often do not obey Newton's Law of viscosity include: polymer melts and solutions; multiphase mixtures (slurries, emulsions, and gas-liquid dispersions); soap solutions; cosmetics and toiletries; food products (jellies, cheese, butter, mayonnaise, soups, etc.); biological fluids (blood, synovial fluid, saliva); and agricultural and dairy wastes. These materials, many of which are textured, often have variable viscosities which change with shear rate and are classified as non-Newtonian fluids.

In these materials the proportionality between the shear stress and shear rate in simple shear flow can be described by

$$\tau_{yx} = -\eta(\dot{\gamma}) \dot{\gamma}_{yx} \quad (1.4)$$

where  $\eta(\dot{\gamma})$  is the non-Newtonian viscosity or the shear rate dependent viscosity. Equation 1.4 defines the generalized Newtonian fluid. The way in which the non-Newtonian viscosity varies with shear rate or shear stress is dependent on the material.

In addition to the viscous properties of non-Newtonian fluids, some non-Newtonian fluids also display an elastic response to an applied deformation or stress. Materials which display both viscous and elastic responses to an applied deformation or stress are further classified as "viscoelastic" fluids. In this work we are interested in the rheological properties of two textured fluids, LCPs and polymer blends, which are classified as viscoelastic fluids. Viscoelastic materials, which often display a shear rate dependent viscosity, are not adequately described by Eq. 1.4 due to their elastic nature. In an ideal viscous fluid the stress which arises as a result of deformation in simple shear flow can be described by Eq. 1.3. At the other extreme is the ideal elastic solid or Hookean solid. In the shearing motion of a Hookean solid between two parallel planes where the upper plane undergoes a displacement  $U$  (see Figure 1.2b), the stress ( $\tau_{yx}$ ) is directly proportional to the strain ( $\gamma_{yx}$ ):

$$\tau_{yx} = -G\gamma_{yx} \quad (1.5)$$

where the coefficient of proportionality,  $G$ , is analogous to the Newtonian viscosity and is called the elastic modulus. When a solid deforms within the linear elastic limit, it regains its original form upon removal of the stress. The elastic behavior observed in polymeric fluids is a consequence of the overlap of macromolecules (called entanglements) or other

interactions such as ionic association. In the case of textured fluids, the elastic nature is the result of surface tension and coalescence of the phases as well as any elastic contributions due to the nature of the material within each phase.

Due to their elastic nature, polymeric and textured fluids display extra normal stresses ( $\tau_{xx}$ ,  $\tau_{yy}$  and  $\tau_{zz}$ ) during flow so that in addition to the viscosity defined above two more material functions can be defined in simple shear flow. All three material functions (also called viscometric functions) can be obtained from three independent quantities of stress (obtained from the non zero components of the stress tensor). In steady simple shear flow of a viscoelastic fluid the stress tensor in rectangular Cartesian coordinates is

$$\boldsymbol{\tau} = \begin{pmatrix} \tau_{xx} + P & \tau_{xy} & 0 \\ \tau_{yx} & \tau_{yy} + P & 0 \\ 0 & 0 & \tau_{zz} + P \end{pmatrix} \quad (1.6)$$

where  $P$  is the isotropic pressure. The three independent quantities of stress in simple shear flow are then

$$\tau_{xy} = \tau_{yx} = -\eta(\dot{\gamma})\dot{\gamma}_0 \quad (1.7)$$

$$\tau_{xx} - \tau_{yy} = N_1 = -\psi_1(\dot{\gamma})\dot{\gamma}_0^2 \quad (1.8)$$

$$\tau_{yy} - \tau_{zz} = N_2 = -\psi_2(\dot{\gamma})\dot{\gamma}_0^2 \quad (1.9)$$

where  $\dot{\gamma}(t) = \dot{\gamma}_0 = \text{constant}$ ,  $N_1$  and  $N_2$  are primary and secondary normal stress differences, respectively, and  $\psi_1$  and  $\psi_2$  are the primary and secondary normal stress coefficients, respectively.

We can now summarize some of the rheological behavior displayed by polymeric and textured fluids (i.e., non-Newtonian viscoelastic fluids) not seen in Newtonian fluids. These differences include but are not limited to, a shear rate or shear stress dependent viscosity, additional normal stresses in shear flow, and other viscoelastic behavior not discussed above such as elastic recoil (memory) and an extensional viscosity which is not simply related to the shear viscosity. In the case of textured fluids like polymer blends and



LCPs, viscoelastic behavior can be a result of surface tension and coalescence of the phases as well as the individual viscoelastic contributions from each phase.

The rheological behavior displayed by viscoelastic fluids (i.e.,  $\eta$ ,  $N_1$ , and  $N_2$ ) can provide valuable insight into the flow induced structural changes that occur in systems containing macromolecules and or texture. The importance of this aspect of rheology in the study of LCPs and polymer blends will become apparent in Sections 1.2 and 1.3. where, in addition to a description of their texture, the rheological behavior associated with these materials is discussed.

## **1.2 Polymer Liquid Crystalline Systems**

The purpose of this section is to introduce liquid crystalline polymers, their texture and their rheological behavior which classifies them as viscoelastic fluids. Additionally, this section will discuss the role which the structure and related rheology of LCPs play in both processing and mechanical properties of products.

Liquid crystallinity is defined as an intermediate state between that of an isotropic fluid and a crystalline solid, and because of this is called a mesophase [3]. While a high degree of molecular order is seen in liquid crystals, they do not display the periodic three dimensional lattice structure of crystalline solids and, therefore, retain the ability to flow. The mesophase structure in liquid crystalline polymers is almost never found to be uniform on a macroscopic scale, but instead LCPs have been shown to consists of many micro-sized "domains" within which the mesophase structure exists and as a whole form a "polydomain" texture (see Figure 1.3) [4]. The polydomain texture in LCPs is characterized by a spacial change in the orientation of the director as a result of discontinuities in the director ( $\mathbf{n}$ ) called "disinclinations". Although liquid crystals flow

under an applied stress, a one or two dimensional order of molecules results in direction dependent properties or anisotropy on a microscopic scale [5].

Three different types of liquid crystalline mesophases can be defined by their orientational and positional order as shown in Figure 1.3. The nematic mesophase (see Fig. 1.3b) is composed of aggregates of rod-like molecules which are highly oriented about a specific direction denoted by the director but lack any positional order of their centers of gravity. This mesophase is characterized by one dimensional order, and consequently the high degree of mobility leads to a low viscosity. The cholesteric mesophase (see Fig. 1.3c) appears to be formed by a set of parallel nematic layers where the director describing each layer varies periodically from layer to layer and results in a periodic helical structure. In the smectic mesophase, which is shown in Figure 1.3d, the molecules are oriented parallel to one direction, while the centers of gravity of molecules are arranged in planes with well defined interlayer spacing that can be detected by X-ray diffraction.

Liquid crystalline order has been observed in both polymer solutions and undiluted polymer systems. The former type is referred to as a lyotropic liquid crystalline polymer (LLCP), and the latter is referred to as a thermotropic liquid crystalline polymer (TLCP). Lyotropic systems are characterized by the fact that the onset of liquid crystalline order is a function of both concentration and temperature, while for the case of thermotropes the transitions are a function of temperature only. In the case of the lyotropic systems, liquid crystalline order (LCO) appears when a critical concentration of the rod-like molecules is achieved. However, once LCO is achieved, temperature can be changed to alter the phase present. For example, on increasing the temperature the fluid can become isotropic, or on decreasing the temperature both solid and liquid crystal phases can exist. In the case of thermotropes, temperature is the primary variable which controls the type of phase present.

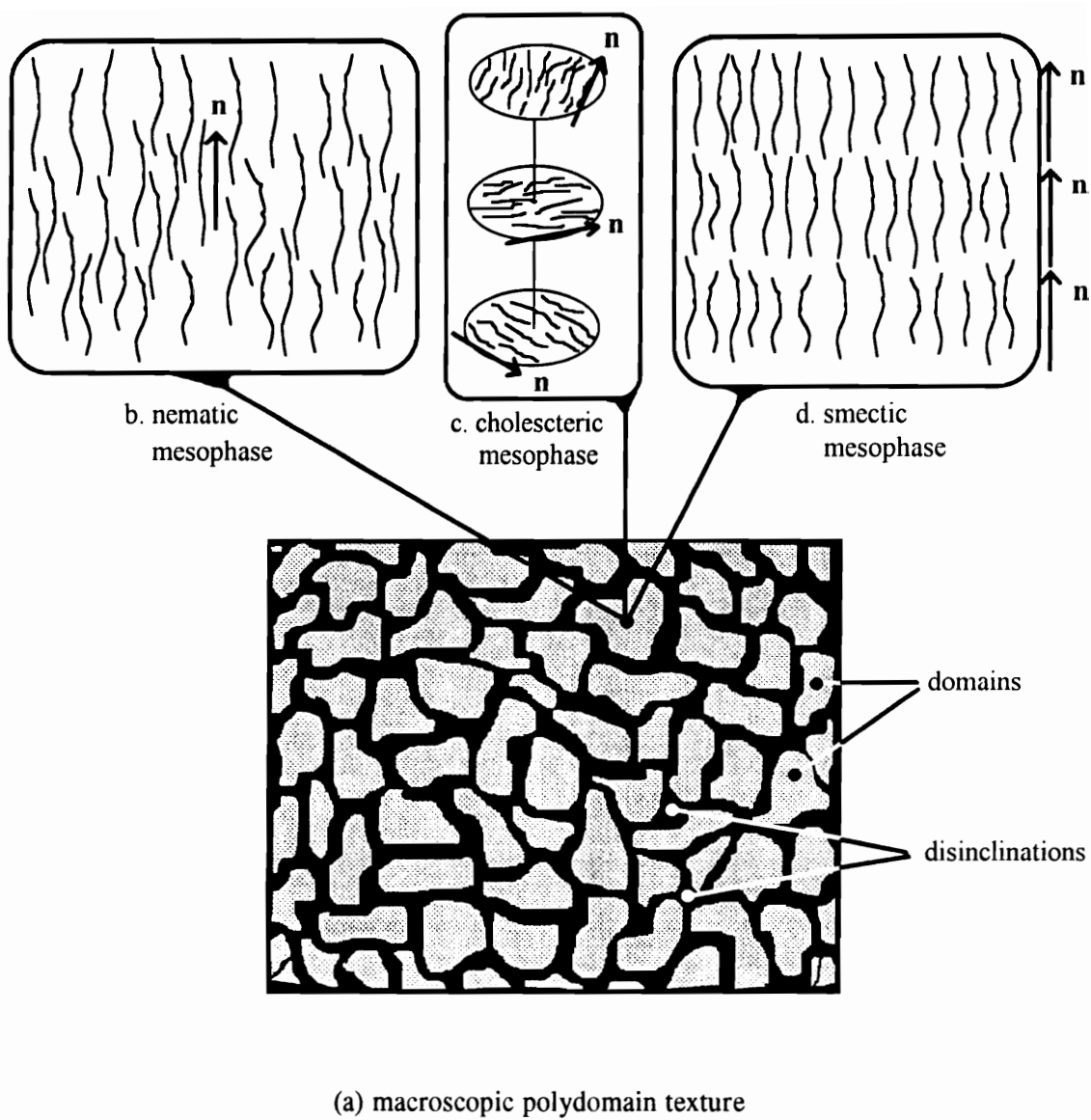


**Figure 1.3. Schematic representations of LCP structure.**

At temperatures below the solidification temperature of the TLCP the material may be a semi-crystalline or an amorphous solid. On increasing the temperature above the melting temperature ( $T_m$ ), in the case of the semi-crystalline solid, or the glass transition temperature ( $T_g$ ), in the case of the amorphous solid, the material becomes fluid but still contains a high degree of local order. Upon a further increase in temperature, some materials form an isotropic state before reaching the decomposition temperature. The molecular order found in both TLCPs and LLCs can also be classified by the three mesophase types described above, i.e., nematic, cholesteric, and smectic mesophases.

The existence of molecular order and a macroscopic polydomain structure is believed to greatly affect the rheological behavior of liquid crystalline polymers. Some of the qualitative rheological phenomena often attributed to LCPs in these studies include behavior not seen in isotropic polymeric liquids such as, apparent yield stresses [13-18], positive steady state first normal stress differences [19-22], and oscillatory behavior following the inception and stepwise change of simple shear flow [23-26]. While some LCPs like poly( $\gamma$ -benzyl-L-glutamate) (PBLG) in m-cresol consistently display some of the above mentioned behavior [19], others like hydroxypropylcellulose (HPC) in H<sub>2</sub>O do not [26]. The lack of generality of these reported phenomena for LCPs and even for the same system studied by different researchers contributes to the lack of a fundamental understanding of their flow behavior [9,19].

The development of orientation and texture in LCPs during flow which is directly related to their rheological behavior, has proven to play an advantageous role in several processes. By taking advantage of the orienting effects of extensional flow, fibers displaying excellent mechanical products can be produced from both lyotropic and thermotropic liquid crystalline polymers in which they are described as solution spun and melt spun, respectively. Additionally, the viscosities of liquid crystalline materials are

considerably lower than those of isotropic systems, allowing for the filling of complex molds, and lower operating pressures which result in lower operating costs.

In summary, LCPs display a complex two phase polydomain texture which includes domains with molecular orientation dispersed in a second phase of isotropic material [4]. The presence of a polydomain texture and molecular orientation in LCPs are believed to be responsible for the unique rheological properties not seen in flexible chain polymers and excellent mechanical properties.

### **1.3 Liquid Crystalline Polymer and Thermoplastic Blends**

In order to economically utilize some of the excellent rheological and mechanical properties of LCPs there has been much interest in combining these materials with thermoplastics in the form of blends [27]. These blends result in another form of textured fluid where the complex structure formed by the phases is analogous to the polydomain structure seen in neat LCPs as illustrated schematically in Fig. 1.1.

While the concept of blending two or more polymers has long been recognized as a cost effective method of generating new materials, it has only in the last decade been recognized that the addition of TLCPs to thermoplastics can have desirable effects on the rheology and mechanical properties of the blend. These effects can include a reduction in system viscosity and reinforcement of the thermoplastic matrix by TLCP fibrils formed during processing. The combination of these two effects allows for the possibility of easily processing materials with improved mechanical properties over those of the neat thermoplastics and lead directly to the importance of understanding the rheological behavior and related morphological or texture development of these blends.

The properties which will result from the blending of two immiscible polymers are to a large extent determined by the texture or morphology which is formed and the interface between the phases (e.g., interfacial adhesion). The blend morphology is in turn a function of interfacial tension, the viscous and elastic properties of each constituent, processing history, and concentration. The distribution of the phases present in binary blends can take on several different forms depending on the many variables mentioned above. In systems where one component is dispersed as drops in a matrix of the other phase, the blend tends to take on the properties of the continuous phase. In other systems the dispersed phase can take on the form of fibrils or ribbons formed in the direction of flow and can lead to properties in which both constituents significantly affect the blend properties. Finally, blends at concentrations at or near phase transition concentration are described as having a co-continuous structure in which the phases are continuous and interpenetrating, and the properties of both phases play a significant role in the properties of the blend. This work is concerned with the development of these types of morphology or texture during flow.

The addition of TLCPs to thermoplastics has been shown to sometimes yield a self-reinforcing polymer system in which LCP fibers are formed in situ (in situ composites) under suitable processing conditions [28]. It has been found that TLCPs orient in elongational flow fields, and in blends with isotropic polymers the formation of TLCP fibers during processing has improved the mechanical properties over those of the neat isotropic polymer [27]. The published work on these systems, which includes studies of different materials, compositions, and processing conditions often lead to conflicting results, and studies directed at the rheology and the development of texture during flow are limited.

The rheological studies of polymer blends have been generally limited to the steady shear viscosity of systems in which the processing temperatures of the constituent polymers

overlap. The results of these investigations are sometimes conflicting and specific to the materials investigated. Some of the most commonly observed results of these investigations are that with the addition of small amounts of LCP the steady shear viscosity of the blend is lower than that of the matrix material and resembles that of the LCP ( shear thinning behavior over a wide range of rates) [29-37]. Additionally, in some cases the steady shear viscosity was seen to be lower than that of the LCP [32]. However, these results conflict with other studies which showed an increase in viscosity with the addition of an LCP [33-35,38]. Although several theories have been proposed to account for a drop in viscosity, which include a lubricating effect by the LCP and the formation of fibrils at the entrance to a capillary [27], others have shown that these theories do not explain the observed rheology [32,36,37,39,40].

While the literature pertaining to polymer blends is extensive, comprehensive rheological data and the corresponding development of texture has not received much attention. The rheological behavior reported is, in general, limited to the viscosity as a function of concentration, processing conditions and materials used. These investigations have not, as of yet, produced a fundamental understanding of the rheology and corresponding texture of these blends and, as a consequence, there are at this time no predictive models generally applicable to these systems.

## **1.4 Models for Textured Materials**

In setting up mathematical models of flows, equations are obtained from the physical principles of conservation of mass and momentum. In addition we need a constitutive equation which describes the response of the material to stress or deformation. Constitutive equations such as those described by Eqs. 1.4 and 1.5 do not adequately

describe the rheological behavior of textured materials such as LCPs and polymer blends. Suitable constitutive equations must be able to separately predict both the stress response and the molecular orientation or changes in the texture as a function of flow history. While there has been considerable activity in predicting the flow behavior of liquid crystalline polymers over the past 15 years, a predictive model of polymer blend rheology is not available at the present time.

The most recent models for LCPs and their modifications stem from the original theories based on the continuum mechanics approach of Leslie [41], Ericksen [42] and Parodi [43] and the molecular theory approach of Doi [44]. In the continuum theory the stress tensor is assumed to be a function of the rate of deformation and a vector which describes the molecular orientation. The molecules are assumed to lie parallel to a common axis denoted by the director  $\mathbf{n}$ . The Doi equation describes the dynamics of rodlike polymers in concentrated solutions by considering the rotational motion of the rods in the isotropic and the liquid crystalline phases. The stress in the fluid during flow is a function of the rate of deformation tensor and an order parameter tensor,  $\mathbf{S}$ , which describes molecular orientation. While these models have been able to simulate some of the observed phenomena, it must be noted that none has been able to comprehensively predict all of them [45]. This problem might be attributed to the lack of a fundamental understanding of the physical mechanisms responsible for the rheological behavior seen in LCPs and the inability or failure of the theories to account for the polydomain texture found in LCPs.

Another approach to model the behavior of textured materials has recently been proposed by Doi and Ohta [1]. The theory proposed by Doi and Ohta attempts to describe a mixture of two immiscible Newtonian fluids by considering the deformation, rupture, and coalescence of many droplets which is shown schematically in Fig. 1.4. The model proposes a semi-phenomenological kinetic equation which describes the time evolution of



droplet size and orientation, and also the macroscopic stress in a flow field. The constitutive equation, which takes into account the macroscopic velocity field and interfacial tension, predicts a shear rate independent viscosity at steady state and a first normal stress difference which is non-zero and is proportional to  $|\dot{\gamma}|$ . Additionally this model predicts transient shear stress behavior which scales with both stress and strain. This scaling phenomena has been reported for several liquid crystalline polymer systems [23,24] while transient experiments on polymer blends with which to compare this behavior have not been reported in the literature.

In summary, while constitutive equations have been developed to model the behavior of LCPs, predictive models for polymer blends do not exist. The models developed for LCPs have considered the influence of molecular orientation on their rheology but have ignored viscoelastic contributions which might arise as a result of their polydomain texture. Failure of these models might be directly attributed to their failure to account for the viscoelastic contribution of the polydomain texture found in these materials. On the other hand, a general theory for textured fluids has been proposed by Doi and Ohta [1]. This theory which was derived for a mixture of two immiscible Newtonian fluids, assumes that the stresses due to a deformation arise as a result of the deformation, rupture, and coalescence of many droplets and might be extended in modified form to model other textured materials.

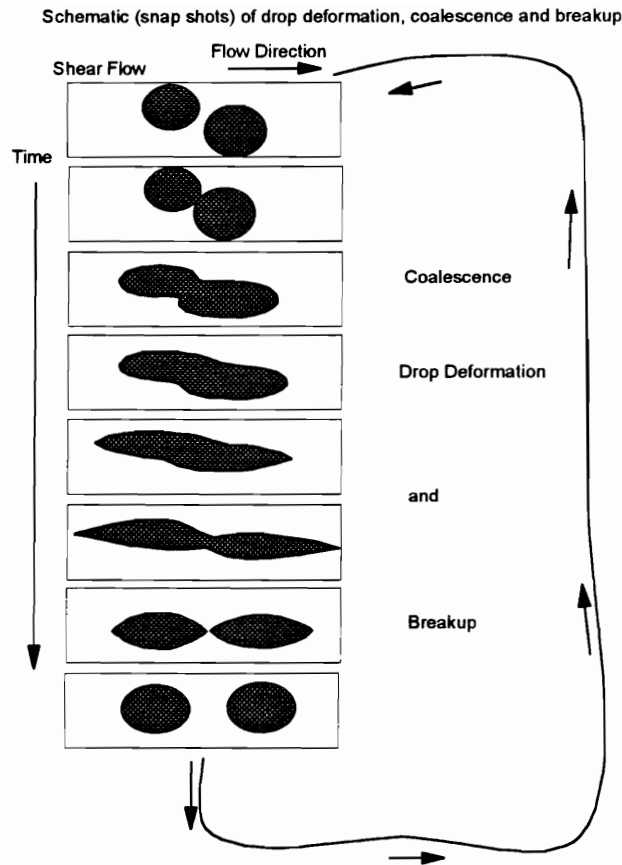


**Figure 1.4. Schematic representation of drop coalescence, deformation and breakup during shear flow.**

## 1.5 Research Objectives

In order to determine the role played by the two phase nature or texture of LCPs and polymer blends, a systematic study of their flow behavior is proposed here. In this section four objectives will be outlined with the intention of providing a better understanding of the rheological behavior and texture of LCPs and polymer blends during shear flow.

In Section 1.2 several aspects of LCP rheology which are considered unusual when compared with that of flexible chain polymers were presented. While unusual rheological behavior (e.g., apparent yield stresses, positive steady state first normal stress differences, and oscillatory behavior following the inception and stepwise change of simple shear flow) is seen in some LCPs, it is at this time not clear whether any of these phenomena are general to polymers containing liquid crystalline order.

**Objective 1:** The first objective of this research is to determine the role played by the liquid crystalline order and a polydomain texture on the rheology of LCPs..

In contrast to the considerable number of rheological studies of pure LCPs, there is a lack of rheological data pertaining to polymer blends. The study of polymer blends, described in Section 1.3, has in general been limited to the steady shear viscosity as a function of concentration. An important aspect of understanding the rheology of polymer blends is to establish how the structure changes during flow. The morphological studies performed on polymer blends have in general been limited to final products such as fibers

and injection molded plaques, while the development of structure during flow has not been related to the rheological behavior of the blend.

**Objective 2:** The second objective of this research is to determine the role played by the two phase texture on the rheology of immiscible polymer blends.

In Section 1.4 it was indicated that the continuum theory of Ericksen and Leslie and the molecular theory of Doi poorly describe the observed rheology of LCPs. It was also stated that a predictive model for polymer blends does not exist. On the other hand, the new theory by Doi and Ohta which is based on deformation, breakup and coagulation of droplets, has been shown to predict viscoelastic behavior for a textured system made up of a mixture of immiscible Newtonian fluids. This model is based on a fluid texture consisting of two phases and is a common feature of both LCPs and polymer blends.

**Objective 3:** The fourth objective of this research is to determine whether the theory proposed by Doi and Ohta can quantitatively or qualitatively predict the rheology of an immiscible polymer blend

The purpose of this chapter was to introduce textured fluids, the viscometric functions required to characterize the rheology of textured fluids, and the two types of textured fluids of interest in this work. This chapter was also intended to indicate that research is still needed in the area of textured fluids consisting of polymer blends and LCPs in order to obtain a fundamental understanding of their rheological behavior. Thereby, the motivation for this research was given and the overall objectives were stated. In the next chapter, the relevant literature pertaining to the rheology and texture of LCPs and polymer blends is reviewed in detail.

## REFERENCES

1. Doi, M., and Ohta, T., *J. Chem. Phys.*, 95(2), 1242, 1991.
2. Moldenaers, P. and Mewis, J., ***J. Non Newt. Fl. Mech.***, 34, 359, 1990.
3. Wendorff, J. F., Finkleman, H., and Ringsdorf, H., ***J. Polym. Sci., Polym. Symp.***, 63, 245, 1968.
4. DeGennes, P. G., "The Physics of Liquid Crystals," Oxford University Press, London , 1974.
5. Miesowicz, M., ***Nature***, 158, 27, 1946.
6. Asada, T., Onogi, S. and Yanase, H., ***Pol. Eng. Sci.***, 24(5), 355, 1984.
7. Aoki, H., White, J. L., and Fellers, J. F., ***J. Appl. Pol. Sci.***, 23, 2293, 1979.
8. Onogi, S. and Asada, T., "Rheology", Vol. 1, G. Astarita, G. Marrucci, and L. Nicolais, eds., Plenum Press, New York, 1980.
9. Wissbrun, K. F., ***J. Rheol.***, 25(6), 619, 1981.
10. Fukada, E., and Date, M., ***Biorheology***, 1, 101, 1963.
11. Marchessault, R. H., Moorehead, F. F. and Walters, N. M., ***Nature***, 184, 632, 1959.
12. Hermans, J. Jr., ***J. Polym. Sci., Part C2***, 129, 1963.
13. Papkov, S. P., Kulichikhin, V. G., Kalmykova, V. D. and Malkin, A. Y., ***J. Polym. Sci. Polym. Phys. Ed.***, 12, 1753, 1974.
14. Yanase, H. and Asada, T., ***Mol. Cryst. Liq. Cryst.***, 153, 281, 1987.
15. Elliot, H. H., ***J. Appl. Pol. Sci.***, 13, 755, 1969.
16. Shimamura, K., White, J. L. and Fellers, J. F., ***J. Appl. Pol. Sci.***, 26, 2165, 1981.
17. Suto, S., White, J. L., and Fellers, J. F., ***Rheol. Acta***, 21, 62, 1982.
18. Sugiyama, H., Lewis, D. N., White, J. L., and Fellers, J. F., ***J. Appl. Pol. Sci.***, 30, 2329, 1985.

19. Kiss, G. and Porter, R. S., **J. Polym. Sci. :Polym. Symp.**, 65, 193, 1978.
20. Moldenaers, P. and Mewis, J., **J. Rheol.**, 30(3), 567, 1986.
21. Navard, P., **J. Pol. Sci.: Pol. Pys. Ed.**, 24, 435, 1986.
22. Kiss, G. and Porter, R. S., **J. Pol. Sci.: Pol. Phys. Ed.**, 18, 361, 1980.
23. Viola, G. G. and Baird, D. G., **J. Rheol.**, 30(3), 601, 1986.
24. Mewis, J. and Moldenaers, P., **Mol. Cryst. Liq. Cryst.**, 153, 291, 1987.
25. Doppert, H. L. and Picken, S. J., **Mol. Cryst. Liq. Cryst.**, 153, 109, 1987.
26. Grizzuti, N., Cavella, and Cicarelli, **J. Rheol.**, 34(8), 1293, 1990.
27. La Mantia, F. P., "Thermotropic Liquid Crystal Polymer Blends", Ed. F. P. La Mantia, Technomic Publishing Co., Pennsylvania, 1993.
28. Siegman, A., Dagan, A., and Kenig, S., **Polymer**, 26, 1325, 1985.
29. Cogswell, F. N., Griffen, B. P., and Rose, J. B., May 31, 1983. U.S. patent 4,386,174.
30. Cogswell, F. N., Griffen, B. P., and Rose, J. B. February 21, 1984. U.S. patent 4,433,083.
31. Cogswell, F. N., Griffen, B. P., and Rose, J. B. February 21, 1984. U.S. patent 4,438,236.
32. Blizard, K. G. and Baird, D. G., **Polym. Eng. Sci.**, 27(9), 653, 1987.
33. Nobile, M. R., Amendola, E., Nicolais, L., Acierno, D., and Carfagna, C., **Polym. Engr. Sci.**, 29(4), 244, 1989.
34. Mehta A., and Isayev, A. I., **Polym. Engr. and Sci.**, 31(13), 971, 1991.
35. Isayev, A. I., and Modic, M., **Polym. Composites**, 8(3), 158, 1987.
36. Kohli, A., Chung, N. and Weiss, R. A., **Polym. Engr. and Sci.**, 29(9), 573, 1989.
37. Crevecoer, G., Ph. D. Thesis, Katholiede Universiteit Leuven, 1991.
38. Weiss, R. A., Huh, W., and Nicolais, L., **Polym. Engr. and Sci.**, 27(9), 684, 1987.

39. Blizard, K. G. and Baird, D. G., **Pol. Engr. Sci.**, Vol 27(9), 653, 1987.
40. James, S. G., Donald, A. M., and MacDonald, W. A., **Mol. Cryst. Liq. Cryst.**, 153:491, 1987.
41. Ericksen, J. L., **Arch. Ration. Mech. Anal.**, 4, 231, 1964.
42. Leslie, F. M., **Arch. Ration. Mech. Anal.**, 28, 265, 1968.
43. Parodi, J. **Phys. (Paris)**, 31, 581, 1970.
44. Doi, M., **J. Pol. Sci. Pol. Phys. Ed.**, 19, 229, 1981.



## **2.0 Literature Review**

This chapter will review the literature pertaining to the rheology of several textured fluids. The textured fluids reviewed here include liquid crystalline polymers, polymer blends, and particulate filled polymers. The first three sections of this chapter will attempt to identify rheological behavior which may be unique to these systems as well as to identify areas in which the rheology and texture of these systems is not well understood. In the last section of this chapter the Doi-Ohta constitutive equation for textured fluids is developed and reviewed.

### **2.1 Rheology of Liquid Crystalline Polymers**

This section will review several aspects of liquid crystalline polymer rheology, but is by no means intended to be comprehensive. Specifically, this review will concentrate on the areas of LCP rheology (introduced in Chapter 1) which differentiate it from the rheology of polymers which do not have texture. The rheological phenomena observed for various LCPs will be described and the theories or explanations presented by several authors to account for their behavior will be presented. In the context of this discussion comparisons will be made to isotropic polymers in order to help make the distinction between behavior seen in systems with liquid crystalline order (LCO) and texture and isotropic polymers. Several reviews on the rheological behavior of LCPs have been given by Baird [46], Wissbrun [9], Wilson[47], and more recently La Mantia [27] and reviews of the rheology of flexible chain polymers are given by Ferry [48], Bird [49], and Tanner [50].

Several liquid crystalline polymers which have received the most academic attention are listed in Table 2.1. Additionally, Table 2.1 indicates the rheological behavior sometimes seen in these LCPs which are not seen in flexible chain polymers such as positive steady state first normal stress differences, scaling of transient behavior, and region I (shear thinning) at low rates. The rheological phenomena listed in Table 2.1 are seen not to be general to all the materials studied, and in fact results obtained by different investigators using the same LCP can be different [51]. Several examples of these studies will be reviewed in the following sections. This section will begin with a review of the viscosity behavior, followed by the steady shear and transient stress behavior. Finally, the thermal and shear history effects are discussed as they are crucial in all aspects of the rheological behavior displayed by these materials and are in themselves areas where the rheological behavior of LCPs are distinguished from most isotropic polymers.

### **2.1.1 Viscosity Behavior of Liquid Crystalline Polymers**

The viscosity behavior of both lyotropic and thermotropic LCPs has been studied extensively. An attempt will be made here to extract those studies which demonstrate the general behavior of LCPs while at the same time highlighting the inconsistencies which exist.

The complex rheology present in LCPs has tentatively been attributed to the domains found in these materials. The use of domains to explain the three region flow curve of lyotropic, nematic, or cholesteric polymers was first presented by Onogi and Asada [8]. The three region flow curve (see Figure 2.1) is described as the evolution of domains from a piled domain structure at low shear rates (region I shear thinning) to a dispersed polydomain structure at intermediate shear rates (region II Newtonian plateau) and, finally,

**Table 2.1 Rheology of Lyotropic and Thermotropic LCPs [51].**

Polymer	Positive $N_1$	Yield Stress	Lack of intrinsic time scale (scaling)	References
PBG	yes	sometimes	yes	8,19,20,195, 196,197
HPC	yes/no	sometimes	yes/no	26,51,95,111, 198
PHIC	unavailable	no	unavailable	199,200,201
PBT,PBO	sometimes	yes	sometimes	202,203,204, 205,206
PPTA,PBA, ABT	unavailable	yes	yes/no	13,207,208, 209
Thermotropes	sometimes	sometimes	sometimes	210,211,99, 212,213,214, 217

PBG = poly- $\gamma$ -benzyl-glutamate

HPC = hydroxypropylcellulose

PHIC = poly(n-hexyl isocyanate)

PBT = poly-p-phenylene-2,6-benzobisthiazole

PPTA = poly-p-phenyleneterephthalamide

PBO = poly-p-phenylene-2,6-benzobisoxazole

PBA = poly-p-benzamide

DABT = poly-4,4'-benzanilidyleneterephthalamide

Thermotropes = include condensation products such as hydroxybenzoic acid (HBA) with ethylene terephthalate (PET), or with 2,6-hydroxynaphthoic acid (HNA)

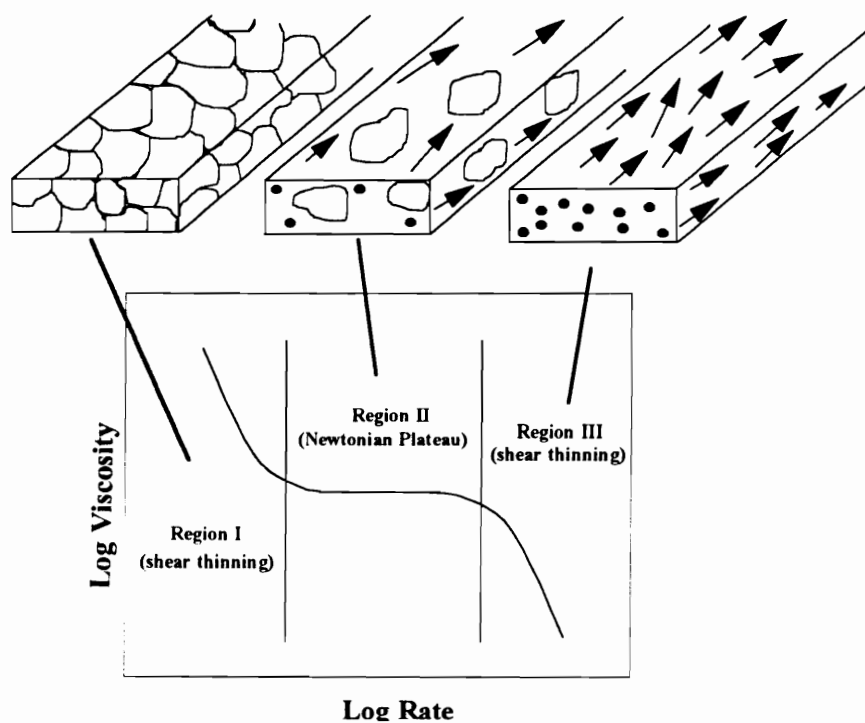


**Figure 2.1 Schematic of proposed three region flow curve [8].**

to a monodomain (region III shear thinning) as the shear rate is increased further. The existence of a three region flow curve believed by some to be general behavior for polymers displaying LCO is seen in only a select few LCPs while a preponderance of systems seem to be better described as displaying either region I or regions II and III behavior.

The general applicability of the three region flow curve to LCPs has been examined by Wissbrun [9], Viola [52], and Wilson [47]. Flow curves of several liquid crystalline polymers are shown in Figure 2.2. This figure shows that while some of these materials show three regions (curves 1,3 and 5) one shows only two (curve 6), and still others show only one region (curves 2,4 and 7). Additionally, those materials which show three regions often have only an inflection at the range in which the region II behavior is believed to exist. The three region flow curve has been widely used in the literature to describe the viscosity behavior of LCPs. While these results show what might be three regions in some LCPs, the number of others which do not show this behavior validates the conclusions of Wissbrun [9], Viola [52], and Wilson [47] that this behavior is not general to LCPs but is instead specific to the materials investigated.

#### **2.1.1.2 Yield Stress**

In the previous section flow curves which would indicate the presence of yield stresses in several LCPs were presented (e.g., shear thinning at low frequencies). If materials described by a three region flow curve and those in which the material is shear thinning at all rates tested are truly features of nematic and cholesteric LCPs, then LCO or a polydomain texture might be associated with this phenomenon. Indeed, yield stresses have been reported in solutions of collagen in dilute HCl [48], in aqueous solutions of wood and cotton cellulose [49], and in aqueous solutions of chitin [48].

The classical definition of a yield stress is a stress, below which, no unrecoverable

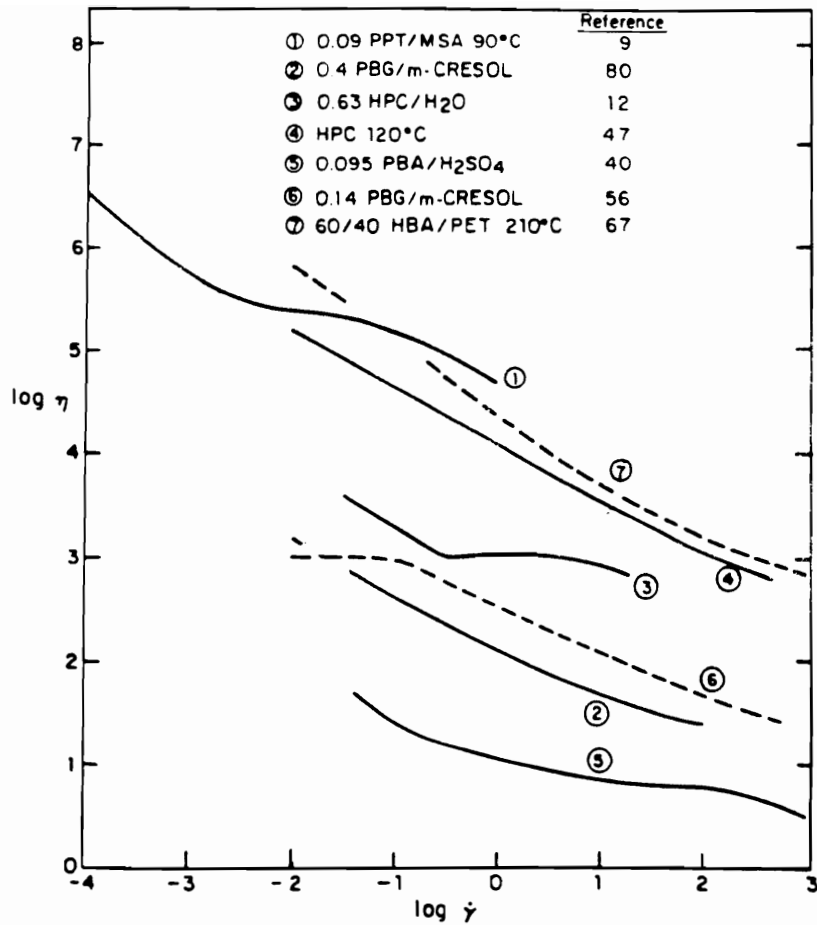


Figure 2.2 Viscosity vs. shear rate for various liquid crystal polymers [9].

(i.e., viscous) flow occurs. Although yield stresses have been reported for many materials, the nature or existence of yield stresses has been the subject of some controversy since by definition experimental proof is not possible (e.g., although no flow occurs below a yield stress within the time constraints of reasonable laboratory experiments, flow may occur at any stress given enough time). The controversy over the existence of a yield stress which has been documented in several recent articles (e.g., Barnes and Walters [53], Astarita [54], Schurtz [55,58], and Evans [56,57]), has at this time not been resolved. Therefore, in this work "apparent yield stresses", as proposed by Evans [57], will be used to describe shear thinning behavior at the lowest rates accessible to the investigator. This nomenclature then, inherently, does not rule out the existence of a zero shear viscosity at rates lower than those used in the various investigations.

Although yield stresses are often attributed to liquid crystalline order in polymers, many examples can be found where no yield stresses are reported. In some cases different investigators have come to different conclusions on the presence of a yield stress. One of the most often studied materials, lyotropic systems of PBLG in m-cresol, has been reported to show a yield stress in some cases while in other cases no yield stress is observed. This material which is cholesteric at rest and forms a nematic mesophase during flow [19], is considered a model system. Although studies have shown a zero shear viscosity for both racemic and optically active solutions of PBLG [19,20,24,59,60], another study on this system [14] has reported shear thinning behavior at rates as low as  $0.01 \text{ s}^{-1}$ . Lyotropic systems of poly(p-phenylene terephthalamide) PPTA in 100% Sulfuric acid have been studied by Baird [61,62] and Aoki [7] and similar solutions of poly(p-benzamine)(PBA) have been investigated Papkov [13]. These solutions, which form the nematic mesophase, are examples of the variety of results which have been observed. While Aoki, Papkov, and Baird have reported a yield stress, Baird has shown that the yield stresses can be eliminated

by preheating the material and careful exclusion of moisture. Hence, the yield stress may be due to small amounts of crystallinity or solid phase.

The existence of yield stresses has been reported in thermotropes such as HPC [15,16,17] and in HBA/PET systems at 260°C [9,18]. A conclusion that LCO in the HBA/PET systems is responsible for the observed yield stresses is questionable since in both studies the presence of residual crystallinity was reported. Additionally, in the investigation by Sugiyama [18], an extrapolation of the data to temperatures higher than 250°C is questionable based on the limited range of shear rates used. The HBA/PET copolyester was also studied by Gotsis and Baird [63] at 260 and 275°C. Their results indicate no yield stress based on the observation of a zero shear viscosity and stress relaxation to zero stress in stress relaxation experiments. Several other studies of liquid crystalline copolyesters have reported a zero shear viscosity in which the materials are believed to be absent of residual crystallinity [64-67].

While LCP systems do show yield stresses in some cases, it cannot be concluded that LCO can, in general, be related to the presence of yield stresses but instead in some cases may be associated with residual crystallinity. The studies discussed above do not provide information as to the differences in the polydomain texture associated with systems in which a yield stress is observed and those displaying a zero shear viscosity. This discussion would lead one to the conclusion that LCPs (both lyotropes and thermotropes) can not in general be described as exhibiting Region I (i.e., shear thinning at the lowest rates tested) behavior as proposed by Onagi and Asada.



### 2.1.1.3 Plateau Viscosity

Some of the earliest rheological data of LCPs involved the concentration dependence of viscosity in lyotropic systems. In these studies it was observed that when the Newtonian plateau viscosity was plotted against concentration, the viscosity increased with concentration to a maximum value at the isotropic anisotropic transition where upon with a further increase in concentration it began to decrease again (see Figure 2.3). This phenomenon can then be associated with the observation that the viscosity of LCPs can be lower than that of the corresponding isotropic state of the material. This behavior has been observed in solutions of PBA [12,68,69], PBLG [19], and PPTA [70] and is regarded as a general behavior for lyotropic liquid crystals [71]. The maximum in viscosity has also been shown to be shear rate dependent by Kiss [19] and Baird [70] shifting to lower concentrations as shear rate increases. In these studies the rate dependence was attributed to a shear induced decrease in the isotropic to anisotropic transition concentration. There is theoretical confirmation of this effect [72] which is based on the lattice theory of Flory and Ronca [73]. In agreement with the studies cited above, this theory shows that the effect of a shear field is to lower the concentration for the isotropic to anisotropic transition.

Thermotropic liquid crystal systems have also been observed to exhibit a maximum in viscosity in passing through the isotropic to anisotropic state. Studies of low molecular weight nematics have shown that as the temperature is raised the material goes through the nematic to isotropic transition and is accompanied by an increase in viscosity [74]. In a similar manner polymeric liquid crystals also show an increase in viscosity at the transition but the transition is much broader due to impurities and a distribution of molecular weights [70] (see Figure 2.4). In some cases the increase in viscosity due to the anisotropic to isotropic transition can be offset by the intrinsic decrease in viscosity with temperature.

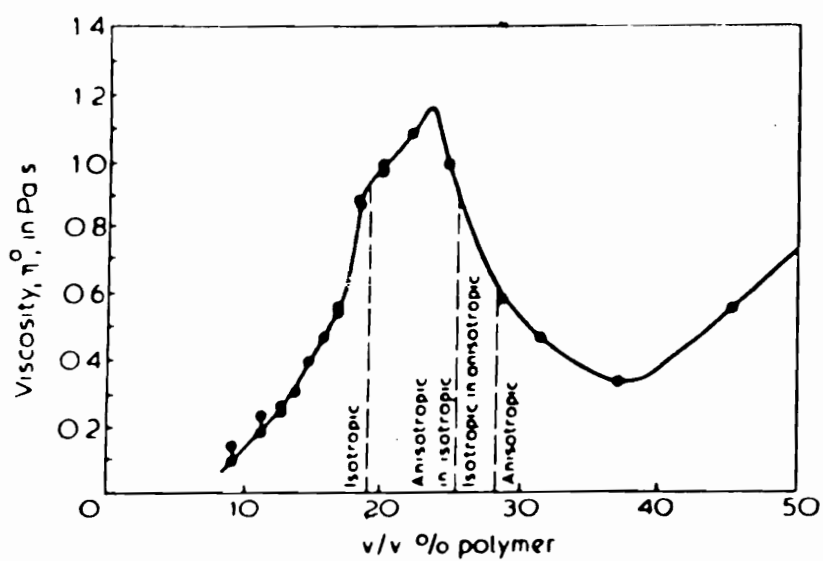


Figure 2.3 Viscosity vs. concentration for 50/50 copolymer of *n*-hexyl and *n*-propylisocyanate, molecular weight 41000, in toluene at 25°C [70].

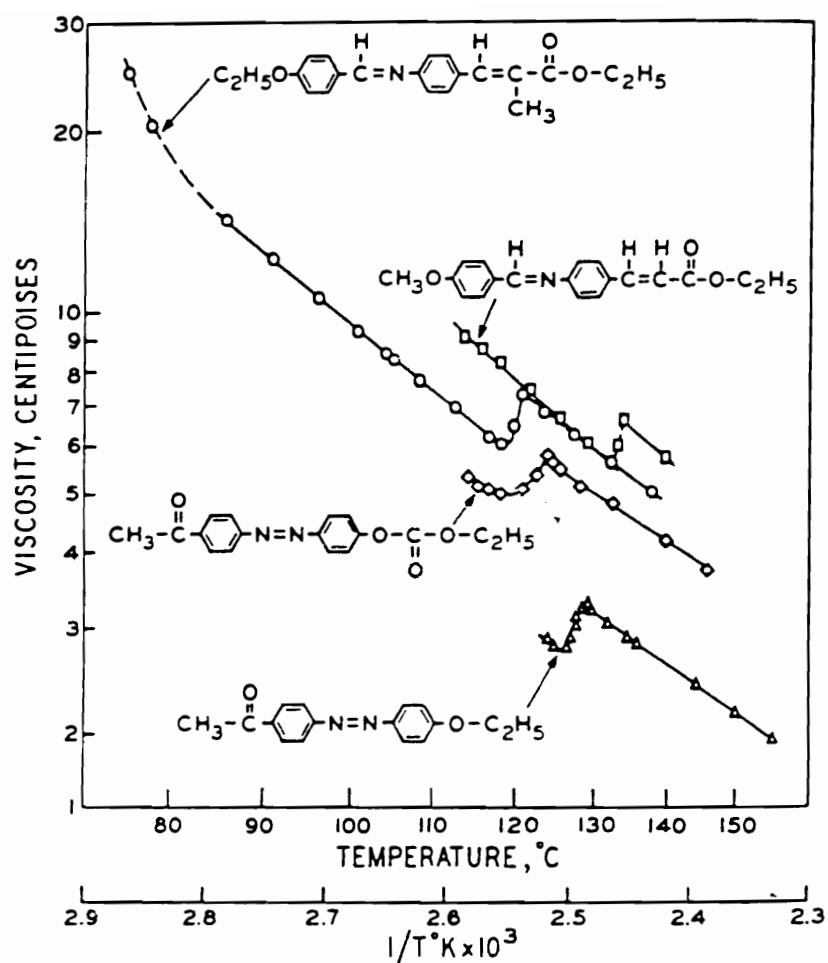


Figure 2.4 Viscosity jump at the isotropic-nematic transition [43].

Since both isotropic and nematic phases have viscosities which decrease with temperature, in some cases a maximum is not observed [75]. The viscosity of HPC was reported by Elliot [15] to decrease as the temperature was raised from 190 to 200°C and then increase as the temperature was increased further. Results of this nature have also been obtained in other studies [17,76,77,78], and have been shown to coincide with the anisotropic to isotropic phase transitions. Additionally, Fujiyama [77] showed that the shape of the viscosity versus temperature curve is rate dependent, with a small shift in the transitions to higher temperatures as the rate was increased. Similar results have been reported by several researchers [64,75,80-83] for several thermotropic copolyesters. In contrast, a study by Bickel [84] showed no increase in viscosity with temperature at the nematic to isotropic transition for a thermotropic copolyester. Instead, a distinct plateau was seen in the temperature versus viscosity curve, and it is possible that the increase in viscosity due to the nematic to isotropic transition was washed out by the decrease in viscosity of the individual phases.

In summary, a maximum in viscosity as a function of concentration or temperature in lyotropic and thermotropic LCPs, respectively, is often seen. The phenomenon that the viscosity of the nematic phase can be lower than that of the corresponding isotropic state in both lyotropic and thermotropic LCPs can be used to determine that a transition has occurred. The accuracy of this method in determining such a transition is of limited use since it may be affected by shear rate dependence, temperature dependence of the individual phases, and polymer dispersity. All of these variables must then be considered when using rheological data of this nature to determine that a transition has occurred.

#### 2.1.1.4 Onset of Shear Thinning

In those LCPs which have a Newtonian plateau, the point at which the transition to shear thinning behavior occurs is fundamentally of rheological interest as well as being an important aspect of their processing behavior. The point at which shear thinning begins provides information that is useful in determining the relaxation time of the polymer [49]. Comparison of the relaxation times for the material in its isotropic and anisotropic states can then be used to elucidate the contribution of liquid crystalline order in the material. Although this information is necessary for modeling the rheology of these systems, no conclusions can be made regarding the shear rate at which the onset of shear thinning in LCPs occurs due to the apparent contradictions in the published literature [9].

Using the information discussed in the previous section, a comparison of systems in which the isotropic and anisotropic phases have equal zero shear viscosities is facilitated. Perhaps the most useful data for comparison of isotropic to anisotropic viscosity behavior exists for lyotropic solutions of PBLG. Wissbrun [9] has compiled data obtained by various investigators working with the PBLG system (see Table 2.2). In this table the shear rate at which the viscosity has reached half of its zero shear value, or plateau ratio value for isotropic and anisotropic solutions, has been summarized. Examination of this data reveals that there is no general agreement on which phase shear thins first and no conclusion can be made for the PBLG systems.

Other studies on PBLG in m-cresol and dichloroacetic acid (DCA) were made by Yang [85,86] in which it was found that the onset of shear thinning for m-cresol solutions occurred at a rate of approximately  $150 \text{ s}^{-1}$  in general agreement with Miller [87] and Izuka [88], while the DCA solutions were Newtonian over nearly the entire range of rates tested. In m-cresol the PBLG molecule exists as a helix, while in DCA the PBLG molecule exists as a random coil (i.e., forms an isotropic solution).

**Table 2.2 Onset of Shear Rate Dependence of Viscosity of PBLG [9].**

Solvent	Form <sup>a</sup>	Concentration (wt %)	Viscosity (poise)	$\dot{\gamma}_{1/2}$ (s <sup>-1</sup> )	Ref.
<i>m</i> -Cresol	I	6	25	100	Kiss and Porter <sup>63</sup>
	C	16	20	1000	
<i>m</i> -Cresol	I	6	4	>500	Aoki, White, and Fellers <sup>64</sup>
	C	10	25	>500	
	C	16	15	>500	
Dioxane	I	4	25	>200	Iizuka <sup>62</sup>
	I	7	150	100	
	C	13	30	100	
CH <sub>2</sub> Br <sub>2</sub>	I	7	16	>200	
	N + I	10	5	150	
	N	13	6	150	

<sup>a</sup> I → isotropic, C → cholesteric, N → nematic, N + I → biphasic.

A comparison of the isotropic and anisotropic viscosity behavior of PPTA solutions also reveal that no general conclusion exists as to the onset of shear thinning behavior in anisotropic versus isotropic solutions. First, Baird [70] found that in isotropic and anisotropic solutions of PPTA in 100%  $\text{H}_2\text{SO}_4$  at  $60^\circ\text{C}$  with the same zero shear viscosities, the anisotropic solution shear thinned first. In a similar study Wong and Berry [89] also found that the anisotropic solution shear-thinned at lower rates than the isotropic solution. On the other hand, Aoki and co-workers who also studied PPTA solutions, found results which conflicted with those of Baird. In their study, which covered a different range of shear rates, no appreciable shear thinning was observed for the anisotropic solution.

Comparison of the viscosity behavior of thermotropic polymers in their isotropic and anisotropic states is limited do to the fact that most thermotropic polymers degrade before the liquid crystal-isotropic transition occurs. The most extensive work on thermotropic systems has been done with the HBA/PET copolymer system [80,90-92]. Although in this system a direct comparison between the isotropic and anisotropic state is not possible, HBA/PET copolymers are reported to exhibit lower values of viscosity and are more shear thinning than the PET homopolymer. Wissbrun [9] and Jackson [92] found that the relaxation times for the 60HBA/PET copolyester were 1000 times greater than that of the PET homopolymer.

In order facilitate a study of the viscosity behavior of a thermotrope in its isotropic and anisotropic states TLCPs can be modified to reduce the nematic to isotropic transition temperature. In one case Wissbrun and Griffin [80] used a copolyester which was modified with aliphatic spacing groups to lower the liquid crystal-isotropic transition temperature. In the isotropic state at  $240^\circ\text{C}$  the viscosity behavior of this copolyester was found to be Newtonian up to the highest rate measured which was  $100\text{ s}^{-1}$ . This copolyester in its anisotropic state at  $210^\circ\text{C}$  was found to be shear thinning at all rates tested. These results

are in question due to the observation of a yield stress which might indicate the presence of residual crystallinity.

In another study using a different copolyester with a crystal to nematic transition at 240°C and a nematic to isotropic transition at 270°C, Tuttle et al. [64] found similar results to those observed above. The nematic state was shown to shear thin while the isotropic state was found to be mostly Newtonian over the rates measured. Blumstein and coworkers [82] compared the viscosity behavior of the nematic and isotropic states of a segmented copolyester. For measurements of viscosity over rates ranging from 2 to 200 s<sup>-1</sup> it was found that both the nematic and isotropic melts were shear thinning while the nematic state proved more shear thinning. In general one can conclude from these investigations that the existence of liquid crystalline order in thermotropic systems is related to shear thinning behavior at lower shear rates and to a greater extent than the same materials in their isotropic state.

Although the factors determining the shear thinning behavior of LCPs have not been established to any degree at this time, they are intuitively related to the characteristics of each system investigated. These characteristics might include, but are not limited to, such variables such as molecular weight, molecular weight distribution, and chain stiffness. A study of a well fractionated thermotropic polyester by Blumstein [82] showed that the polydisperse samples were more shear thinning than the fractionated samples.

In summary, while the viscosity behavior of both lyotropic and thermotropic polymers have been studied extensively, many aspects of their behavior cannot be labeled as general to LCPs. The three region flow curve as proposed by Onogi and Asada has been widely used to describe the viscous behavior of LCPs but does not adequately describe the behavior seen in most systems containing liquid crystalline order. Many LCPs have been shown to exhibit yield stresses, but association of this phenomenon to systems containing



liquid crystalline order is hampered by the fact that this behavior is also associated with the presence of crystalline solids. The liquid crystalline state is associated with a lower viscosity than the corresponding isotropic state. There does not seem to be any clear conclusion as to the onset of shear thinning behavior in the anisotropic versus isotropic states. However, there is some evidence in thermotropic systems that the anisotropic phase shear thins at lower rates than the isotropic phase. Contrary evidence in lyotropic systems does not allow for a definitive conclusion to their shear thinning behavior.

### **2.1.2 Normal Stress Behavior**

The importance of the first normal stress difference ( $N_1$ ) as a rheological property related to the elastic nature of viscoelastic materials was briefly discussed in the introduction. In the study of LCPs the behavior of the first normal stress difference has proven to display behavior not seen in isotropic polymers. In this section the steady state normal stress behavior of LCPs is reviewed. To facilitate a review of the literature on first normal stress difference behavior, the sign convention used in this section will be opposite of that used in Chapter 1 Eq. 1.8 (i.e., in this section a negative first normal stress difference corresponds to a positive first normal stress difference by the sign convention used in Chapter 1).

In addition to the viscosity behavior reviewed above, many of the same investigations have examined the normal stress behavior of PPTA and PBLG solutions. These investigations have found the same concentration dependence of  $N_1$  as was observed for the viscosity (i.e., a maximum is seen when  $N_1$  is plotted against concentration as shown in Fig. 2.5. [7,19,70]. Using solutions of PPTA in 100%  $H_2SO_4$  Baird [70] found that  $N_1$  was the same for the solutions in both their isotropic and anisotropic states. In

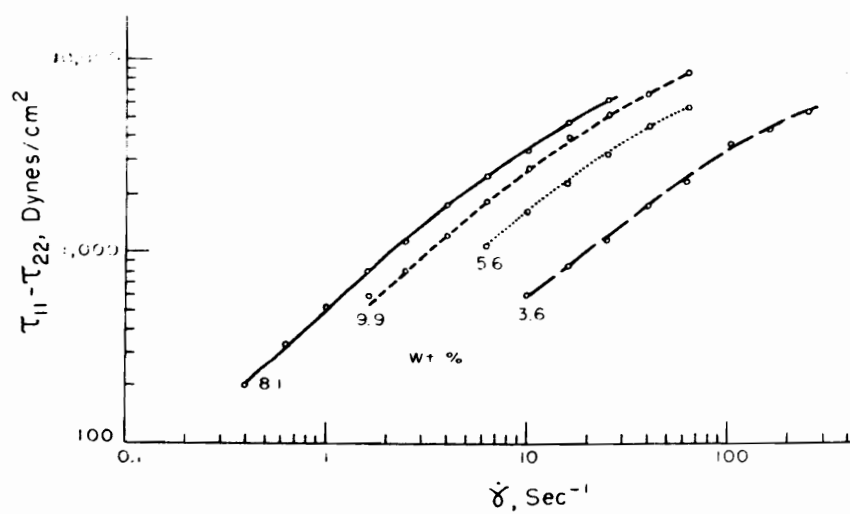


**Figure 2.5** First normal-stress difference versus shear rate for isotropic solutions of PBG in m-cresol [19].

contrast to these results, Aoki et. al. [7] found that  $N_1$  was an order of magnitude greater for anisotropic than isotropic solutions of PPTA. Two explanations for this discrepancy are that the shear rates used in each study covered different ranges and that Aoki did not take care to use 100%  $H_2SO_4$  so that coagulation of the PPTA solution was possible.

Another phenomenon reported for some LCPs like PBLG [19,94] and HPC [26] is the existence of a negative steady state first normal stress difference (see Figure 2.6). Kiss and Porter [19,94] reported negative values of  $N_1$  for steady state shear flow over well defined shear rate ranges for solutions that were anisotropic. Similar results were obtained in studies by Mewis and Moldenaers [59] for PBLG systems in which they also showed that the data could be normalized to compensate for the effect of temperature. Explanations for this behavior were not given in these investigations but Kiss and Porter succeeded in ruling out the possibility of secondary flow effects. In another study by Iizuka [88] negative values of  $N_1$  were reported but without explanation were attributed to surface tension.

In aqueous solutions of HPC, the appearance of negative steady state  $N_1$  values at intermediate shear rates has been reported by Grizzuti et al. [26]. In another study on the same material by Ernst and Navard [95], positive  $N_1$  values have been reported for all rates measured. In order to explain these discrepancies Grizzuti and co-workers listed several considerations. The first consideration was that the materials were obtained from different suppliers. Secondly a mercury sealing technique was used by Grizzuti and co-workers to protect the sample from drying and was not used in the work by Ernst and Navard. Finally, due to sensitivity limits of the normal force transducer values of less than 100 Pa as measured by Ernst and Navard could not be considered reliable.

Thermotropic systems have also been reported to show negative values of  $N_1$ . In studies by Wissbrun [96], Gotsis [97], and Baird et al. [98] transient negative values of  $N_1$  have been reported for the 60HBA/PET copolyester. Additionally, Gotsis [99] also

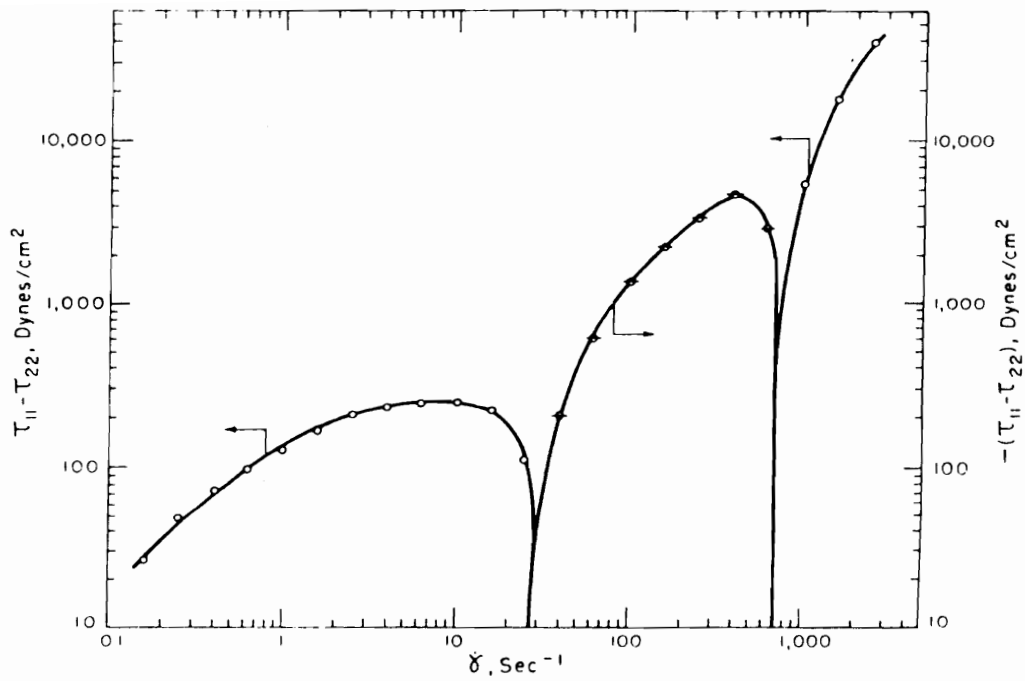


Figure 2.6 The primary normal stress difference vs. the shear rate [19].

reported negative values of  $N_1$  over defined shear rates and temperatures for the 80HBA/PET copolyester. In this investigation explanations for the negative values of  $N_1$  included the existence of a suspension of crystalline material in the mesophase, texture development in the mesophase, boundary layer effects, and changes in density due to shear induced crystallization. The 80HBA/PET copolyester has been shown to contain residual crystallinity at temperatures within the range in which negative values of  $N_1$  were reported [99].

Several theories which provide evidence for the existence of negative values of  $N_1$  have been proposed. It has been shown by Ogagawa, Cox, and Mason [100] that monodisperse suspensions of rigid spheroids at low concentrations in a Newtonian solvent could exhibit negative  $N_1$  values during steady shear flow. Using the continuum theories of Leslie [101] and Ericksen [102], Currie [103] has shown that negative values of  $N_1$  can be predicted in shear flow for the case where the molecules are oriented in the flow direction and for a range of orientation conditions at the fluid boundary. Another theoretical model has been proposed by Chaffey and Porter [104] in which negative values of  $N_1$  can exist due to a tendency for perfect molecular alignment, which creates a compressive force during steady flow.

Using a 2-dimensional analog of the molecular theory of Doi [44], Marrucci and Maffettone [105] and Larson [106] have explained the existence of negative values of  $N_1$ . In these papers negative values of  $N_1$  are generated in a 2-dimensional system of rodlike molecules when the action of shear flow is to broaden the orientation distribution from the equilibrium value in the fluid at rest. This was shown to occur at low shear rates and when the intermolecular potential is large, resulting in a narrow distribution of orientations in the systems at equilibrium. At low shear rates the rotational nature of the shear flow then causes tumbling of domains of rods. When the shear rate is increased, the viscous forces

overcome the elastic forces due to a spread in the orientation distribution and the value of  $N_1$  then becomes positive. Rheo-optical results support the picture of tumbling domains through a low degree of macroscopic molecular orientation. This theory also predicts the existence of positive values of  $N_1$  at very low shear rates in the systems in which the negative values of  $N_1$  are seen at intermediate shear rates.

Although theories which attempt to describe the existence of negative values of  $N_1$  seem applicable, it must be noted that the basis for these results are conflicting. The Leslie-Ericksen theory predicts negative  $N_1$  values when the molecules take on a stable flow induced alignment, while the theory as proposed by Marrucci and Maffettone predicts negative values of  $N_1$  only when there is large scale tumbling of the domains. While there is some rheo-optical evidence supporting the phenomenon of large scale tumbling of domains, both theories are also unable to simultaneously predict the correct viscosity and  $N_1$  behavior for these LCPs. Thus, while individual aspects of the rheological behavior are predicted by these theories, their inadequacy in other areas of rheological behavior leaves some doubt as to their correctness.

Negative values of  $N_1$  have not only been reported for systems thought to be liquid crystalline but also for block copolymers and concentrated suspensions. Other systems which have been reported to exhibit transient negative  $N_1$  values include lecithin in dodecane [107], lubric grease [108], and styrene-butadiene-styrene block copolymers, and concentrated suspensions of high density polyethylene in a thermoset polyester resin [109].

In summary, the existence of negative values of  $N_1$  has been associated with LCO in some systems, in others it may be associated with the presence of residual crystallinity. Although, the theoretical basis for the existence of negative values of  $N_1$  in systems containing LCO is described by two theories, limitations of these theories in other aspects of their rheology raises some doubt as to their applicability. Finally, negative values of  $N_1$

cannot be considered a general feature in LCPs but one that is specific to the system studied.

### 2.1.3 Comparison of Steady State and Dynamic Behavior

Dynamic mechanical measurements provide a sensitive means to probe the behavior of materials in their undeformed state and allow the investigator to examine the structure found in the material at equilibrium. This is accomplished by using very small strain levels thereby minimizing the effects due to orientations, disentanglement of molecules, or thixotropic breakdown. Additionally, angular frequencies higher than the corresponding shear rates used in steady shearing tests can often be obtained [56]. A comparison of the dynamic and steady shear behavior (where the material being tested is subjected to large total strains) can give information about the structural changes which occur in the material. These results give insight into the flow mechanisms and can also be used to test constitutive equations.

Relationships between dynamic and steady shear quantities have been developed [72], which are stated as follows:

$$\eta(\dot{\gamma}) \approx \eta^*(\omega) \quad \text{for} \quad \dot{\gamma} = \omega \quad \dot{\gamma} \rightarrow 0 \quad (2.1)$$

$$N \approx 2G' \quad (2.2)$$

where  $\eta$  is the steady shear viscosity,  $\eta^*$  is dynamic viscosity,  $\dot{\gamma}$  is the shear rate,  $\omega$  is the frequency, and  $G'$  is the storage modulus. This relationship in Eq. 2.1, called the Cox-Merz rule, and Eq. 2.2 have been shown to generally apply to isotropic solutions and melts of flexible-chain polymers [49,50]. The applicability of these relationships at low

deformation rates has been confirmed by Baird [61] and Wissbrun [80] using isotropic solutions of PPTA/H<sub>2</sub>SO<sub>4</sub> and isotropic and anisotropic copolyester melts, respectively.

Comparisons of the steady state and dynamic behavior have been the focus of several investigations and a tabulation of some of their results can be seen in Table 2.3. It can be seen in this table that  $\eta$  and  $\eta^*$  are generally similar in magnitude for the systems examined. Similar results were found by Baird [110] who reported good agreement between  $N_1$  and  $2G'$  at low rates for the HBA/PET copolyester at 275°C, and  $\eta < \eta^*$  at high rates. Yanase and Asada [14] reported similar results where  $\eta$  and  $\eta^*$  are nearly equal for anisotropic solutions of PBLG. In a study also using an anisotropic solution of PBLG, Moldenaers [20] found that  $\eta > \eta^*$  conflicting with the results reported by Yanase and Asada. In another investigation by Suto [17] of anisotropic melts of HPC  $\eta$  and  $\eta^*$  were found to be qualitatively similar but  $\eta^*$  was an order of magnitude higher.

Comparisons of  $N_1$  and  $2G'$  in the literature have shown a wide range of results. In anisotropic solutions of PPTA at 60°C, Baird [62] found good agreement, while Aoki [7] found  $N_1 > 2G'$  at the same temperature. However, in measurements at 25°C Aoki also found good agreement between  $N_1$  and  $2G'$ . In work published by Kiss and Porter [19] on the PBLG system they report  $N_1 > 2G'$  at all shear rates which was later confirmed by Mewis and Moldenaers [59]. Conflicting results have also been observed for the 60HBA/PET system. While Baird [110] reports good agreement between  $N_1$  and  $2G'$  at 275°C (above the highest crystalline melting point as determined by DSC), Wissbrun reports that for the same system  $N_1$  is greater than  $2G'$  by a factor of 5 to 100 at all temperatures tested.

Despite the many experimental investigations comparing the steady shear to dynamic properties of LCPs, few theoretical predictions have been proposed. A general



**Table 2.3 Steady Shear versus Dynamic Properties [9].**

				Ref.
PPT (60°C)		$\eta(\dot{\gamma}) \approx \eta^*(\omega)$	$N_1(\dot{\gamma}) \approx 2G'(\omega)$	Baird <sup>65</sup>
		$\eta \approx \eta^*$	$N_1 \gg 2G'$	Aoki et al. <sup>64</sup>
	(25°C)	$\eta^* \gg \eta$	$N_1 \approx 2G'$	Aoki et al. <sup>64</sup>
PBLG		$\eta \approx \eta^*$	$N_1 > 2G'$	Kiss and Porter <sup>56,63</sup>
Thermotropic Polyesters	High temp.	$\eta \approx \eta^*$	$N_1 > 2G'$	Wissbrun <sup>67</sup>
	Low temp.	$\eta^* > \eta$	$N_1 > 2G'$	

phenomenological equation using the Doi theory has been given by Larson and Mead [111] to predict the viscoelasticity of a nematic fluid based on the assumption of a monodomain system in small amplitude deformation. Their equations predict that the properties or rheological quantities  $G'$ ,  $G''$ , and  $\eta^*$  depend on the orientation of the director, and at certain orientations the director just "wags" or oscillates in phase with the deformation and results in zero values for the linear viscoelastic properties.

Using the same theory, Larson and Mead [111] also made predictions for a polydomain system using two different mathematical methods of averaging the contributions from different domains. The first case uses a Voigt average so that all of the domains undergo a similar strain history. This then results in a stress which is the sum of the stress contributions of all possible director orientations. The result is then the upper limit of stress response, with  $G'$  proportional to  $\omega^2$  and  $G''$  proportional to  $\omega$  at low frequencies. This prediction is in contrast to experimental studies on 60HBA/PET by Gotsis and Baird [60,89] where it was shown that  $G'$  is proportional to  $\omega$  at low rates. At low shear rates the Doi theory for a monodomain predicts that  $N_1$  is directly proportional to the shear rate [45]. In the second averaging scheme, which is a Reuss average, proposed by Larson and Mead, each domain is subjected to the same shear stress. In this scheme the system stress is controlled by the lowest modulus layer. This model then predicts the shear modulus to be zero at all rates since certain layers will be at orientations for which there is zero shear stress. This theory is shown to predict failure of the Cox-Merz rule for liquid crystalline systems.

In an attempt to account for the polydomain texture, Burghardt [113] has predicted the response of a nematic liquid crystal to oscillating shear flow using the continuum formulation of Leslie and Ericksen. In his work, Burghardt, neglecting fluid inertia, reported that the influence of the distortional elastic effects are important and at both low

and high frequencies viscous forces dominate. At low frequencies the director rotates in phase with the shear rate while, at high shear rates, the director rotates in phase with the applied shear strain and at intermediate rates the distortional elastic effects lead to viscoelastic behavior in the macroscopic response. This theory predicted that  $G'$  was proportional to  $\omega^2$ , and the value of  $G''$  was proportional to  $\omega$  at low frequencies. The dynamic viscosity  $\eta^*$  was found to equal the steady shear viscosity  $\eta$  at low rates but begins to deviate from steady shear values at higher rates. Although qualitative agreement is seen in the viscosity behavior predicted and experimental results, the elastic contributions to the stress would more likely be significant at low rates, where viscous stress is relatively weak. Additionally, the dependence of  $G'$  on  $\omega$  disagrees with that seen experimentally as discussed above which leads to the conclusion that the Leslie-Ericksen theory in the present form can not predict the viscoelastic behavior of LCPs.

In summary, good agreement between  $\eta$  and  $\eta^*$  at low shear rates is often seen in liquid crystalline polymers. At the same time  $N_1$  and  $2G'$  are seen to sometimes show agreement while in other cases no general agreement is seen. Although the Cox-Merz rule is seen to hold for some LCP systems it does not, in general, hold for these materials and no analogous theoretical relationship has been proposed which is successful in describing the relationship between steady shear and dynamic shear flow. It is possible that such a relationship is not possible due to the differences in the polydomain texture and the sensitivity of this texture to the large differences in strain in steady shear versus small amplitude dynamic shear flow [114].

#### 2.1.4 Shear History and Transient Behavior

The effects of deformation on the texture of LCPs has been demonstrated in the previous section where the steady shear and small amplitude dynamic rheological properties have been shown to be different in many cases. In transient experiments the development of structure which includes the effects of orientation on individual molecules as well as the macroscopic changes in the polydomain texture found in LCPs can be studied.

The effects of previous shear history on the rheological behavior of both thermotropic and lyotropic liquid crystalline polymers has been shown by numerous investigators [20,23,24,64,80,110,115]. Some of the effects due to the application of a pre-shear history include a decrease in viscosity, hysteresis during frequency sweeps of dynamic tests, and secondary stress overshoots upon startup of steady shear flow. This section will review these phenomena and the explanations for their occurrence.

In an investigation by Wissbrun and Griffin [80] the pre-shear history effects on a thermotropic polyester with solid-nematic and nematic-isotropic transition temperatures of 185°C and 212°C, respectively, have been studied. While testing in the nematic state at 210°C they found that the dynamic viscosity  $\eta^*$  and storage modulus  $G'$  were reduced by shearing the sample prior to the tests (see Figure 2.7) and the dynamic viscosity was seen to be reduced more with an increase in the prior shear rate. Additionally, a hysteresis was observed in the dynamic viscosity, (i.e., the viscosity varied depending on the direction of the frequency sweep). Prior to the aforementioned investigation, Wissbrun [93] also reported hysteresis for an anisotropic melt of a copolyester, which at temperatures in which it was isotropic, did not show shear history effects or hysteresis. A decrease in the complex modulus was reported in a similar study by Tuttle [64]. This result has been explained by Wissbrun and Griffin [80] as being due to the change in the polydomain

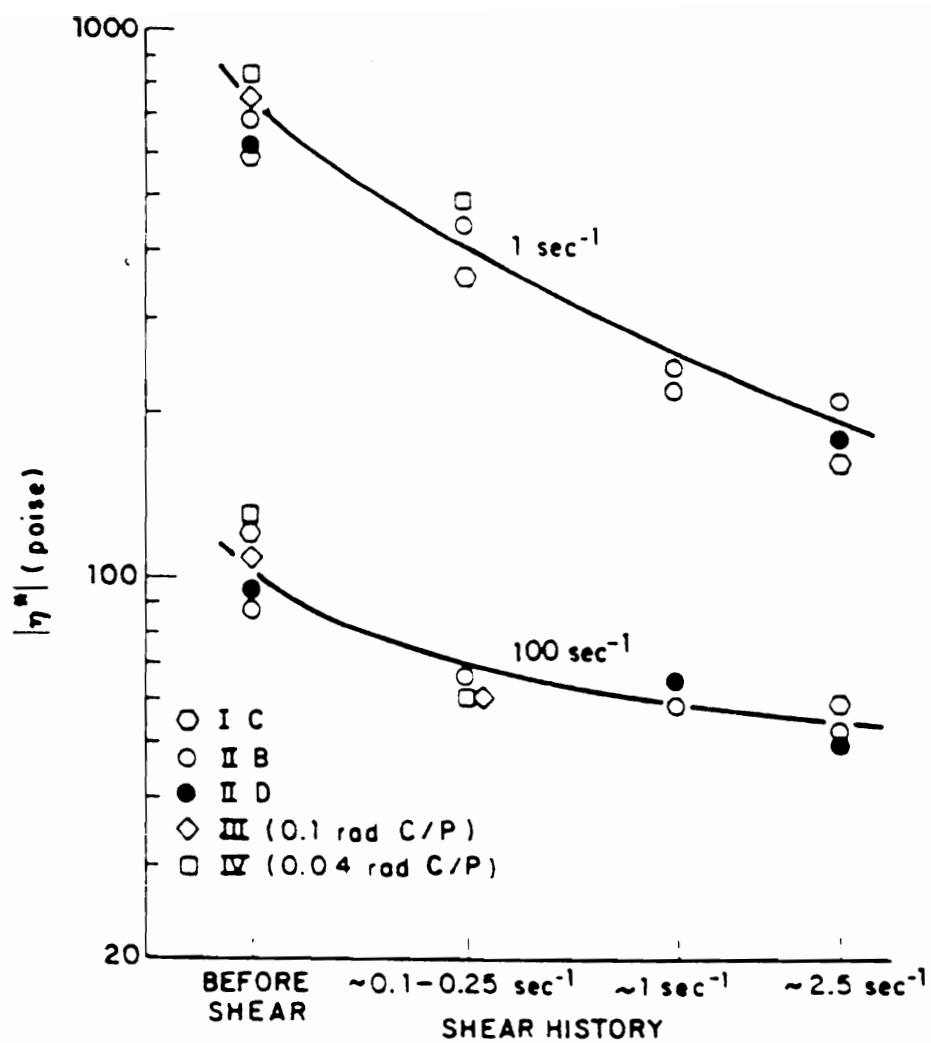


Figure 2.7 Effect of preshear on the dynamic viscosity of a thermotropic LCP [80].

texture of the melt with shear and the relaxation of this texture. The presence of residual crystallinity at the test temperature was ruled out by Griffin [116] using DSC data.

To quantitatively measure the effects of pre-shear history on viscosity for various materials Cogswell [115] used a capillary rheometer, modified with a rotating cylindrical bob inside the barrel. The materials investigated included a 20 wt. % solution of PPTA in  $\text{H}_2\text{SO}_4$  at  $85^\circ\text{C}$  and a thermotropic copolyester. The PPTA solution became paste-like with a yield stress of  $10^5$  dyne/cm<sup>2</sup> after standing for 16 hours. However, upon subsequent shearing a low viscosity state was reformed. With no pre-shearing, extrusion of the thermotropic copolyester below its melting temperature formed an inextensible paste-like extrudate. Pre-shearing this material resulted in a uniform highly oriented extrudate. Investigating the possibility that this was being caused by viscous heating it was found that the a temperature  $20^\circ\text{C}$  higher was required for the same ease of extrusion and orientation. An explanation for the paste-like textures observed for both of the samples discussed here was attributed to the formation of crystallinity which was then broken up upon application of the shear.

In an effort to produce reproducible results for oscillatory shear flow of aqueous solutions of HPC, Grizzuti and co-workers [26] carefully examined the effects of deformation history. It was found that after cessation of steady shear the dynamic viscosity, which increased with time, took on the order of 2 hours to reach an equilibrium value. Additionally, the effects of using two different pre-shear rates was investigated. It was found by observing the evolution of the dynamic viscosity over time that while the characteristic time did not change with prior shear rate, the initial dynamic viscosity decreased with increasing the prior shear rate, and the final equilibrium dynamic viscosity increased with an increase in the prior shear rate.

Lyotropic solutions of PBLG have also been investigated by Moldenaers and Mewis

[20]. In contrast to the results described above, a decrease in  $\eta^*$  was observed with time after cessation of steady shearing flow. Additionally, the time it took for  $\eta^*$  to reach a steady state value was 1 to 2 orders of magnitude greater than the time for stress relaxation upon cessation of steady flow, and was found to be independent of temperature, strain amplitude, and frequency. While Moldenaers and Mewis concluded that this behavior was due to structural changes in the material and was general for liquid crystalline polymers, the results cited above for thermotropic polymers show this generalization to be in error. It was also noted by Wissbrun [80], that the reformation of the equilibrium polydomain structure would result in an increase in viscosity.

The development of orientation and structure have been studied by examining the transient rheological behavior of several LCPs. Stress growth experiments have been performed on lyotropic solutions of PBLG and HPC. In studies of PBLG solutions Mewis and Moldenaers [80] found 3 overshoot peaks. The appearance of multiple overshoots has been reported in the literature by several investigators (see Figure 2.8) [24-26,117]. In an investigation by Grizzuti et al. [26] the transient response following start up of steady shear is described by a large initial peak, followed by a sequence of damped oscillations until the steady state value is reached. The authors determined that these oscillations, which were observed at all shear rates measured, are not an instrumental artifact, and they also stated that the oscillations are not observed in an isotropic solution of HPC. A similar response in the transient behavior of  $N_1$  was also observed (see Figure 2.8). These results are in disagreement with similar data obtained in start-up experiments by Doppert and Picken [25], as well as in step-up experiments by Mewis and Moldenaers [24], where a shear rate independent wavelength of the oscillations was found. Grizzuti et al. [26] attributed these discrepancies to the range of shear rates investigated and that in HPC solutions no Newtonian plateau is observed. They also explain these transients as being

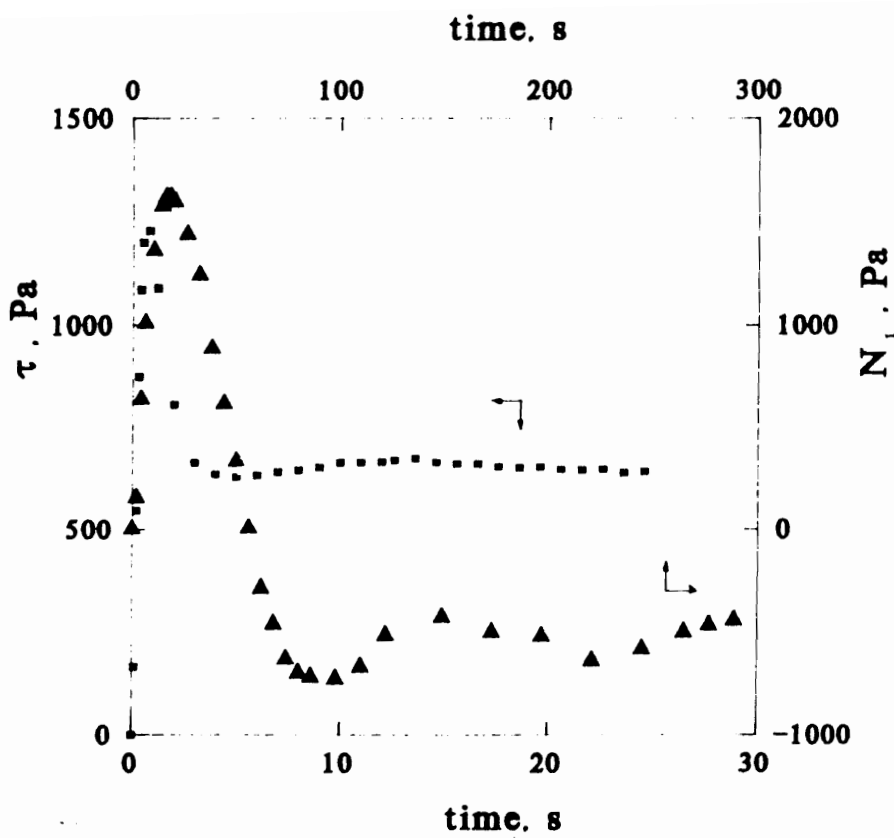


Figure 2.8 Start-up of shear flow. Shear rate  $\dot{\gamma} = 5 \text{ s}^{-1}$ . (■) shear stress; (▲) first normal stress difference [26].



due to a modification of the polydomain structure which upon cessation of flow, recovery is governed by the action of an elastic force (Frank elasticity) , which tends to restore the original situation, and a viscous force, which resists the process.

In the case of thermotropic systems Viola and Baird [23,52] studied the stress growth and relaxation behavior of the 60/40 and 80/20 HBA/PET copolyesters. The 60HBA/PET copolyester was tested at temperatures of 250, 260, and 275°C where overshoots were observed at all rates measured. These overshoots increased in magnitude with an increase in rate but all overshoots occurred at approximately the same total strains. At temperatures of 250°C, two overshoots were observed, the first occurring at 1-2 strain units and the second at 50-60 strain units. An explanation for this behavior was given by Baird [110] in which he attributed the first peak to the development of orientation of the domain structure, and the second peak to the two phase nature of this system. Figure 2.9 shows the relaxation of structure monitored using interrupted stress growth tests. Recovery of the second peak is shown to occur within 6 seconds while the first peak is shown not to have recovered even after 3 minutes. Also, the first peak was absent upon reversal of the shear direction. The stress was shown to relax to zero in just a few seconds using stress relaxation experiments. These results indicated that the time scales for the relaxation of orientation and texture are much greater than those for stress. Similar results were obtained for the 80HBA/PET copolyester but at different temperatures.

The effect of preshear on the transient stress behavior of a thermotropic copolyester was also studied by Cogswell [115] and Kim and Denn [218]. In the study by Cogswell, the melt was sheared until steady state was reached and then allowed to relax until a specified stress was reached before starting the second shear at the same rate. It was shown that the stress rose to its equilibrium value almost immediately. When the sample was presheared at a higher rate prior to the routine described above, the stress exhibited a large

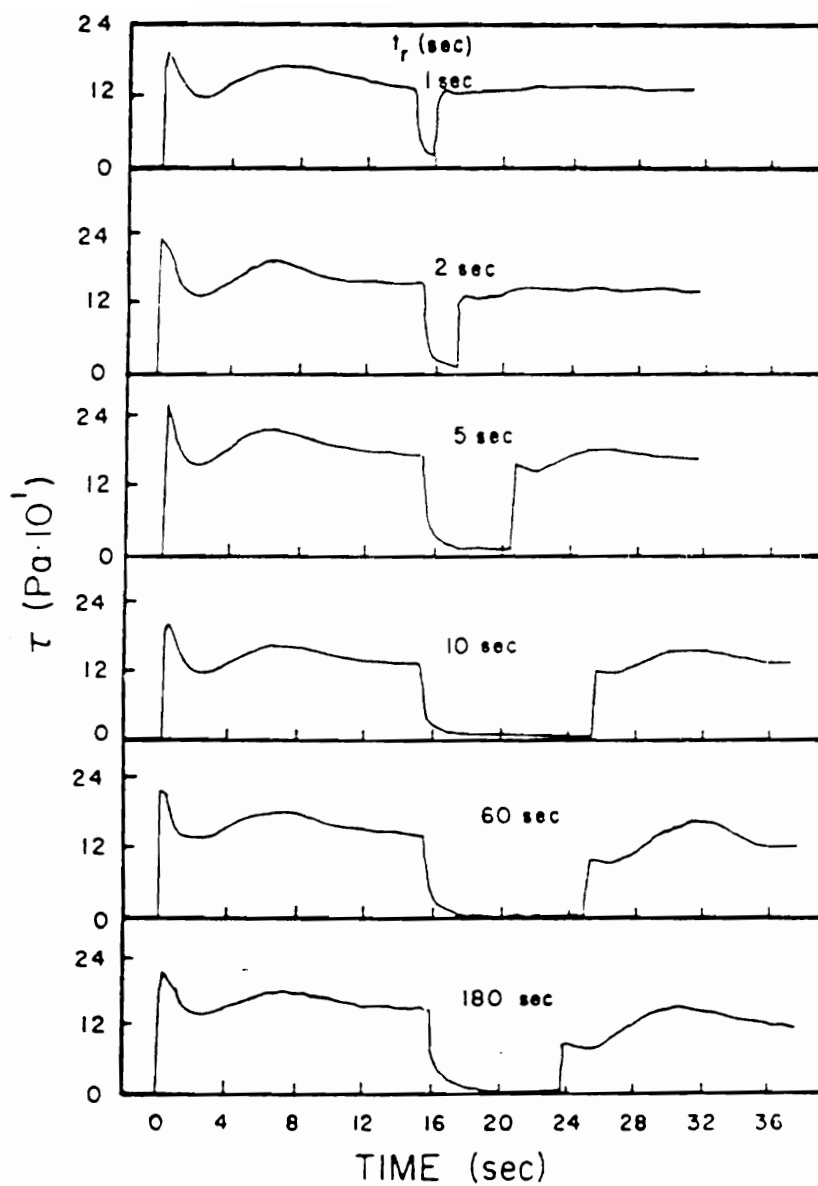


Figure 2.9 The effect of varying the relaxation time  $t_r$  for interrupted stress growth of 60HBA/PET at 275°C and  $\dot{\gamma} = 10 \text{ s}^{-1}$  [110].

overshoot before reaching its equilibrium value. This behavior was attributed to the reorganization of texture. It was proposed that upon shearing the domain structure which exists in the quiescent state is broken up into smaller domains and upon increasing the shear rate the domains are eventually completely broken up. Cogswell explained that the relaxation to an equilibrium domain structure was fast enough after shearing at higher rates that the structure had to be broken up again resulting in a large overshoot peak. A faster relaxation time with an increase in the shear rate is confirmed in the transient experiments of Baird [110] and Viola and Baird [23].

The changes of orientation and polydomain texture during flow are believed to cause the unusual oscillatory behavior sometimes seen in transient experiments. The oscillatory behavior seen during the start up of steady shear is believed to exist in materials which contain anisotropic inclusions whenever convective flow effects dominate rotational Brownian motion [119]. Recently, Grizzuti *et al.* [26] described the phenomenon as the modification of the polydomain structure from an equilibrium condition to one where the domains are changed in size, and the director describing each domain is orienting due to the flow field. The recovery of the structure is governed by the action of an elastic force which tries to recover to the equilibrium condition and a viscous force which resists this process. These competing mechanisms are believed to produce a series of damped oscillations.

In summary, the existence of dramatic pre-shear history effects on dynamic and transient experiments can be attributed to the liquid crystalline order found in LCPs. While the effect of pre-shearing is often seen to reduce the viscosity of the material, the opposite effect has also been seen. In transient experiments, multiple overshoots are often seen, while in isotropic materials only one overshoot is observed. The magnitude of the overshoots has been shown to be dependent on the pre-shear history of the material. While the transient phenomenon are usually explained in terms of the development of orientation

and structure of the polydomain texture of LCPs, theories have been unable to predict all of the rheological phenomena observed.

## **2.2 Rheology of Polymer Blends**

In this section will be reviewed the rheology of a textured fluid consisting of binary mixtures of polymers. As was illustrated in Fig. 1.1, the structure formed by the polymer phases is analogous to the structure formed by polydomain LCPs discussed in the previous section. Additionally, as with polydomain LCPs, the development of texture during flow of polymer blends results in rheology which is not seen in either neat blend constituent. The rheology of polymer blends will be divided into two subsections. The first section will deal with blends consisting of mixtures of two immiscible flexible chain polymers. In the second section the rheology of blends in which one of the components is a liquid crystalline polymer is reviewed. It will be indicated in this section that there is a lack of experimental data on these systems. Studies have predominantly included only the steady shear properties of blends as a function of concentration and temperature while other aspects of their rheology such as transient behavior have been largely ignored.

### **2.2.1 Blends of Isotropic Polymers**

The rheological behavior of polymer blends show a number of peculiarities that have not been explained at this time. This section will give an overview of some of the behaviors observed in polymer blends and attempts to explain this behavior. The rheological behavior of polymer blends results in a viscosity which relative to the mean of the blend components can be: 1) lower (negative deviation); 2) higher (positive deviation);

and 3) higher and lower (positive-negative deviation) depending on shear stress or rate. Tabulation of polymer blends displaying positive and negative deviation are given in Table 2.4. A review of each of these three cases will be presented next.

In studies of the concentration dependence of viscosity for mixtures of immiscible polymer blends often results in a blend viscosity which lies between that of the neat blend components. The concentration dependence of the viscosity of polystyrene (PS) - polyethylene (PE) blends has been investigated by Van Oene [120]. The concentration dependence of this blend at various shear stresses and 170°C is shown in Fig. 2.10. It can be seen that the viscosity lies between that of the neat blend components at both large and small differences in the viscosity of the constituents and the blend viscosity does not show a minimum or maximum as the composition is changed. The morphology of this blend was found to be in the form of stratified layers or ribbons at 10 and 30% PE while at 70 and 90% PE the PS was found to be dispersed in the form of droplets in a PE matrix. On the other hand, Van Oene found that a minimum in viscosity is observed when the viscosities of the parent polymers are more nearly the same by increasing the temperature of the blend to 210°C (see Figure 2.11). This figure shows that at shear stresses higher than  $5 \times 10^5$  dyn/cm<sup>2</sup> the viscosity of the mixture of 10/90 PE/PS is lower than that of the neat blend components and between that of the neat blend components at stress below  $5 \times 10^5$  dyn/cm<sup>2</sup>.

An extensive rheological study of high density polyethylene (HDPE) and polystyrene (PS) blends has been made by Han and Kim [121]. In this study, Han and Kim examined the viscosity and first normal stress difference of HDPE/PS blends as a function of temperature and composition. Some of their results obtained at three different stresses using a capillary rheometer are shown in Fig. 2.12. The normal stress behavior was found to be independent of temperature for a given stress while a temperature dependence was

**Table 2.4 Viscosity of polymer blends [122].**

**a. Positive Deviation Blends**

Polymers	Temperature (°C)
PE/Ethylene vinyl acetate	160-200
POM/CPA	190
PS/PMMA	200
LDPE/PA-6	240
HDPE/PP	200
PE/PMMA	160

**b. Negative Deviation Blends**

Polymers	Temperature (°C)
iPP/EPR	200
PE/EPDM	190
PC/PMMA	250
PS/LDPE	200
PET/PA-6	275
iPP/HDPE	180-210
PS/PC	180-260

**c. Positive-Negative Deviation Blends**

Polymers	Temperature (°C)
PS/HDPE	200-240
PS/PBD	-
PBD/PIP	-
POM/PE	140-200
POM/HDPE	140-200
iPP/PE	140-270

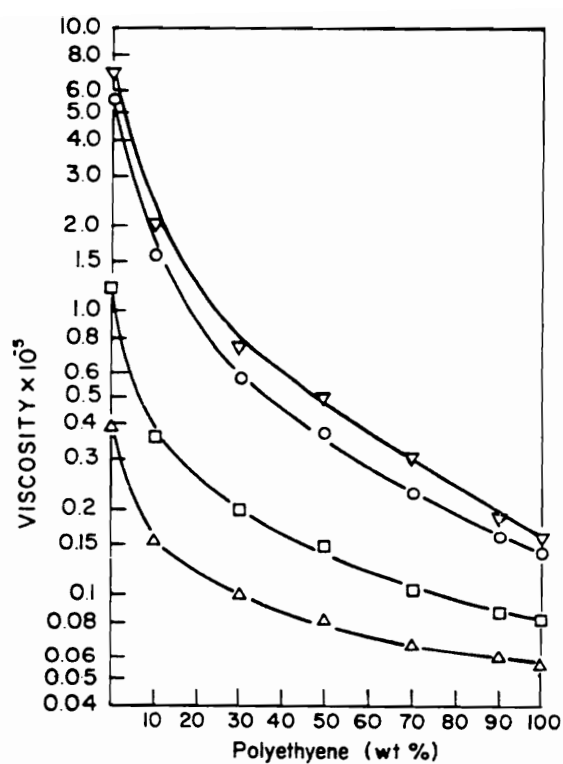


**Figure 2.10** Composition dependence of the viscosity of polystyrene-polyethylene blends at various shear stresses ( $T=170^{\circ}\text{C}$ ): Shear stress ( $\text{dyn}/\text{cm}^2$ ) ( $\nabla$ )  $0.5 \times 10^5$  ( $\circ$ )  $1 \times 10^5$ ; ( $\square$ )  $5 \times 10^5$ ; ( $\Delta$ )  $10 \times 10^5$  [120].

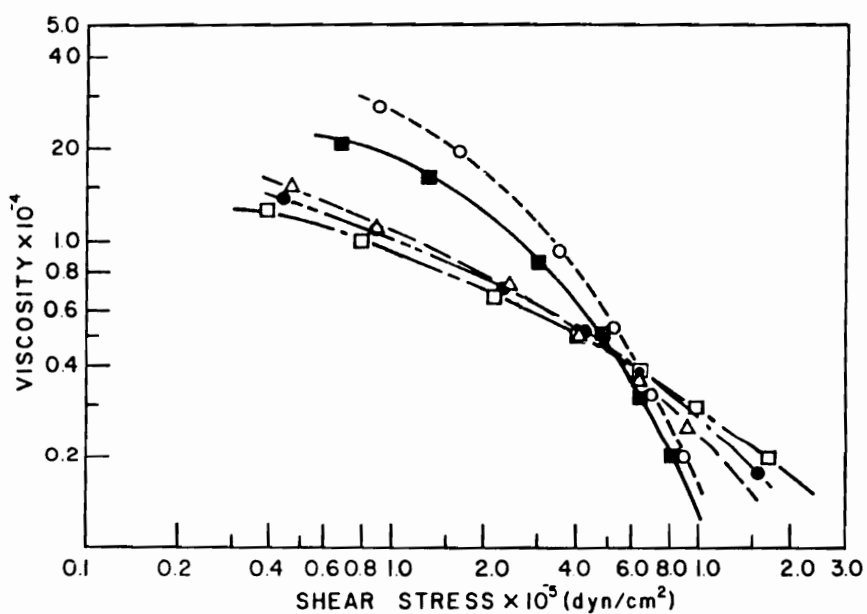


**Figure 2.11** Viscosity as a function of shear stress of polystyrene-polyethylene blends at  $T=210^{\circ}\text{C}$ . ( $\circ$ ) polystyrene ( $\blacksquare$ ) 90/10 PS/PE; ( $\triangle$ ) 50/50 PS/PE; ( $\bullet$ ) 30/70 PS/PE; ( $\square$ ) polyethylene [120].



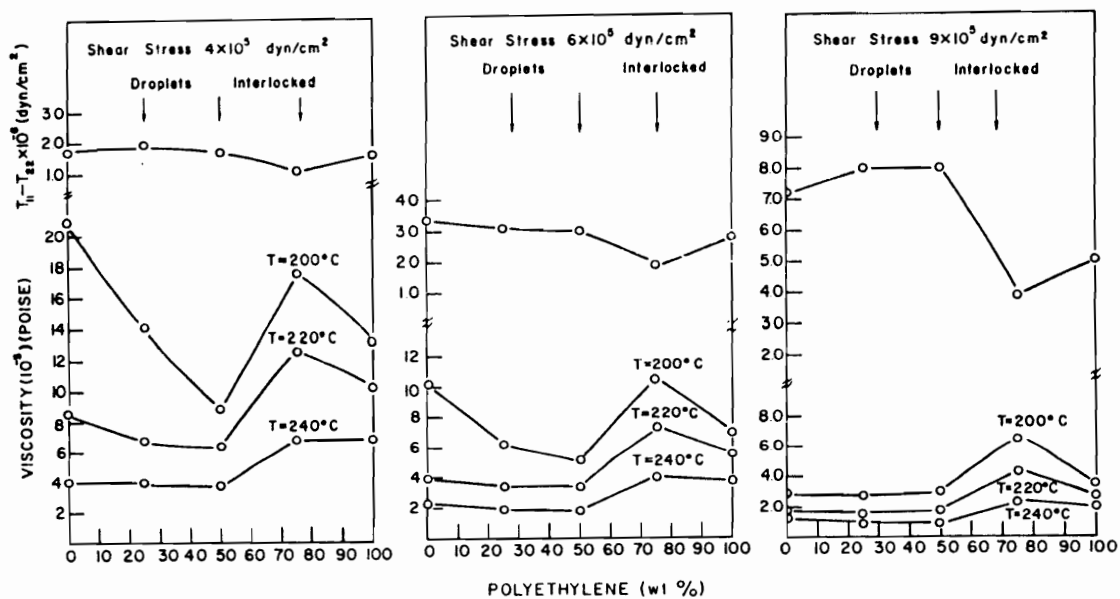
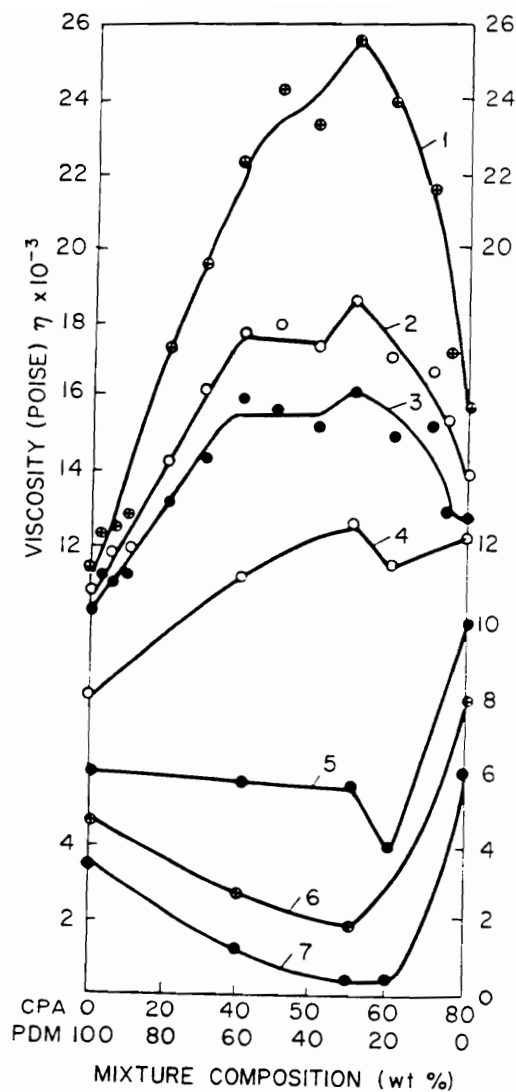


Figure 2.12 Comparison of the composition and temperature dependence of the viscosity and normal stress of blends of polystyrene and polyethylene at various shear stresses [121].

seen in the viscosity. The viscosity is seen to go through both a minimum and a maximum as the composition is varied depending on the shear stress used. The minimum in viscosity can be seen to be lower than that of the neat blend components and corresponds to a 50/50 composition ratio at all three stress levels. The first normal stress difference is seen to show a minimum at a 75/25 HDPE/PS composition and corresponds to the composition where a maximum in viscosity is observed. Han and Kim observed that the morphology of the blends at composition ratios of 75/25 and 50/50 HDPE/PS consisted of PS drops dispersed in a continuous phase of HDPE. At a composition ratio of 25/75 HDPE/PS no clear continuous phase was observed, but instead the two components seemed interlocked. The authors concluded that in the blends that consisted of dispersed droplets the normal stress difference tended to increase and also tended to have a minimum in viscosity. The blend with an interlocked morphology had a larger viscosity but a lower normal stress difference.

In another study, Ablazova and Vinogradov et al. [123,124], studied the composition dependence of viscosity of the immiscible blend of formaldehyde with 2% of 1,3-dioxalane (POM) and a mixed copolyamide (CPA), a copolymer of 44% caprolactum, 37% hexamethylene adipate, and 19% hexamethylene sebacate. Their results shown in Fig. 2.13 show a strong dependence of viscosity on both shear stress and composition. In contrast to the results obtained by Han and Kim [121], at stresses up to  $6.3 \times 10^5$  dyn/cm<sup>2</sup> the viscosity was observed to be higher than that of the neat blend components with a maximum observed at a composition of approximately 55/45 CPA/POM. At stresses higher than 6.3 dyn/cm<sup>2</sup> the viscosity was seen to be lower than that of both neat components with a minimum occurring at a composition of approximately 60/40 CPA/POM. The morphology of this blend was found to be in the form of POM fibers in a matrix of CPA, and the shear stresses at which the fibrous structure was found corresponded to the region



**Figure 2.13** Composition dependence of the viscosity of blends of CPA and POM as a function of shear stress: (curve 1) 1.27; (curve 2) 3.93; (curve 3) 5.44; (curve 4) 6.30; (curve 5) 12.59; (curve 6) 19.25; (curve 7) 31.62 ( $\times 10^{-5}$  dyn/cm<sup>2</sup>) [124].

in which a sharp viscosity minimum was observed.

The occurrence of viscosity maxima or minima in thermoplastic-thermoplastic blends is not well understood at this time. Although some attempts to correlate morphology with rheology have been published little is known of the relationship between the observed viscosity behavior as a function of the elastic nature of the blend components and other factors such as interfacial tension or compatibility.

### **2.2.2 LCP/thermoplastic Blends**

While the previous section briefly discussed the behavior of polymer-polymer blends consisting of flexible chain components, this section will focus on the rheology of systems where one polymer component is a liquid crystalline polymer. In general these studies have been limited to steady shear viscosity as a function of temperature and concentration and a fundamental understanding of the development of texture and its correlation to rheological behavior is lacking. In these systems the phenomena of positive, negative and positive-negative deviation are well documented [27,126]. The phenomena of a drop in viscosity with the addition of small amount of TLCP and the formation of a reinforcing fibrillar LCP structure have received both academic and industrial interest [27]. Indeed the addition of small amounts of TLCP to flexible chain polymers as a processing aid and to act as reinforcing agents has been patented [29,30,31,125]. Attempts to relate blend viscosity as a function of the blend composition and viscosity ratio of blend components has been published by La Mantia [126] (see Table 2.5).

The steady shear viscosity as a function of concentration of blends of polycarbonate (PC) with polyethyleneterephthalate-*co-p*-oxybenzoate copolyester (HBA/PET) with 60% HBA content (PET/60HBA) has been studied by Blizzard and Baird [72], Acierno et al.

**Table 2.5 Viscosity behavior of TLCP/thermoplastic blends [126].**

Blends Showing Flow Curves Between Those of the Two Components

System	Viscosity Relationship	References
PC-HBA60/PET	$\eta_{TP} > > \eta_{LCP}$	39
PC-HNA/HBA	$\eta_{TP} > \eta_{LCP}^*$	35
PES-HNA/HBA	$\eta_{TP} > \eta_{LCP}$	131
PS-C <sub>10</sub> C <sub>12</sub> F <sub>3</sub>	$\eta_{TP} > > \eta_{LCP}$	38
CPVC-HBA60/PET	$\eta_{TP} > > \eta_{LCP}$	132
PC and PET-HBA60/PET	$\eta_{TP} > > \eta_{LCP}$	133
PC-HNA/HBA/TA/HQ	$\eta_{TP} > > \eta_{LCP}$	148
PC-HBA60/PET	$\eta_{TP} > > \eta_{LCP}$	33
PC-HNA/HBA	$\eta_{TP} > \eta_{LCP}$	134
PC-HNA/TA/APH	$\eta_{TP} > > \eta_{LCP}$	135
PEI-LCP(Bayer)	$\eta_{TP} > \eta_{LCP}$	136
PC-HNA/HBA	$\eta_{TP} > \eta_{LCP}^*$	137
PSPH-LCP(BASF)	$\eta_{TP} > \eta_{LCP}^O$	138

Blends Showing Flow Curves Between Those of the Two Components

System	Viscosity Relationship	References
PC-HNA/HBA	$\eta_{TP} > > \eta_{LCP}^*$	35
PS-HBA60/PET	$\eta_{TP} > \eta_{LCP}$	133
PC-HNA/HBA	$\eta_{TP} > \eta_{LCP}^*$	137
PA 6-HNA/HBA	$\eta_{TP} > > \eta_{LCP}$	28
PA 12-HNA/HBA	$\eta_{TP} > > \eta_{LCP}$	139
PBT-HNA/TA/APH	$\eta_{TP} > > \eta_{LCP}$	140
PA 6-HNA/TA/APHQ	$\eta_{TP} > > \eta_{LCP}$	141
PSPH-LCP(BASF)	$\eta_{TP} > > \eta_{LCP}^O$	138

\* At high shear rates

<sup>O</sup>At high temperatures

HBA = 4-hydroxybenzoic acid HNA = 2-hydroxy-6-naphthoic acid

APH = 4-aminophenol

HQ = hydroquinone

TA = terephthalic acid

PSPH = polysulfone

PES = polyester sulfone

C<sub>10</sub>C<sub>12</sub>F<sub>3</sub> = polyester from sebacic and dodecanedioic

acids and 4,4'-dihydroxy- $\alpha,\alpha'$ -dimethylbenzalazine

[127] Nobile et al. [128], and White et. al. [129]. These investigations have shown a blend viscosity at low concentrations of PET/60HBA which is lower than that of the neat PC with the exception that Acierno[127] and Nobile [128] found that at low shear rates the viscosity of the blend was higher than that of the neat PC (see Figure 2.14). In all cases [127-129] the blend viscosity was found to be between that of the neat blend components with the exception that Baird [32] found that blends containing 50 and 70% LCP were lower than those of the neat blend components (see Figure 2.15). Additionally, it was observed that when the LCP content was greater than 10% the rate dependence of the viscosity became strongly shear thinning and resembled that observed in pure LCPs. The morphology associated with the rheology reported above at low shear rates in both capillary and cone and plate rheometers has been found to be in the form of droplets with sizes on the order of a few microns [32,127-129]. These droplets are found to decrease in size with increasing shear rate [32] and increase with increasing LCP concentration [129].

In another study by Isayev and Modic [130] blends of PC with hydroxybenzoic acid (HBA) and 2,6-hydroxynaphthoic acid (HNA) with 75 mole % HNA (PC with HBA/75HNA) were studied. In this system, Isayev and Modic observed that at low shear rates the viscosity of the blends was lower than that of the neat blend constituents and at higher shear rates (where viscosity of the PC is higher) the viscosity of the blend lies between that of the neat blend components. Additionally, Isayev and Modic found that at 50 mole % LCP content the viscosity of the blend was higher than that of each neat blend constituent. This is in contrast to a similar system in which the LCP contained 70 mole % rather than 75% HNA (i.e., PC-HBA/70HNA blends). Isayev and Modic found that while the rheological behavior of PC-HBA/70HNA was similar to that of the PC-HBA/75HNA blend no maximum at an LCP content of 50% was observed. Additionally, both systems are reported to exhibit a yield stress. As was seen in the blends of PC with HBA/PET

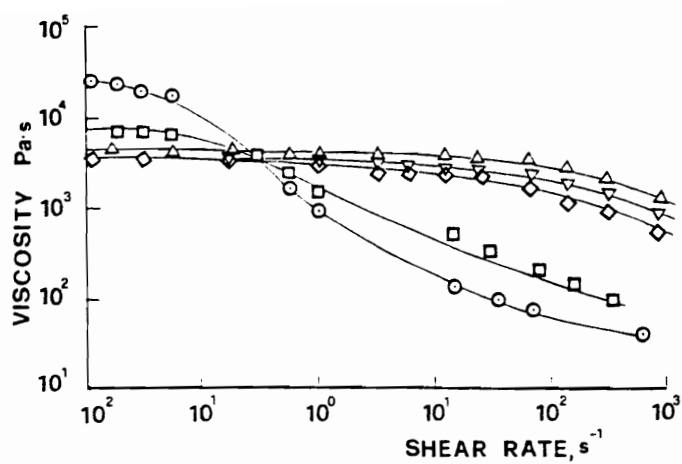


**Figure 2.14** Viscosity vs. shear rate for PC-PET/60HBA blends. The LCP content is  $\Delta$  0%;  $\nabla$  5%;  $\diamond$  10%;  $\square$  90%; and  $\circ$  100% [128].

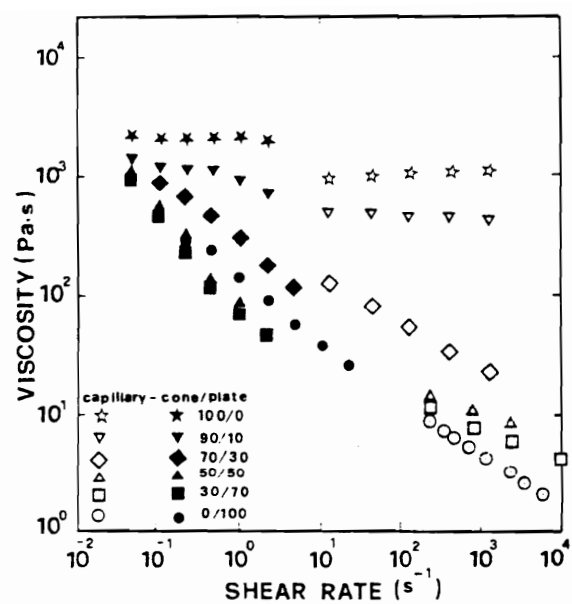


Figure 2.15 Viscosity vs. shear rate for PC-PET/60HBA blends [39].



discussed above (see Figure 2.15) the PC-HBA/HNA exhibit an increase in their shear thinning behavior upon increase in LCP content.

In blends where the LCP phase is the dispersed phase La Mantia [126] has pointed out that as a general rule in capillary flow a drastic reduction of the viscosity over that of the thermoplastic matrix is observed [33,35,39,131-138,148]. In some of these systems a minimum in the viscosity composition curves (i.e., the blend viscosity is lower than that of both constituents at certain compositions) is found [28,35,133,137-141]. Additionally, in some cases an apparent yield stress is found by the observation of a strong increase in the viscosity at very low shear rates. La Mantia draws two conclusions from the data tabulated in Table 2.5:

1) the viscosity of the blends decreases and is between that of the two components when the ratio of the viscosities  $\eta_{TP}/\eta_{LCP}$  is  $\gg 1$ ; and

2) the viscosity of the blends shows minima when  $\eta_{TP}/\eta_{LCP}$  is about 1 or less.

The conclusions presented above are in general valid only at a specific temperature and shear rate. It has been shown that both behaviors have been observed in the same blend by changing the temperature [138] or the shear rate [35,137]. However, in some cases the general rule of a reduction in viscosity of the thermoplastic matrix is not observed in the viscosity at low shear rates where a yield stress is observed [35,128,129,134], in blends of PC-HNA/HBA [35] that show a maximum at 50% composition, and PA12-HNA/HBA [127] blends in the composition range of 20 to 80% where both minima and maxima are observed.

The effect of the molecular weight of the thermoplastic component of TLCP/thermoplastic blends on their rheology was investigated by La Mantia and Valenza [126]. In this study a high and a low intrinsic viscosity PC and a high and low molecular weight PP were used as the blend constituents. In blends containing the low molecular

weight PC with HNA/TA/AP (where the viscosities are similar in magnitude), the viscosity was found to be below that of the constituents at low shear rates and between them at higher shear rates. The viscosity of blends using the high intrinsic viscosity PC with the copolyesters of HNA/TA/AP (where the PC viscosity is substantially higher than that of the HNA/TA/AP) was found to lie between those of the constituents at all rates tested. Similar results were obtained in blends of low and high molecular weight PP with the LCP synthesized from sebacic acid, 4-hydroxybenzoic acid, and 4,4'-dihydroxybiphenyl (SBH). The authors proposed two mechanisms to account for the reduction of viscosity in the presence of a LCP: 1) incompatibility between the two phase and 2) formation of fibrils at the entrance of the capillary which lubricated the thermoplastic matrix. The authors concluded that since compatibility is only slightly influenced by molecular weight, it could be considered responsible for the reduction of the viscosity but not for the presence of minima. A reduction in viscosity in the presence of a LCP has been attributed the lubricating effect of fibrils forming at the entrance to the capillary [35,38,39]. La Mantia and Valenza point out cases where the relaxation time of the fibrils is less than the residence time in the capillary or if breakup of the fibrils occurs at high shear rates the lubrication mechanism cannot account for the drops in viscosity observed. Additionally systems studied using cone and plate rheometers have shown similar drops in viscosity [608]. An adequate explanation for the phenomenon discussed above has not available at this time.

A reduction in viscosity has also been attributed directly to the morphology of the blend. It has been shown that a transition from a droplet to a fibrillar morphology occurred when the viscosity of the two phases was similar [133,143-149,149]. When  $\eta_{TP} \gg \eta_{LCP}$  the particles of the dispersed phase were smaller and were formed directly during shear flow [141,146]. Additionally, fibrils formed in the converging flow at the entrance to the capillary were broken up into small particles when  $\eta_{TP} \gg \eta_{LCP}$  [141,149]. La Mantia

[147] proposed that the decrease of viscosity of biphasic systems is much larger with increasing particle size or in the presence of short fibers. Therefore, the presence of a minimum was correlated to a blend morphology consisting of large drops or short fibers because of the larger decrease of the viscosity. In a recent review La Mantia [27] proposed that minimum in viscosity versus composition curves could occur only when slippage between the phases occurs.

The presence of yield stresses in some systems [35,140,141] has been attributed to the solid like LCP particles dispersed in the thermoplastic matrix. La Mantia has associated this phenomenon with similar behavior seen in neat LCPs and the structural model proposed by Onagi and Asada [8] in which under an applied stress piled domains are transformed to a dispersed polydomain system and finally to a monodomain continuous phase. In LCP based blends the LCP piled polydomains behave like hard inclusions in the matrix. A given stress must be transmitted from the matrix (which has Newtonian and shear thinning zones) to the LCP phase and give rise to the Newtonian and the shear thinning zones .

Although transient data obtained from experiments such as start up of steady shear could provide valuable insight to the development of structure in TLCP/thermoplastic blends, this data is greatly lacking. In an investigation by Nobile et al. [150] the transient behavior of a blend of polyetherimide (PEI) and a TLCP based on hydroxybenzoic acid (HBA), terephthalic acid, hydroquinone, and 4-4' dihydroxybiphenol (K161 Bayer) was studied. The data show an overshoot which appeared at shear rates lower than that required to produce an overshoot for the pure matrix (see Figure 2.16a, b and c). Additionally, it was observed that steady state was not obtained even after 250 strain units while pure polyetherimide reaches steady state in less than 50 units of strain. Nobile et al. associated these results with a continuous decrease in the stress with the continuous deformation and orientation of the second phase during the experiment. Furthermore, it was pointed out that

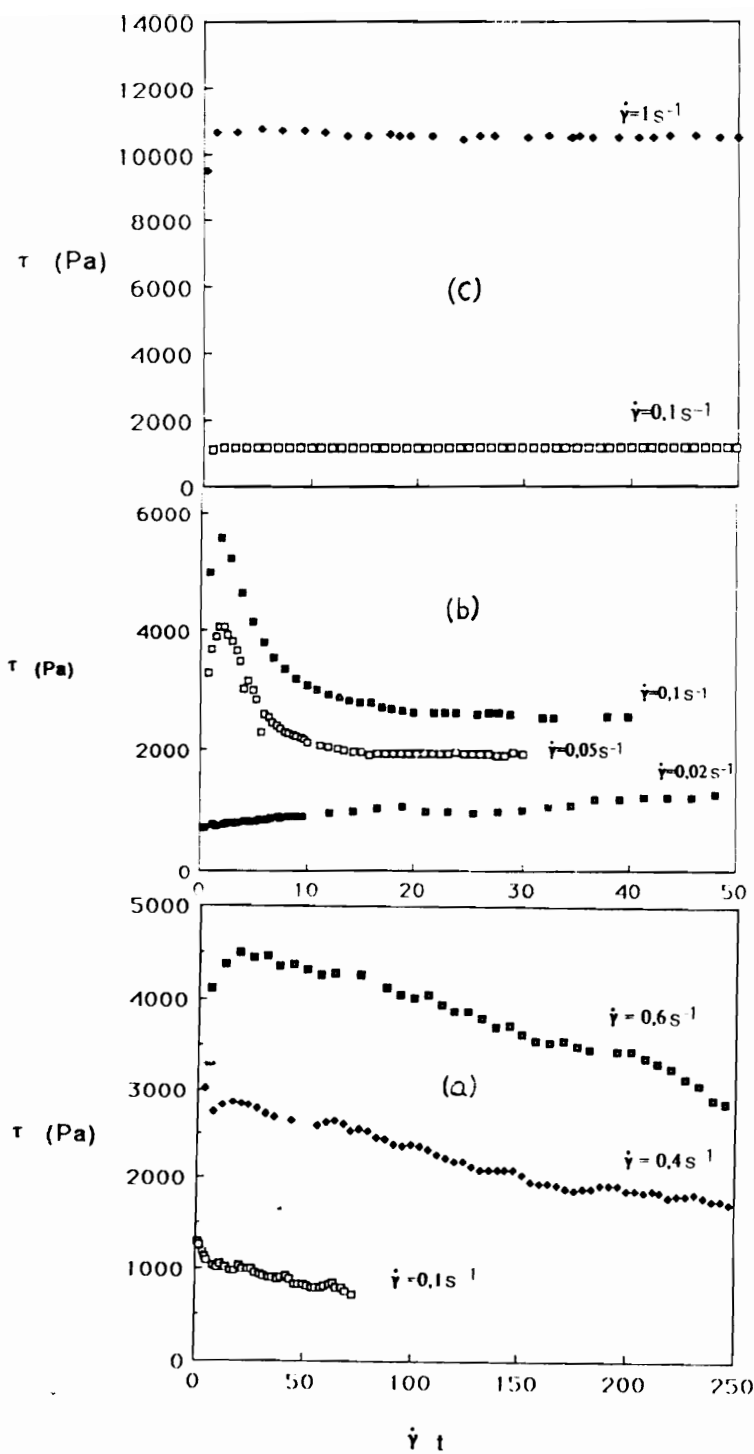


Figure 2.16 Transient shear stress vs. strain a) TLCP ; b) PEI; c) PEI/TLCP 90/10 at 330°C [150].

these results raise questions as to the validity of rate sweep experiments where it was possible that steady state had not been reached.

A comparison of dynamic and steady shear rheology has been presented by Biing-Lin [151]. In this study using a blend of chlorinated polyethylene (CPVC) and PET/60HBA dynamic oscillatory strain sweeps showed a strain dependent behavior and an increase in the storage modulus  $G'$  with an increase in strain. In frequency sweep experiments both pure blend components and the blend showed strong shear thinning behavior. It can be seen that the dynamic viscosity of the LCP is larger than that of the CPVC and the viscosity of the blend lies between that of the pure components. These results are in contrast to steady shear results obtained using a capillary rheometer (see Figure 2.17). Although the steady shear viscosity, as in the case of the dynamic viscosity, showed a blend viscosity which was between that of the pure components, the rate and concentration dependence were seen to differ markedly. Additionally, the magnitude in steady shear was much lower. These results were explained by Biing-Lin [151] as being a result of aligned domains of the LCP in the flow direction while in the dynamic experiment the LCP domains were retained in the blends resulting in an increase in the viscosity of the matrix.

While researchers have attempted to apply several predictive theories to model the rheological behavior of these systems, the models are largely empirical and limited in their applicability[27]. These models range from simple mixing rules which are a function of concentration and component viscosity to more complicated formulations which take into account other factors such as interfacial tension. Several empirical relations which have been developed to model the viscosity versus composition dependence of polymer blends are shown in Table 2.6. These equations are various forms of rather simple mixing rules. In cases where no minima is observed the blend viscosity of polymer-polymer blends is

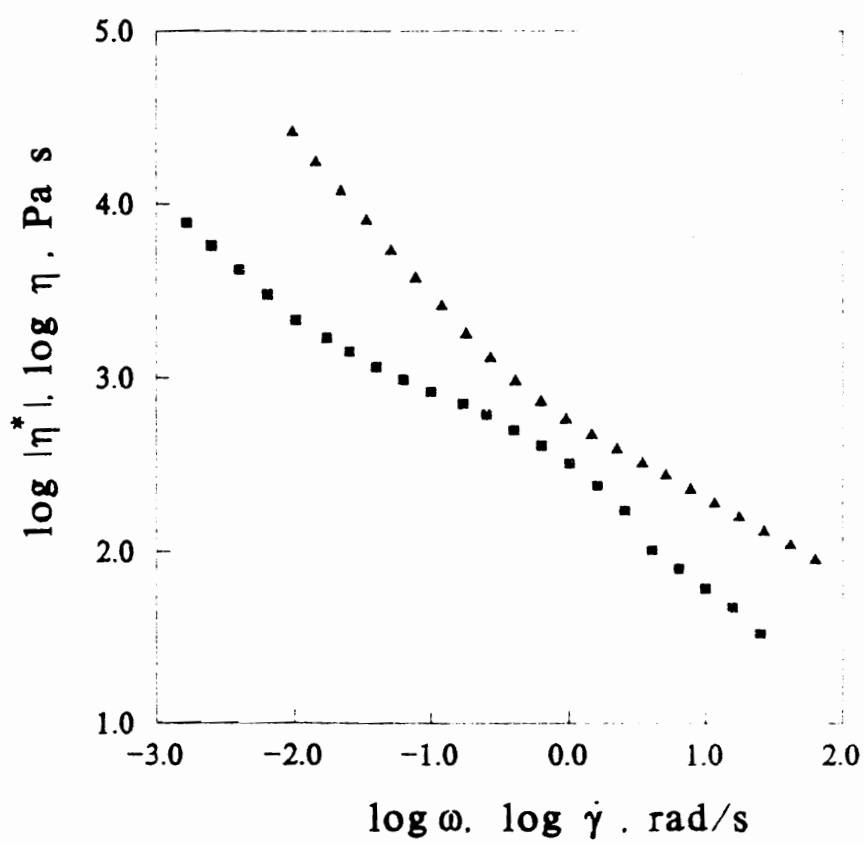


Figure 2.17 Comparison between steady shear and complex viscosities. (■)  $\eta$ ; (▲)  $\eta^*$  [126].

**Table 2.6 Empirical Relations for Predictions of Blend Viscosity**

Equation Number	Equation	Reference
2.3	$\log \eta = \phi_1 \log \eta_1 + \phi_2 \log \eta_2$	152
2.4	$\frac{1}{\eta} = \frac{w_1}{\eta_1} + \frac{w_2}{\eta_2}$	153
2.5	$\frac{1}{\eta} = \frac{w_2}{\eta_1} + \frac{w_1}{\eta_2}$	154
2.6	$\ln \eta = x_1 \ln \mu_1 + x_2 \ln \mu_2$	155
2.7a	upper bound: $\eta_{mix}^* = \eta_2 + \frac{\phi_1}{1/(\eta_1 - \eta_2) + 2\phi_2/5\eta_2}$	156
2.7b	lower bound: $\eta_{mix}^* = \eta_1 + \frac{\phi_2}{1/(\eta_2 - \eta_1) + 2\phi_1/5\eta_1}$	

Equations 5a and b are modified for non-Newtonian fluids by

replacing 2/5 in denominator with 1/2

$\eta, \mu$  and  $\eta_{mix}^*$  = Viscosity of the mixture

$\phi_i$  = weight fraction of component i

$w_i$  = volume or weight fraction of component i

$\mu_i$  = Newtonian viscosity of component i

$x_i$  = mole fraction of component i

lower than values predicted using various empirical relationships developed. In the case of PS/PE blends studied by Van Oene [120] and discussed earlier, Figure 2.18 shows that at  $10^5 \text{ dyn/cm}^2$  the viscosity of this blend was seen to be similar and to fall below the lower bound predicted by Eq. 2.7b and above that predicted the inverse additivity law (Eq. 2.4). Upon increasing the shear stress to  $10^6 \text{ dyn/cm}^2$  the viscosity of the blend is seen to fall below that predicted by the inverse additivity law. The lowest curve in Figure 2.18 is predicted when a sheath core morphology formed by complete segregation of the polymers takes place. It is seen that the viscosity of this blend was lower than that predicted by various models but higher than that assuming complete segregation of the blend constituents. Furthermore, the models cannot predict a viscosity maximum or minimum as observed in some systems regardless of the viscosity ratios.

In summary, although a considerable amount of research has been devoted to polymer blends in which one component is an LCP, a fundamental understanding of their rheology and texture has not been reached at this time. The viscosity behavior of these blends shows concentration dependence which appears to be a function of the ratio of viscosity of the blend constituents. Correlation of this and other rheological behavior to other factors such as the contribution from the interface and elastic nature of the components is unavailable and requires further research.



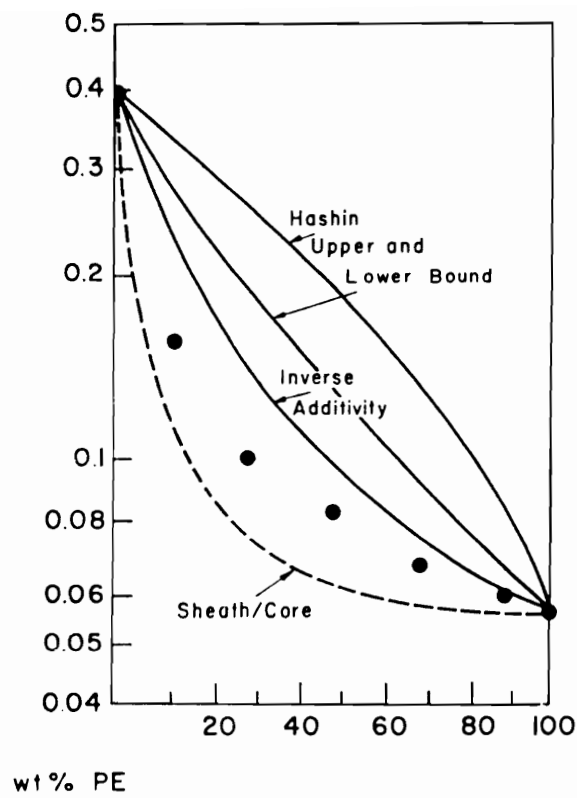


**Figure 2.18** Comparison of observed composition dependence with theoretical predictions at  $T = 170^{\circ}\text{C}$  [126].

## 2.3 Rheology of Filled Polymers

The texture developed in some polymer blends has been shown in some cases to consist of a dispersed phase in the form of fibrils. Little is known of the rheology and development of orientation of the dispersed phase of these systems at temperatures above that of the matrix phase below that of the dispersed phase. In this section analogous systems such as particulate and fiber filled polymer will be reviewed in order to obtain an understanding of the rheology of commonly used filled systems.

The rheology of polymers filled with particulates and fibers has received a great deal of attention [157,159-193]. These studies cover a wide array of polymers and fillers several of which are summarized in Table 2.7 for particulate filled systems and Table 2.8 for fiber filled systems. These tables give polymer/filler used, geometric details of the filler, volume fraction, experimental details and rheological properties observed including the presence of a yield stress.

The rheological properties of polymer/filler systems are functions of the nature of the polymer-filler interface which has been shown in low molecular weight materials to be a few angstroms thick, but a much thicker layer is found in high molecular weight materials [157]. A thicker polymer-filler interfacial layer acts to increase the particle size and concentration dependence of the rheological properties. Some of the interfacial conditions which exist in these systems include no adherence between the polymer and particle, a fraction of the particles are partially or fully wet, or the polymer may fully wet all the particles.

In order to enhance the filler dispersion and adhesion to the polymer, various chemicals called "coupling agents" and "wetting agents", respectively are used [158]. A suitable coupling agent contains pendant groups capable of reacting both with the polymer

**Table 2.7 Summary of Particulate Filled Polymers [159]**

Polymer/Filler	Dia ( $\mu\text{m}$ )	Aspect Ratio	$\dot{\gamma}_{\min}$	$\dot{\gamma}_{\max}$	$\sigma_y$ (yield Stress)	Reference
Polypropylene						
CaCO <sub>3</sub>	2.5	-	100	500	-	178
Glass Beads	5-44	-	100	500	-	178
Talc	10	-	0.001	10,000	yes	162
Glass Beads	44	-	0.001	0.1	yes	162
Polyethylene						
Mica	100	35	0.01	20,000	no	177
CaCO <sub>3</sub>	2	1	0.01	100	yes	170
Glass Beads	36-100	1	0.01	100	yes	169
Polystyrene						
CaCO <sub>3</sub>	0.5	-	0.2	1000	yes	172
Carbond Black	0.045	-	0.2	1000	yes	172
TiO <sub>2</sub>	0.18	-	0.2	1000	yes	172
Franklin Fiber	1.5-2	100	0.2	1000	yes	172
Mica	5	25-30	0.2	1000	no	172
Glass Beads	10	-	0.2	1000	no	172

**Table 2.8 Summary of Fiber Filled Polymers [159].**

Polymer/Filler	Dia ( $\mu\text{m}$ )	Aspect Ratio	$\dot{\gamma}_{\min}$	$\dot{\gamma}_{\max}$	$\sigma_y$ (yield Stress)	Reference
Polypropylene						
Glass Fiber	10	50	3	1000	no	177
Glass Fiber	10	1000	1	1000	no	170
Glass Fiber	10	300	0.01	10	-	169
Polyethylene						
Glass Fiber	12.7	157	.005	1000	no	181
Glass Fiber	725	35	100	1000	no	186
Polystyrene						
Glass Fiber	12.7	45	0.01	20	-	181
Glass Fiber	12.7	112	0.01	20	-	182
Aramid-Kevlar	12.2	120	0.01	20	-	182
Cellulose	12.0	20	0.1	1000	-	182

and filler surfaces. The extent of coupling then depends on the strength of the covalent bonds between polymer and filler formed. Wetting agents merely act to increase wetting.

### **2.3.1 Viscous Effects**

Rheological studies of particulate filled polymers have shown dramatic changes in the viscoelastic properties of the matrix [158,159]. The steady shear viscosity is found to be dependent on the particle diameter. In systems containing particles with diameters  $\leq 1 \text{ m}\mu$ , a yield stress is often observed with large increases in viscosity at low shear rates [160,162,165,168,169,170,173]. On the other hand, systems containing particles with diameters of  $\geq 5 \text{ m}\mu$  a yield stress is generally not observed [161,177]. These phenomena have been attributed to interparticle interaction to form a network or gel-like structure. In many cases it is found that agglomeration of filler particles occurs [158] (often associated with partial wetting) which can also contribute to an observed yield stress.

In order to characterize the influence of coupling agents rheological experiments have been performed [178,179,185]. The effect of the addition of silane and titanate coupling agents on the rheological properties of stainless steel microspheres in a low density polyethylene matrix has been studied [25]. In this study, an increase in both viscosity and shear modulus indicated that polymer-filler adhesion was enhanced. A silane coupling agent was also used in calcium carbonate filled polypropylene in another work by Han [178]. It was found that the addition of coupling agents which increase viscosity decrease elasticity and those which decrease viscosity increase elasticity. The effect on the viscosity of the addition of a silane coupling agent to mica filled polypropylene has been investigated by Boira and Chaffey [185]. A reduction in both the viscosity and the shear rate dependence of the viscosity was observed in the presence of the silane coupling agent. In

another study, using a titanate coupling agent, Han [179] also found a decrease in the viscosity. Han indicated that the titanate might not have acted as a true coupling agent but instead may have acted as a lubricant or a surfactant, which reduced resistance to flow [158]. Coupling agents have also been used in glass fiber filled polypropylene melts [179]. Although it appears that coupling agents act to reduce the viscosity of the filled polymer the effectiveness of coupling agents is not well understood nor is their effect on the rheological properties .

The effect of a wetting agent on the yield stress observed in talc filled polypropylene has been studied by Chapman and Lee [162]. In their study the surface of the talc particles was chemically treated prior to compounding. This treatment was found to lower the viscosity relative to the untreated filler system at low shear rates but did not result in a zero shear viscosity. The authors attributed the decrease in the viscosity to the deactivation of polar groups on the talc surface which reduced particle agglomeration. Particle agglomeration can result in a larger effective particle size.

In general, the addition of a particulate filler results in an increase in viscosity which becomes more pronounced at lower shear rates and has been attributed to an increase in the polymer relaxation times as the filler particles hinder polymer chain relaxation [177]. The viscosity at low shear rates appears to be strongly dependent on inter-particle interactions while at high shear rates the rheological properties of the polymer dominate. The flow curves for filled and unfilled samples tend to converge at high shear rates [161-165,168-170,177]. The yield value found in these systems has been found to depend on particle size, coupling and wetting agents, and concentration. In a study using carbon black filled polystyrene Lobe and White [165] observed a zero shear viscosity at 5% filler content while as the concentration of filler increased a yield stress was seen to develop.

In systems containing fillers in the form of fibers, the viscosity is found, in general,

to increase over the pure polymer with the increase being largest at low shear rates (i.e., below  $1 \text{ s}^{-1}$ ) and tend toward the same value at high shear rates (see Figure 2.19). In a study by Czarnecki and White [182] the effect of fiber length on the viscosity was observed. In order to obtain shorter fibers the filled polymer mixing times were increased in the compounding equipment. A reduction in viscosity was observed with an increase in compounding time. The authors attributed the drop in viscosity to lower fiber aspect ratios and ruled out effects due to polymer degradation. In another investigation by Maschmeyer and Hill [183] the effect of an increase in glass fiber length in silicone oil was investigated. In this study, the addition of a small amount of long fibers, while keeping the overall fiber concentration constant, was found to increase the viscosity as well as nonNewtonian behavior at low shear rates. It was postulated that at low shear rates the matrix may flow in between the stationary fibers greatly increasing the resistance to flow, and at higher shear rates, the fibers begin to tumble end over end in the shear field. End over end tumbling has been observed using visualization techniques for dilute suspensions of steel fibers in a polypropylene melt by Crowsen et al. [180]. Crowsen proposed that the end over end rotation increases the probability of collisions due to hydrodynamic interactions among the fibers and tends to increase viscous dissipation in the sheared sample. Shorter fibers would then reduce the probability of fiber interaction.

### 2.3.2 Elastic Nature

In polymers the first normal stress coefficient is found in general to be reduced by the addition of particles [165,168,173]. This phenomena is illustrated by Lobe and White [165] with carbon black filled polystyrene and by Tanaka and White [168] for carbon black, titanium dioxide and calcium carbonate filled polystyrene melts. Similar results were

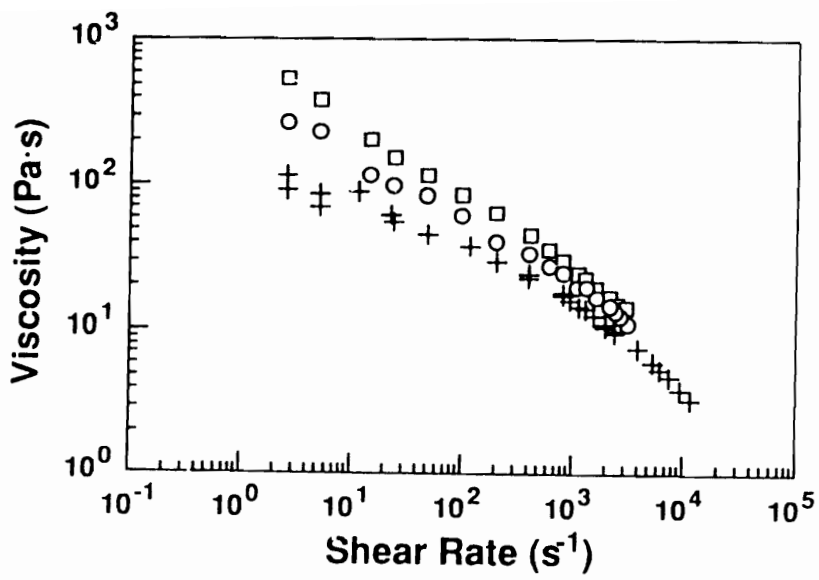


**Figure 2.19** Shear viscosity vs. apparent shear rate, for HDPE suspensions at 170°C. The concentrations of fibers for the sets of data are, from top to bottom, 40%, 10%, 0% [187].



obtained by Minagawa and White [173] who also found the first normal stress difference coefficient ( $\psi_1$ ) to be a decreasing function of shear rate and to increase with  $\text{TiO}_2$  content in polyethylene and polystyrene melts at the same shear rates.

The elastic nature of particulate filled polymer has also been studied by determining the dependence of the storage modulus ( $G'$ ) on frequency. The presence of yield stresses in particulate filled polymers is thought to give rise to a plateau value of  $G'$  at low frequencies. The dynamic response of carbon black filled polystyrene solutions was studied by Onagi and Matsumoto [163]. In their system, a plateau in  $G'$  was observed, but the authors concluded that it did not represent a yield stress but instead was due to a structure formed by carbon black interactions. The value of the plateau  $G'$  was found to decrease with decreasing strain. The relaxation time of this structure was found to be longer than the longest relaxation time of polystyrene in either the melt or solution state. Similar dynamic experiments on filled polymer melts for this system were not performed.

The elastic nature of fiber filled polymers in contrast to their viscous behavior is not found to be qualitatively similar to particulate filled polymers. Typical measurements of normal stresses in shear flow are qualitatively different in fiber filled polymers relative to particulate filled polymers. In general, the first normal stress differences in fiber filled polymers have been found to increase with both shear rate and shear stress compared to the unfilled base polymer [172,181,184]. Aramid (Kevlar), cellulose, and glass fiber filled polystyrene were studied by White et al. [172]. In all cases the first normal stress difference ( $N_1$ ) was found to increase with fiber content at the same shear stress. Additionally, it was found that ( $N_1$ ) decreased with decreasing fiber aspect ratio.

In summary, the viscous and elastic nature of particulate and fiber filled polymers are a function of concentration, geometry and interfacial phenomena. The addition of fillers to polymers, in general, increases viscosity for both particulate and fiber fillers. In

contrast, while the addition of fillers in the form of fibers has been shown to increase  $N_1$ , particulate fillers generally act to reduce  $N_1$ .

## 2.4 Mathematical Models for Viscoelastic Behavior of Textured Fluids

In Chapter 1 it was indicated that a suitable constitutive equation for textured materials must be able to separately predict both the stress response and the molecular orientation or changes in the phase structure as a function of flow history. Early attempts to model the viscoelastic nature of fluids were based on linear combinations of viscous and elastic properties. By considering a series combination of viscous and elastic behavior one early model is the Maxwell model:

$$\tau + \lambda \dot{\tau} = -\mu_o \dot{\gamma} \quad (2.8)$$

This equation is distinguished from a Newtonian fluid by the term reflecting an influence of the rate of change of stress whose importance is weighed by a relaxation time. While this model and other models which are functions of the shear rate alone are capable of roughly modeling the response of a homogenous viscoelastic fluids at small deformations (i.e., within the linear viscoelastic region) they are entirely inadequate at describing the response of a fluid at large deformations (i.e., in the nonlinear regime) and non homogeneous fluids in which molecular orientation and texture play a role in their rheology. In an attempt to model the response of viscoelastic materials with texture, constitutive equations have been developed which account for the nonlinear nature of viscoelastic fluids and in some cases account for the role played by the development of molecular orientation and texture as seen in such fluids as LCPs and mixtures of immiscible fluids.

At this time attempts to model the rheology of textured fluids consisting of polymer blends have been limited to various empirical equations which predict blend viscosity as a function of the viscosity of the blend constituents. On the other hand, in the case of textured fluids consisting of LCPs, several constitutive equations have been developed to model the rheology of LCPs as a function of molecular orientation and flow history. Two of these models which have been widely used to model the rheology and molecular orientation of LCPs include the molecular theory of Doi [44] and the continuum model of Ericksen and Leslie [101,102]. These theories, which consider the LCP as a monodomain system (i.e., no texture is present), have been able to predict some of the rheological behavior displayed by LCPs, neither has proven adequate in their predictions. Ericksen's theory has been shown to be incapable of describing the transient shear flow behavior of a thermotropic copolyester [8,95], and the theory proposed by Doi is incapable of predicting both a yield stress and negative first normal stress differences. Recent attempts to account for the polydomain texture seen in LCPs using both Ericksen's and Doi's theories have used various averaging schemes in which the stress is an average of the contribution of stress from each domain (defined by a separate director) making up the system. While the modifications discussed above have improved certain aspects of their predictions, their inability to correctly account for the polydomain texture found in LCPs could play a crucial role in their failure to adequately model their rheological behavior.

Recently, a new constitutive equation proposed by Doi and Ohta [1] has been developed for mixtures of immiscible Newtonian fluids. This theory predicts the fluid response to a deformation as a function of the shear rate and the deformation and relaxation of the interface (drop deformation, coalescence and breakup) and has been shown to predict various aspects of textured fluid rheology often seen in both LCPs and polymer blends. In this work we are interested in the applicability of this theory to both LCPs and polymer

blends.

#### **2.4.1 Constitutive Equations for Textured Materials**

The theory proposed by Doi and Ohta is based on a two phase structure. It might be proposed that the complex polydomain texture in LCPs and two phase texture of polymer blends plays a significant and similar role in their rheology. It has been shown that the theory by Doi and Ohta predicts rheological behavior for a mixture of two immiscible Newtonian fluids which is similar in some respects to that of LCPs. The most interesting similarities are that this theory predicts yield stresses, nonlinear behavior (i.e., stress is never a linear function of strain), and a fluid which has no intrinsic time constant (scaling). The lack of an intrinsic time constant has been reported for several LCP systems and yield stresses have been reported for both LCPs and polymer blends. While there is limited data on the rheological behavior of LCP/thermoplastic systems and no correlation of this behavior to the development of the complex structure in these blends the Doi-Ohta theory might apply in modified form to mixtures of viscoelastic fluids such as LCPs and their blends with thermoplastics. The theory of Doi and Ohta will be considered in this section in detail as it was derived for a mixture of two immiscible Newtonian fluids.

##### **2.4.1.1 Derivation of Doi Ohta Equation**

In this section the theory by Doi and Ohta is reviewed. This theory is based on the observed behavior that when two immiscible fluids are sheared, a rather complex interface is formed due to the coagulation, rupture, and deformation of droplets. The dynamics and rheological properties of this system are discussed and a semi-phenomenological kinetic

equation is derived which describes the time evolution of droplet size and orientation, and also the macroscopic stress in a flow field. The theory is then shown to predict rheological properties such as a steady state viscosity which is independent of shear rate and a first normal stress difference which is nonzero and proportional to the magnitude of the shear rate.

As was mentioned above, the system considered in the development of the Doi-Ohta theory is that of two immiscible fluids having the same viscosity and density. The interface of the fluid is regarded as a mathematical surface with no thickness. The Reynolds number is assumed to be small enough so that the inertial effects are negligible. The theory is then based on the following formulation for the stress tensor developed from the theory of Kirkwood [219,220] and applied by Doi [221] for emulsions of two immiscible liquids having the same viscosity,  $\eta_o$ , and density,

$$\tau_{\alpha\beta} = -\eta_o (\kappa_{\alpha\beta} + \kappa_{\beta\alpha}) + \frac{\Gamma}{V} \int (n_\alpha n_\beta - \frac{1}{3} \delta_{\alpha\beta}) dS + p \delta_{\alpha\beta} \quad (2.9)$$

where  $\kappa_{\alpha\beta} = \partial \underline{v}_\alpha / \partial \underline{r}_\beta$  is the macroscopic velocity gradient,  $\Gamma$  is the interfacial surface tension,  $p \delta_{\alpha\beta}$  is the isotropic pressure, and the integral is over all the interfaces of surface  $S$  where  $n_\alpha n_\beta$  are the components of the normal to the surface in the system of volume  $V$ . The macroscopic fluid velocity  $\underline{v}$  is obtained by using the spatial average of the microscopic flow so that the intricate details associated with the characteristic size of the domains is removed. Equation 2.9 indicates that the stress due to the two phase nature of the system is determined by the tensor [220]

$$q_{\alpha\beta} = \frac{1}{V} \int (n_\alpha n_\beta - \frac{1}{3} \delta_{\alpha\beta}) dS \quad (2.10)$$

which is called the interface tensor. Doi and Ohta have derived the interface tensor

(Equation 2.10) for the macroscopic velocity field given by,

$$\bar{\mathbf{v}}(\mathbf{t}, \mathbf{r}) = \boldsymbol{\kappa}(\mathbf{t}) \cdot \mathbf{r} \quad (2.11)$$

and assuming an incompressible fluid where,

$$\text{div } \mathbf{v} = 0 \quad \text{or} \quad \text{Tr } \boldsymbol{\kappa} = \kappa_{\alpha\alpha} = 0. \quad (2.12)$$

The time evolution equation of the interface tensor (Eq. 2.10) is derived by considering that the interface tensor is determined by two factors. The first factor is the flow field which enlarges and orients the interface and the other is the interfacial tension which opposes these effects. The derivation then considers each of these effects separately so that

$$\frac{dq_{\alpha\beta}}{dt} = \left. \frac{dq_{\alpha\beta}}{dt} \right|_{\text{flow}} + \left. \frac{dq_{\alpha\beta}}{dt} \right|_{\text{interfacial tension}} \quad (2.13)$$

The following two sections show the derivation of the first term in Eq. 2.13 assuming the interfacial tension is negligible (i.e.,  $\Gamma = 0$ ) and the second term assuming that the macroscopic velocity gradient tensor is equal to zero (i.e.,  $\boldsymbol{\kappa} = 0$ ), respectively.

#### 2.4.1.2 Deformation by Macroscopic Flow

In order to derive the time evolution of the first term in Equation 2.13, Doi and Ohta considered the case of  $\Gamma = 0$ . Assuming that the viscosity of each phase is equal, every point in the material moves with the macroscopic velocity given by Eq. 2.12, and a point  $\mathbf{r}$  on the surface moves according to

$$\frac{d}{dt} \mathbf{r} = \boldsymbol{\kappa} \cdot \mathbf{r} \quad (2.14)$$

A unit vector normal to the interface can be shown to change according to

$$\frac{d}{dt} \mathbf{n} = -\boldsymbol{\kappa}^T \cdot \mathbf{n} + \boldsymbol{\kappa} : \mathbf{n} \mathbf{n} \mathbf{n} \quad (2.15)$$

and the surface area can be shown to change as

$$\frac{d}{dt} \Delta S = -\boldsymbol{\kappa} : \mathbf{n} \mathbf{n} \Delta S. \quad (2.16)$$

Thus

$$\frac{d}{dt} (\overline{\eta_\alpha \eta_\beta} \Delta S) = -\overline{\eta_\alpha \eta_\beta \kappa_{\mu\beta}} \Delta S - \overline{\eta_\beta \eta_\mu \kappa_{\mu\alpha}} \Delta S + \overline{\eta_\alpha \eta_\beta \eta_\mu \eta_\nu \kappa_{\mu\nu}} \Delta S \quad (2.17)$$

where  $\overline{\eta_\alpha \eta_\beta}$  is defined by

$$\overline{\eta_\alpha \eta_\beta} = \frac{1}{V} \int dS \eta_\alpha \eta_\beta \quad (2.18)$$

Then from Equation 2.16 it follows that

$$\frac{d}{dt} \overline{\eta_\alpha \eta_\beta} = -\overline{\eta_\alpha \eta_\mu \kappa_{\mu\beta}} - \overline{\eta_\beta \eta_\mu \kappa_{\mu\alpha}} + \overline{\eta_\alpha \eta_\beta \eta_\mu \eta_\nu \kappa_{\mu\nu}} \quad (2.19)$$

To get a closed equation for the second moment,  $\overline{\eta_\alpha \eta_\beta}$ , Doi and Ohta used a decoupling approximation as proposed by Doi [44] for the fourth moment  $\overline{\eta_\alpha \eta_\beta \eta_\mu \eta_\nu}$ :

$$\overline{\eta_\alpha \eta_\beta \eta_\mu \eta_\nu \kappa_{\mu\nu}} = A \overline{\eta_\alpha \eta_\beta} \cdot \overline{\eta_\mu \eta_\nu \kappa_{\mu\nu}}$$

i.e.,

$$\overline{\eta_\mu \eta_\nu \kappa_{\mu\nu}} = A \bar{1} \cdot \overline{\eta_\mu \eta_\nu \kappa_{\mu\nu}} \quad (2.20)$$

Where

$$\bar{1} = \frac{1}{V} \int dS \equiv Q \quad (2.21)$$

is the area of the interface per unit volume and  $A = 1/Q$ . Equation 2.20 now gives

$$\overline{\eta_\alpha \eta_\beta \eta_\mu \eta_\nu \kappa_{\mu\nu}} = \frac{1}{Q} \overline{\eta_\alpha \eta_\beta} \overline{\eta_\mu \eta_\nu \kappa_{\mu\nu}} \quad (2.22)$$

Now using Equation 2.22 and

$$\overline{\eta_\alpha \eta_\beta} = q_{\alpha\beta} + \frac{Q}{3} \delta_{\alpha\beta} \quad (2.23)$$

Equation (2.19) can be rewritten to yield the first term in Equation 2.13,

$$\left. \frac{dq_{\alpha\beta}}{dt} \right|_{flow} = -q_{\alpha\gamma} \kappa_{\gamma\beta} - q_{\beta\gamma} \kappa_{\gamma\alpha} + \frac{2}{3} \delta_{\alpha\beta} \kappa_{\mu\eta} q_{\mu\eta} - \frac{Q}{3} (\kappa_{\alpha\beta} + \kappa_{\beta\alpha}) + \frac{q_{\mu\nu} \kappa_{\mu\nu}}{Q} q_{\alpha\beta} \quad (2.24)$$

Similarly, by considering  $d\Delta S/dt$ , the time evolution of  $Q$  is:

$$\left. \frac{dQ}{dt} \right|_{flow} = -q_{\alpha\beta} \kappa_{\alpha\beta} \quad (2.25)$$

For special cases,  $q_{\alpha\beta}$  and  $Q$  can be calculated rigorously. By comparing such a result with those obtained by Equation 2.25, the accuracy of the decoupling approximation used has been estimated. Such a comparison has demonstrated that Equation 2.24 works quite well



in both shear and elongational flows.

#### 2.4.1.3 Relaxation by Interfacial Tension

The time evolution equations for  $q_{\alpha\beta}$  and  $Q$  have been obtained in the preceding section by neglecting interfacial tension to obtain the first term in Eq. 2.13. In this section it will be shown how Doi and Ohta derived the second term in Eq. 2.13 where the macroscopic velocity gradient is zero (i.e.,  $\kappa=0$ ) and the effect of the interfacial tension  $\Gamma$  drives the relaxation of the deformed interface.

Crudely speaking, the interfacial tension has two effects on the system: (i) it decreases the area of the interface, and (ii) it makes the system isotropic. The area is  $Q$ , and the degree of the anisotropy can be expressed by  $q_{\alpha\beta}/Q$ . Doi and Ohta have assumed (for lack of a better estimate and simplicity) a first order relaxation mechanism for the relaxation of the interfacial area and anisotropy:

$$\left. \frac{d}{dt} Q \right|_{relax} = -r_1 Q, \quad (2.26)$$

$$\left. \frac{d}{dt} \left( \frac{q_{\alpha\beta}}{Q} \right) \right|_{relax} = -r_2 \left( \frac{q_{\alpha\beta}}{Q} \right), \quad (2.27)$$

where  $r_1$  and  $r_2$  are the relaxation rates,  $r_1$  representing the decrease of the interfacial area (size relaxation), and  $r_2$  the relaxation of anisotropy (shape relaxation). These relaxation rates are in general determined by the viscosity  $\eta_o$ , the interfacial tension  $\Gamma$ , and the configuration of the interface. The configuration of the interface can be characterized by  $q_{\alpha\beta}$  and  $Q$ . Doi and Ohta then disregard the dependence on  $q_{\alpha\beta}$  and assume that relaxation rates  $r_1$  and  $r_2$  are determined by  $\eta_o$ ,  $\Gamma$ , and  $Q$ . Then by dimensional analysis

$$r_1 = c_1 \frac{\Gamma Q}{\eta_o}, \quad r_2 = c_2 \frac{\Gamma Q}{\eta_o} \quad (2.28)$$

where  $c_1$  and  $c_2$  are positive numbers which may depend on the volume fraction,  $\phi$ .

From Equations 2.26, 2.27 and 2.28 we have,

$$\left. \frac{\partial}{\partial \alpha} q_{\alpha\beta} \right|_{relax} = -\lambda Q q_{\alpha\beta}, \quad (2.29)$$

and

$$\left. \frac{\partial}{\partial \alpha} Q \right|_{relax} = -\lambda \mu Q^2, \quad (2.30)$$

where

$$\lambda = (c_1 + c_2) \Gamma / \eta_o \quad \text{and} \quad \mu = c_1 / (c_1 + c_2) \quad (2.31)$$

There are two mechanism which drive the relaxation of  $Q$ . The first mechanism is that due to shape relaxation of individual droplets (the interfacial area of an elongated droplet decreases as the droplet becomes spherical). The second mechanism is associated with droplet coagulation (the interfacial area decreases when two droplet coagulate to form a larger droplet). In dilute mixtures the shape relaxation occurs much faster than the size relaxation ( the relaxation due to coagulation) which would be infinitely slow. In the case of concentrated mixtures these two mechanisms are expected to occur with similar speed. This can be concluded if it is assumed that there is only one length scale in the system and therefore only one time scale. Based on this argument, Equation 2.30 assumes that the relaxation of  $Q$  is controlled by a single relaxation rate and no distinction is made between the relaxation caused by droplet coagulation and shape relaxation driven by interfacial tension.

In the absence of flow Eq. 2.29 indicates that the system will form a macroscopically phase separated state of  $Q=0$ . While this could occur in systems

containing 1:1 volume fractions (which would result in a bicontinuous phase), in systems where the volume fraction is not 1:1 the final state might not reach  $Q=0$ . This is due to the fact that once the droplets forming the minority phase become spherical no further relaxation can occur. Doi and Ohta have modified Equation 2.30 to account for this possibility

$$r_1 = c_1 \frac{\Gamma}{\eta_o} \left( \sum q_{\alpha\beta}^2 \right)^{1/2}, \quad (2.32)$$

which assures that the relaxation stops when the droplets of the minority phase become spherical.

There is only one dimensionless parameter ( $\mu$ ) found in Eqs. 2.29 and 2.30. If the system is characterized by three parameters  $\eta$ ,  $\Gamma$ , and  $\phi$ , then  $\mu$  might be a function of the volume fraction  $\phi$ . The dimensionless parameter represents the rate of the shape relaxation relative to the total relaxation rate. If  $\mu = 0$ , then the shape relaxation is rapid, and if  $\mu = 1$ , the shape relaxation is slow. In this case we might consider  $c_1$  to represent a function of the volume fraction of the dispersed phase so that at low volume fractions no coagulation takes place and the degree of anisotropy is low and the decrease in the interfacial area  $Q$  remains constant with  $\mu$  equal to zero ( $c_1$  is zero and  $r_1$  is zero). Doi and Ohta have regarded  $\mu$  as a phenomenological parameter.

#### 2.4.1.4 Constitutive Equation

Combining Equations 2.24, 2.25, 2.26, and 2.27 we have

$$\begin{aligned} \frac{dq_{\alpha\beta}}{dt} = & -q_{\alpha\gamma}\kappa_{\gamma\beta} - q_{\beta\gamma}\kappa_{\gamma\alpha} + \frac{2}{3}\delta_{\alpha\beta}\kappa_{\mu\eta}q_{\mu\eta} \\ & - \frac{Q}{3}(\kappa_{\alpha\beta} + \kappa_{\beta\alpha}) + \frac{q_{\mu\nu}\kappa_{\mu\nu}}{Q}q_{\alpha\beta} - \lambda Qq_{\alpha\beta}, \end{aligned} \quad (2.33)$$

$$\frac{dQ}{dt} = -q_{\alpha\beta}\kappa_{\alpha\beta} - \lambda\mu Q^2. \quad (2.34)$$

Equations 2.33 and 2.34 are the time evolution equation for the interface shape and size in flow. Given  $q_{\alpha\beta}$  and  $Q$ , the stress can be calculated using,

$$\tau_{\alpha\beta} = -\eta_o(\kappa_{\alpha\beta} + \kappa_{\beta\alpha}) + \Gamma q_{\alpha\beta} + p\delta_{\alpha\beta} \quad (2.35)$$

Thus the set of Eqs. 2.33, 2.34 and 2.35 give the rheological constitutive equation.

### 2.4.2 Scaling Property

The Doi-Ohta theory derived above has properties quite different from those of the usual viscoelastic materials like polymeric fluids. Consider for example the solution of Eqs. 2.33, and 2.34 for a given velocity gradient  $\kappa(t)$ :

$$\mathbf{q} = \mathbf{q}(t; [\kappa(t)]) \quad Q = Q(t; [\kappa(t)]) \quad (2.36)$$

Then it can be shown that under a different velocity gradient given by

$$\tilde{\kappa}(t) = c\kappa(ct) \quad (2.37)$$

where  $c$  is an arbitrary number, that the solution to Eqs. 2.33 and 2.34 is:

$$\mathbf{q}(t; [\tilde{\kappa}(t)]) = c\mathbf{q}(t; [c\kappa(t)]) \quad (2.38)$$

$$Q(t; [\tilde{\kappa}(t)]) = cQ(t; [c\kappa(t)]) \quad (2.39)$$

and from Eq. 2.9 that

$$\sigma(t;[\tilde{\kappa}(t)]) = c\sigma(t;[c\kappa(t)]) \quad (2.40)$$

where  $\sigma = \tau$ .

This equation states that the stress at time  $t$  under the velocity gradient  $\tilde{\kappa}(t) = c\kappa(ct)$  is  $c$  times larger than the stress at time  $ct$  under the velocity gradient  $\kappa(t)$ . The consequences and significance of this scaling relationship are discussed next as it applies to steady, transient and oscillatory shear flow.

### 2.4.3 Steady Shear Flow Predictions

Under steady shear flow with shear rate  $\dot{\gamma}$  in simple shear flow, the shear stress and the first normal stress differences are proportional to the shear rate:

$$\sigma_{yx} = \eta(\phi)\dot{\gamma} \quad \sigma_{xx} - \sigma_{yy} = \eta_N(\phi)|\dot{\gamma}| \quad (2.41)$$

where the constants  $\eta$  and  $\eta_N$  are functions of  $\mu$  and are shown in Figure 2.20. It follows immediately from Eq. 2.41 that the steady state viscosity is independent of shear rate (i.e., there is no shear thinning or shear thickening). This result should hold rigorously since it is a result of dimensional analysis: the steady-state viscosity should be determined by  $\Gamma$ ,  $\eta_0$ ,  $\phi$ , and  $\dot{\gamma}$ . This conclusion is only valid at steady state with respect to the breakup and coagulation of droplets. In dilute systems this result would not hold since there is a characteristic size of droplets which gives a shear rate dependent viscosity at the steady state.

Although the viscosity is independent of shear rate, this model shows other rather interesting rheological behavior. It can be shown that the first normal stress difference is

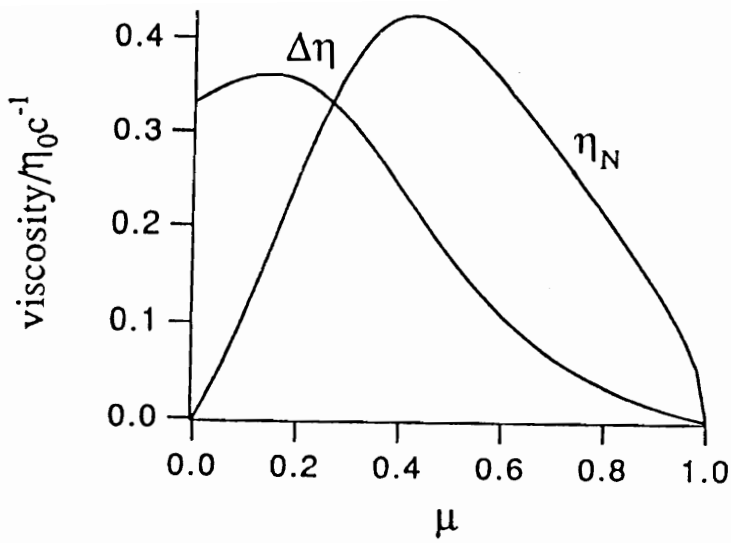


**Figure 2.20.** Extra shear viscosity  $\Delta\eta$  and the normal viscosity  $\eta_N$  for steady shear flow and  $\Delta\eta = \eta - \eta_0$  and  $c^{-1} = 1/(c_1 + c_2)$  and  $\eta_N$  is defined by Eq. 2.41 [1].

nonzero and proportional to  $|\dot{\gamma}|$ . This singular behavior is due to the fact that even at infinitely small shear rates the structure can change drastically.

#### 2.4.4 Transient Shear Flow Predictions

The predictions of the Doi-Ohta equations for transient shear flows show complex rheological responses not seen in the individual blend components (i.e., Newtonian). Consider the transient experiment where the shear rate is changed from  $\dot{\gamma}_1$  to  $\dot{\gamma}_2$  at time  $t = 0$  (see Figure 2.21). The shear stress calculated by the constitutive equation is then shown in Fig. 2.22. In Fig. 2.22  $\Delta\sigma$  is the extra shear stress due to the surface tension obtained from Eq. 11 by  $\Delta\sigma \equiv \sigma_{xy} - \eta_0 \dot{\gamma}$ . The growth curve can be superimposed if the stress  $\Delta\sigma$  is normalized by  $\Delta\sigma_1$ , the extra stress for the shear rate  $\dot{\gamma}_1$  and the time is normalized by  $1/\dot{\gamma}_1$ : i.e.,  $\Delta\sigma(t, \dot{\gamma}_1, \dot{\gamma}_2)$  is written as

$$\Delta\sigma(t, \dot{\gamma}_1, \dot{\gamma}_2) = \Delta\sigma_1(t, \dot{\gamma}_1 / \dot{\gamma}_2) \quad (2.42)$$

so that for a fixed value of  $\dot{\gamma}_1 / \dot{\gamma}_2$ , the plot of  $\Delta\sigma(t, \dot{\gamma}_1, \dot{\gamma}_2) / \Delta\sigma_1$  against  $\dot{\gamma}_1 t$ , becomes independent of the magnitude of  $\dot{\gamma}_1$ . This is a special case of the more general scaling relation described by Eqs. 2.38, 2.39, and 2.40. Fig. 2.23 shows the growth of the shear stress when a shear flow is started for an isotropic system. In Fig. 2.23 the time is scaled by  $\dot{\gamma}_0 = \lambda Q_0$  where  $Q_0$  is the surface area of the interface before the application of the flow.

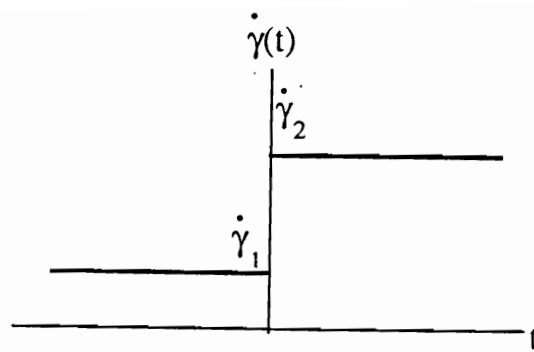


**Figure 2.21. Stepwise change of the shear rate [1].**



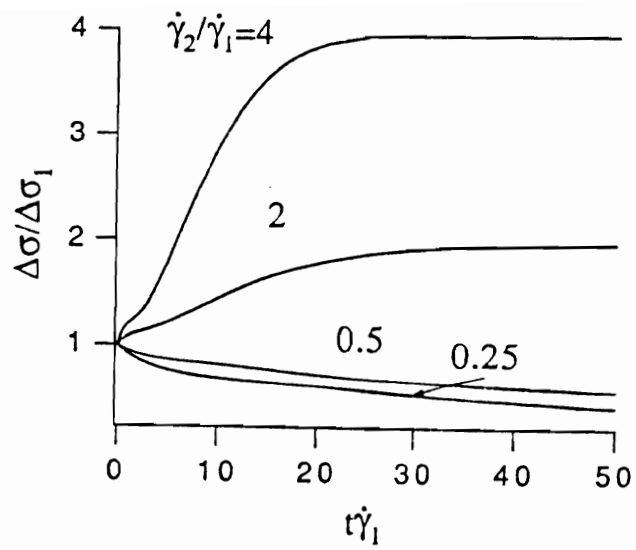


**Figure 2.22.** Calculated shear stress for a step change in the shear rate. The parameter  $\mu$  is chosen to be 0.9 [1].

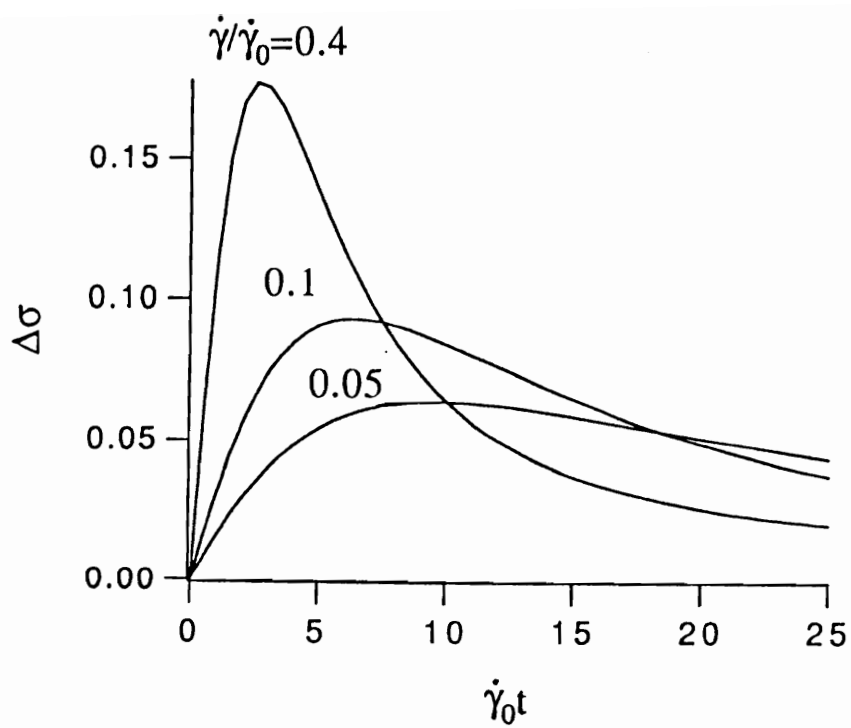


**Figure 2.23** Calculated shear stress when a shear flow of constant shear rate  $\dot{\gamma}$  is started for an isotropic system at time  $t = 0$ . The parameter  $\mu$  is chosen to be 0.9 [1].

### 2.4.5 Oscillatory Shear Flow Predictions

In an oscillatory shear flow, the shear strain changes with time according to:

$$\gamma(t) = \gamma_0 \sin(\omega t) \quad \text{or} \quad \dot{\gamma}(t) = \gamma_0 \omega \cos(\omega t) \quad (2.43)$$

At a condition of steady oscillation the stress is a function of  $\gamma_0$ ,  $t$ , and  $\omega$ , and can be written as

$$\sigma = \sigma(t, \gamma_0, \omega) \quad (2.44)$$

In the oscillatory flow described by

$$\tilde{\gamma}(t) = \gamma_0 \sin(c\omega t) \quad \text{or} \quad \tilde{\dot{\gamma}}(t) = \gamma_0 c \omega \cos(c\omega t) \quad (2.45)$$

the stress is obtained using Eq. 2.40

$$\sigma(t, \gamma_0, \omega) = c \sigma(t, \gamma_0, c\omega) \quad (2.46)$$

and the stress  $\sigma(t, \gamma_0, \omega)$  can be written as

$$\sigma(t, \gamma_0, \omega) = \omega \sigma(\gamma_0, \omega) \quad (2.47)$$

From these results it can be seen that a plot of  $\sigma / \omega$  versus the shear strain is independent of the frequency. Similarly to Eq 2.41, Eq. 2.47 can be obtained by dimensional analysis and should hold as long as the system is governed by hydrodynamics characterized by  $\eta_0$ ,  $\Gamma$ , and  $\phi$ .

In summary, the constitutive equation proposed by Doi and Ohta describes the rheology and texture of systems which, during flow, form complex patterns controlled by a mechanism of drop deformation, breakup, and coalescence. While this theory has been derived for mixtures of two immiscible Newtonian fluids, a similar mechanism as is mathematically described by the Doi-Ohta constitutive equation is seen in other textured fluids which include those consisting of polydomain LCPs and two component polymer blends. The rheology predicted by the Doi-Ohta constitutive equation shows some similarities to rheological phenomena seen in LCPs and polymer blends (e.g., yield stresses, scaling phenomena). Comparisons of predicted rheology and texture of textured fluids using the Doi-Ohta constitutive equation with experimental data have not been published at this time. An extension of this constitutive equation to systems such as LCPs and polymer blends and comparison of predicted to experimental data might prove useful in obtaining a better understanding of the rheological behavior and development of texture of these materials. A comparison of predicted and experimental results might also prove useful in evaluating the validity of the mechanism proposed the constitutive equation and its contribution to the material response to an applied deformation.

## 2.5 Research Objectives

In Chapter 1 textured fluids and their rheology were introduced along with the general objectives of this work intended to further the state of understanding of fluids with texture. In support of these objectives this chapter has reviewed the literature pertaining to these materials in order to gain a better understanding of the rheological phenomena associated with textured fluids and to give insight into the areas in which an understanding of them is lacking.

Several of the phenomena which have been observed in the textured fluids include yield stress, concentration and temperature dependence which cannot be explained in terms of various mixing rules, and transient shear and first normal stress difference behavior which is unique with respect to other homogenous systems (e.g., scaling with respect to strain, large strains before steady state is reached, and large overshoots).

In order to obtain a fundamental understanding of the rheological behavior of LCPs and TLCP/thermoplastic blends, a systematic study of their rheology is proposed here. In this section four objectives will be outlined with the intention of providing a better understanding of the rheological behavior and morphology of LCPs and TLCP/thermoplastic blends during flow.

**Objective 1:** The first objective of this research is to determine the role played by the LCO and a polydomain texture on the rheology of LCPs. In particular by using a nearly model, nematic lyotropic system it will be determined whether rheological behavior such as a three region flow curve, negative steady state first normal stress differences and oscillations at the startup of shear flow are truly common features of LCPs. This is done by comparing the rheology of an anisotropic and isotropic

solution where differences in rheology can be attributed to LCO and a polydomain texture.

**Objective 2:** The second objective of this research is to determine the role played by the two phase texture on the rheology of polymer blends as a function of viscosity ratio, surface tension, and concentration. Specifically, the rheology will be investigated using steady shear, dynamic oscillatory, and various transient experiments. Special attention will be given to comparisons of the rheology of polymer blends above the melting temperature of both blend constituents (with a texture ranging from a dispersed phase in the form of drops and fibrils to a co-continuous texture) with that of the neat blend constituents. This will be done in an attempt to isolate rheological behavior which can be attributed to the texture formed by the blends from that due to intermolecular interactions or chain entanglements as seen in both the blends and neat blend constituents.

**Objective 3:** The fourth objective of this research is to determine if the Doi-Ohta constitutive equation can quantitatively or qualitatively model the rheology of a mixture of nearly Newtonian fluids. Specifically, by using a model system consisting of an immiscible mixture of two polymers which are nearly Newtonian and by using rheological experiments in which the shear rate is lower than the longest relaxation time of the blend components ( $De < 1$ ), comparison of predicted and experimental rheology will be carried out.

## REFERENCES

1. Doi, M., and Ohta, T., *J. Chem. Phys.*, 95(2), 1242, 1991.
2. Moldenaers, P. and Mewis, J., ***J. Non Newt. Fl. Mech.***, 34, 359, 1990.
3. Wendorff, J. F., Finkleman, H., and Ringsdorf, H., ***J. Polym. Sci., Polym. Symp.***, 63, 245, 1968.
4. DeGennes, P. G., "The Physics of Liquid Crystals," Oxford University Press, London , 1974.
5. Miesowicz, M., ***Nature***, 158, 27, 1946.
6. Asada, T., Onogi, S. and Yanase, H., ***Pol. Eng. Sci.***, 24(5), 355, 1984.
7. Aoki, H., White, J. L., and Fellers, J. F., ***J. Appl. Pol. Sci.***, 23, 2293, 1979.
8. Onogi, S. and Asada, T., "Rheology", Vol. 1, G. Astarita, G. Marrucci, and L. Nicolais, eds., Plenum Press, New York, 1980.
9. Wissbrun, K. F., ***J. Rheol.***, 25(6), 619, 1981.
10. Fukada, E., and Date, M., ***Biorheology***, 1, 101, 1963.
11. Marchessault, R. H., Moorehead, F. F. and Walters, N. M., ***Nature***, 184, 632, 1959.
12. Hermans, J. Jr., ***J. Polym. Sci., Part C2***, 129, 1963.
13. Papkov, S. P., Kulichikhin, V. G., Kalmykova, V. D. and Malkin, A. Y., ***J. Polym. Sci. Polym. Phys. Ed.***, 12, 1753, 1974.
14. Yanase, H. and Asada, T., ***Mol. Cryst. Liq. Cryst.***, 153, 281, 1987.
15. Elliot, H. H., ***J. Appl. Pol. Sci.***, 13, 755, 1969.
16. Shimamura, K., White, J. L. and Fellers, J. F., ***J. Appl. Pol. Sci.***, 26, 2165, 1981.
17. Suto, S., White, J. L., and Fellers, J. F., ***Rheol. Acta***, 21, 62, 1982.
18. Sugiyama, H., Lewis, D. N., White, J. L., and Fellers, J. F., ***J. Appl. Pol. Sci.***, 30, 2329, 1985.

19. Kiss, G. and Porter, R. S., **J. Polym. Sci. :Polym. Symp.**, 65, 193, 1978.
20. Moldenaers, P. and Mewis, J., **J. Rheol.**, 30(3), 567, 1986.
21. Navard, P., **J. Pol. Sci.: Pol. Pys. Ed.**, 24, 435, 1986.
22. Kiss, G. and Porter, R. S., **J. Pol. Sci.: Pol. Phys. Ed.**, 18, 361, 1980.
23. Viola, G. G. and Baird, D. G., **J. Rheol.**, 30(3), 601, 1986.
24. Mewis, J. and Moldenaers, P., **Mol. Cryst. Liq. Cryst.**, 153, 291, 1987.
25. Doppert, H. L. and Picken, S. J., **Mol. Cryst. Liq. Cryst.**, 153, 109, 1987.
26. Grizzuti, N., Cavella, and Cicarelli, **J. Rheol.**, 34(8), 1293, 1990.
27. La Mantia, F. P., "Thermotropic Liquid Crystal Polymer Blends", Ed. F. P. La Mantia, Technomic Publishing Co., Pennsylvania, 1993.
28. Siegman, A., Dagan, A., and Kenig, S., **Polymer**, 26, 1325, 1985.
29. Cogswell, F. N., Griffen, B. P., and Rose, J. B., May 31, 1983. U.S. patent 4,386,174.
30. Cogswell, F. N., Griffen, B. P., and Rose, J. B. February 21, 1984. U.S. patent 4,433,083.
31. Cogswell, F. N., Griffen, B. P., and Rose, J. B. February 21, 1984. U.S. patent 4,438,236.
32. Blizard, K. G. and Baird, D. G., **Polym. Eng. Sci.**, 27(9), 653, 1987.
33. Nobile, M. R., Amendola, E., Nicolais, L., Acierno, D., and Carfagna, C., **Polym. Engr. Sci.**, 29(4), 244, 1989.
34. Mehta A., and Isayev, A. I., **Polym. Engr. and Sci.**, 31(13), 971, 1991.
35. Isayev, A. I., and Modic, M., **Polym. Composites**, 8(3), 158, 1987.
36. Kohli, A., Chung, N. and Weiss, R. A., **Polym. Engr. and Sci.**, 29(9), 573, 1989.
37. Crevecoer, G., Ph. D. Thesis, Katholiede Universiteit Leuven, 1991.
38. Weiss, R. A., Huh, W., and Nicolais, L., **Polym. Engr. and Sci.**, 27(9), 684, 1987.



39. Blizard, K. G. and Baird, D. G., **Pol. Engr. Sci.**, Vol 27(9), 653, 1987.
40. James, S. G., Donald, A. M., and MacDonald, W. A., **Mol. Cryst. Liq. Cryst.**, 153:491, 1987.
41. Ericksen, J. L., **Arch. Ration. Mech. Anal.**, 4, 231, 1964.
42. Leslie, F. M., **Arch. Ration. Mech. Anal.**, 28, 265, 1968.
43. Parodi, J. **Phys. (Paris)**, 31, 581, 1970.
44. Doi, M., **J. Pol. Sci. Pol. Phys. Ed.**, 19, 229, 1981.
45. Moldenaers, P. and Mewis, J. **Rheol.** 37(2), 367, 1993.
46. Baird, D. G., in "Liquid Crystalline Order in Polymers," A. Blumstein ed., Academic Press, 1978.
47. Wilson, T., PhD Dissertation, Virginia Polytechnic Institute and State University, Blacksburg, VA, 1991.
48. Ferry, J. D., "Viscoelastic Properties of Polymers", 3rd ed., Wiley, New York, 1980.
49. Bird, R. B., Armstrong, r. C., Hassager, O., "dynamics of Polymeric Liquids," Vol. 1, John Wiley Pub., New York, 1977. Vol. 1, 2nd ed., 1987.
50. Tanner, R. I., "Engineering Rheology," Oxford University Press, New York, 1985.
51. Baek, S.-G., Magda, J. J., and Larson, R. G., **J. Rheol.**, 37(6), 1993.
52. Viola, G. G, PhD Dissertation, Virginia Polytechnic Institute and State University, Blacksburg, VA, 1985.
53. Barnes, H. A., and Walters, K., **Rheol. Acta**, 24, 323, 1985.
54. Astarita, G., **J. Rheol.**, 34, 275, 1990.
55. Schurtz, J., **Rheol. Acta**, 29, 170, 1990.
56. Evans, D. I., and Haisman, J. **Text. Stud.** 10, 347, 1979.
57. Evans, D. I., **J. Rheol.**, 36(7), 1313, 1992.
58. Schurz, J., **J. Rheol.**, 36(7), 1319, 1992.

59. Mewis, J. and Moldenaers, P., **Chem. Eng. Commun.**, 53, 33, 1987.
60. Larson, R. G., and Mead, D. W., **J. Rheol.**, 33(8), 1251, 1989.
61. Baird, D. G., **J. Appl. Pol. Sci.**, 13, 755, 1978.
62. Baird, D. G., and Ballman, R. L., **J. Rheol.**, 23(4), 505, 1979.
63. Gotsis, A. D. and Baird, D. G., **J. Rheol.**, 29(5), 539, 1985.
64. Tuttle, J. R., Bartony, H. E., and Lenz, R. W., **Polym. Eng. Sci.**, 27(15), 2256, 1987.
65. Kalika, D. S., Giles, D. W., and Denn, M. M., **J. Rheol.**, 34(2), 139, 1990.
66. Mackley, M. R., **Mol. Cryst. Liq. Cryst.**, 153, 249, 1987.
67. Kalika, D. S., Nuel, L. and Denn, M. M., **J. Rheol.**, 33(7), 1059, 1989.
68. Mishra, R. K., **Mol. Cryst. Liq. Cryst.**, 29, 201, 1975.
69. Kulichikhin, V. G., Kudryavtsev, G. I., and Papkov, S. P., **Intern. J. Polymeric Mater.**, 9, 1982.
70. Baird, D. G., **J. Rheol.**, 24(4), 465, 1980.
71. Aharoni, S. M., **Polymer**, 21, 1413, 1980.
72. Bahar, I. and Erman, B., **J. pol. Sci.: Part B: Pol. Phys.**, 24, 1361, 1986.
73. Flory, P. J. and Ronca, G., **Mol. Cryst. Liq. Cryst.**, 54, 289, 1979.
74. Porter, R. S. and Johnson, J. F., "Rheology," Erich ed., Vol. 4, Ch. 5, Academic Press, New York, 1967.
75. Kiss, G., **J. Rheol.**, 30(3), 585, 1986.
76. Chen, J., White, J. L. and Kyu, T., **SPE ANTEC**, 723, 1986.
77. Fujiyama, M., **J. Appl. Pol. Sci.**, 40, 67, 1990.
78. Horio, M., Kamei, E., and Matsumobu, K., **J. Soc. Rheol.**, Japan, 36, 27, 1988.
79. Moldenaers, P., Yanase, H., and Mewis, J., **ACS Symp. Ser.**, 435, 370, 1990.

80. Wissbrun, K. F. and Griffin, A. C., **J. Polym. Sci.:Polym. Phys. Ed.**, 20, 1835, 1982.
81. Acierno, D. La Mantia, F. P., Polizzotti, G., Ciferri, A., Krigbaum, W. R. and Kotek, R., **J. Pol. Sci. Pol. Phys. Ed.**, 21, 2027, 1983.
82. Blumstein, A., Thomas, O. and Kumar, S., **J. Pol. Sci. Pol. Phys. Ed.**, 24, 27, 1986.
83. Wunder, S. L., Ramachandran, S., Gochanour, C. R. and Weinberg, M., **Macromolecules**, 19, 1696, 1986.
84. Bickel, a., Shaw, M. T., and Samulski, E. T., **J. Rheol.**, 28, 647, 1984.
85. Yang, J. T., **J. Am. Chem. Soc.**, 80, 1783, 1958.
86. Yang, J. T., **J. Am. Chem. Soc.**, 81, 3902, 1959.
87. Miller, W. G., Wu, C. C., Wee, E. L., Santee, G. L., Rai, J. H., and Goebel, K. G., **Pure Appl. Chem.**, 38, 25, 1974.
88. Iizuka, E., **Mol. Cryst. Liq. Cryst.**, 25, 287, 1974.
89. Wong, C. P. and Berry, G. C., **Polymer**, 20, 229, 1979.
90. Jackson, W. J. Jr. and Kuhfuss, H. F., **J. Pol. Sci. Pol. Chem. Ed.**, 14, 2043, 1976.
91. Jerman, R. and Baird, D. G., **J. Rheol.**, 25(2), 275, 1981.
92. Jackson, W. J. Jr., **Br. Polym. J.**, 12(4), 154, 1980.
93. Metzner, A. B., **J. Rheol.**, 29(6), 739, 1985.
94. Kiss, G. and Porter, R. S., **Mol. Cryst. Liq. Cryst.**, 60, 267, 1980.
95. Ernst, B. and Navard, P., **Macromolecules**, 22, 1419, 1989.
96. Wissbrun, K. F., **Br. Polym. J.**, 12(4), 163, 1980.
97. Gotsis, A. D., M.S. Thesis, Virginia Polytechnic Institute and State University, Blacksburg VA, 1984.
98. Baird, D. G., Gotsis, A. D. and Viola, G. G., **Polym. Prepr. Am. Chem. Soc. Div. Polym. Chem.**, 24(2), 292, 1983.

99. Gotsis, A. D., **Rheol. Acta.**, 25, 275, 1986.
100. Ogagawa, A. Cox, R. G. and Mason, S. G., **J. Colloid Interface Sci.**, 45, 303, 1973.
101. Leslie, F. M., *Advances in Liquid Crystals*, Vol. 4, Ed. by G. H. Brown, Academic Press, New York, 1979.
102. Erickson, J. L., "The Mechanics of Viscoelastic Fluids," Ed. by R. S. Rivlin, (AMD Vol. 22), ASME, New York, 1977.
103. Currie, P. K., **Mol. Cryst. Liq. Cryst.**, 73, 1, 1981.
104. Chaffey, E. and Porter, R. S., **J. Rheol.**, 30(3), 601, 1986.
105. Marrucci, G. and Maffettone, P. L., **Macromolecules**, 22, 4076, 1989.
106. Larson, R. G., **Macromolecules**, 23, 3983, 1990.
107. Duke, R. W., and Chapoy, L. L., **Rheol. Acta**, 15, 548, 1976.
108. Hutton, J. F., **Rheol. Acta**, 14, 979, 1979.
109. Lem, K. W. and Han, C. D., **J. Rheol.**, 27(3), 263, 1982.
110. Baird, D. G., in "Polymeric Liquid Crystals," A. Blumstein ed., Plenum Press, New York, 1985.
111. Larson, R. G. and Mead, D. W., **J. Rheol.**, 32(3), 185, 1989.
112. Prilutski, G. M., Ph.D. Dissertation, University of Delaware, 1984.
113. Burghardt, W. R., **J. Rheol.**, 35(1), 49, 1991.
114. Burghardt, W. R., **J. Rheol.**, 35(1), 49, 1985.
115. Cogswell, F. N., **Br. Polym. J.**, December, 170, 1980.
116. Griffin, A. C. and Haven, S. J., **J. Pol. Sci. Pol. Phys. Ed.**, 19, 951, 1981.
117. Metzner, A. B. and Prilutski, G. M., **J. Rheol.**, 30(3), 661, 1986.
118. Kim, W. N., and Denn, M. M., **J. Rheol.**, 36(8) 1992.
119. Hinch, E. J., and Leal, L.G., **J. Fluid Mech.**, 51, 753, 1973.

120. Van Oene, H., "Polymer Blends", Vol. 1., Ed. Paul and Newman, Acad. Press, New York, 1978.
121. Han, C. D. and Kim, Y. W., **Trans. Soc. Rheol.** 19, 245, 1975.
122. Blizard, K. G., Masters Thesis, Virginia Polytechnic Institute and State University, Blacksburg, VA, 1986.
123. Ablazova, T. I., Tsebrenko, M. B., Yudin, A. B., Vinogradov, G. V., and Yarlykov, B. V., **Polymer**, 19, 1781, 1975.
124. Vinogradov, G. V., Yarlykov, B. V., Tsebrenko, M. V., Yudin, A. V., and Ablazova, T. I., **Polymer**, 16, 609, 1975.
125. Froix, M. F. July 3, 1980. U.S. patent 4,460735.
126. La Mantia, F. P., and Valenza, A., **Makromol. Chem., Macromol. Symp.** 56, 151, 1992.
127. Acierno, D., Amendola, E., Nicolais, L., and Nobile, N. R., **Mol. Cryst. Liq. Cryst.**, 153:553, 1987.
128. Noble, M. R., Amendola, E., Nicolais, L., Acierno, D., and Carfagna, C., **Polym. Eng. Sci.**, 29(4), 244, 1989.
129. Shuang, P., Kyu, T., and White, J. L., **Polym. Eng. Sci.**, 28(17), 1095, 1989.
130. Ysayev, A. I, and Modic, M., **Polym. Composites**, 8(3):158, 1987.
131. Kiss, G., **Polym. Eng. Sci.**, 27, 412, 1987.
132. Lee, B. L., **Polym. Eng. Sci.**, 28, 1107, 1988.
133. Zhuang, P., Kyu, T., and White, J. L., **Polym. Eng. Sci.**, 28, 1095, 1988.
134. Malik, T. M., Carreau, P.J., and Chapleau, N., **Polym. Eng. Sci.**, 29, 600, 1989.
135. Valenza, A., La Mantia, F. P., Paci, M., and Magagnini, P. L., *Int. Polym. Process.*, in press.
136. Nobile, M. R., Acierno, D., Incarnato, L., Amendola, E., Nicolais, L., and Carfagna, C., *J. Appl. Polym. Sci.*, 41, 2723, 1990.
137. Brinkman, T., Heidemeyer, P., and Michaeli, W., The Sixth Annual Meeting, PPS, Nizza, 1990.

138. Kulichikhin, V. G., Vasil'eva, O. V., Litvinov, I. A., Parsamyan, I. L., and Plate, N. A., *J. Appl. Polym. Sci.*, 42, 363, 1991.
139. Chung, T. S., *SPE ANTEC*, 1987.
140. La Mantia, F. P., Valenza, A., Paci, M., and Magagnini, P. L., *Rheol. Acta*, 28, 417, 1989.
141. La Mantia, F. P., Valenza, Magagnini, P. L., and Paci, M., *Polym. Eng. Sci.*, 30, 7, 1990.
142. Siegmman, A., Dagan, A., and Kenig, S., *Polymer*, 7, 1071, 1988.
143. Taylor, G. I., *Proc. R. Soc.*, A146, 501, 1934.
144. Tsebrenko, M. V., Rezanova, N. M., and Vinogradov, G. V., *Polym. Eng. Sci.*, 20, 1023, 1980.
145. White, J. L., and Min, K., *Adv. Polym. Technol.*, 5, 225, 1986.
146. La Mantia, F. P., Saiu, M., Valenza, Paci, M., and Magagnini, P. L., *Eur. Polym. J.*, 26, 323, 1990.
147. Han, "Multiphase Flow in Polymer Processing", Academic Press, New York, 1981.
148. Kohli, A., Chung, N., and Weiss, R. A., *Polym. Eng. Sci.*, 29, 573, 1989.
149. Beery, D., Siegmman, A., and Kenig, S., *J. Mat. Sci. Lett.*, 7, 1071, 1988.
150. Nobile, M. R., Arcieno, D., Incarnato, L., and Nicolais, D., *J. Rheol.*, 34(7), 1181, 1990.
151. Biing-Lin, L., *Polym. Eng. Sci.*, 28(17), 1988.
152. Plochocki, A. P., Ch. 21 in "Polymer Blends", (D.R. Paul and S. Newman, Eds.) Academic Press, New York, 1978.
153. Heitmiller, R. F., Naar, R. Z., and Zabusky, H. H., *Appl. Polym. Sci.*, 8, 873, 1964.
154. Hayashida, K., in "Proc. Fifth Intern. Congr. Rheol., Vol. 4, University of Tokyo Press, Tokyo, 1970.
155. Carley, J. F., *Polym. Eng. Sci.*, 21, 249, 1981.

156. Hasin, Z., in "Second-order effects in Elasticity Plasticity and Fluid Dynamics" (M. Reiner and D. Abir, eds.) Mcmillan, New York, 1964.
157. Bigg, D. M., **Polym. Eng. Sci.**, 22, 512, 1982.
158. Rosen, M. J., "Sufactants and Interfacial Phenomena", 2nd Ed., Ch. 6 and 9, John Wiley & Sons, New York, 1989.
159. Pisipati, R. M., Ph.D. Dissertation, Virginia Polytechnic Institute and State University, Blacksburg, VA, 1983.
160. Geisbusch, P., and Menges, G., SPE 36th ANTEC 113, 1978.
161. Goel, D. C., **Polym. Eng. Sci.**, 20, 103, 1982.
162. Chapman, F. M., and Lee, T. S., SPE J. 26, 37, 1970.
163. Onogi, S., and Matsumoto, T., **Poly. Eng. Rev.**, 1,44, 1981.
164. Kitano, T., Nishimura, T., Kataoka, T., and Sakai, T., **Rheol. Acta.**, 19, 671, 1980.
165. Lobe, V. M., and White, J. L., **Polym. Eng. Sci.** Report, 118, Univ. of Tennessee.
166. Schmidt, L. R., GE Report 76CRD202, Aug. 1976.
167. Faulkner, D. L., and Schmidt, L. R., GE Report 76CRD200, Aug. 1976.
168. Tanaka, H., and White, J. L., **Polym. Eng. Sci.**, 20, 949, 1980.
169. Kataoka, T., Kitano, T., Sasahara, M., and Nishijima, K., **Rheol. Acta**, 17, 149, 1978.
170. Kataoka, T., Kitano, T., Oyanagi, Y., and Sasahara, M., **Rheol. Acta**, 18, 635, 1979.
171. Nakajima, N., and Collins, E. A., **Rubber Chem. Tech.**, 48, 615, 1975.
172. White, J. L., and Crowder, J. W., **J. Appl. Polym. Sci.**, 18, 1013, 1974.
173. White, J. L., Czarnecki, L., and Tanaka, H., **Rubber Chem. Tech.**, 53, 823, 1980.
174. Minagawa, N., and White, J. L., **J. Appl. Polym. Sci.**, 20, 501, 1976.

175. Matsumoto, T., Hitomi, C., and Onogi, S., **Trans. Soc. Rheol.**, 19, 541, 1975.
176. Chaffey, C. E., **Ann. Rev. Matl. Sci.**, 13, 1983.
177. Chaffey, C. E., Proc. 2nd. World Congress of Chemical Engineering, Montreal, Vol. VI, 301, 1981.
178. Fisa, B. and Utracki, L. A., NRCC-IMRI Symposium on Rheology of Polymers, 65th CIC Chem. Conf., Toronto, May, 1982.
179. Han, C. D., Weghe, T. V. D., Shete, P., and Haw, J. R., **Polym. Eng. Sci.**, 21, 196, 1981.
180. Han, C. D., Sandford, C., and Yoo, H. J., **Polym. Eng. Sci.**, 18, 849, 1978.
181. Crowson, R. J., Folkes, M. J., and Bright, P. F., **Polym. Eng. Sci.**, 20, 925, 1980.
182. Chan, Y., White, J. L., and Oyanagi, Y., **J. Rheol.** 22, 507, 1978.
183. Czarnecki, L., and White, J. L., **J. Appl. Polym. Sci.**, 25, 1217, 1980.
184. Kitano, T., and Kataoka, T., **Rheol. Acta.**, 20, 403, 1981.
185. Mutel, A. T., and Kamal, M. R., NRCC-IMRI Mini-Symposium on 'Composites-82', Montreal, Nov. 1982.
186. Boira, M. S., and Chaffey, C. E., **Polym. Eng. Sci.**, 17, 715, 1977.
187. Beecraft, M. L., and Metzner, A. B., **J. Rheology**, 36(1), 1992.
188. Moskal, E. A., SPE-RETEC, Oakbrook Ill., Oct. 2-4, Paper 'H-1", 1979.
189. White, J. L., and Oyanagi, Y., SPE ANTEC, 35, 290, 1977.
190. Charier, J. M., and Rieger, J. M., **Fiber Sci. Tech.**, 7, 161, 1979.
191. Kubat, J., and Stromwall, H. E., **Plast. Rubber Process**, 5, 45, 1980.
192. Kuntson, B. A., White, J. L., and K. B., Abbas, **Rheology**, 3, 83, 1980.
193. Wu, S. **Polym. Engr. Sci.**, 19, 638, 1979.
194. Mewis, J., and Metzner, A. B., **J. Fluid Mech.**, 62, 593, 1974.
195. Burghardt, W. R. and Fuller, G. G., **Macromolecules**, 24, 2546, 1991.



196. Asada, T., Tanaka, T., and Onogi, S., **J. Appl. Polym. Sci. Appl. Polym. Symp.**, 41, 229, 1985.
197. Gleeson, J. T., Larson, R. G., Kiss, G., and Cladis, P. E., **Liq. Cryst.**, 11, 341, 1992.
198. Mortier, M., Moldenaers, P., and Mewis, J., "Theoretical and Applied Rheology", edited by P. Moldenaers and R. Keunings, Proc. XIth Int. Congr. Rheology, Brussels, Belgium, Aug. 17-21, Elsevier, New York, 1992.
199. Marsano, E., Carpaneto, L., Ciferri, A., and Wu, Y., **Liq. Cryst.** 3, 1561, 1988.
200. Yang, I.-K., and Shine, A., **J. Rheol.**, 36, 1079, 1992.
201. Yang, I.-K., and Shine, A., **Macromolecules**, 26 1529, 1993.
202. Einaga, Y., Berry, G. C., and Chu, S. G., **J. Polym. Sci. Polym. Phys. Ed.** 17, 239, 1985.
203. Srinivasarao, M., and Berry, G. C., **J. Rheol.**, 35, 379, 1991.
204. Berry, G. C., **J. Rheol.**, 35, 943, 1991.
205. Ernst, B., Denn, M. M., Pierini, P., Rochefort, W. E., **J. Rheol.**, 36, 289, 1992.
206. Chow, A. W., Hamlin, R. D., Ylitalo, C. M., **Macromolecules**, 25, 7135, 1992.
207. Kulichkhin, V. G., **Mol. Cryst. Liq. Cryst.**, 169, 51, 1989.
208. Picken, S., Aerts, Visser, R., and Northolt, M. G., **Liq. Cryst.**, 3, 1073, 1988.
209. Picken, S., Aerts, J., Doppert, H. L., Reuvers A. J., and Northolt, M. G., **Macromolecules**, 24, 1366, 1991.
210. Wissbrun, K. F., **Brit. Polym. J.**, 12, 163, 1980.
211. Prasadaraao, M., Pearce, E. M., and Han, C. D., **J. Appl. Polym. Sci.**, 27, 1343, 1982.
215. Srinivasarao, M., Garay, R. O., Winter, H. H., and Stein, R. S., **Mol. Cryst. Liq. Cryst.**, 223, 29, 1992.
216. Giles, D. W., and Denn, M. M., **J. Rheol.**, to be published, 1993.
217. Kim, S. S. and C. D. Han, **J. Rheol.**, 37(5), 1993.

- 218. Kirkwood, J. G., **Rec. Trac. Chim.**, 68, 649, 1949.
- 220. Erpenbeck, J. J., and Kirkwood, J. G., **J. Chem. Phys.**, 38, 1023, 1963.
- 221. Doi, M. in, "Physics of Complex and Supramolecular Fluids", S. A. Safran and N. A. Clark, John Wiley & Sons, New York, 1987.
- 222. Press, W. H., Flannery, B. P., Teukolsky, S. A., and Vetterling, W. T., "Numerical Recipes", Cambridge University Press, New York, 1987.
- 223. Sukhadia, A. M., PhD Dissertation, Virginia Polytechnic Institute and State University, Blacksburg, VA, 1991.
- 224. Ciferri, A., Krigbaum, W. R., and Meyer, R. B., "Polymeric Liquid Crystals", Academic Press (1982).

### 3.0 Rheological Properties of Liquid Crystalline Polymers

#### Preface

This chapter addresses the first objective of this thesis. The role played by liquid crystalline order (LCO) and a polydomain texture on the rheology of a liquid crystalline polymer (LCP) is investigated. In particular, by using a nematic lyotropic system it will be determined whether rheological behavior such as a three region flow curve, negative steady state first normal stress differences and oscillations of the stress during the start up of shear flow are truly common features of LCPs. This is done by comparing the rheology of an anisotropic solution to that of an isotropic solution where differences in rheology can be attributed to liquid crystalline order and a polydomain texture. This chapter is organized as a manuscript which will be submitted to the *Journal of Rheology* for publication.

## Rheological properties of poly-p-phenyleneterephthalamide/H<sub>2</sub>SO<sub>4</sub> solutions

G. K. Guenther, D. G. Baird and R. M. Davis

*Virginia Polytechnic Institute & State University, Department of Chemical Engineering,  
Polymeric Materials and Interfaces Laboratory, Blacksburg, VA 24061-2011*

### Synopsis

The rheological properties of solutions of poly-p-phenyleneterephthalamide (PPT) in sulfuric acid (H<sub>2</sub>SO<sub>4</sub>) were studied in both the anisotropic and isotropic states to determine whether certain behavior could be attributed to liquid crystalline order. The state of the solutions was determined using polarized light intensity measurements as a function of temperature and concentration. The solution at a PPT concentration of 6.7 wt. % was isotropic over all temperature ranges as it did not transmit polarized light. At a concentration of 12.6 wt. % PPT the state of the solution was found to be largely anisotropic at temperatures ranging from 53 to 65 °C by a peak in the intensity of transmitted polarized light as a function of temperature. Several of the rheological phenomena commonly attributed to liquid crystalline order in polymers (e.g., three region flow curve, negative steady state first normal stress difference ( $N_1$ ), and oscillatory behavior at the start up of steady shear flow) were not observed in the 12.6 wt. % solution at 60 °C. The rheological behavior of the anisotropic and isotropic solution was found to be similar. The solution in both its anisotropic and isotropic state exhibited a two region flow curve (Newtonian plateau and shear thinning region at rates ranging from  $10^{-4}$  to  $10^2$  sec<sup>-1</sup>), a positive steady state first normal stress difference which increased with shear rate, and a transient shear stress which displayed a single overshoot before reaching a steady state value. This work showed that the presence of liquid crystalline order was by itself not a sufficient condition for the observation of rheological phenomena such as a three region flow curve, negative  $N_1$ , and oscillatory behavior at the start up of shear flow.

### 3.1 INTRODUCTION

The study of liquid crystalline polymer (LCP) rheology has been the subject of much interest and some controversy over the past two decades as was first recognized in early reviews [Baird (1978b); Wissbrun (1981)]. The fact that LCP rheology is much more complex than that of isotropic polymeric fluids is revealed by substantial literature on this subject [LaMantia (1993)], which as of yet, has not produced a fundamental understanding of LCP flow behavior [Sigillo and Grizzuti (1994)].

Academic and industrial interest in liquid crystalline polymers stems from their use in fibers with exceptionally high modulus and strength [Preston (1975); Ciferri *et al.* (1977)]. Other useful properties attributed to some LCPs include low melt viscosity, low thermal expansion coefficient, high use temperatures, excellent solvent resistance, and often low gas permeability [Chung (1986); Chiou and Paul (1987); LaMantia (1993)]. Some of the most recent interest in LCPs stems from the ability to use them as reinforcing agents in thermoplastic matrices [Dutta *et al.* (1990)].

Some of the rheological phenomena attributed to liquid crystalline order in polymers and not seen in isotropic polymeric liquids include apparent yield stresses [Aoki *et al.* (1979); Wissbrun (1981); Asada *et al.* (1984)], negative steady state first normal stress differences ( $N_1$ ) [Kiss and Porter (1978); Kiss and Porter (1980); Moldenaers and Mewis (1986); Navard (1986), Gotsis and Baird (1985)], and oscillatory behavior following the inception and stepwise change of simple shear flow [Mewis and Moldenaers (1987); Doppert and Picken (1987); Grizzuti *et al.* (1990)]. While some LCPs like poly( $\gamma$ -benzyl-L-glutamate), PBLG, in m-cresol consistently display some of the above mentioned behavior, others like hydroxypropylcellulose (HPC) in  $H_2O$  [Grizzuti *et al.* (1990)] and poly-p-phenylene terephthalamide in sulfuric acid (PPT/ $H_2SO_4$ ) [Baird (1978a); Viola (1985)] do not. The lack of generality of these reported phenomena in the same or similar

systems [Sigillo and Grizzuti (1994)] adds to the complexity in understanding the rheology of these materials.

The high degree of molecular order or liquid crystalline order (LCO) in LCPs is almost never found to be uniform on a macroscopic scale, but instead LCPs are believed to consist of many micro-size "domains" within which LCO exists and as a whole form a "polydomain" texture [Onogi and Asada (1980)]. Because a microstructure exists during flow, LCPs fall into a class of materials referred to as "textured fluids". Under an applied flow field textured fluids undergo complex structural changes and as a consequence may exhibit rheological properties which are a function of their texture [Doi and Ohta (1987)].

The shear rate dependence of the viscosity reported for some LCPs was tentatively attributed to "domains" found in these materials by Onogi and Asada (1980). The domain concept was used to account for the flow behavior of lyotropic nematic or cholesteric polymers which display a three region flow curve. The three region flow curve was explained by Onogi and Asada as the evolution of domains from a piled domain structure at low shear rates (region I shear thinning) to a dispersed polydomain structure at intermediate shear rates (region II Newtonian plateau) and, finally, to a monodomain (region III shear thinning) as the shear rate was increased further. The presence of an apparent yield stress (i.e., region I shear thinning as described by Onogi and Asada) was reported for PPT systems by Aoki *et al.* (1979). In an investigation by Baird (1978a) the presence of an apparent yield stress in the PPT system was attributed to coagulation of the sample due to the limited solubility of PPT in  $H_2SO_4$  in the presence of moisture. A Newtonian plateau was observed when coagulation was prevented by exclusion of moisture.

The existence of negative steady state first normal stress difference values was reported for lyotropic systems (e.g., PBLG and HPC) [Kiss and Porter (1978); Kiss and Porter (1980); Moldenaers and Mewis (1986); Navard (1986)]. The reported negative first

normal stress difference for some LCPs corresponds to a fluid, which when sheared between parallel plates, pulls the plates together and is contrary to what happens for most polymeric systems. In the work by Kiss and Porter (1980) using a solution of PBLG in m-cresol, negative  $N_1$  values were observed at shear rates between 20 and 700  $\text{sec}^{-1}$  while positive values were observed at shear rates below and above this region. An explanation of this phenomenon was given by Marrucci and Maffettone (1989) in which the behavior was attributed to changes in the dynamics of director orientation in nematic materials. This theory described the occurrence of negative  $N_1$  values as the transition from directors which are "tumbling" at low to intermediate shear rates to one where the directors were aligning in the flow direction. The ability of directors to tumble was linked to an imbalance between the orienting effect of shear flow induced torque on the director and the nematic potential which tried to restore an equilibrium orientation distribution.

Thermotropic systems were reported to show negative values of  $N_1$ . In studies by Wissbrun (1980), Baird *et al.* (1983), Gotsis (1984), and Gotsis and Baird (1986) negative transient and steady state values of the first normal stress difference were reported for a copolyester of hydroxybenzoic acid (HBA) and poly(ethylene terephthalate) (PET). In the investigation by Gotsis and Baird (1986) possible explanations for the observed negative steady state values of the first normal stress difference at low shear rates included the existence of a suspension of crystalline material in the mesophase, texture development in the mesophase, boundary layer effects, and changes in density due to shear induced crystallization. The HBA/PET copolyester was shown to contain residual crystallinity at temperatures within the range in which negative values of  $N_1$  were reported. Crystallization of the HBA segments during the experiment would probably cause an increase in the density of the system and give rise to a negative  $N_1$  value.

The existence of an oscillatory response of the stresses occurring at the start up of shear flow was reported for several lyotropic LCP systems which include poly-p-pheneleneterephthalamide in sulfuric acid (PPT/H<sub>2</sub>SO<sub>4</sub>) [Doppert and Picken (1987)], HPC in water [Grizzuti *et al.* (1990)], and PBLG in m-cresol [Mewis and Moldenaers (1987)]. The oscillatory response at the start up of shear flow in these systems consisted of an initial overshoot of the stress followed by a series of damped oscillations before reaching steady state. In the work by Grizzuti *et al.* (1990) an explanation of the observed oscillatory behavior was provided. At the start up of shear flow it was proposed that the polydomain structure was changed from an equilibrium condition to one where the domains were changed in size and orientation. The stresses arose as a result of an elastic force which tried to recover to the equilibrium condition and a viscous force which resisted this process. These competing forces were believed to produce a series of damped oscillations. While an oscillatory response at the start up of shear flow was reported by Doppert and Picken (1987) for the PPT/H<sub>2</sub>SO<sub>4</sub> solution, Viola (1985) and Viola and Baird (1986) reported a single overshoot followed by a monotonic decrease to steady state values for the same system.

In the case of thermotropic systems, Viola (1985) and Viola and Baird (1986) studied the stress growth and relaxation behavior of HBA/PET copolyesters at 250, 260, and 275 °C. Overshoots at start up of shear flow were observed for the HBA/PET copolyesters at all shear rates measured. These overshoots increased in magnitude with an increase in shear rate while the strain at which the overshoots occurred remained constant. At 250 °C two overshoots were observed; the first occurring at 1-2 strain units and the second at 50-60 strain units. An explanation for this behavior was given by Baird (1985) in which the first peak was attributed to the development of orientation of the domain structure and the second peak to the two phase nature of the system.



The objective of this work is to determine if liquid crystalline order leads to a three region flow curve, negative steady state first normal stress difference, and oscillatory behavior at the start up of steady shear flow in an anisotropic solution of poly-p-phenyleneterephthalamide (PPT) in sulfuric acid ( $\text{H}_2\text{SO}_4$ ). This system was chosen because at a certain concentration of PPT it forms a truly nematic lyotropic LCP fluid [Minagawa and White (1976)]. The nematic system is devoid of potential problems associated with cholesteric systems such as a shear induced cholesteric-nematic transition analogous to unwinding of the helix [Onogi *et. al.* (1980)] and the observation that at low shear rates the helical screw axes were perpendicular to the direction of shear while at higher shear rates the helical screw axes tilted to a direction parallel to the direction of shear [Pochan and Marsh (1972)]. Special attention is given to comparing the rheological behavior of the solution in its anisotropic state to that of the solution in its isotropic state in order isolate any rheological behavior which may be due to LCO.

## 3.2 EXPERIMENTAL

### 3.2.1 Materials

The solutions used in this investigation were based on poly-p-phenyleneterephthalamide (PPT) ( $M_w = 40,100$  supplied by DuPont) and 100% sulfuric acid ( $\text{H}_2\text{SO}_4$ ). 100%  $\text{H}_2\text{SO}_4$  was prepared by mixing the appropriate amounts on a molar basis of 96.5%  $\text{H}_2\text{SO}_4$  with oleum (30% free  $\text{SO}_3$ ) (e.g., 80 ml of 96.5%  $\text{H}_2\text{SO}_4$  was mixed with 40 ml of oleum in an ice bath). Two solutions were prepared by blending 2 cm long PPT fibers, which had been washed in acetone, in proportions of 14 and 30 grams, respectively, with 120 ml of 100%  $\text{H}_2\text{SO}_4$  in a Helicone Mixer (Model 2CV) at 60°C under

a nitrogen atmosphere. These concentrations were chosen based on a reported transition from the anisotropic to isotropic state at 25 °C of 9.5% PPT for a similar molecular weight PPT [Aoki *et. al.* (1979)]. The solutions were extruded directly from the mixer into containers which were then kept sealed under vacuum until use.

The concentration of each solution was estimated by washing weighed amounts of the PPT/H<sub>2</sub>SO<sub>4</sub> solutions in water for a minimum of three hours to remove the H<sub>2</sub>SO<sub>4</sub>. The washed samples were dried in a vacuum oven at 100 °C for six hours before they were weighed again. The difference in weight prior to and following the washing process represented the weight of the 100% H<sub>2</sub>SO<sub>4</sub> in the original sample. Finally, the weight of the sample after the washing and drying process represented the weight of the PPT in the solution and was then used in conjunction with the original weight of the solution to determine the concentration of the sample. The concentrations of the solutions were determined using this procedure to be 6.7 wt. % and 12.6 wt. % PPT. There was a discrepancy between the concentrations based on the amounts of the starting materials and that determined by the coagulation experiments. This difference may be partially due to the inability to completely remove H<sub>2</sub>SO<sub>4</sub> during the coagulation and washing process. In any event the 6.7 wt. % and 12.6 wt. % PPT solutions will be referred to as the 6.7% and 12.6% solutions, respectively, in the following discussion.

### 3.2.2 Optical Measurements

In order to confirm the state of the solutions, measurements of transmitted polarized light were carried out on both solutions using a Zeiss polarizing light microscope and a Linkam THM 600 hot stage in conjunction with a Linkam PR600 temperature controller. The intensity of transmitted polarized light was measured by mounting a

cadmium sulfide photocell on the camera/video output of a Zeiss polarizing light microscope. The photocell was sensitive to light at wavelengths from 2500 to 8000 Angstroms with a relative response greater than 50% for the range of visible light. Data was obtained by measuring the resistance (using an ohmmeter) as a function of temperature for samples with a thickness of 0.05 mm at a heating rate of 1 °C/min. Resistance values were calibrated to zero intensity over a range of temperatures using a 6.7% solution as the zero intensity baseline (this method also corrected for the change in measured resistance as a function of temperature). Finally, the intensity of transmitted polarized light ( $I$ ) was assumed to be proportional to the inverse of the resistance ( $\Omega$ ) (e.g.,  $I \propto 1/\Omega$ ).

### 3.2.3 Rheological Measurements

The rheological data was obtained using two different rheometers and four different test modes. Viscosity ( $\eta$ ), first normal stress difference ( $N_1$ ), and shear stress ( $\sigma$ ) measurements were carried out using the steady shear modes of a Rheometrics Mechanical Spectrometer (RMS 800) at shear rates ranging from 0.1 to 3 sec<sup>-1</sup> while the magnitude of the complex viscosity ( $|\eta^*|$ ), storage modulus ( $G'$ ) and loss modulus ( $G''$ ) were obtained as a function of angular frequency ( $\omega = 2\pi f$ ) in the range 0.1 to 100 rad/sec. All tests were run using a cone and plate fixture having a cone angle of 0.1 rad and a diameter of 12.5 mm under nitrogen atmosphere. In addition, a thin coating of Vaseline was applied to all the free surfaces of the samples to minimize the sample exposure to moisture which would result in coagulation at the edges as discussed below.

Steady shear viscosity data at shear rates from 0.0001 to 0.1 sec<sup>-1</sup> was obtained using the shear sweep and creep modes of a Bohlin CS Rheometer using a cone and plate fixture having a cone angle of 0.095 radian and a diameter of 30 mm. In the creep

experiments the viscosity was calculated from the slope of the compliance versus time curve after steady state conditions had been reached.

### 3.2.4 Preliminary Rheological Experiments

In order to obtain accurate data using each of the methods described above, several preliminary experiments were carried out. Strain sweeps were carried out in order to determine the range of linear viscoelastic behavior. Time sweeps were used to quantify the effects of coagulation at the exposed sample surface. The effect of preshear history on the steady shear and transient data was evaluated using several transient experiments.

To establish the linear viscoelastic range of the solutions, strain sweeps at a fixed angular frequency were carried out. The 6.7% and 12.6% solutions displayed a linear response up to 0.1 and 0.2 strain units, respectively. Based on these results frequency sweeps were carried out on both solutions using strain amplitudes of 0.08 which met the required criterion of linear viscoelasticity.

The length of time each solution could remain in the test fixtures before coagulation of the exposed surface affected measurements was determined using time sweep experiments at a fixed angular frequency and strain amplitude (e.g.,  $\omega = 1$  rad/sec and  $\gamma_o = 0.08$ , respectively). The highly sensitive nature of the  $\text{H}_2\text{SO}_4$  solutions to moisture was documented by Kwolek (1972) and Baird (1978a) and was a result of the limited solubility of PPT in  $\text{H}_2\text{SO}_4$  as the concentration of the solvent concentration dropped below 100%  $\text{H}_2\text{SO}_4$  in the presence of moisture. Time sweep experiments indicated that the increase in the values of  $|\eta^*|$ ,  $G'$  and  $G''$  due to coagulation occurred despite the use of a Vaseline barrier at the exposed sample surface. The increases in  $|\eta^*|$ ,  $G'$  and  $G''$  due to coagulation were greatest for the 12.6% solution. It was determined that the 12.6% solution could

remain in the test fixtures for a maximum of 5 minutes before films formed by coagulation at the surface produced errors in  $|\eta^*|$ ,  $G'$ , and  $G''$  greater than the experimental error (i.e.,  $\pm 5\%$ ). Experimental error on the results of the dynamic oscillatory experiments was found to be random and within a  $\pm 5\%$  range by comparing results at the same conditions for at least three different samples. In the case of the solution at a concentration of 6.7%, the sample could remain in the test fixtures for up to 20 minutes before errors in the rheological properties exceeded approximately  $\pm 5\%$ .

The effect of preshear history on the steady shear and transient rheological measurements was evaluated using step-up, step-down and interrupted stress growth experiments. Based on these results it was concluded that steady state data could be obtained independent of the preshear history of each sample and comparisons of steady state data obtained using creep and steady shear tests could be made. As the transient response of the samples was sensitive to deformation history which occurred during loading of the sample into the cone and plate fixtures, the sample was allowed to relax for approximately one minute before beginning the start up of shear flow measurements. Preshearing lead to better reproducibility of the transient response, but altered the response significantly.

### 3.2.5 Creep Experiments

In creep experiments the times required to reach steady state at very low shear stresses (e.g., 5 Pa) were very long. For example, if we consider the extreme case of a creep experiment performed on a 12.6% solution at 60 °C and a shear stress of 5 Pa (i.e., a shear rate on the order of  $0.0001 \text{ sec}^{-1}$ ), steady state was reached at approximately 20 strain units in 55 hours. Based on a time limitation of 5 minutes for experiments before coagulation adversely affected measurements and the length of time to reach steady state for

low shear stress creep experiments, steady shear viscosity measurements would be limited to much larger shear stresses than those required to obtain viscosity data at shear rates below  $0.1 \text{ sec}^{-1}$ . For this reason the creep experiments were modified to reduce the length of time required to reach steady state, and data obtained using this method was corrected for the affects of coagulation. Step-down creep experiments reduced the time required to reach steady state conditions at very low shear stresses by first applying a large shear stress for a short period of time and then stepping down to the lower shear stress. The lower shear stress corresponded to the shear stress at which the steady shear viscosity data was desired. Data from start up of shear flow experiments and step-down experiments was used to determine the conditions used for carrying out step-down creep experiments (e.g., initial shear stress and length of time at each shear stress). First, using transient start up of steady shear flow experiments, the largest strain required to reach steady state for both solutions at various shear rates was determined to be on the order of 20 strain units. Using this information an initial shear stress in step-down creep experiments of 1000 Pa, which corresponded to a shear rate of approximately  $1 \text{ sec}^{-1}$ , was applied for 20 seconds. Next, the time required to reach steady state when the shear stress was stepped down to the low final shear stresses at which the steady shear viscosity data was desired was estimated using step-down experiments. Step-down experiments on the RMS-800 were performed by stepping down from an initial shear rate of  $1 \text{ sec}^{-1}$  to various final shear rates ranging from 0.1 to  $0.01 \text{ sec}^{-1}$ . The time required to reach steady state for each of these tests was then used to extrapolate to the time required to reach steady state stepping down from a shear rate of  $1.0 \text{ sec}^{-1}$  to values lower than  $0.01 \text{ sec}^{-1}$  as would be required in step-down creep experiments. Using this procedure steady shear viscosity measurements at a shear stress of 5 Pa from step-down creep experiments could be obtained in approximately 17 minutes, which was a substantial reduction from the 55 hours required in normal creep experiments.

Based on the results presented above indicating a time limitation of 5 minutes for rheological measurements on the 12.6% solution before the effects of coagulation became prominent, a correction for the increase in viscosity with time due to coagulation was used on the viscosity data. The method by which the viscosity data was corrected will be discussed in the results section of this paper.

### 3.3 RESULTS AND DISCUSSION

The results of this work are presented in the following four sections. In the first section, the state of the solution as a function of concentration and temperature is determined using polarized light microscopy. The role played by liquid crystalline order on the magnitude of the complex viscosity,  $|\eta^*|$ , and the steady shear viscosity,  $\eta$ , as a function of angular frequency and shear rate, respectively, is examined in the second section. In addition, the temperature dependence of  $|\eta^*|$  for both isotropic and anisotropic solutions is investigated in order to isolate differences in the temperature dependence of the rheological properties of an anisotropic solution. In the third section, the role played by liquid crystalline order on the steady state first normal stress difference,  $N_1$ , and storage modulus,  $G'$ , as function of shear rate and angular frequency, respectively, is examined by comparison of the results for an anisotropic solution with those of a solution in its isotropic state. Finally, in the fourth section, the role played by liquid crystalline order on the transient shear stress and first normal stress difference at the start up of steady shear flow is examined.

### 3.3.1 State of the Solution

In order to confirm the state of the solutions, the intensity of transmitted polarized light for both solutions was measured in the quiescent state. The 6.7% solution was confirmed to be isotropic over all temperatures as it did not transmit polarized light. In order to investigate the state of the 12.6% solution as a function of temperature, the intensity of transmitted polarized light was measured as a function of temperature (see Fig. 3.1). It can be seen from Fig. 3.1 that in the temperature range of 53 to 65 °C the intensity of transmitted polarized light is highest and this corresponds to a material which is believed to be largely anisotropic. The increase in intensity for the 12.6% solution with an increase in temperature from 53 to 65 °C may be associated with a melting of the solid phase, and this indicates a biphasic condition may exist over this temperature range (i.e., crystalline-anisotropic). As the temperature of the sample is increased above 65 °C a decrease in the intensity is observed which is associated with a phase transition from a largely anisotropic material at 65 °C to a material in which both anisotropic and isotropic phases coexist. At a temperature of approximately 90 °C the solution appears to be isotropic because the intensity of transmitted polarized light is zero. The coexistence of up to three phases for both lyotropic [Papkov (1984); Uematsu (1984)] and thermotropic [Lenz (1985); Blumstein *et. al.* (1985)] liquid crystalline polymers has previously been documented .

### 3.3.2 Viscosity

The magnitude of the complex viscosity and the steady shear viscosity of the solution in its isotropic and anisotropic state as a function of angular frequency and shear rate, respectively, was investigated. By comparison of the rate and temperature dependence



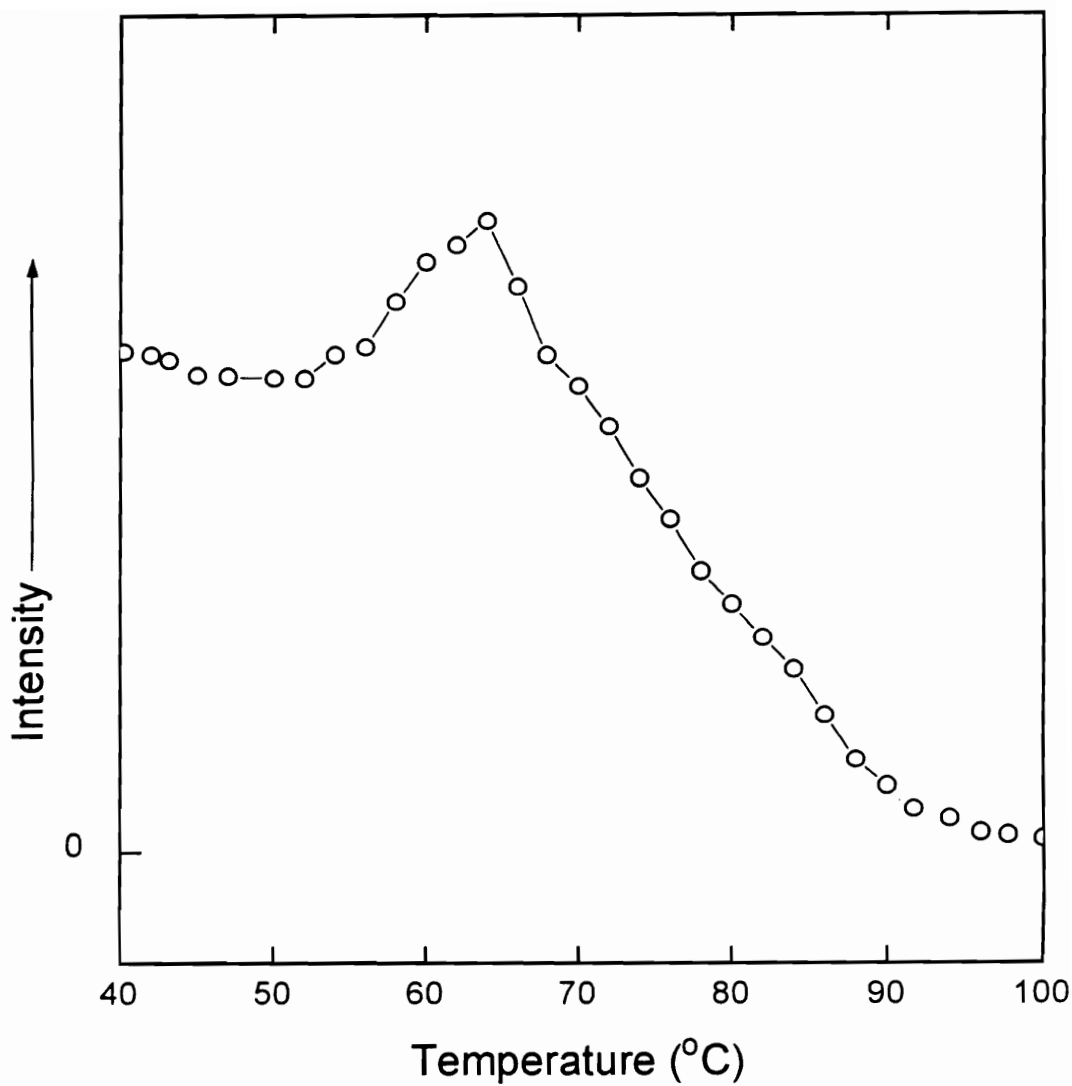


**Figure 3.1** Intensity of transmitted polarized light as function of temperature for 12.6% PPT/H<sub>2</sub>SO<sub>4</sub> solution.

of the viscosity for the 6.7% and 12.6% solutions, the role played by LCO and a polydomain texture on the viscosity was examined.

Although the step-down creep experiments described earlier substantially reduced the time required to obtain steady state viscosity data from creep experiments at low stresses (e.g., 17 minutes versus 55 hours), the increase in the measured viscosity from coagulation at the exposed sample surface for the 12.6% solution was still significant. In order to adjust for the increase in measured viscosity for the 12.6% solution due to coagulation in step-down creep experiments, the measured viscosity was corrected using data from time sweep and step-down experiments. First, using the increase in the magnitude of the complex viscosity  $|\eta^*|$  as a function of time at several frequencies (see Fig. 3.2), the increase in measured steady shear viscosity ( $\eta_{\text{measured}}$ ) due to coagulation was determined by assuming that the increase in  $|\eta^*|_{\text{measured}}$  as a function of time and angular frequency is equal to the increase in  $\eta_{\text{measured}}$  as a function of time and shear rate. The assumption of  $|\eta^*| \cong \eta$  was found to hold at rates of  $\omega$  and  $\dot{\gamma}$  below 1.0 rad/sec and 1.0 sec<sup>-1</sup>, respectively. The increase in  $|\eta^*|_{\text{measured}}$  as a function of time (t) and  $\omega$  obtained from time sweep experiments was fit by the following function,

$$|\eta^*|_{\text{measured}} \cong \eta_{\text{measured}} = \eta_{\text{actual}} + [374 - (280 \cdot \dot{\gamma})] \cdot \eta_{\text{actual}} \cdot t \quad (3.1)$$

where  $\eta_{\text{actual}}$  is the initial viscosity at time t=0 of the solution free of the effects of coagulation, and the time, t, has units of minutes. Next, using the data obtained from the step-down experiments described earlier and shown in Fig. 3.3, the time to reach steady state stepping down from an initial shear rate ( $\dot{\gamma}_i$ ) of 1 sec<sup>-1</sup> to some lower final shear rate ( $\dot{\gamma}_f$ ) was found to be fit by the following function,

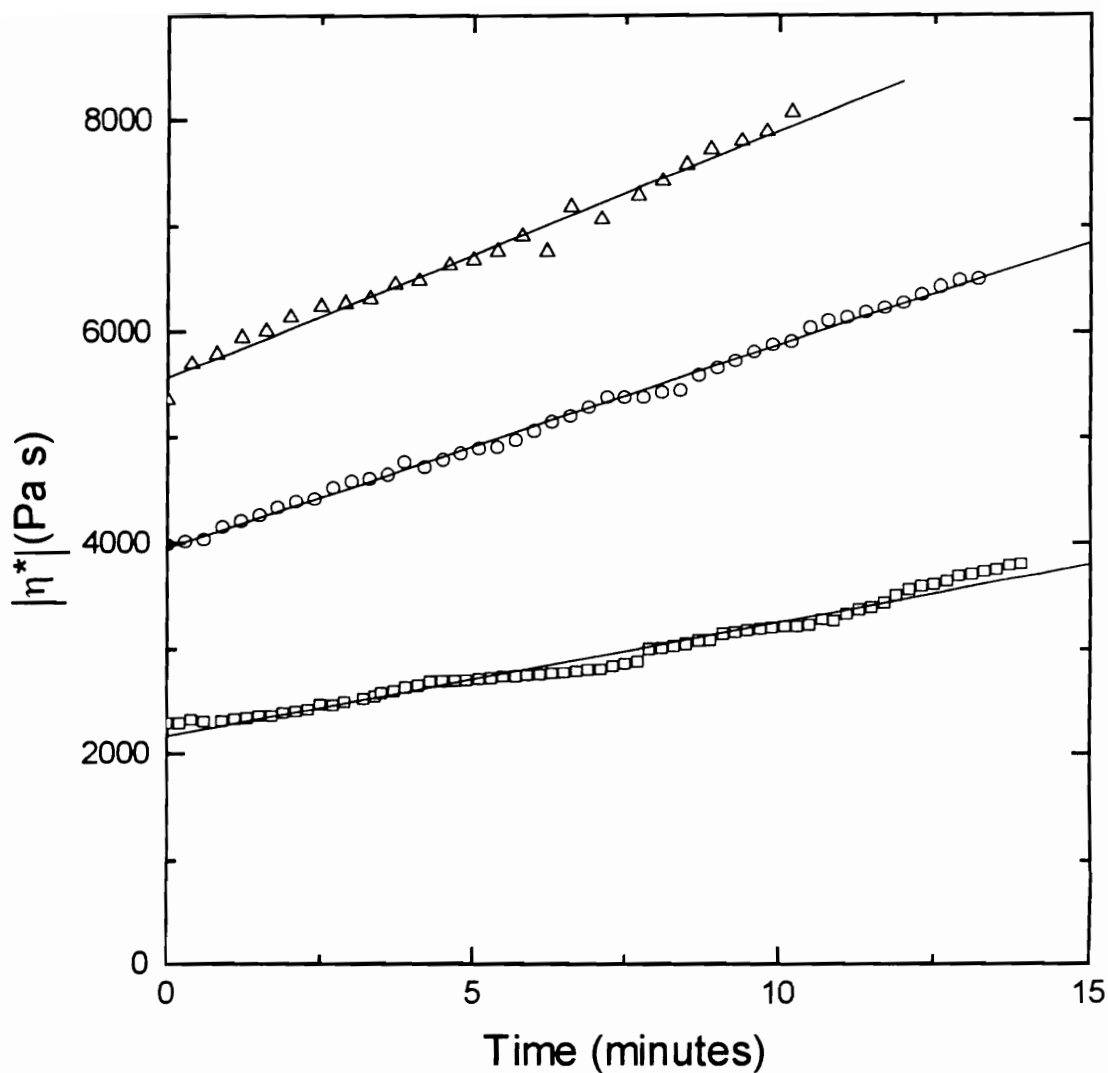


**Figure 3.2** Increase in the magnitude of the complex viscosity of the 12.6% PPT/H<sub>2</sub>SO<sub>4</sub> solution at 60 °C as a function of time at frequencies of: (Δ) 0.3; (○) 0.5; (□) 1.0 rad/sec. The line a statistical fit of the data using Eq. (3.1) where  $\dot{\gamma} = 0.3, 0.5$ , and 1.0 rad/sec.

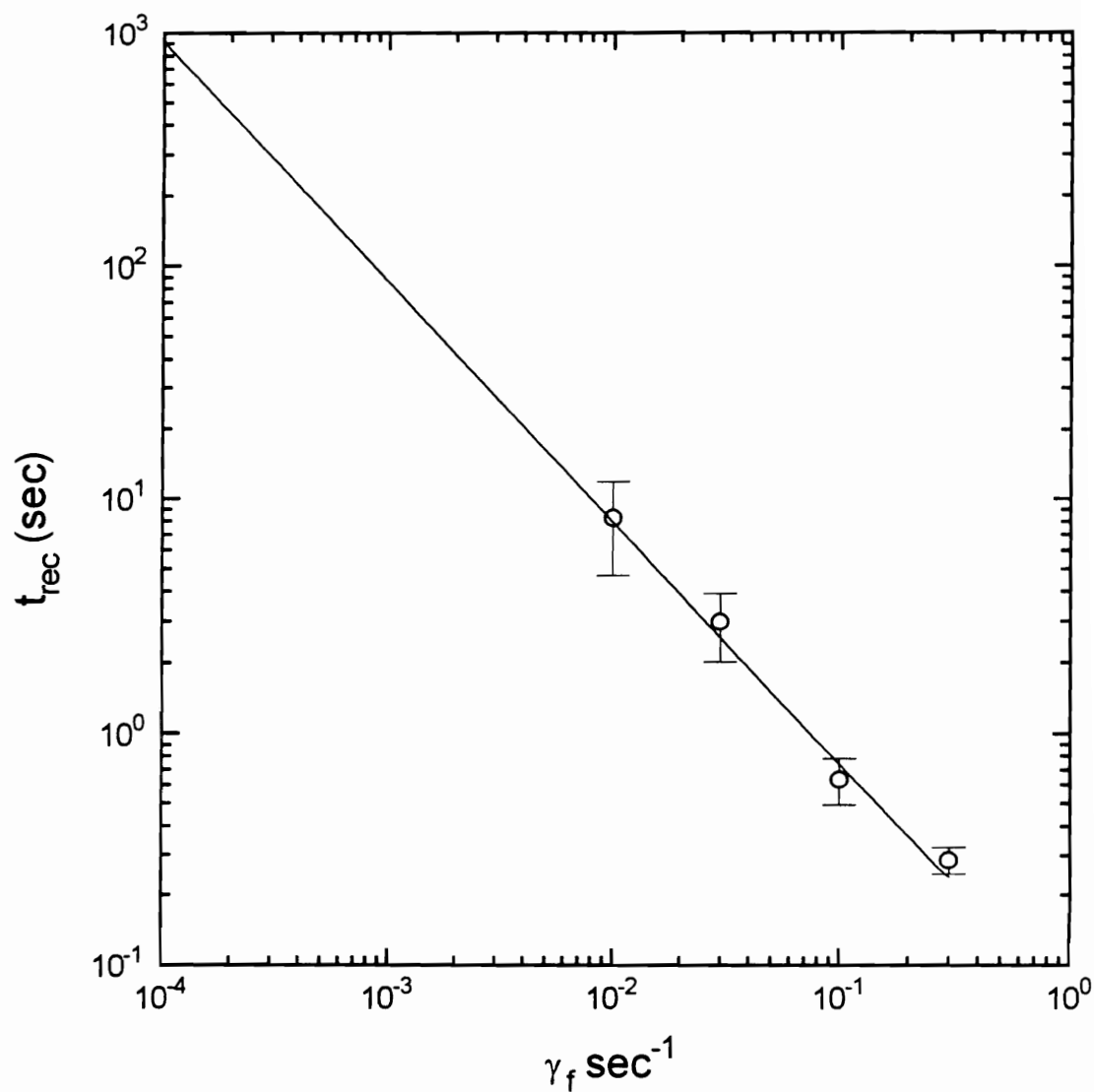


**Figure 3.3** Increase in the time required to reach steady state in step-down experiments from an initial shear rate of  $1 \text{ sec}^{-1}$  as a function of the final shear rate for 12.6% PPT/ $\text{H}_2\text{SO}_4$  solution. The line represents a statistical fit of the data using Eq. (3.2).

$$t_{\text{rec}}(\dot{\gamma}_f) = 0.0686(\dot{\gamma}_f)^{-1.0312} \quad (3.2)$$

where  $t_{\text{rec}}$  is the time, in minutes, required to reach steady state stepping down from an initial shear rate ( $\dot{\gamma}_i$ ) of  $1 \text{ sec}^{-1}$  to a lower final shear rate ( $\dot{\gamma}_f$ ). Using the expression for the increase in viscosity as function of time [Eq. (3.1)] and the recovery time [Eq. (3.2)] in conjunction with the duration of the initial shear rate ( $t_i$ ) the actual viscosity was obtained by correcting the measured viscosity for the effects of coagulation at the exposed sample surface using the following expression:

$$\eta_{\text{actual}}(\dot{\gamma}_f) = \frac{\eta_{\text{measured}}(\dot{\gamma}_f)}{1 + (374 - 280 \dot{\gamma}_f)(0.0686 \dot{\gamma}_f^{-1.0312} + t_i)} \quad (3.3)$$

where  $t_i$  has the unit of minutes.

The magnitude of the complex viscosity and steady shear viscosity as a function of angular frequency and shear rate, respectively, for the isotropic (6.7%) and the anisotropic (12.6%) solutions at  $60^\circ\text{C}$  is shown in Figs. 3.4 and 3.5, respectively. The magnitude of the complex viscosity and the steady shear viscosity of the 6.7% solution at  $60^\circ\text{C}$  (see Fig. 3.4) displays shear thinning behavior at high shear rates and a Newtonian plateau at rates below  $0.1 \text{ sec}^{-1}$ . Good agreement is observed between the steady shear viscosity obtained using both step-down creep tests and steady shear tests and between  $|\eta^*|$  and  $\eta$ . Steady shear viscosity data could not be obtained at higher shear rates due to edge fracture and loss of material from the gap. Edge fracture and loss of material from the gap is correlated to increasingly erratic behavior of the shear stress with increasing strain during steady shear experiments at shear rates above  $0.1 \text{ sec}^{-1}$ . The magnitude of the complex viscosity and the steady shear viscosity of the 12.6% solution at  $60^\circ\text{C}$  display shear thinning behavior at

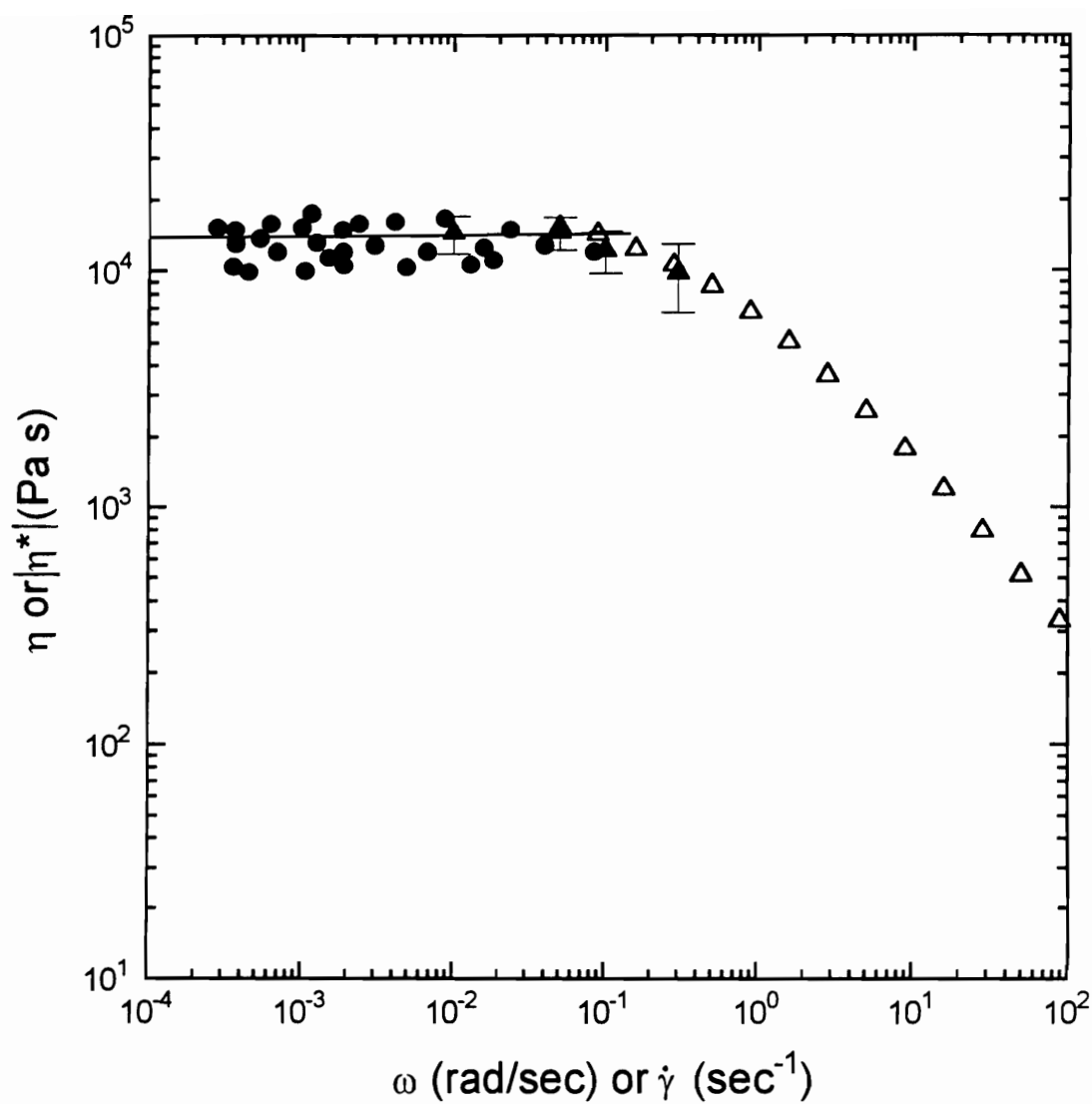


**Figure 3.4** Flow curve for the 6.7% PPT/H<sub>2</sub>SO<sub>4</sub> solution at 60 °C: (Δ) magnitude of the complex viscosity; (▲) steady shear viscosity from steady shear experiments; and (●) steady shear viscosity from step-down creep experiments. The line represents linear regression analysis of the creep data.

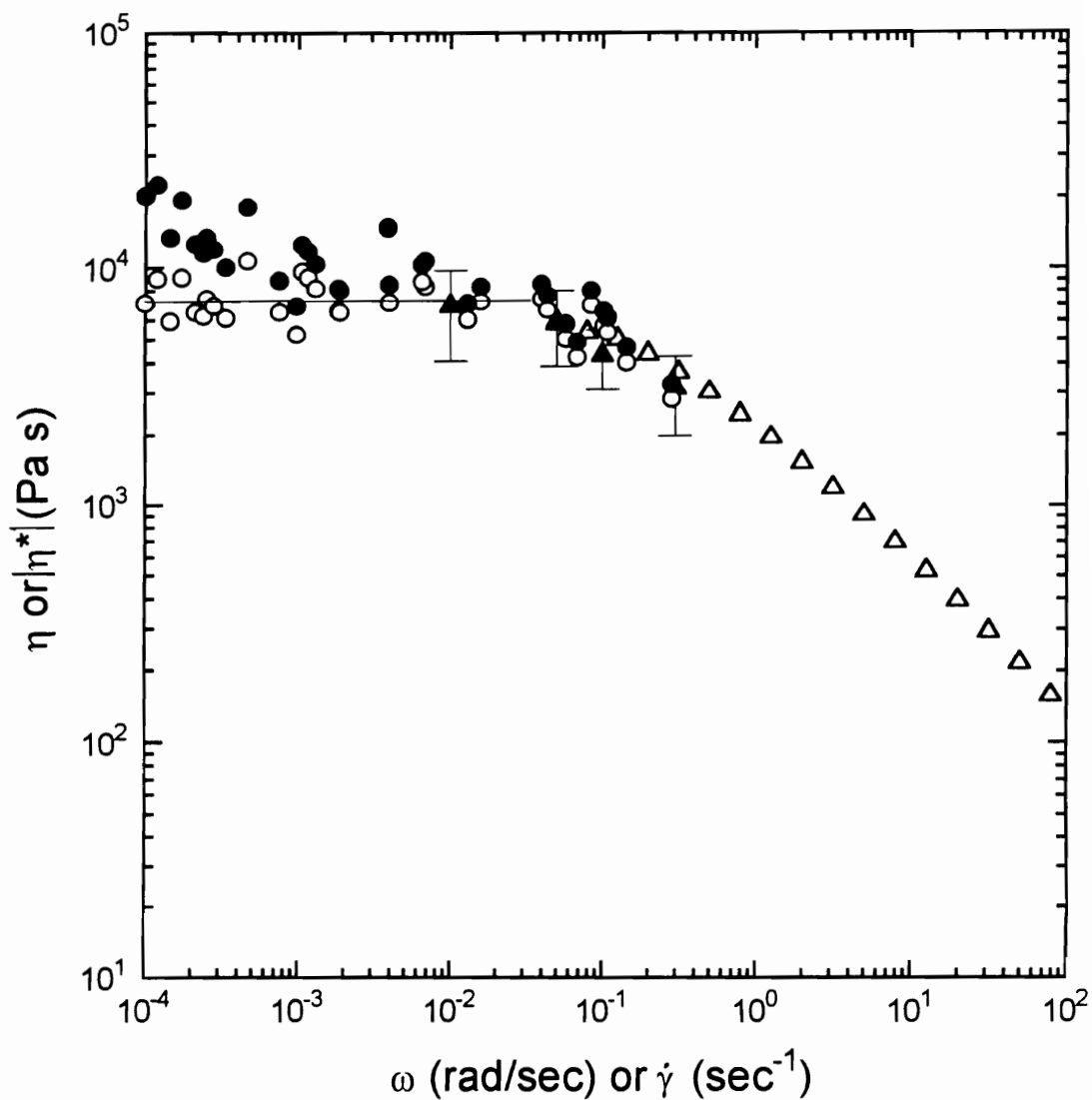


**Figure 3.5.** Flow curve for 12.6% PPT/H<sub>2</sub>SO<sub>4</sub> solution at 60 °C: (Δ) magnitude of the complex viscosity; (▲) steady shear viscosity from steady shear experiments; (●) steady shear viscosity from step-down creep experiments; and (○) creep data corrected for coagulation using Eq. (3.3). The line represents linear regression analysis of the corrected creep data.

high frequencies and shear rates (see Fig. 3.5). At low shear rates the steady shear viscosity of the 12.6% solution at 60 °C obtained using creep experiments is shear thinning, but when corrected for the effects of coagulation using Eq. (3.3) a Newtonian plateau is observed. The steady shear viscosity measured using steady shear and step-down creep experiments is in good agreement. In addition, good agreement between  $\eta$  and  $|\eta^*|$  is observed. A comparison of the magnitude of the viscosity of the isotropic and anisotropic solutions reveals that it is lower for the anisotropic solution despite a substantially higher concentration. This observation corresponds with published data in which it was shown using plots of the Newtonian plateau viscosity against concentration that the viscosity of the anisotropic solution was lower than that of the isotropic solution [Wissbrun (1980)]. While the appearance of the flow curves for the 6.7% and 12.6% solutions is similar (e.g., a Newtonian plateau at low shear rates, a shear thinning region at high rates, and agreement between  $|\eta^*|$  and  $\eta$ ), the presence of LCO results in a viscosity which is lower in magnitude than that of the isotropic solution at 60 °C. At first appearance it seems that the anisotropic solution exhibits an apparent yield stress, but when the measured viscosity is corrected for the effects of coagulation, a Newtonian plateau is observed.

Because the shear rates obtained from the step-down creep experiments were very low and experimental error (e.g., effects due to moisture and equipment resolution) was as high as 17% for the 12.6% solution at 60 °C, a statistical analysis was performed to determine if there was any indication of a third region of shear thinning behavior at the lowest rates obtained. Specifically, an analysis, based on the linear fit of the 12.6% solution creep data at 60 °C encompassing shear rates of 0.0001 to 0.05 sec<sup>-1</sup> was carried out in order to determine if the viscosity data taken at the lowest shear rates showed any tendency to deviate from the horizontal line and thus a Newtonian plateau. The analysis of the viscosity data at shear rates between 0.0001 and 0.003 relative to the horizontal line



showed a Gaussian distribution of the error typical of random scatter. Although this analysis showed a good fit with no indication of another shear thinning region, one cannot rule out that if data was obtained at rates lower than those obtained here, a change in the shear rate dependence might be observed. However, based on the data presented here only two regions are observed in the flow curve for the 12.6% solution at 60 °C with no indication of another shear thinning region beginning at the lowest rates investigated.

Another method by which the anisotropic and isotropic solutions were compared in order to determine the role played by liquid crystalline order was to examine the temperature dependence of the viscosity. The magnitude of the complex viscosity at various temperatures for the 6.7% and 12.6% solutions is shown in Figs. 3.6 and 3.7, respectively. The 6.7% solution shows a temperature dependence of  $|\eta^*|$  typical of melts and solutions of flexible chain polymers. The effect of increasing temperature on intermolecular interactions results in a family of  $|\eta^*|$  versus  $\omega$  curves similar in shape but decreasing in magnitude and the value of  $\omega$  at which the transition from Newtonian to shear thinning behavior occurs is decreased. In sharp contrast to the effect of temperature on  $|\eta^*|$  for the 6.7% solution,  $|\eta^*|$  for the 12.6% solution increases with an increase in temperature, and the value of  $\omega$  at which shear thinning behavior begins does not appear to change. The change in  $|\eta^*|$  at a fixed angular frequency over a range of temperatures for the 12.6% solution is seen in Fig. 3.8. The data reported in Fig. 3.8 shows a decrease in  $|\eta^*|$  with increasing temperature until at 65 °C a minimum in  $|\eta^*|$  is observed after which further increases in temperature lead to an increase in  $|\eta^*|$ . The results shown in Fig. 3.8 can be correlated with the results obtained using transmitted polarized light intensity measurements shown in Fig. 3.1. The minimum in  $|\eta^*|$  is associated with a solution which is believed to be largely anisotropic at 65 °C and the increase in  $|\eta^*|$  with increasing temperature above 65 °C is associated with a solution which is becoming more isotropic.

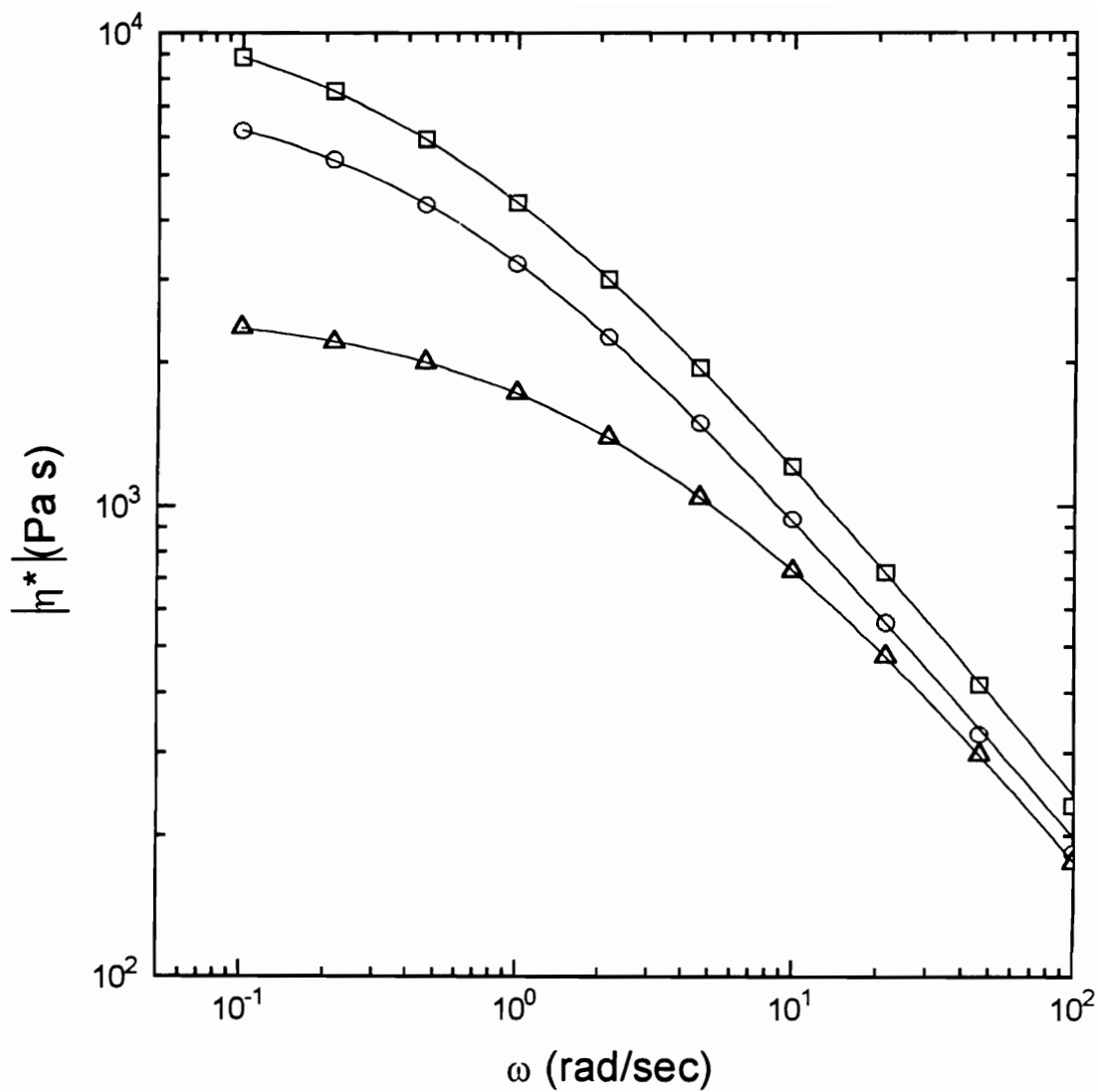


**Figure 3.6** Magnitude of the complex viscosity versus frequency as a function of temperature for the 6.7% PPT/H<sub>2</sub>SO<sub>4</sub> solution: ( $\square$ ) 40 °C; ( $\circ$ ) 60 °C; and ( $\Delta$ ) 75 °C. The lines represent a best fits using the Carreau-Yasuda model.

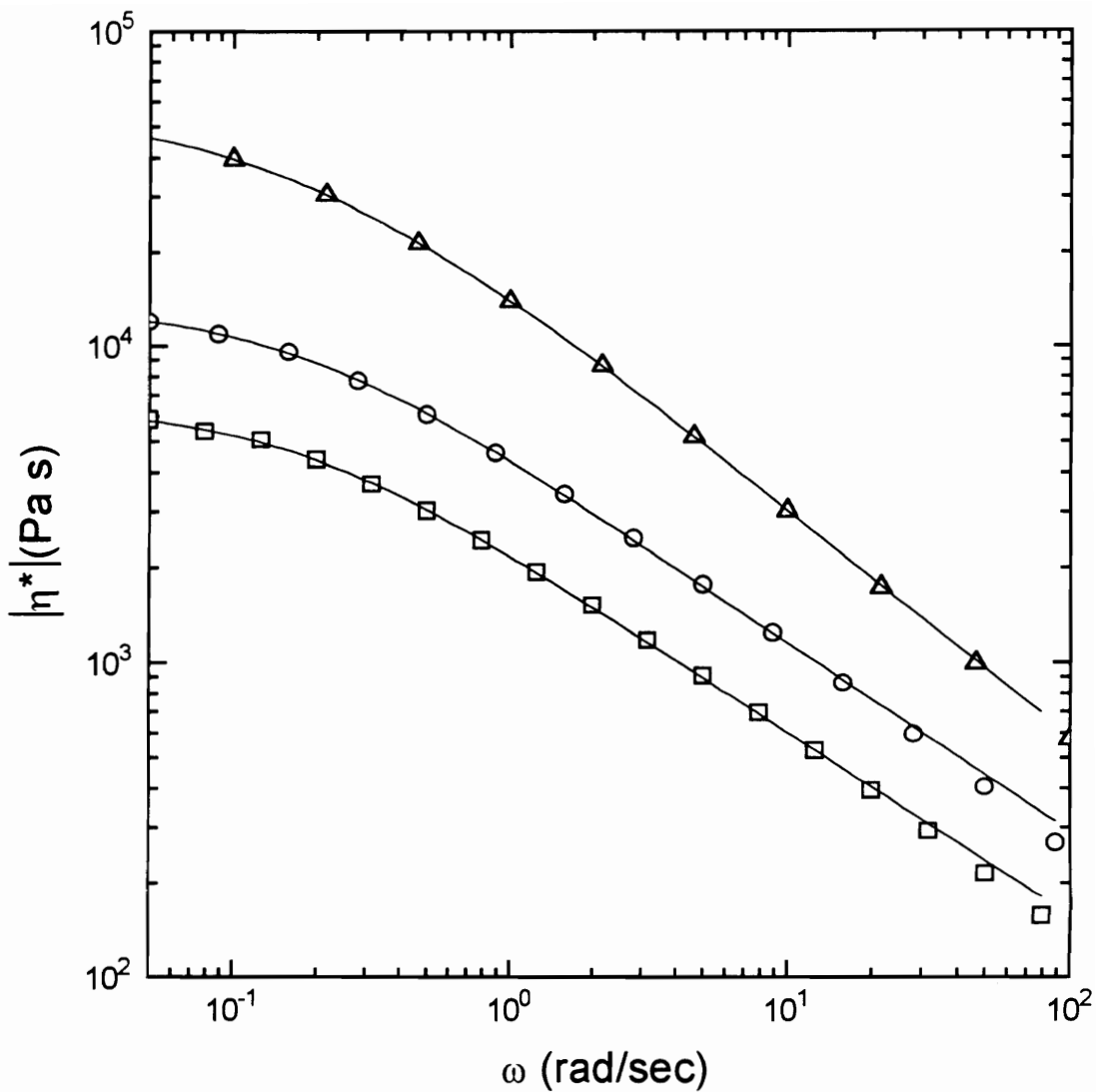


**Figure 3.7** Magnitude of the complex viscosity versus frequency as a function of temperature for the 12.6% PPT/H<sub>2</sub>SO<sub>4</sub> solution: ( $\square$ ) 60 °C; ( $\circ$ ) 75 °C; and ( $\Delta$ ) 90 °C. The lines represent best fits using the Carreau-Yasuda model.

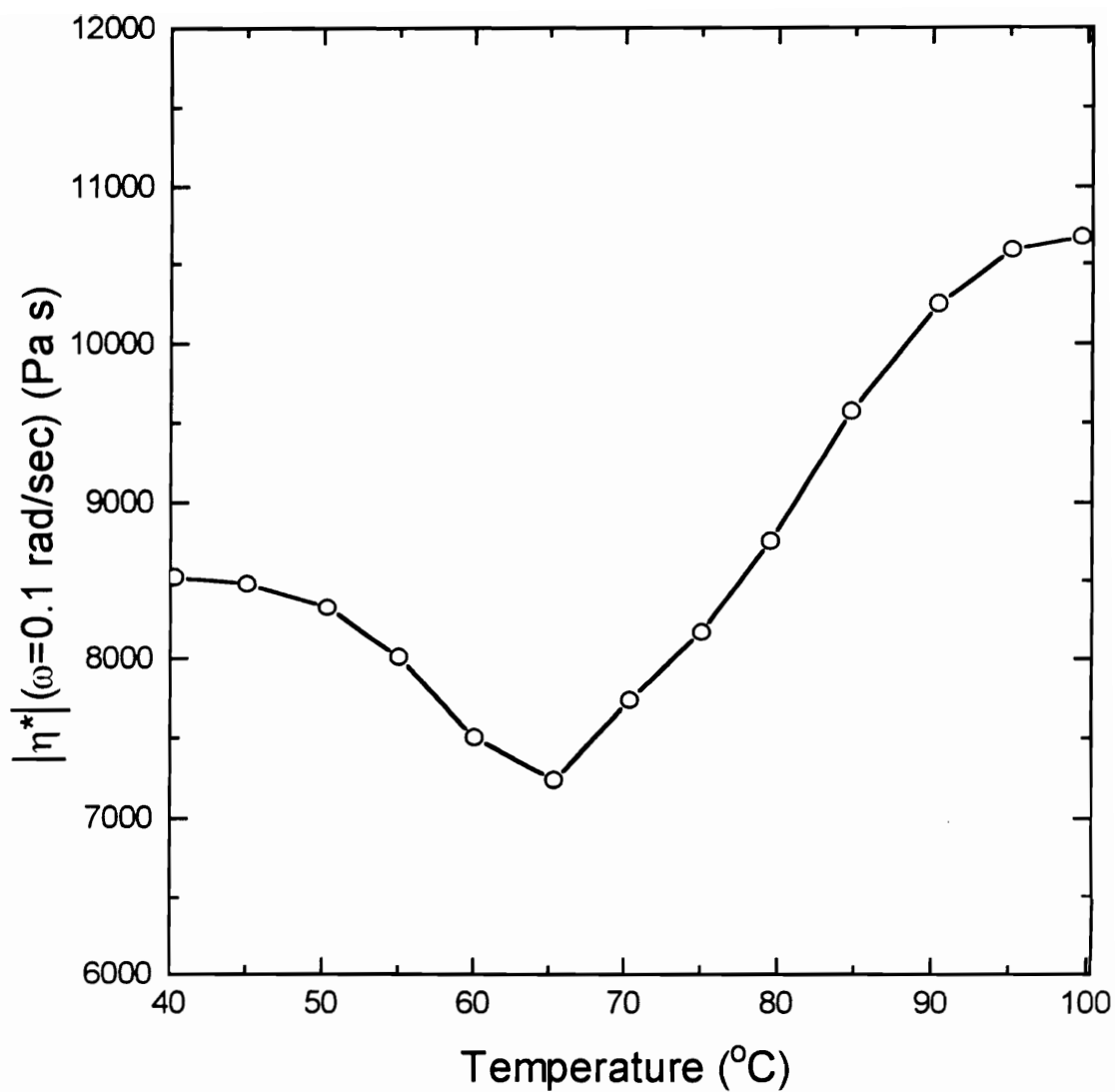


**Figure 3.8** Magnitude of the complex viscosity versus temperature for a 12.6% PPT/H<sub>2</sub>SO<sub>4</sub> solution.

The fit of an empiricism for  $\eta(\dot{\gamma})$  is next used to analyze the changes in the shape and magnitude of the viscosity as a function of concentration and temperature. An accurate fit of the flow curves for both solutions at all temperatures investigated was obtained using the Carreau-Yasuda model given below and shown in Figs. 6 and 7 assuming an infinite shear viscosity ( $\eta_\infty$ ) of zero and  $\eta = |\eta^*|$

$$\frac{\eta - \eta_\infty}{\eta_0 - \eta_\infty} = \left[ 1 + (\lambda \dot{\gamma})^a \right]^{\frac{(n-1)}{a}} \quad (3.4)$$

where  $\eta_0$  represents the magnitude of the zero shear viscosity,  $a$  is a dimensionless parameter that describes the breadth of the transition region between the Newtonian plateau and the power-law region,  $\lambda$  is a time constant describing the location of the transition region, and  $n$  is the power-law exponent describing the degree of shear thinning behavior. The parameters in the Carreau-Yasuda model obtained by fitting  $|\eta^*|$  data for the 6.7% and 12.6% solutions at all temperatures investigated is listed in Table 3.1. The effect of LCO on the shape and magnitude of  $|\eta^*|$  as a function of  $\omega$  is seen by a comparison of the data listed in Table 3.1 for the 6.7% and 12.6% solutions at 60 °C (i.e., isotropic and anisotropic solutions, respectively). The effect of LCO order on the flow curve of the solution at a concentration of 12.6% relative to the solution at a concentration of 6.7% is to decrease  $\eta_0$ , narrow the transition from the Newtonian region to the power-law region (i.e.,  $a$  increases), decrease the rate at which the transition from Newtonian to shear thinning behavior occurs (i.e., increase the time constant  $\lambda$ ), and decrease the degree of shear thinning in the power law region (i.e.,  $n$  increases). The same qualitative changes in the Carreau-Yasuda parameters as seen with a decrease in concentration from 12.6% to 6.7% at 60 °C are seen with an increase in temperature of the 12.6% solution from 60 °C to 90 °C where the increase in temperature causes a decrease in the anisotropy of the solution.

**TABLE 3.1** Carreau-Yasuda model parameters for the 6.7% and 12.6% PPT/H<sub>2</sub>SO<sub>4</sub> solutions fit to the magnitude of the complex viscosity versus angular frequency data.

6.7% PPT/H <sub>2</sub> SO <sub>4</sub>				
	$\eta_0$ (Pa s)	<b>n</b>	<b>a</b>	$\lambda$ (sec <sup>-1</sup> )
40 °C	11,995(±13)	0.2599(±.011)	0.6763(±.0131)	1.8558(±.08)
60 °C	7816(±8.3)	0.2752(±.01)	0.6960(±.009)	1.7824(±.06)
75 °C	2623(±4.9)	0.2397(±.008)	0.6643(±.005)	0.2989(±.014)
12.6% PPT/H <sub>2</sub> SO <sub>4</sub>				
	$\eta_0$ (Pa s)	<b>n</b>	<b>a</b>	$\lambda$ (sec <sup>-1</sup> )
60 °C	6489(±34)	0.4189(±.009)	1.1534(±.017)	5.9575(±.45)
75 °C	13,545(±123)	0.4018(±.014)	1.1172(±.015)	6.0727(±.39)
90 °C	58,112(±48)	0.2817(±.011)	0.9012(±.031)	5.9774(±.72)

In the case of the solution at a concentration of 6.7%, increasing the temperature decreases  $\eta_o$  and the time constant  $\lambda$  while  $n$  and  $a$  remain essentially constant. Based on an analysis using the Carreau-Yasuda parameters the presence of liquid crystalline order and a polydomain texture results in a decrease of  $|\eta^*|$ , a decrease in the value of  $\omega$  at which the transition from the Newtonian to shear thinning behavior occurs, a sharpening of the transition region and a decrease in the degree of shear thinning in the power-law region relative to the solution in its isotropic state.

Another method by which the role played by liquid crystalline order was investigated was the application of time-temperature superposition to the viscosity of both the isotropic and anisotropic solutions. In the case of the isotropic solution, it was seen that as the temperature was increased the magnitude of  $|\eta^*|$  decreased and the value of  $\omega$  at which the transition from the Newtonian to shear thinning behavior occurred increased. In fact, application of time temperature superposition, which was shown to work quite well for a broad range of polymer melts and solutions [Ferry (1980)], worked quite well for the 6.7% solution (see Fig. 3.9). On the other hand,  $|\eta^*|$  of the 12.6% solution does not display the same temperature dependence as seen in the isotropic fluid due to the phase changes which occur, and, therefore, time-temperature superposition was not applicable. The phase transition observed using light intensity measurements as a function of temperature for the 12.6% solution (see Fig. 3.1) was the cause of the failure of time-temperature superposition (e.g., as the temperature was increased a transition from an anisotropic solution to a biphasic solution and finally to an isotropic solution).

Other evidence for the presence of liquid crystalline order and a phase transition which occurs with a change in concentration or temperature was observed when one examined a plot of the dimensionless viscosity ( $\eta/\eta_o$ ) versus the dimensionless shear rate ( $\dot{\gamma}/\dot{\gamma}_o$ ) for the 6.7% and 12.6% solutions at all temperatures investigated. It is known that

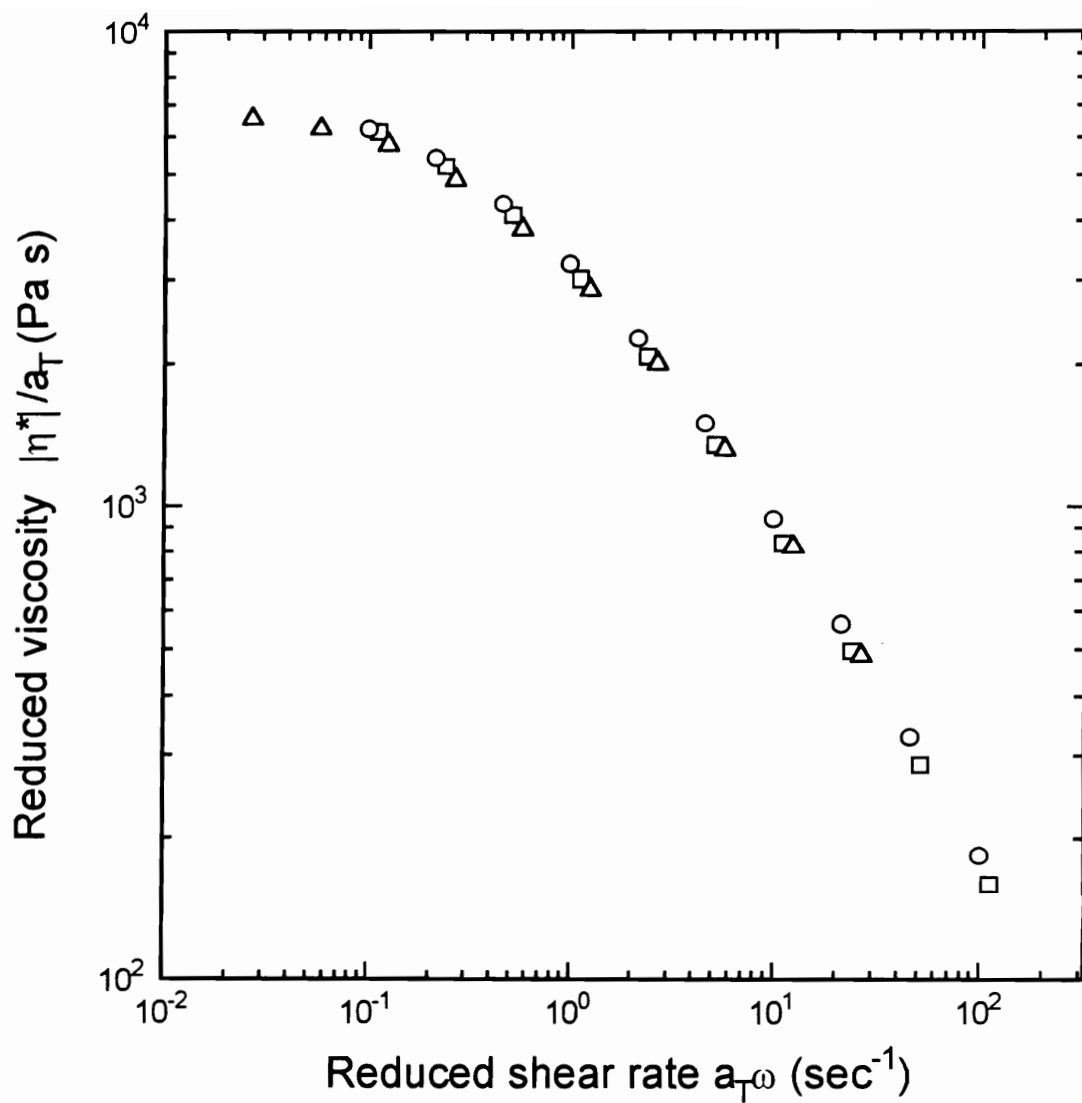


**Figure 3.9** Master curve for the magnitude of the complex viscosity as function of frequency shifted to a reference temperature of  $T_0=60\text{ }^{\circ}\text{C}$  for a 6.7% PPT/ $\text{H}_2\text{SO}_4$  solution where the values were taken at temperatures of ( $\square$ ) 40  $^{\circ}\text{C}$ , ( $\circ$ ) 60  $^{\circ}\text{C}$ , and ( $\Delta$ ) 75  $^{\circ}\text{C}$ .



for concentrated polymer solutions that for a given polymer-solvent system that viscosity versus shear rate curves taken at varying concentrations and temperatures lie on a single curve when plotted in reduced form [Graessly (1974)]. In our work the critical shear rate ( $\dot{\gamma}_o$ ) was arbitrarily taken to be the value of the dimensionless shear rate at which  $(\eta - \eta_s)/(\eta_o - \eta_s) = 0.8$  and the zero shear viscosities were taken from Table 3.1. The data for the 6.7% and 12.6% solutions at various temperatures are plotted in this manner in Fig. 3.10. It can be seen that the viscosity for the 6.7% solution at 40 °C, 60 °C, and 75 °C and the 12.6% solution at 90 °C all lie on a single curve while a deviation from this curve is observed for the viscosity data of the 12.6% solution at 60 °C and 75 °C. As the anisotropic nature of the 12.6% solution decreases with increasing temperature from 60 °C to one in which both isotropic and anisotropic phases coexist at 75 °C, the corresponding curve is seen to shift closer to that formed by the solution in its isotropic state. Finally, as the temperature of the 12.6% solution is increased further to 90 °C the phase transition to an isotropic solution is complete and the curve overlaps with those formed by the 6.7% solution. The presence of liquid crystalline order in the 12.6% solution at 60 °C and a biphasic solution at 75 °C results in a small deviation of the curve of dimensionless viscosity versus dimensionless shear rate from the curve formed by the solution in its isotropic state.

### 3.3.3 Steady State First Normal Stress Difference and Storage Modulus

The rate dependence of the steady state first normal stress difference ( $N_1$ ) and storage modulus ( $G'$ ) for the anisotropic and isotropic solutions was investigated next. The shear rate dependence of  $N_1$  was examined to determine whether any differences in the elastic response of the anisotropic and isotropic solutions existed. Specifically, it was

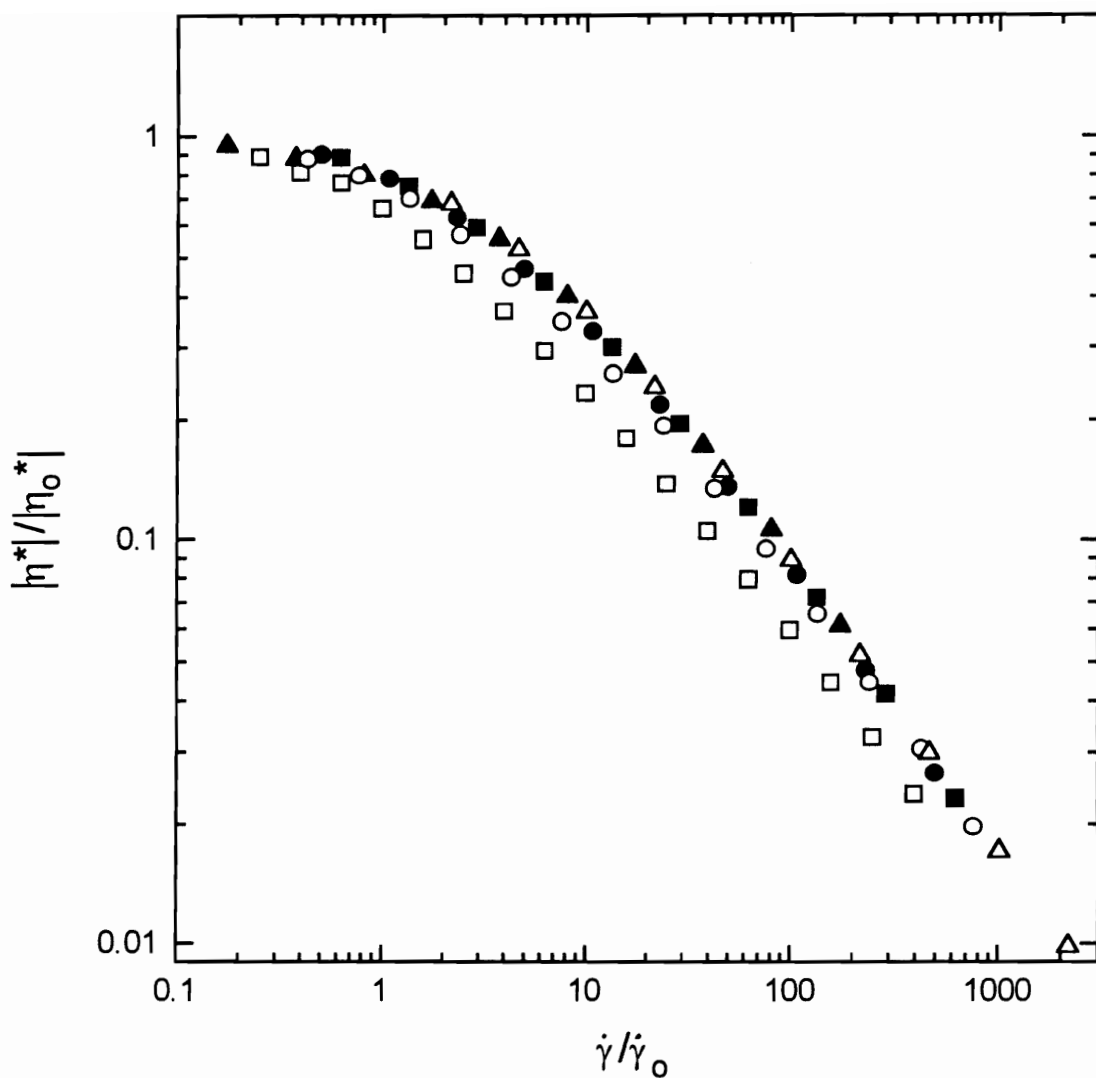


**Figure 3.10** Dimensionless complex viscosity versus dimensionless shear rate for a 6.7% PPT/H<sub>2</sub>SO<sub>4</sub> solution at (■) 40 °C, (●) 60 °C, and (▲) 75 °C and a 12.6% PPT/H<sub>2</sub>SO<sub>4</sub> at (□) 60 °C, (○) 75 °C, and (△) 90 °C.

determined whether negative steady state first normal stress differences were observed in anisotropic solutions. Additionally, steady state values of  $N_1$  were compared to the small strain values of  $2G'$  obtained from the dynamic oscillatory experiments for both anisotropic and isotropic solutions. This was done in order to isolate the effect on the elasticity of the anisotropic solution resulting from a highly deformed polydomain texture (i.e.,  $N_1$ ) relative to the elasticity arising from a polydomain texture which is relatively undeformed (i.e.,  $G'$ ).

The values of  $N_1$  as a function of shear rate and  $2G'$  as a function of  $\omega$  obtained from dynamic oscillatory experiments for the 6.7% and 12.6% solutions at 60 °C are shown in Fig. 3.11. This figure shows that the values of  $N_1$  and  $2G'$  of both solutions increase monotonically as shear rate and angular frequency are increased and that values of  $N_1$  remain positive over the whole range tested and show no tendency to exhibit negative values. The magnitudes of  $N_1$  and  $2G'$  are higher for the isotropic solution than those of the anisotropic solution. A qualitative comparison of the isotropic and anisotropic solutions shows that the rate dependence of  $N_1$  and  $2G'$  are similar for both solutions. Additionally, good agreement is observed between  $N_1$  and  $2G'$  for both the anisotropic and the isotropic solutions over the angular frequencies and shear rates measured.

### 3.3.4 Start Up of Steady Shear Flow

The transient behavior during start up of steady shear flow of the 6.7% and 12.6% solutions at several temperatures was investigated. The role played by liquid crystalline order and the presence of a polydomain texture were examined by comparing the transient shear stress and first normal stress difference at the start up of steady shear flow for both solutions as a function of temperature.

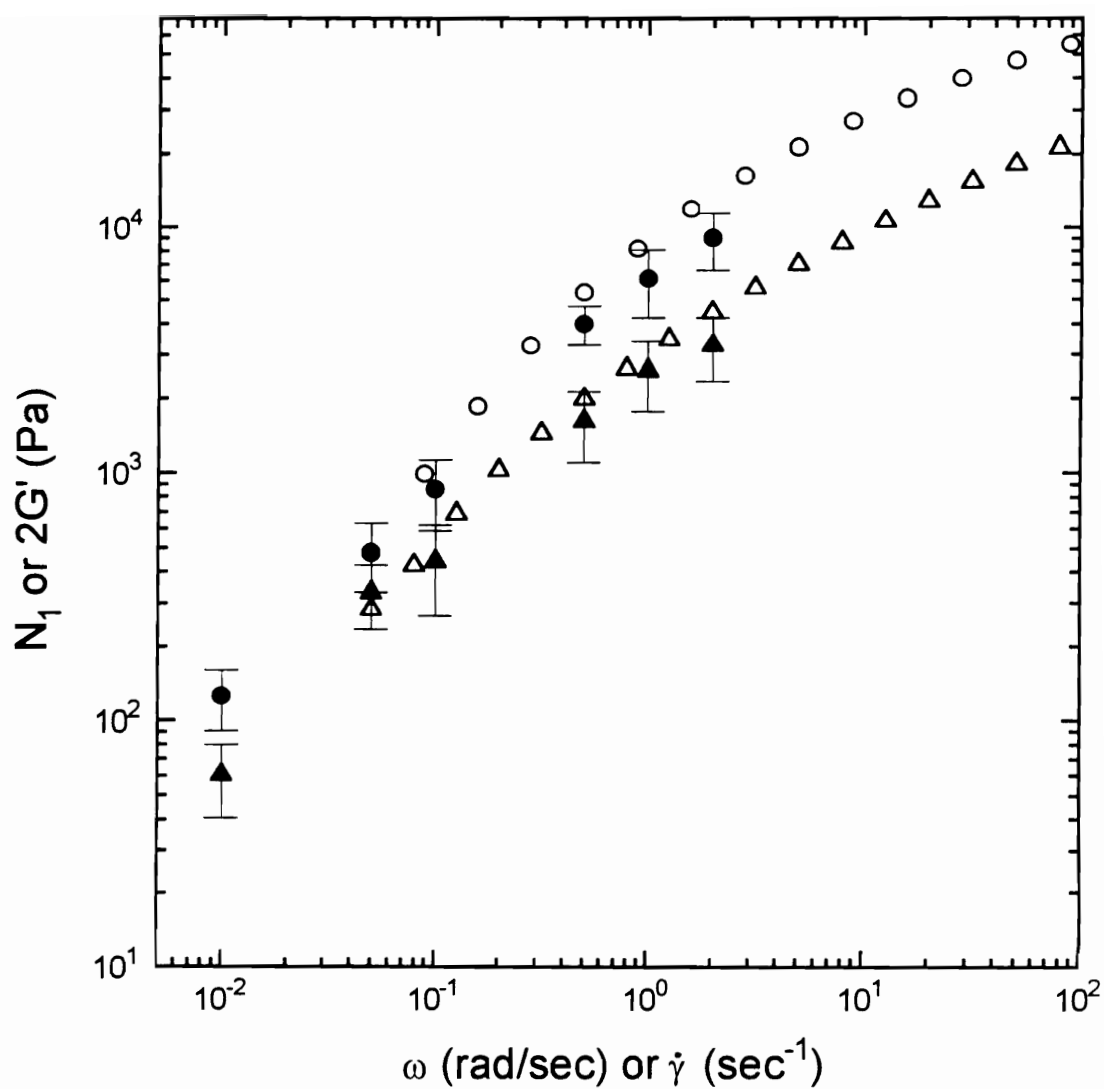


**Figure 3.11** First normal stress difference and  $2G'$  as a function of shear rate and frequency, respectively, at 60 °C:  $N_1$  (●) 6.7% PPT/H<sub>2</sub>SO<sub>4</sub> solution, (▲) 12.6% PPT/H<sub>2</sub>SO<sub>4</sub> solution;  $2G'$ , (○) 6.7% PPT/H<sub>2</sub>SO<sub>4</sub> solution, (Δ) 12.6% PPT/H<sub>2</sub>SO<sub>4</sub> solution.

The transient shear stress and first normal stress difference of the 6.7% and 12.6% solutions at various temperatures versus strain are shown in Figs. 3.12, 3.13, 3.14 and 3.15. The data shown in these figures was obtained at a shear rate of  $1 \text{ sec}^{-1}$  and was representative of the results obtained at lower shear rates. In addition, the shear rate of  $1 \text{ sec}^{-1}$  represented the upper limit of shear rate from which accurate steady shear data could be obtained due to edge fracture and loss of material from the gap. The transient behavior of some LCPs (e.g., PBLG and HPC) was reported to show an oscillatory response during the start up of steady shear flow [Mewis and Moldenaers (1987); Doppert and Picken (1987); Grizzuti *et. al.* (1990)]. It can be seen in Fig. 3.12 that the shear stress for the 6.7% solution shows a single overshoot followed by a monotonic decrease to steady state values with little change in the magnitude of the overshoot relative to steady state values as the temperature is increased. Similarly, the shear stress at the start up of steady shear flow for the 12.6% solution is seen in Fig. 3.13 to show an overshoot followed by a monotonic decrease to steady state values. The magnitude of the overshoot relative to the steady state values increases slightly with temperature. Differences in the transient shear stress at the start up of steady shear flow are observed in the strain at which the overshoot occurs. The overshoot in shear stress for the 12.6% solution occurs at lower strains than that for the 6.7% solution (e.g., 1.2 and 1.8 strain units, respectively). In the case of the first normal stress difference for the 6.7% solution shown in Fig. 3.14, there is little overshoot observed. In sharp contrast to the transient behavior of the first normal stress difference seen for the 6.7% solution, the first normal stress difference at the start up of steady shear flow for the 12.6% solution (see Fig. 3.15) displays an overshoot followed by an undershoot during which negative values are observed and then finally a slow increase to positive steady state values which are higher than those of the overshoot. The effect of an increase in temperature and the corresponding

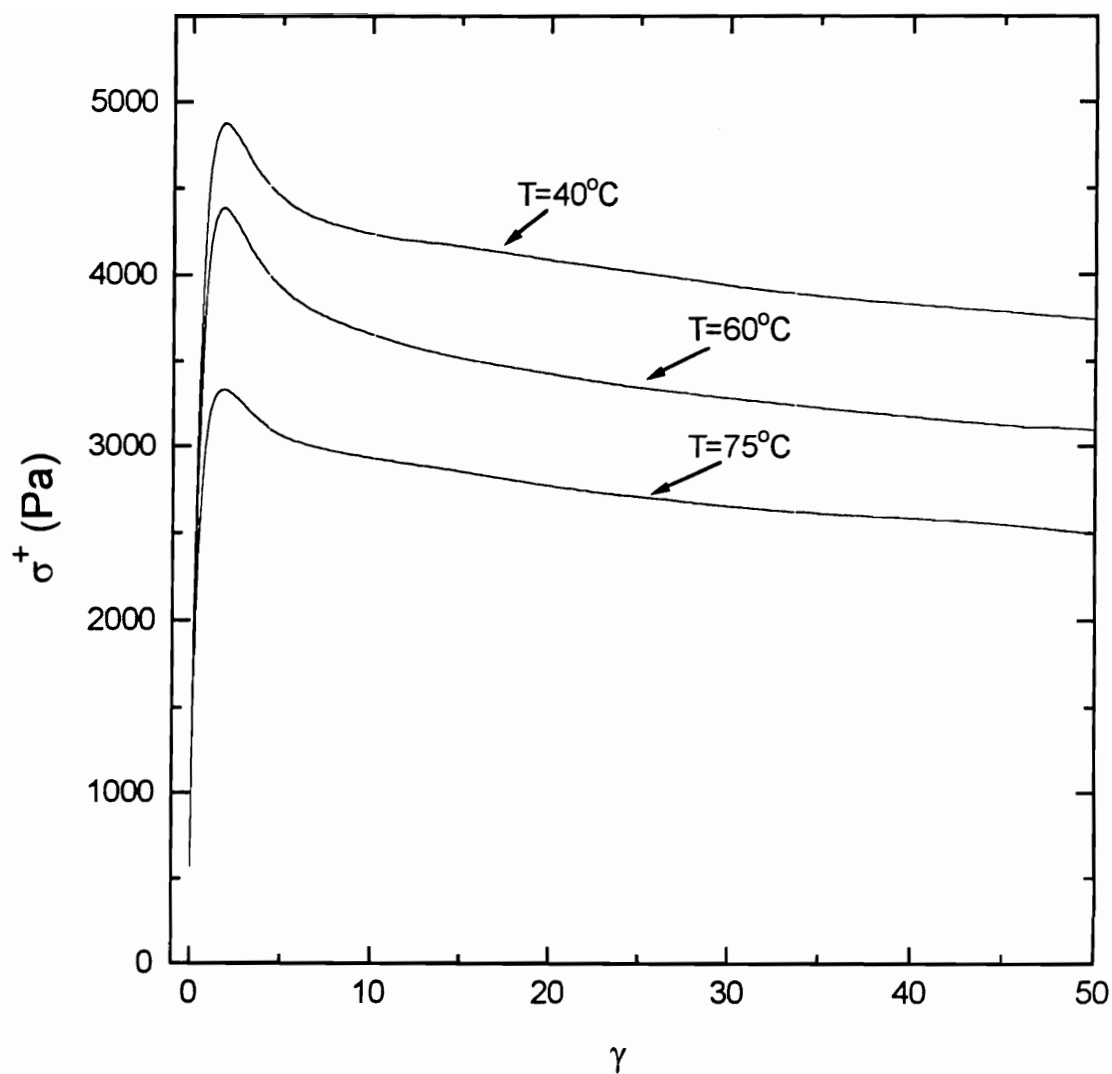


**Figure 3.12** Transient shear stress at a constant shear rate of  $1 \text{ sec}^{-1}$  at the start up of steady shear flow versus strain at  $40^\circ\text{C}$ ,  $60^\circ\text{C}$ , and  $75^\circ\text{C}$  for the 6.7% PPT/ $\text{H}_2\text{SO}_4$  solution.

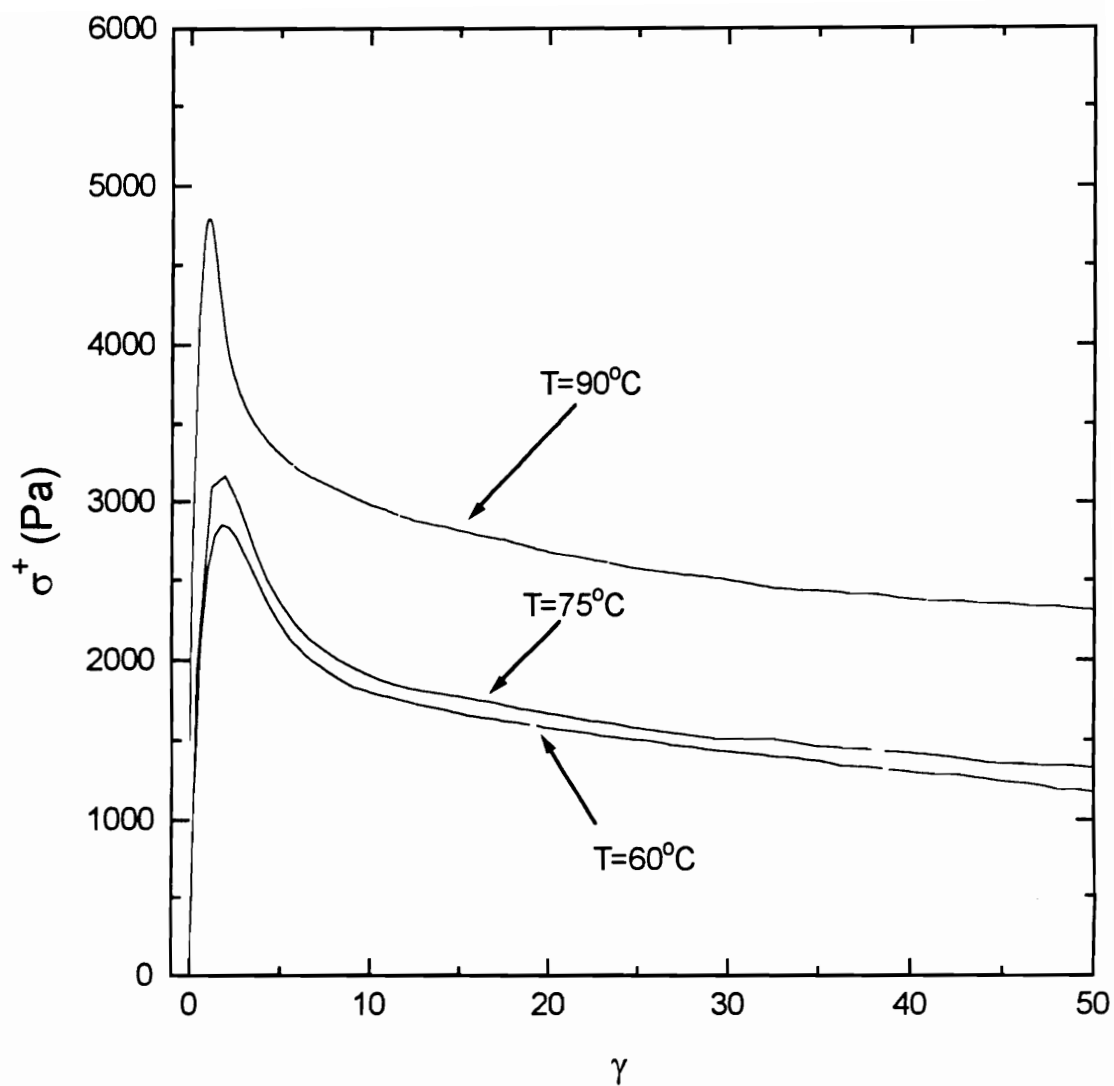


**Figure 3.13** Transient shear stress at a constant shear rate of  $1 \text{ sec}^{-1}$  at the start up of steady shear flow versus strain at 60 °C, 75 °C, and 90 °C for the 12.6% PPT/ $\text{H}_2\text{SO}_4$  solution.

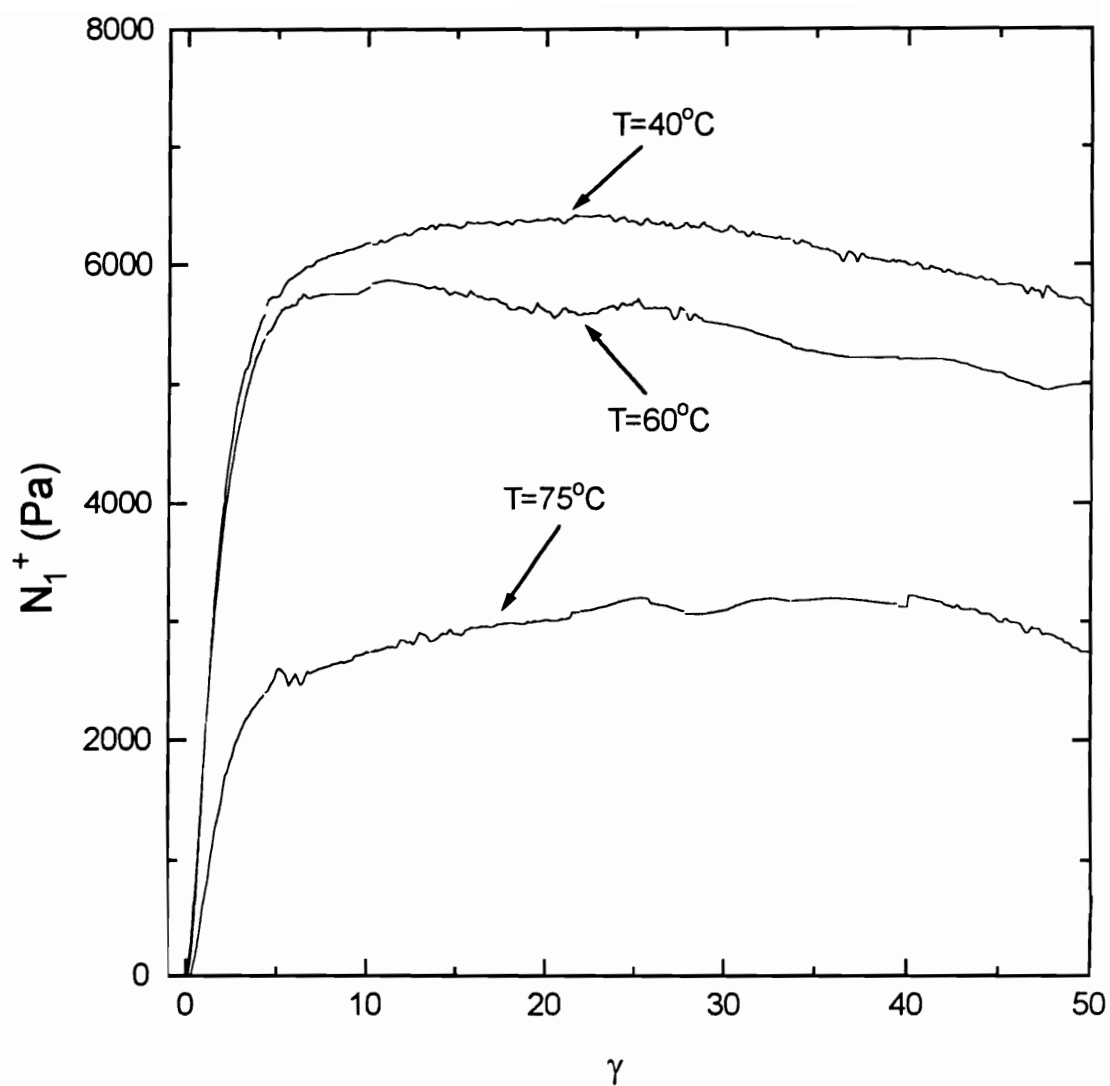


**Figure 3.14** Transient first normal stress difference at a constant shear rate of  $1 \text{ sec}^{-1}$  at the start up of steady shear flow versus strain at  $40^\circ\text{C}$ ,  $60^\circ\text{C}$  and  $75^\circ\text{C}$  for the 6.7% PPT/ $\text{H}_2\text{SO}_4$  solution.



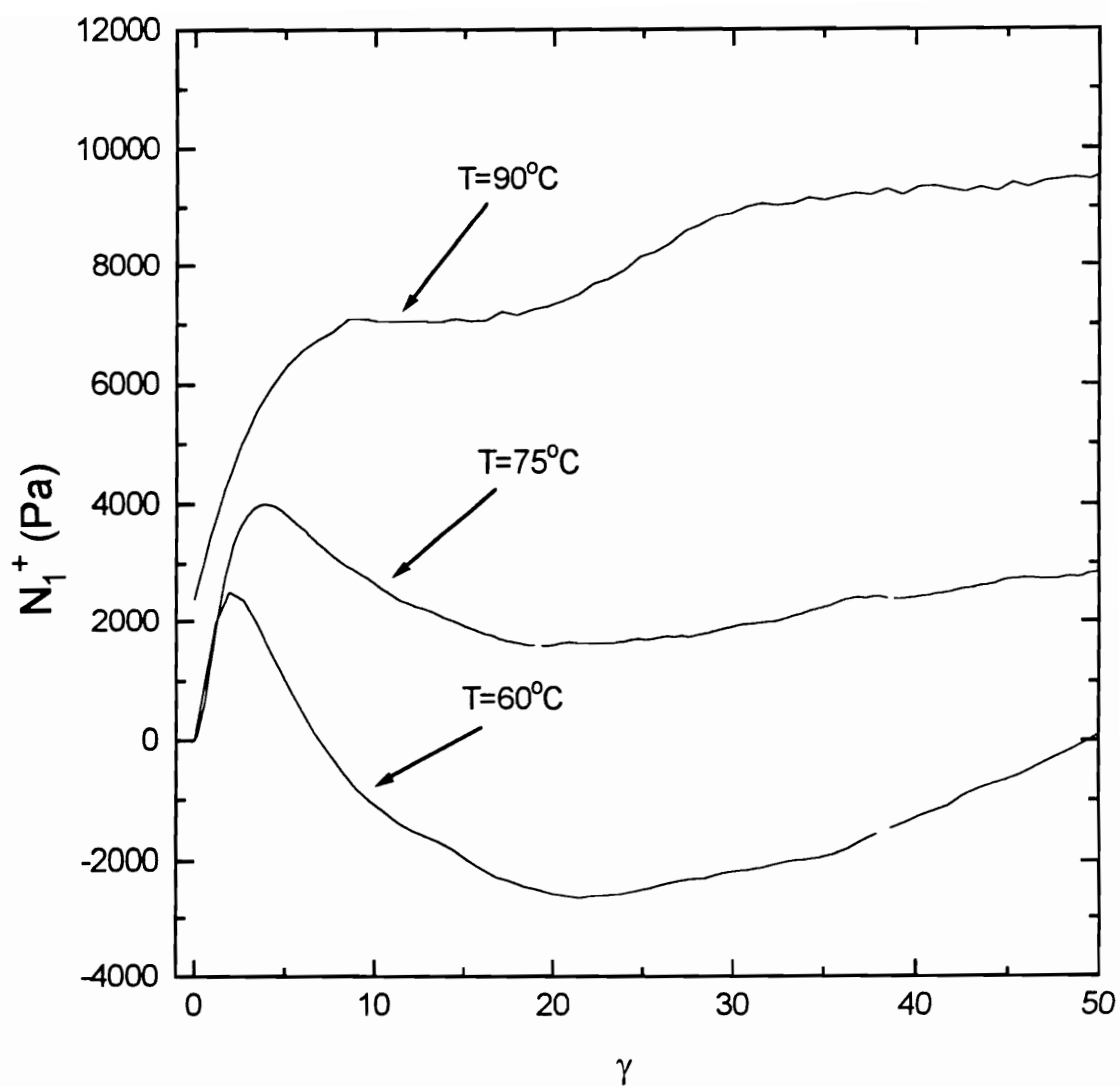


**Figure 3.15** Transient first normal stress difference at a constant shear rate of  $1 \text{ sec}^{-1}$  at the start up of steady shear flow versus strain at  $60^\circ\text{C}$ ,  $75^\circ\text{C}$  and  $90^\circ\text{C}$  for the 12.6% PPT/ $\text{H}_2\text{SO}_4$  solution.

decrease in the anisotropy decreases the amount of undershoot which occurs and increases the strain at which the overshoot occurs (overshoot occurs at 2 strain units at 60 °C, 4 strain units at 75 °C). At 90 °C the first normal stress difference for the 12.6% solution displays a shoulder at approximately 5.5 strain units before increasing to the final steady state value. A comparison of the results for the 6.7% isotropic solution to the results for the 12.6% anisotropic solution indicates a qualitative difference in the first normal stress difference behavior. The presence of liquid crystalline order and a polydomain texture is seen qualitatively in the first normal stress difference behavior where a negative undershoot following an initial overshoot is observed in the anisotropic solution and is not observed in the isotropic solution. Similar qualitative differences between the isotropic and anisotropic solution are not seen in the transient shear stress behavior. In addition, a comparison of the 12.6% solution at 60 °C and 90 °C reveals similar qualitative differences as discussed above for the 6.7% and 12.6% solutions at 60 °C where the undershoot in the first normal stress difference is reduced but an inflection can still be seen and may be due to the presence of residual anisotropy.

### 3.4 CONCLUSIONS

Several of the phenomena commonly reported to be characteristic of LCPs (e.g., three region flow curve, a negative steady state first normal stress difference, and oscillatory behavior upon inception of steady shear) were not observed in anisotropic solutions of PPT in sulfuric acid. This work showed that the presence of liquid crystalline order was, by itself, not a sufficient condition for the appearance of these rheological phenomena. The solution in its anisotropic and isotropic state exhibited a two region flow curve, a positive steady state first normal stress difference which increased with shear rate,

and a transient shear stress which displayed a single overshoot before reaching steady state. Although an apparent yield stress was observed at low rates for the anisotropic solution, when the viscosity data was corrected for the effects of coagulation a Newtonian plateau was observed.

Although similar qualitative rheological behavior was observed for the anisotropic and isotropic solutions, small differences in the shape and magnitude of the flow curve and transient first normal stress difference for the anisotropic solution relative to the isotropic solution were observed. The presence of liquid crystalline order in the anisotropic solution relative to the isotropic solution resulted in a decrease in the magnitude, a sharper transition from Newtonian to shear thinning regions, a decrease in the rate at which the transition from Newtonian to shear thinning regions occurs, and a decrease in the degree of shear thinning at high shear rates. The transient first normal stress difference for the anisotropic solution displayed an overshoot followed by a negative undershoot before increasing to positive steady state values while the isotropic solution displayed a monotonic increase to steady state values.

These results suggest that the rheological behavior of this system may be related to a transition from the resistance to flow offered by individual entangled rods to that of aggregates or clusters of rods. The dissipative effects of the aggregates may be less than those of the individual molecules. Likewise the elastic energy associated with the recovery of the deformed aggregates may be lower than that due to Brownian motion associated with the individual molecules.

### **3.5 ACKNOWLEDGMENTS**

The authors gratefully acknowledge the Virginia Institute of Materials Systems for support of this work.

### 3.6 References

- Aoki, H., J. L. White, and J. F. Fellers, "A Rheological and Optical Properties Investigation of Aliphatic (Nylon 6,6, PyBLG) and Aromatic (Kevlar, Nomex) Polyamide Solutions," J. Appl. Polym. Sci. **23**, 2293-2314 (1979).
- Asada, T., S. Onogi, and H. Yanase, "A Rheo-Optical Study on the Reformation of Structure in Racemic Poly(g-benzyl glutamate) Liquid Crystals" Polym. Eng. Sci. **24**, 355-360 (1984).
- Baird, D. G., "Viscometry of Anisotropic Solutions of Poly-p-Phenyleneterephthalamide in Sulfuric Acid," J. Appl. Polym. Sci. **22**, 2701-2706 (1978a).
- Baird, D. G., *Liquid Crystalline Order in Polymers* (A. Blumstein ed., Academic Press, 1978b).
- Baird, D. G., A. D. Gotsis, and G. G. Viola, "Transient Shear Flow Behavior of Thermotropic Liquid Crystalline Copolyesters," Polym. Prepr. Am. Chem. Soc. Div. Polym. Chem. **24**, 292-295 (1983).
- Baird, D. G., *Polymeric Liquid Crystals*, (A. Blumstein ed., Plenum Press, New York, 1985).
- Blumstein, A., M. M. Gauthier, O. Thomas, and R. B. Blumstein, "Structure-Property Correlations in some Nematic Main-chain Polyesters," Faraday Discuss. chem. Soc. **79**, 33-39 (1985).
- Chung, T. S., "The Recent Developments of Thermotropic Liquid Crystalline Polymers," Polymer. Eng. Sci. **26**, 901-919 (1986).
- Chiou, J. S. and D. R. Paul, "Gas Transport in a Thermotropic Liquid-Crystalline Polyester," J. Polym. Sci., Part B: Polym. Phys. **25**, 1699-1707 (1987).
- Ciferri, A., *Ultra-High Modulus Polymers*, (Applied Science Publishers, Essex, England Ltd., 1979).

- Doppert, H. L. and S. J. Picken, "Rheological Properties of Aramid Solutions: Transient and Rheo-Optical Measurements," *Mol. Cryst. Liq. Cryst.* **153**, 109-116 (1987).
- Dutta, D., H. Fruitwala, A. Kohli, and R. A. Weiss, "Polymer Blends Containing Liquid Crystals: A Review," *Polymer. Eng. Sci.* **30**, 1005-1018 (1990).
- Ferry, J. D., *Viscoelastic Properties of Polymers*, (3rd ed., Wiley, New York, 1980).
- Gotsis, A. D., "A Study of the Rheological Behavior of Two Thermotropic Liquid Crystalline Copolyesters," M.S. Thesis, Virginia Polytechnic Institute and State University, Virginia (1984).
- Gotsis, A. D. and D. G., Baird, "Rheological Properties of Liquid Crystalline Copolyester Melts. II. Comparisons of Capillary and Rotary Rheometer Results," *J. Rheol.* **29**, 539-556 (1985).
- Gotsis, A. D., *Rheol. Acta.*, **25**, 275 (1986).
- Graessly, W. W., *Adv. Polym. Sci.* **16**, 1-179 (1974).
- Grizzuti, N., S. Cavella, and P. Cicarelli, "Transient and steady-state rheology of a liquid crystalline hydroxypropylcellulose solution," *J. Rheol.* **34**, 1293-1310 (1990).
- Hinch, E. J. and L. G. Leal, "Time-dependent shear flows of a suspension of particles with weak Brownian rotations," *J. Fluid Mech.* **51**, 753 (1973).
- Kiss, G. and R. S. Porter, "Rheology of Concentrated Solutions of Poly(g-benzyl glutamate)," *J. Polym. Sci. :Polym. Symp.* **65**, 193-211 (1978).
- Kiss, G. and R. S. Porter, "Rheology of Concentrated Solutions of Helical Polypeptides," *J. Polym. Sci.: Polym. Phys. Ed.* **18**, 361-388 (1980).
- Kwolek, J. L., U.S. Patent No. 3,671,542 (1972).
- LaMantia, F. P., *Thermotropic Liquid Crystalline Polymer Blends* (Technomic, Pennsylvania, 1993).

- Lenz, R. W., "Balancing Mesogenic and Non-mesogenic Groups in the Design of Thermotropic Polyesters," *Faraday Discuss. chem. Soc.* 21-32, **79** (1985).
- Marrucci, G. and P. L. Maffettone, "Description of the Liquid-Crystalline Phase of Rodlike Polymers at High Shear Rates," *Macromolecules* **22**, 4076-4082 (1989).
- Mewis, J. and P. Moldenaers, "Transient Rheological Behavior of a Lyotropic Polymeric Liquid Crystal," *Mol. Cryst. Liq. Cryst.* **153**, 291-300 (1987).
- Minagawa, N. and J. L. White, "The Influence of Titanium Dioxide on the Rheological and Extrusion Properties of Polymer Melts," *J. Appl. Polym. Sci.* **20**, 501-523 (1976).
- Moldenaers, P. and J. Mewis, "Transient Behavior of Liquid Crystalline Solutions of Poly(benzylglutamate)," *J. Rheol.* **30**, 567-584 (1986).
- Nardard, P., "Formation of Band Textures in Hydroxypropylcellulose Liquid Crystals," *J. Polym. Sci.: Polym. Phys. Ed.* **24**, 435-442 (1986).
- Onogi, S. and T., Asada, "Rheology and Rheo-optics of Polymer Liquid Crystals," In: *Rheology*, (Plenum Press, New York, 1980).
- Onogi, Y., J. L. White, and J. F. Fellers, "Rheo-optics of Shear and Elongational Flow of Liquid Crystalline Polymer Solutions: Hydroxypropylcellulose/Water and Poly-p-phenylene terephthalamide/Sulfuric Acid," *J. Non-Newt. Fluid Mech.* **7**, 121-151 (1980).
- Papkov, S. P., "Liquid Crystalline Order in Solutions of Rigid-Chain Polymers," *Adv. Polym. Sci.* **59**, 75-102 (1984).
- Pochan, J. N. and D. G. Marsh, "Mechanism of Shear Induced Structural Changes in Liquid Crystals-Cholesteric Mixtures," *J. Chem. Phys.* **57**, 1193-1200 (1972).
- Preston, J., "High-Strength/High-Modulus Organic Fibers," *Polym. Eng. Sci.* **15**, 199-206 (1975).

- Sigillo, I. and N. Grizzuti, "The effect of molecular weight on the steady shear rheology of lyotropic solutions. A phenomenological study," *J. Rheol.* **38**, 589-599 (1994).
- Uematsu, I., and Y. Uematsu, "Polypeptide Liquid Crystals," *Adv. Polym. Sci.* **59**, 37-73 (1984).
- Viola, G. G., "Rheological Characteristics, and the Development of Molecular Orientation and Texture During Flow for a Liquid Crystalline Copolymer of Para-hydroxybenzoic acid and Polyethylene Terephthalate," Ph.D. Dissertation, Virginia Polytechnic Institute and State University, Virginia, 1985.
- Viola, G. G. and D. G. Baird, "Studies on the Transient Shear Flow Behavior of Liquid Crystalline Polymers," *J. Rheol.* **30**, 601-628 (1986).
- Wissbrun, K. F., "Observations on the Melt Rheology of Thermotropic Aromatic Polyesters," *Brit. Polym. J.* **12**, 163-169, (1980).
- Wissbrun, K. F., "Rheology of Rod-like Polymers in the Liquid Crystalline State," *J. Rheol.* **25**, 619-662 (1981).



## 4.0 Rheology of an Immiscible Polymer Blend

### Preface

This chapter addresses the second objective of this thesis. The role played by the two phase nature and degradation on the rheological properties of an immiscible polymer blend is investigated. Two different blend preparation methods are used in order to help isolate the effects of polymer degradation on the observed rheological properties from those which are due to the two phase texture and interfacial tension. Specifically, the complex and steady shear viscosity, storage modulus, steady state first normal stress difference, and transient shear stress and first normal stress difference for an immiscible polymer blend are investigated. This chapter is organized as a manuscript which will be submitted to the *Journal of Applied Polymer Science* for publication.

## **Rheology of a Textured Fluid Consisting of Poly(ethylene terephthalate) and Nylon 6,6**

G. K. GUENTHER and D. G. BAIRD, *Virginia Polytechnic Institute & State University,  
Department of Chemical Engineering, Polymeric Materials and Interfaces Laboratory,  
Blacksburg, VA 24061-2011*

### **Synopsis**

The rheology and development of texture of immiscible polymer blends based on poly(ethylene terephthalate) (PET) and nylon 6,6 at composition ratios of 75/25, 50/50 and 25/75 w/w PET/nylon 6,6 were studied. The blends were prepared by mixing in an extruder and by dry blending and mixing between cone and plate fixtures in a nitrogen atmosphere. The rheology of these blends was found to be a function of both polymer degradation and the two phase morphology. An accelerated degradation rate in air was observed for the 75/25 and 50/50 w/w PET/nylon 6,6 blends relative to the neat polymers while the blend at a weight ratio of 25/75 w/w PET/nylon 6,6 displayed a rate of degradation similar to that of the neat polymers. The values of the steady shear viscosity ( $\eta$ ),  $|\eta^*|$ , storage modulus ( $G'$ ) and steady state first normal stress difference ( $N_1$ ) for melt blended 75/25 and 50/50 w/w PET/nylon 6,6 samples were lower than those of the neat polymers and were determined to be a consequence of the higher rate of degradation of these blends during extrusion relative to that of the neat polymers. The role played by the two phase nature on the blends was observed for all samples prepared by dry blending and mixing in cone and plate fixtures under a nitrogen atmosphere and for the melt blended 25/75 w/w PET/nylon 6,6 blend. The two phase nature of the dry blended samples and the extruded 25/75 w/w PET/nylon 6,6 sample resulted in values of  $|\eta^*|$ ,  $\eta$ ,  $G'$ , and  $N_1$  which were higher than those of the neat polymers. Transient behavior observed for the blends using stepwise changes of shear rate was found to superimpose when plotted in reduced form indicating that at rates lower than the longest relaxation time of the neat polymers there was no intrinsic time constant associated with the deformation of the interface in the blends.

## 4.1 INTRODUCTION

Immiscible polymer blends represent complex systems in which the rheological properties are not only a function of the viscoelastic properties of the component polymers but also the morphology which is developed and any reactions which might occur at melt temperatures.<sup>1</sup> In the case of binary blends of immiscible polymers the morphology can in general take the form of one component dispersed in a continuous phase of the second component or both components can be continuous resulting in an interpenetrating network. The morphology of immiscible polymer blends during flow is constantly changing and as a consequence the blend may exhibit rheological properties which are functions of their texture and are not seen in the individual polymers.<sup>2-5</sup>

While the literature pertaining to immiscible polymer blends is extensive as demonstrated in an early review by Paul and Newman,<sup>1</sup> comprehensive rheological data including transient data and the corresponding development of texture is lacking. Rheological studies of polymer blends have generally focused on the correlation of specific rheological properties with the state of miscibility or lack thereof. Some of the rheological observations which were related to immiscibility in polymer blends include: 1) lack of agreement between the blend viscosity and that based on the log additivity rule,<sup>6</sup> 2) lack of agreement between the steady shear and corresponding small strain dynamic oscillatory responses,<sup>7</sup> 3) bimodality in the Cole-Cole plot of the imaginary versus real part of the dynamic viscosity,<sup>8</sup> and 4) a broad relaxation spectrum relative to that of the neat polymers due to the contribution from the interface.<sup>4</sup> While the above observations were reported for many immiscible polymer blends, they were not exclusive to immiscible systems and were also observed in miscible systems.<sup>9-11</sup>

The viscosity of polymer blends relative to the log additivity of the viscosity of the

neat polymer was used to classify polymer blends in investigations by Utracki and Kamal<sup>6</sup> and LaMantia.<sup>12</sup> This method placed polymer blends in one of three categories based on a blend viscosity which relative to the log additivity of the viscosity of the blend components was lower (negative deviation), higher (positive deviation), or both lower and higher (positive-negative deviation) depending on concentration. Systems in which a positive deviation was observed included immiscible blends where strong interdomain interactions were present and miscible blends in which the intersegmental interactions may be nonrepulsive. Polymer blends which displayed partial miscibility or a limited miscibility at low concentrations fell into the category of negative deviation blends. Finally, polymer blends in which both positive and negative deviations were observed included those blends where, depending on concentration or shear rate, a phase inversion or a concentration dependent transition of structure occurred. For example, in a study of high density polyethylene (HDPE) and polystyrene (PS) blends by Han and Kim<sup>13</sup> the viscosity was seen to go through both a minimum and a maximum as the composition was varied for a given stress. The minimum in viscosity was observed at a composition of 50/50 HDPE/PS and the maximum at a composition of 75/25 HDPE/PS. The minimum in viscosity corresponded to a morphology of dispersed HDPE droplets and the maximum to a co-continuous morphology. With an increase in the stress, the minimum in viscosity was no longer observed and was correlated to a shift of the onset of the co-continuous morphology to a lower HDPE content.

The presence of yield stresses in immiscible polymer blends was described as evidence of interactions during flow of the dispersed phase in an investigation by Utracki.<sup>2</sup> An apparent yield stress was reported in a study by Chuang and Han<sup>7</sup> using an immiscible blend of poly(methyl methacrylate) (PMMA) with polystyrene (PS), a miscible blend of two low-density polyethylenes (LDPE) of different molecular weights, and a miscible blend of

PMMA with Poly(vinylidene fluoride) (PVDF). In Chuang and Han's study, each material was examined over a range of compositions and temperatures. Their results showed an apparent yield stress by an upturn in the viscosity at low shear rates for the immiscible system consisting of PMMA with PS while a Newtonian plateau was observed for both miscible blends. On the other hand, an apparent yield stress was not always observed in immiscible systems as was demonstrated in a study by Utracki *et al.*<sup>6,14</sup> In the study by Utracki *et al.* a Newtonian plateau was observed using an immiscible blend of poly(ethylene terephthalate) (PET) and nylon 6,6. Although a Newtonian plateau was observed, the shear rate at which the transition from Newtonian to shear thinning behavior occurred was lower in the blend than in either neat polymer.

Although transient data obtained from experiments such as the start up of steady shear flow could provide valuable insight into the development of texture in immiscible polymer blends, very little work of this nature has been reported. In an investigation by Nobile *et al.*<sup>15</sup> the transient behavior of a blend of polyetherimide (PEI) and a thermotropic liquid crystalline polymer (TLCP) based on hydroxybenzoic acid, terephthalic acid, hydroquinone, and 4-4' dihydroxybiphenol (K161, from Bayer) at a weight ratio of 90/10 PEI/K161 was reported. The data showed an overshoot which appeared at shear rates lower than that required to produce an overshoot for the pure matrix. Additionally, it was observed that steady state was not obtained even after 250 strain units while pure polyetherimide reached steady state in less than 50 strain units. Nobile *et al.* associated the continuous decrease in the stress with the continuous deformation and orientation of the TLCP phase during flow.

The rheological properties of immiscible polymer blends may, in addition to the morphology, be a function of chemical changes such as those associated with polymer degradation and reactions which may occur as the polymers are mixed. An example of a

system in which reactions and degradation were observed in blends consisting of poly(ethylene terephthalate) (PET) and nylon 6,6. The literature pertaining to polyester/polyamide blends is fairly extensive.<sup>2,6,14,16-19</sup> At certain concentrations (e.g., nylon 6,6 concentrations of between 5 and 35 wt. %) PET/nylon 6,6 blends were reported to fall into the category of negative deviation blends.<sup>6,14,20</sup> The origin of a blend viscosity which is lower than that of the log additivity of the neat polymers was complicated by the fact that in addition to a two phase morphology extensive degradation was also reported to occur in this system. While these observations were each treated separately, it is likely that they were interrelated.

The degradation behavior of PET/nylon 6,6 blends was investigated by Utracki *et al.*<sup>14</sup>. It was shown using measurements of viscosity versus time that in blends consisting of nylon 6,6 levels ranging from 5 to 35 wt. % that the rate of decrease in the viscosity with time for the blends was greater than that of the neat polymers. In addition, the temperature dependence of the degradation process measured in terms of the apparent overall activation energy of degradation for the blends was higher than values calculated from a simple additivity rule using the activation energies of the component polymers. Utracki *et al.* attributed the degradation of PET to random chain scission and the degradation of nylon 6,6 to random cleavage of C-N bonds. The accelerated degradation of the blends was postulated to be a result of the initial catalytic effect of the amide groups on the degradation of PET which in turn accelerated the degradation of the nylon 6,6. On the other hand, although degradation may be purely thermal for these polymers, accelerated degradation in the presence of trace amounts of water for polymers containing hydrolysable linkages such polyamides and polyesters may also play a role.

The formation of block copolymers by ester interchange reaction in polyester/polyamide blends was documented in the patent literature.<sup>21-23</sup> The times required

for the interchange reaction were reported to range from 5 to 30 hours for reaction temperatures ranging from 220 °C to 290 °C. The copolymers which were formed at the interface were found to compatibilize the system, reducing interfacial tension and the contribution of the interface to the rheological properties of the blend.<sup>3-5</sup>

In a study by Pillon and Utracki<sup>16</sup> the ester interchange reaction was used to form copolymers of PET and nylon 6,6 in order to compatibilize the blend. A catalyst consisting of p-toluenesulfonic acid (TsOH) was introduced to facilitate the ester-amide interchange reaction. It was shown that the extent of the interchange reaction reached 23.3% in the presence of the TsOH catalyst as measured by NMR methods. Blending was carried out in an extruder with a residence time of 2 minutes and a maximum barrel temperature of 370 °C. No indication of the exchange reaction was detected when no catalyst was used by blending in an extruder with a maximum barrel temperature of 300 °C and a residence time of 4 minutes. In a study by Kimura *et al.*<sup>19</sup> the rate at which the exchange reaction occurred was demonstrated using a blend consisting of poly(butylene terephthalate) and polyarylate. Kimura *et al.* showed using intrinsic viscosity measurements and melting point depression as a function of reaction time that appreciable transesterification occurred only after approximately 100 minutes. Although compatibilization of polyester/polyamide blends due to the ester interchange reaction was reported, the time scale for the reaction was on the order of hours and was much longer than the time scale of most blending processes.

It is clear that the rheology of blends of PET and nylon 6,6 can be complicated by several factors including degradation, transesterification, and interfacial tension. However, it is apparent that under most normal blending operations there is not sufficient time for transesterification to occur. Hence, the primary goal of this work is to separate the effect of degradation on the rheology of the blend from that of interfacial tension. To accomplish this we compare the rheological properties of blends prepared under normal mixing

conditions to those prepared under controlled conditions where degradation is minimized.

## **4.2 EXPERIMENTAL**

The materials and methods used in this work are presented in this section. First, the polymers used and the blend preparation methods are presented. Next, the methods used to determine the state of the texture (microscopy) and the rheological properties are discussed.

### **4.2.1 Materials and Sample Preparation**

The polymers used in this investigation were poly(ethylene terephthalate) (PET) and nylon 6,6. The PET supplied by Dupont was PTX-267 ( $M_w = 25,000$ ) and has a melting temperature of 257 °C determined using differential scanning calorimetry. The recommended drying conditions for PET are 120 to 125 °C for 3 to 4 hours in vacuum which yields a moisture content of 0.02 %. The nylon 6,6 supplied by Monsanto was Vydyne 66b ( $M_w = 30,000$ ) and was determined to have a melting temperature of 263 °C determined using differential scanning calorimetry. The recommended drying conditions for nylon 6,6 are 75-80 °C for 3 to 4 hours in vacuum.

Due to the extensive degradation and ester interchange reaction reported for blends of these two polymers, two different blend preparation methods were used. In order to provide blends with a minimum residence time and exposure to moisture during blending, PET and nylon 6,6 were mixed using the following procedure. First, the neat polymers in pellet form were granulated in a Thomas Scientific granulator which produced samples with particle sizes ranging from 0.05 to 0.5 mm in diameter. Quantities of the granulated



polymers corresponding to the appropriate weights required to produce blends with weight ratios of 25/75, 50/50 and 75/25 w/w PET/nylon 6,6 were placed in separate containers and dried in a vacuum oven (PET at 125 °C and nylon 6,6 at 75 °C for 36 hours). After drying, samples were dry blended under vacuum by mixing in a plastic desiccator and then immediately placed back into a vacuum oven at 100 °C. In order to provide further mixing, dry blended samples were presheared for 1 minute at 5 sec<sup>-1</sup> in a cone and plate fixture under a nitrogen atmosphere prior to performing all rheological experiments. The samples prepared in the above manner will be referred to as DB-75/25, DB-50/50 and DB-25/75 for the 75/25, 50/50 and 25/75 PET/nylon 6,6 w/w blends, respectively, and the neat polymers simply as PET and nylon 6,6 in the following discussion.

The second blend preparation method used consisted of melt blending in an extruder. The neat polymers in pellet form were dried in a vacuum oven prior to dry blending. PET was dried for 36 hours at 125 °C in a vacuum oven and nylon 6,6 was dried for 36 hours in a vacuum oven at 75 °C to insure a minimum moisture content in the samples. Weighed amounts of the dried polymers were dry blended and stored in a vacuum oven at 100 °C. Dry blended pellets in proportions of approximately 30 grams at a time were removed from the oven and immediately loaded into the hopper of a 2.54 cm Killion extruder. New pellets from the oven were added to the hopper only after the last pellets from the previous charge had reached the feed section of the extruder. Extrusion was carried out at 20 RPM with an attached capillary die with a diameter of 0.3175 cm and a L/D of 10. The barrel temperatures from the feed zone to the die were 260, 275, 290, 290 and 270 °C, respectively. The extrusion conditions described above correlate to a residence time at melt temperatures during the blending process of 4.5 minutes based on the flow rate and screw and barrel dimensions. The neat polymers were subjected to the same processing histories as the blends. The samples prepared in the above manner will be referred to as

MB-75/25, MB-50/50 and MB-25/75 for the 75/25, 50/50 and 25/75 w/w PET/nylon 6,6 blends, respectively, and MB-PET and MB-nylon 6,6 for neat PET and neat nylon 6,6, respectively, in the following discussion.

#### 4.2.2 Rheological Measurements

Rheological experiments were carried out on the blends and neat polymers using a Rheometrics Mechanical Spectrometer (RMS-800) with a cone and plate fixture having a cone angle of 0.1 rad and a diameter of 12.5 mm. Steady shear viscosity ( $\eta$ ) and first normal stress difference ( $N_1$ ) data was obtained after the sample was sheared long enough to reach steady state conditions. The magnitude of the complex viscosity ( $|\eta^*|$ ) and storage modulus ( $G'$ ) were obtained as a function of angular frequency ( $\omega = 2\pi f$ ) in the range 0.1 to 100 rad/sec. Dynamic oscillatory experiments were run using strain amplitudes ( $\gamma_0$ ) in the linear viscoelastic range (e.g.,  $\gamma_0 = 0.08$ ). All experiments were carried out at a temperature of 290 °C under a nitrogen atmosphere unless otherwise stated. Dry blended samples were presheared under a nitrogen atmosphere at 5 sec<sup>-1</sup> for 1 minute using a nitrogen atmosphere to provide additional mixing. A recovery time of 30 seconds was allowed following the preshear prior to starting subsequent rheological measurements. Time sweep experiments were carried out on all samples at 280, 290, and 300 °C under both nitrogen and air atmospheres in which  $|\eta^*|$  at  $\omega = 1$  rad/sec and  $\gamma_0 = 0.08$  was measured.

#### 4.2.3 Microscopy

The state of mixing and morphology of the blends prepared by both dry and melt

blending was examined by means of scanning electron microscopy. Scanning electron microscopy was carried out using a Cambridge Stereoscan S200 electron microscope. Melt blended samples were prepared by means of cryogenic fracture of extruded strands after immersion in liquid nitrogen for 5 minutes. Dry blends were prepared by first preshearing each blend between parallel plates for 1 minute at a shear rate of  $5 \text{ sec}^{-1}$ . The blend was then removed from the test fixtures and was cryogenically fractured after immersion in liquid nitrogen for 5 minutes. The fractured samples were fixed to aluminum stubs and sputter coated.

## 4.3 RESULTS

The rheological results of this work are organized as follows. The stability of the samples with respect to degradation is discussed in terms of the decrement of  $|\eta^*|$  with time. The information obtained on the degradation behavior of the blends and neat polymers is then used to isolate the effect of degradation which occurred during melt blending from that due to the two phase morphology on the rheological properties of the blends. Specifically, the role played by the two phase nature of the blends and degradation on the dynamic oscillatory, steady shear and transient behavior of the blends is discussed.

### 3.3.1 Viscosity

The change in the magnitude of the complex viscosity,  $|\eta^*|$ , of the blends and neat polymers as a function of time and temperature was examined because of the extensive degradation reported to occur in PET and nylon 6,6 as well as their blends.<sup>14</sup> Once the

decrease in  $|\eta^*|$  due to degradation for the samples was determined, the role played by the two phase nature of the blends on  $|\eta^*|$  and the steady shear viscosity,  $\eta$ , as a function of angular frequency and shear rate, respectively, was examined.

The decrease in  $|\eta^*|$  with time for the blends and neat polymers in air at temperatures of 290 and 300 °C is shown in Figure 4.1. A logarithmic decay of  $|\eta^*|$  with time is observed for all samples. Similar results were reported for PET, nylon 6,6 and their blends by Utracki *et al.*<sup>14</sup> and were explained in terms of the mechanism of random chain scission which was described by first order degradation kinetics.<sup>24</sup> The magnitude of the complex viscosity of PET is seen to decrease by 30% and 45% in 5 minutes at 290 and 300 °C, respectively. The magnitude of the complex viscosity of nylon 6,6 is seen to decrease by 10% and 28% in 5 minutes at 290 and 300 °C, respectively. At 290 °C the DB-25/75 and DB-50/50 blends degrade at a rate intermediate to that observed for the two neat polymers while the blend rich in PET (e.g., DB-75/25) degrades at a rate faster than that observed for both neat polymers. Both the DB-50/50 and DB-75/25 blends show a rate of decrease in complex viscosity with time as the temperature is increased to 300 °C which is faster than that of the neat polymers at the same temperature.

In order to quantify the decrease in the magnitude of the complex viscosity with time, the isothermal logarithmic decrement of viscosity (D) for all samples was computed by fitting time sweep data taken at  $\omega = 1$  rad/sec,  $\gamma_0 = 0.08$  and temperatures of 280, 290 and 300 °C using the relationship,

$$D = \left( \frac{d \ln |\eta^*|}{dt} \right) \cdot (-10^3). \quad (4.1)$$

The parameter D was estimated for the samples subjected to extrusion. Assuming that the

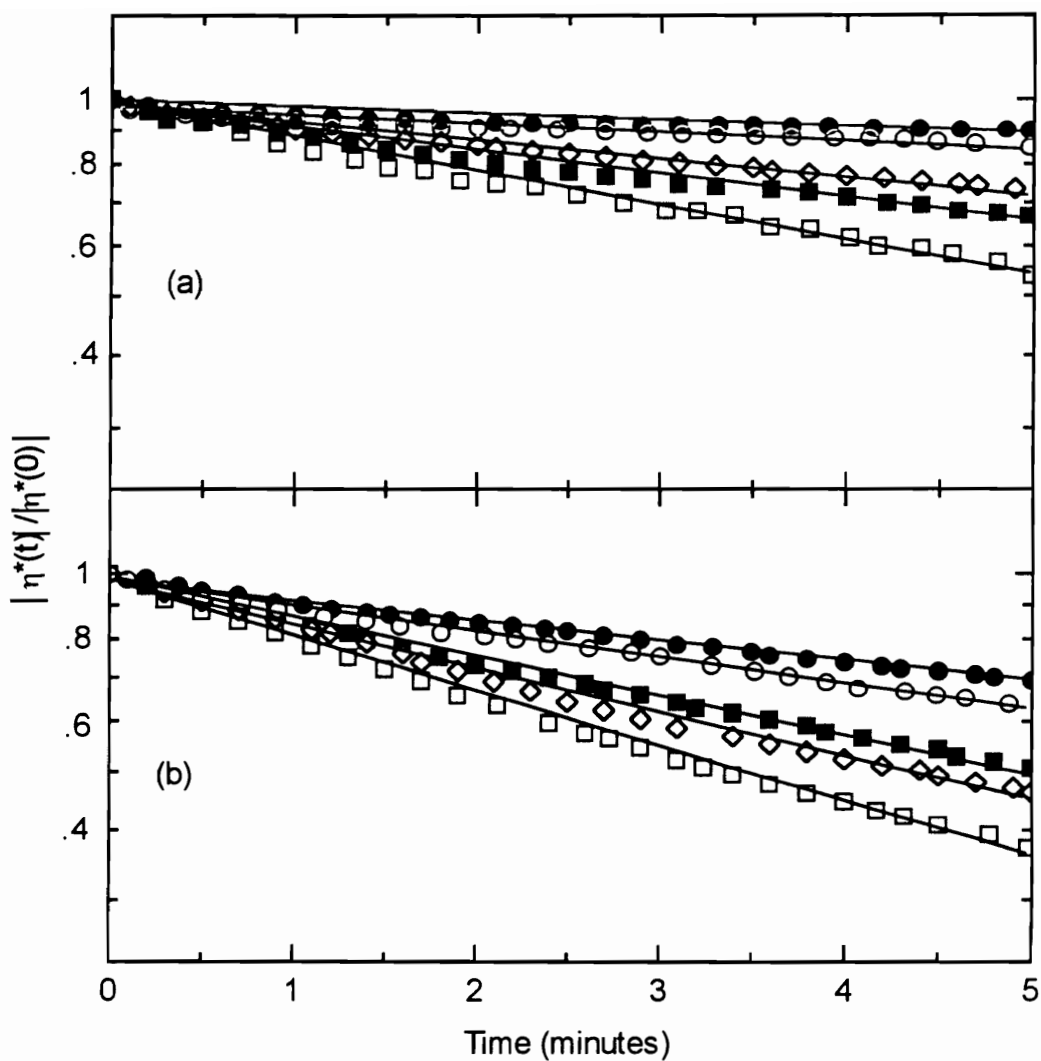


**Figure 4.1** Normalized magnitude of the complex viscosity as a function of time at a fixed frequency of 1 rad/sec and a strain of 5% in air at (a) 290 °C and (b) 300 °C for melt blended PET/nylon 6,6 samples: (■) 100/0; (□) 75/25; (◇) 50/50; (○) 25/75; and (●) 0/100. The lines represent best fits using eq. (1).

degradation occurring during extrusion resulted in a logarithmic decrease in viscosity with time as described by eq. (4.1) and based on a residence of 4.5 minutes a value for the parameter D was calculated for each sample using the magnitude of the complex viscosity of the samples measured before extrusion (e.g.,  $|\eta^*|$  at time = 0) and after extrusion (e.g.,  $|\eta^*|$  at time = 4.5 minutes). The estimated value of the parameter D for the blends was calculated using the value of  $|\eta^*|$  at 1 rad/sec for the presheared dry blends and the value of  $|\eta^*|$  at 1 rad/sec for the extruded blends. The estimated value of the parameter D for the extrusion process for the neat polymers was calculated using  $|\eta^*|$  at 1 rad/sec for the neat polymers measured before and after subjecting them to extrusion. The values of D calculated by fitting eq. (4.1) to the time sweep data and estimated for the extrusion process for the blends and neat polymers are shown in Figure 4.2 and listed in Table 4.1. The results show that the rate of decrease of  $|\eta^*|$  with time due to degradation for the blend at a weight ratio of 25/75 w/w PET/nylon 6,6 corresponds to that predicted using the weighted average of the values of D for the neat polymers. On the other hand, blends of 75/25 and 50/50 w/w PET/nylon 6,6 have values of D higher than the weighted average of D for the neat polymers. Based on these results the magnitude of the viscosity of melt blended 25/75 PET/nylon 6,6 blend relative to the extruded neat polymers is independent of the degradation occurring during extrusion. However, the viscosity of the melt blended 75/25 and 50/50 PET/nylon 6,6 system is reduced relative to that of the neat polymers.

The temperature dependence of the degradation process was calculated in terms of the apparent overall activation energy of degradation ( $E_D$ ). The overall activation energy of the degradation process was calculated by fitting the logarithmic decrement of viscosity data shown in Figure 4.2 obtained using time sweep experiments at  $\omega = 1$  rad/sec,  $\gamma_0 = 0.08$  and temperatures of 280, 290 and 300 °C in air using the following relationship,

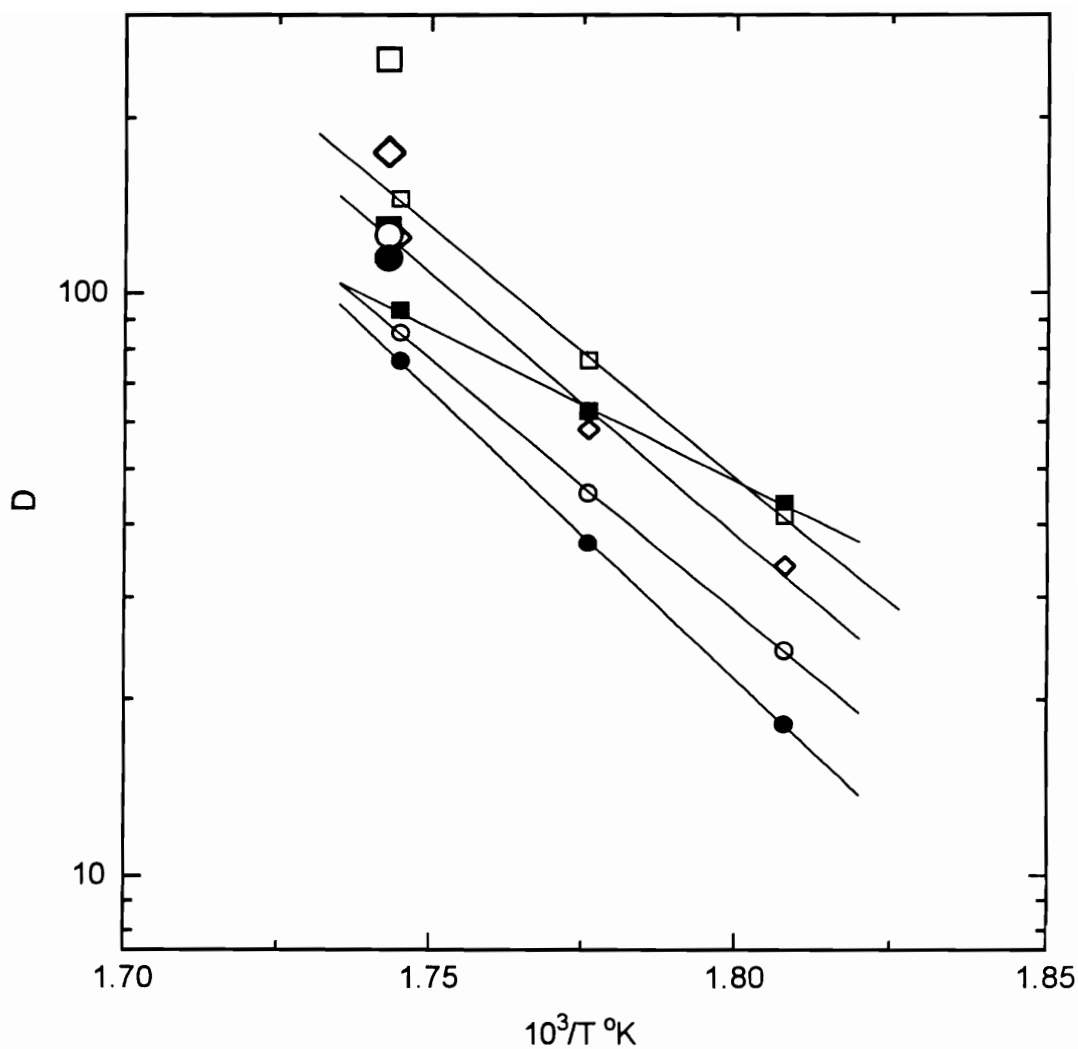


**Figure 4.2** Logarithmic decrement of viscosity as a function of reciprocal temperature samples based on time sweep measurements for PET/nylon 6,6 samples: (■) 100/0; (□) 75/25; (◇) 50/50; (○) 25/75; and (●) 0/100 and estimated for PET/nylon 6,6 samples subject to extrusion: (■) 100/0; (□) 75/25; (◇) 50/50; (○) 25/75; and (●) 0/100 estimated for the extrusion process. The lines represent best fits using eq. (2).

**TABLE 4.1** Logarithmic decrement of viscosity (D) and the apparent overall activation energy of degradation ( $E_D$ ) in air for PET/nylon 6,6 blends.

PET/nylon 6,6 w/w	D ( $\pm 2$ )			$E_D$ ( $\pm 4$ )	
	[ln(Pa s)/s]			(kcal/mole)	
	280 °C	290 °C	300 °C	Extrusion <sup>(a)</sup>	
100/0	43.53	62.52	93.03	129.32	26
75/25	41.28	76.35	145.01	251.81	38
50/50	33.89	58.22	124.85	175.26	41
25/75	24.25	45.42	85.32	125.97	49
0/100	18.12	37.19	76.42	114.87	45

(a) Calculated from the magnitude of the complex viscosity of samples before and after extrusion.



$$E_D = R \left( \frac{d \ln D}{d(1/T)} \right) \quad (4.2)$$

where R is the gas constant. The values for  $E_D$  determined using eq. (4.2) are listed in Table 4.1. The values for  $E_D$  reported here are within the range reported in the literature for PET<sup>14,24-26</sup> and nylon 6,6.<sup>14,27-29</sup> In addition, the value of  $E_D$  for the 75/25 w/w PET/nylon 6,6 blend is in agreement with  $E_D$  reported for this blend at the same weight ratio by Utracki *et al.*<sup>14</sup>. The estimated values of D for the samples subjected to the extrusion process are also shown in Figure 4.2 plotted at the maximum barrel temperature used during extrusion (e.g., 290 °C). It can be seen that for the extruded neat polymers and blends, the values of D estimated for the samples subjected to the extrusion process at 290 °C far exceed those calculated from time sweep measurements at 290 °C and do not fall on the curves predicted using eq. 4.2. This discrepancy may be related to the conditions during extrusion (e.g., viscous heating and exposure to moisture) which are not experienced during time sweep experiments.

In order to determine the stability of the blends and neat polymers during rheological experiments, time sweeps were also performed on the samples at 290 °C under a nitrogen atmosphere. The change in  $|\eta^*|$  with time for the melt and dry blended samples and the neat polymers before and after extrusion in a nitrogen atmosphere are shown in Figure 4.3. A logarithmic decrease in the viscosity with time is also observed for samples tested in nitrogen. The values of the parameter D for the samples tested in nitrogen calculated using eq. (4.1) are listed in Table 4.2. It can be seen by comparison of the values of D listed in Tables I and II that the rate of degradation in nitrogen is lower than in air. The degradation behavior of the neat polymers both before and after extrusion is seen to be the same. In the case of PET, a decrease in  $|\eta^*|$  of approximately 9% in 5 minutes is

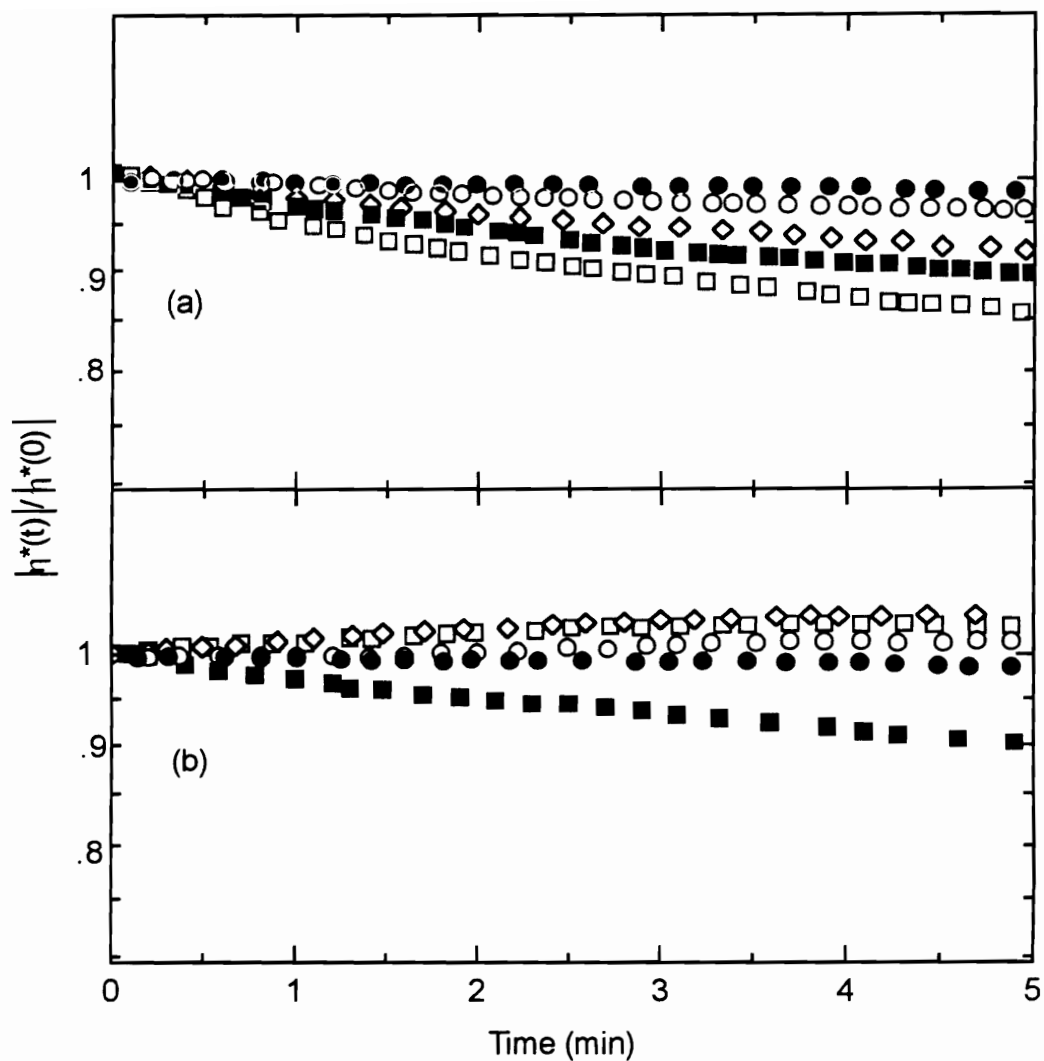


**Figure 4.3** Normalized magnitude of the complex viscosity as a function of time at a fixed frequency of 1 rad/sec and a strain of 5% in nitrogen for (a) melt blended and (b) dry blended PET/nylon 6,6 samples: (■) 100/0; (□) 75/25; (◇) 50/50; (○) 25/75; and (●) 0/100 at 290 °C.

**TABLE 4.2** Logarithmic decrement of viscosity (D) in nitrogen PET/nylon 6,6 blends.

PET/Nylon 6,6 w/w	D ( $\pm 2$ ) [ln(Pa s)/s]
Dry Blends	
100/0	18.75
75/25	0 <sup>(a)</sup>
50/50	0 <sup>(a)</sup>
25/75	0 <sup>(a)</sup>
0/100	9.72
Melt blends	
100/0	20.15
75/25	34.50
50/50	20.98
25/75	19.74
0/100	9.91

(a) An increase in complex viscosity was observed in these blends and may be related to a relaxing morphology following preshearing.

observed while  $|\eta^*|$  for nylon 6,6 is seen to remain essentially constant within a time frame of 5 minutes. The rate of the decrease in  $|\eta^*|$  with time for the MB-25/75 and MB-50/50 is seen to be between that of the neat polymers (e.g., 3% and 7%, respectively in 5 minutes) while the MB-75/25 blend complex viscosity decreases at a rate higher than that of neat PET (e.g., 14% in 5 minutes). On the other hand, in the case of the dry blended samples the complex viscosity is seen to increase slightly with time until approximately 3 minutes after which no further change is observed. The increase in complex viscosity (e.g.,  $< 4\%$  in 5 minutes) with time for the dry blended samples may be related to the incomplete relaxation of the morphology after preshearing because time sweeps were started approximately 30 seconds after cessation of the preshear. The results presented here are in contrast to those reported by Utracki *et al.*<sup>14</sup> in which it was reported that the degradation process measured in terms of the decrease in viscosity with time were the same in both air and nitrogen atmospheres.

The role played by degradation and the two phase morphology of the blends on  $|\eta^*|$  as a function of angular frequency and steady shear viscosity as a function of shear rate was investigated. The magnitude of the complex viscosity of the MB-25/75, MB-50/50, and MB-75/25 blends as a function of angular frequency is shown in Figure 4.4 along with that of the neat extruded polymers (MB-PET and MB-nylon 6,6). The magnitude of the complex viscosity of the MB-75/25 and MB-50/50 blends is below that of the neat polymers. The reduced  $|\eta^*|$  of the MB-75/25 and MB-50/50 blends relative to that of the neat polymers can be correlated directly to the higher rate of degradation of the blends during extrusion than that of the neat polymers. A higher value of  $|\eta^*|$  for the MB-75/25 and MB-50/50 blends than the neat polymers would be observed in the absence of degradation. The MB-25/75 blend has higher values of  $|\eta^*|$  than those of the neat polymers at all but the highest angular frequency measured. Because the parameter D calculated from

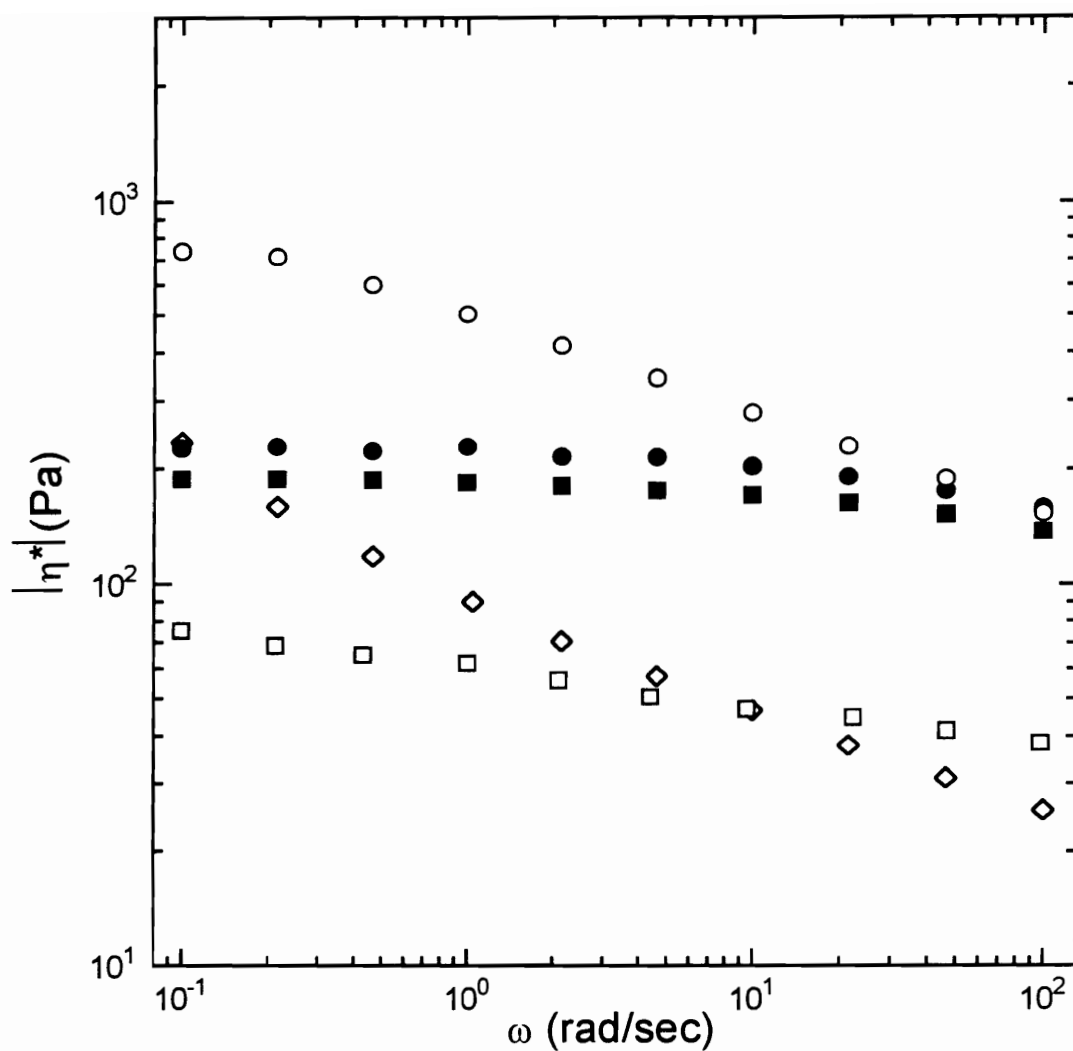


**Figure 4.4** Magnitude of the complex viscosity as a function of frequency at 290 °C for melt blended PET/nylon 6,6 samples: (■) 100/0; (□) 75/25; (◇) 50/50; (○) 25/75; and (●) 0/100.

time sweep experiments and estimated for the extrusion process for the 25/75 PET/nylon 6,6 blend is between that of the neat polymers (see Table 4.1 and Figure 4.1), the higher values of  $|\eta^*|$  relative to those of the neat polymers can be attributed to the two phase nature of the blend and not to degradation. The steady shear viscosity as a function of shear rate for the MB-25/75, MB-50/50, and MB-75/25 blends shown in Figure 4.5 displays similar qualitative behavior as the complex viscosity as a function of angular frequency for these blends. It can also be seen that both the 75/25 and 50/50 PET/nylon 6,6 blends display a greater degree of shear thinning than the neat polymers with the highest degree of shear thinning being seen in the 75/25 blend. The observed shear thinning cannot be explained in terms of degradation occurring during the dynamic oscillatory and steady shear experiments. An apparent yield stress was observed by Utracki *et al.*<sup>14</sup> in PET/nylon 6,6 blends by an upturn of the viscosity at low shear rates at 280 °C but was not observed at 285 °C and 290 °C. Utracki *et al.* attributed the apparent yield stress to associations of the dispersed phase at 280 °C which were destroyed at 285-290°C. The higher viscosity of the MB-25/75 blend than that of the neat polymers can most likely be attributed to the two phase morphology. The lower viscosity of the MB-75/25 and MB-50/50 blends relative to the neat polymers can be attributed to degradation.

In order to confirm that the lower values of viscosity for the MB-75/25 and MB-50/50 blends relative to those of the neat polymers are a result of the accelerated degradation which occurs for these blends relative to the neat polymers during extrusion, frequency sweeps were also carried out on the dry blended samples and neat polymers without subjecting them to extrusion (see Fig. 4.6). The data in Figure 4.6 shows that all three blends display a higher viscosity than the neat polymers. These results show that the blend rich in PET (e.g., DB-75/25) has the highest viscosity followed by the DB-50/50 blend and finally the DB-25/75 blend. In contrast to the melt blended samples, the

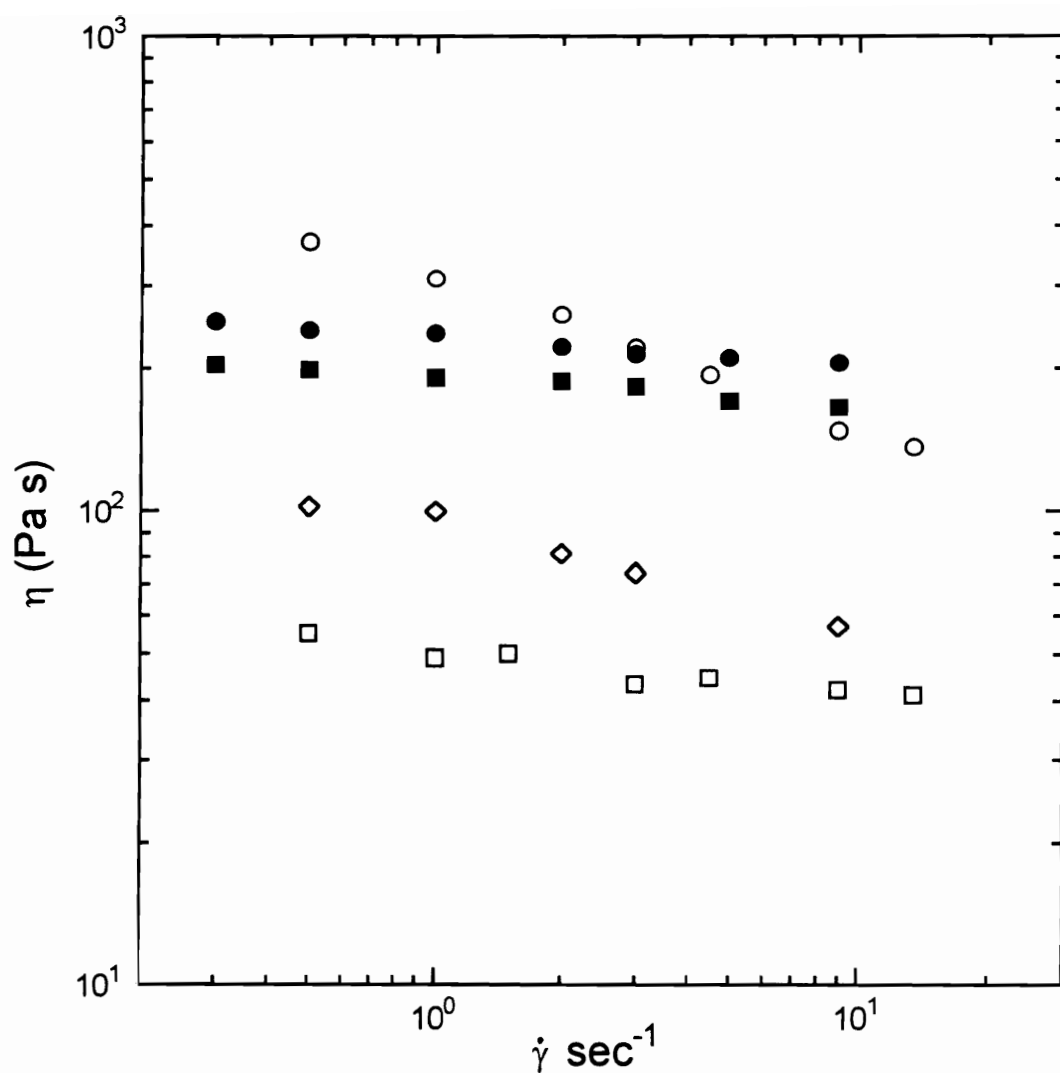


**Figure 4.5** Steady shear viscosity as a function of shear rate at 290 °C for melt blended PET/nylon 6,6 samples: (■) 100/0; (□) 75/25; (◇) 50/50; (○) 25/75; and (●) 0/100.

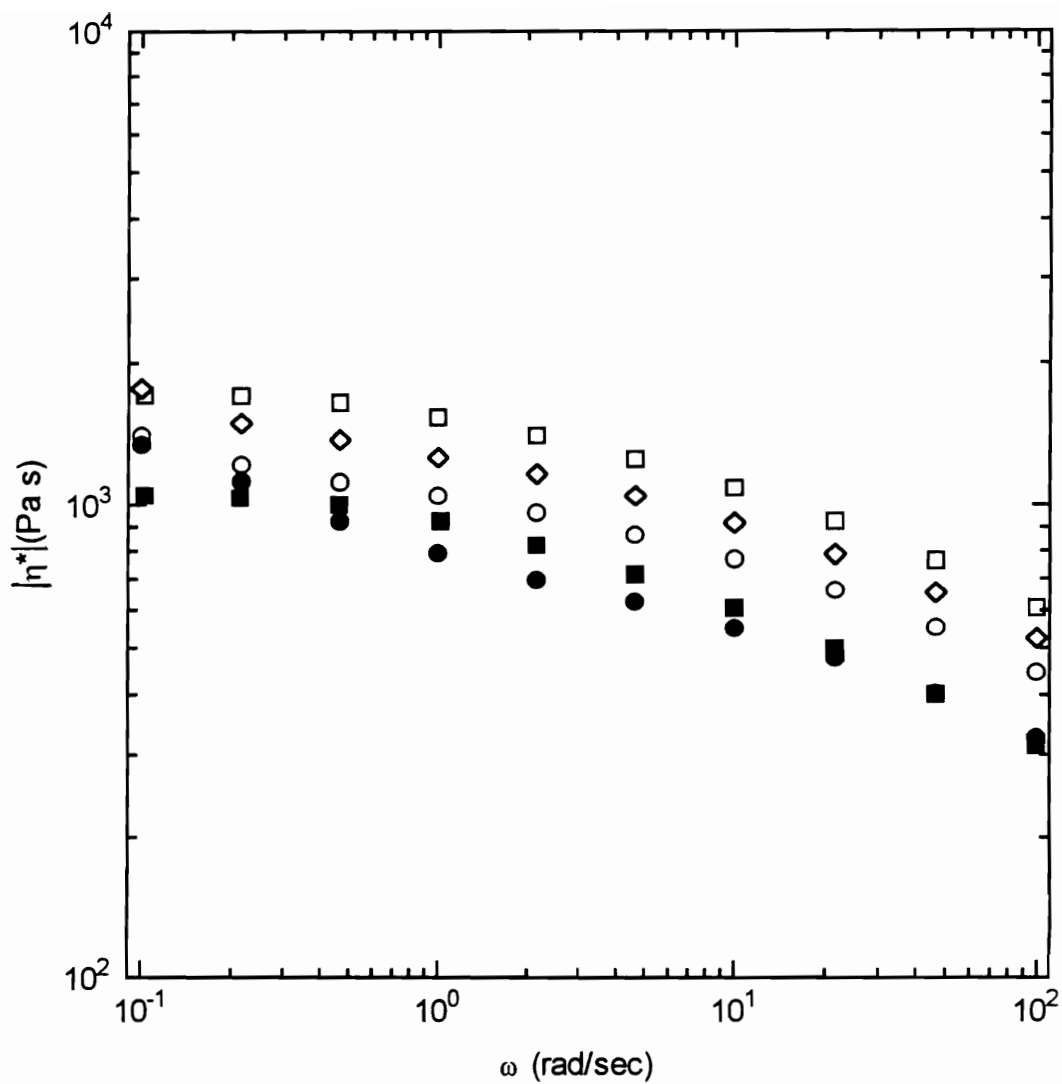


**Figure 4.6** Magnitude of the complex viscosity as a function of frequency at 290 °C for dry blended PET/nylon 6,6 samples: (■) 100/0; (□) 75/25; (◇) 50/50; (○) 25/75; and (●) 0/100.



enhanced shear thinning behavior relative to the neat polymers is not observed in the dry blended samples which may be due to the shear thinning behavior of the neat polymers themselves.

The magnitude of the complex viscosity and the steady shear viscosity and rate of degradation of the blends relative to that of the neat polymers can also be correlated to the morphology of the blends. The higher rate of degradation and lower viscosity of the MB-75/25 and MB-50/50 blends as compared to the neat polymers corresponds to a larger dispersed phase size than is observed in the MB-25/75 blend (see Fig. 4.7). The dispersed phase of nylon 6,6 for the MB-75/25 and MB-50/50 blends (Figs. 4.7a and 4.7b, respectively) has dimensions in the range of 10 to 30  $\mu\text{m}$  in diameter. The MB-25/75 blend (see Fig. 4.7c) has a dispersed phase of PET with dimensions on the order of 5  $\mu\text{m}$  in diameter. A similar dispersed phase size for the MB-25/75 blend is seen for the dry blended samples at all three weight ratios (see Fig. 4.8) and also corresponds to a viscosity which is higher than that of the neat polymers. The DB-75/25 and DB-50/50 blends (see Figs. 4.8a and 4.8b) have a dispersed phase of nylon 6,6 with drop sizes ranging from 1 to 5  $\mu\text{m}$  in diameter and the DB-25/75 blend (see Fig 4.8c) has a dispersed phase of PET with drop sizes also ranging from 1 to 5  $\mu\text{m}$ . A higher rate of degradation of the blend relative to the neat polymers corresponds to a larger dispersed phase size and a blend viscosity which is lower than that of the neat polymers. The dispersed phase size is small and the viscosity of the blend is higher than that of the neat polymers when the rate of degradation of the system during blending is similar to that of the neat polymers (e.g., MB-25/75 blend) or when the extent of degradation is low (i.e., dry blended samples). The larger dispersed phase size of the MB-75/25 and MB-50/50 blends may be related to the fact that PET degrades more during blending and hence it is more difficult to reach the critical Weber number (e.g., ratio of viscous stresses to interfacial stresses at which a droplet will burst).

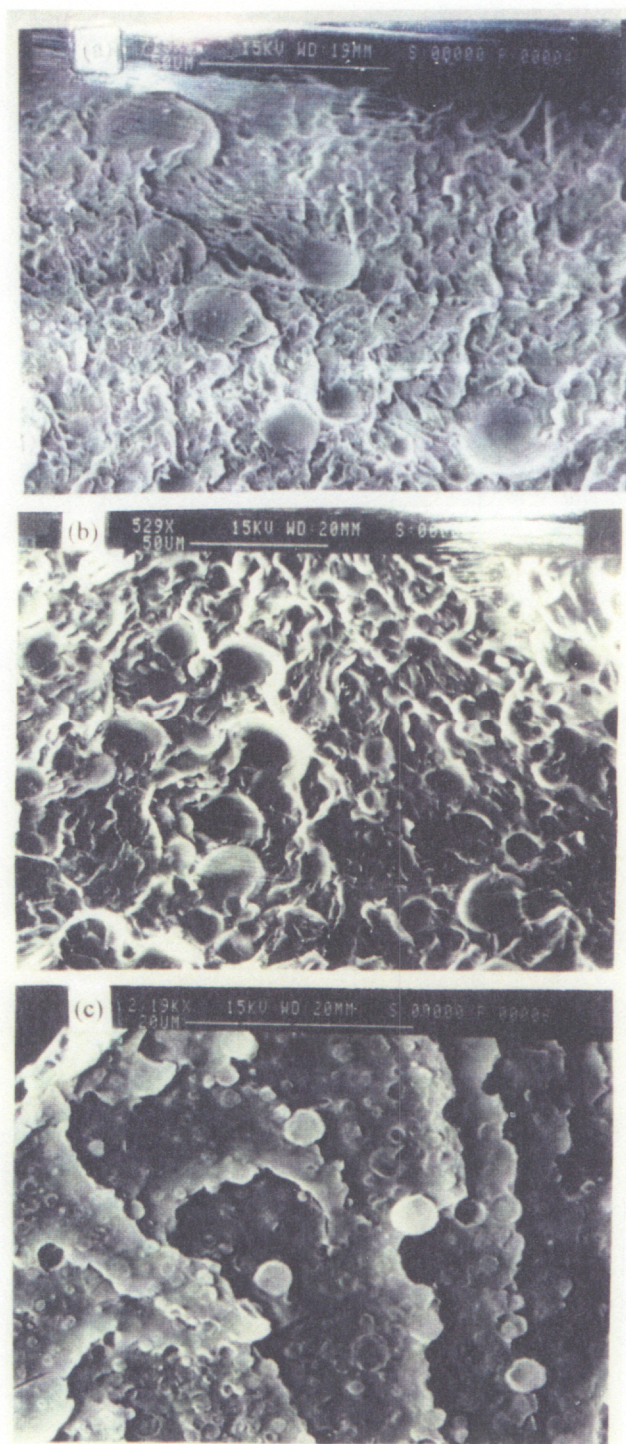


**Figure 4.7** Scanning electron micrographs of melt blended PET/nylon 6,6 samples: (a) 75/25; (b) 50/50; and (c) 25/75.



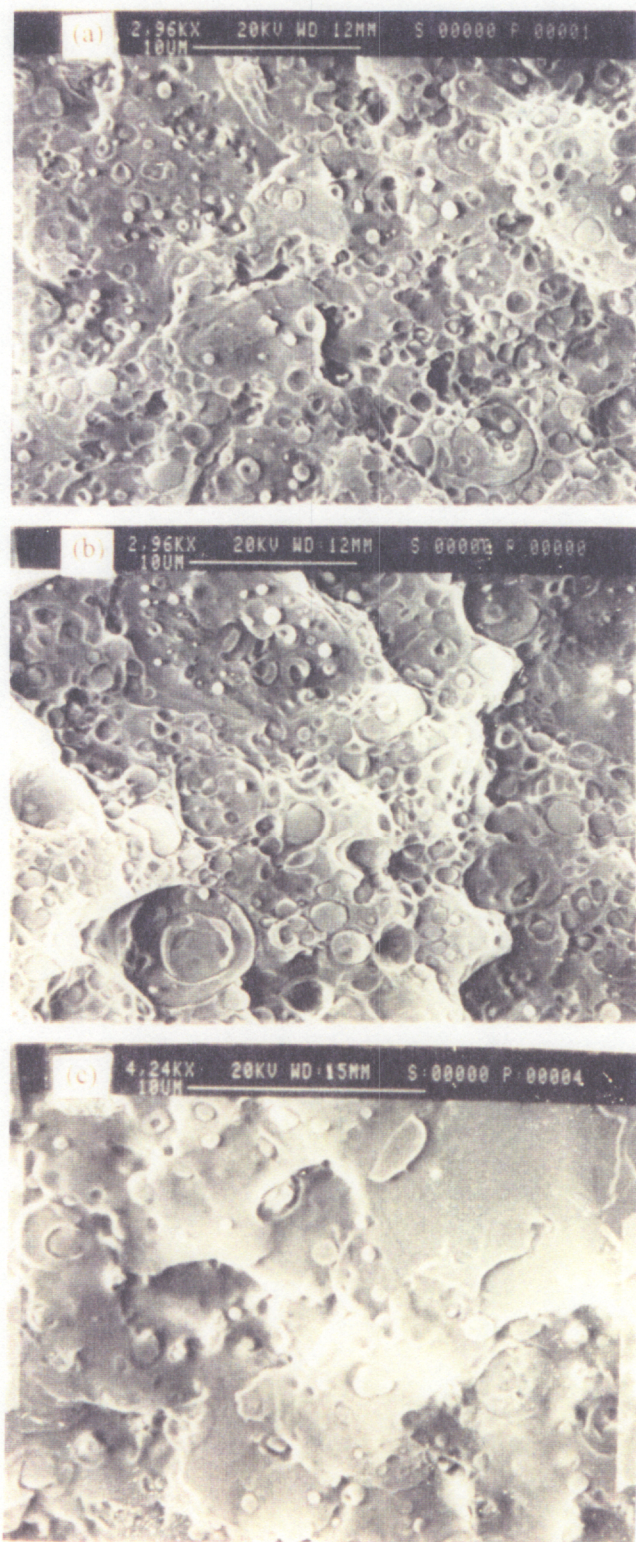


**Figure 4.8** Scanning electron micrographs of dry blended PET/nylon 6,6 samples: (a) 75/25; (b) 50/50; and (c) 25/75.

The effect of large strains and deformation on the dispersed phase during shear flow was examined by comparing  $\eta$  and  $|\eta^*|$  for the blends to those of the neat polymers. The magnitude of the complex viscosity of the blend relative to that of the neat polymers (see Fig. 4.4) is higher than the steady shear viscosity of the blend relative to that of the neat polymers (see Fig. 4.5). This may be due to the deformability of the dispersed phase during shear flow. The deformability of the dispersed phase of the MB-25/75 blend is demonstrated in Figure 4.9 in which the sample was quenched following shear flow. It can be seen that the drops of the dispersed phase (PET) readily deform during shear flow and result in a texture consisting of both drops (with diameters on the order of 5 microns) and deformed drops or fibrils (with diameters ranging from 5 to 25 microns) oriented in the flow direction. At a shear rate of  $0.5 \text{ sec}^{-1}$  the value of  $\eta$  of the MB-25/75 blend is 1.7 times higher than  $\eta$  based on the weighted average (by weight fraction) of  $\eta$  of the neat polymers. At  $\omega = 0.46 \text{ rad/sec}$  the value of  $|\eta^*|$  of the MB-25/75 blend is 3 times higher than  $|\eta^*|$  based on the weighted average (by weight fraction) of  $|\eta^*|$  of the neat polymers. These results indicate that the contribution from the two phase morphology is lower when the dispersed phase is oriented in the flow direction than when the dispersed phase is in the form of drops.

#### 4.3.2 Steady State First Normal Stress Difference and Storage Modulus

Next we turn our attention to the elastic properties of the blends as determined by  $N_1$  and  $G'$ . The elastic properties of the PET/nylon 6,6 blend system measured in terms of  $N_1$  and  $G'$  display similar deviation from those of the neat polymers as was observed in the



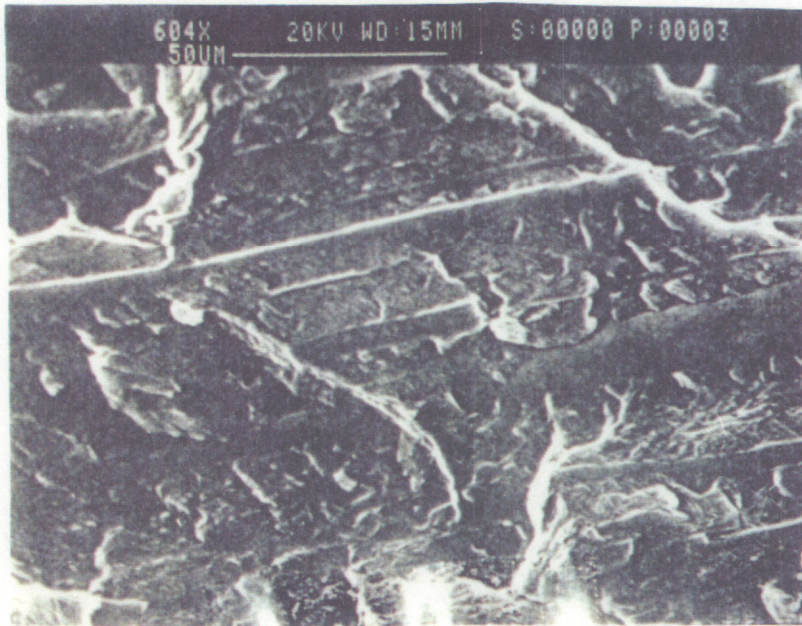


**Figure 4.9** Scanning electron micrographs of melt blended 25/75 PET/nylon 6,6 sample quenched after shear flow.

viscous properties at 290 °C. It can be seen in Figures 4.10 and 4.11 that the MB-75/25 blend shows a negative deviation of both  $N_1$  and  $G'$  from those of the neat polymers. The MB-50/50 blend displays  $N_1$  and  $G'$  values which are similar in magnitude to those of the neat polymers. In the case of the MB-25/75 blend a positive deviation of  $N_1$  and  $G'$  from those of the neat polymers is observed. The lower values of  $N_1$  and  $G'$  of the MB-75/25 and MB-50/50 blends relative to those of the neat polymers may be related to the higher rate of degradation of the samples during melt blending.

In order to determine the role played by the two phase morphology obtained by blending PET and nylon 6,6 in the absence of significant degradation on  $G'$ , the storage modulus of the dry blended samples was also measured and is shown in Figure 4.12 along with that of the neat polymers. It can be seen that a positive deviation is observed at all three weight ratios with  $G'$  for the DB-75/25 blend being the highest.

A comparison of the relative deviation of the values of  $N_1$  and  $G'$  of the blends at all three concentrations from that of the blend constituents reveals the effect of the different textures present during each rheological test (e.g., drops, elongated drops, and fibrils in steady shear experiments and only drops in small amplitude dynamic oscillatory experiments). At a shear rate of  $0.5 \text{ sec}^{-1}$  the value of  $N_1$  of the MB-25/75 blend is 3.2 times higher than  $N_1$  based on the weighted average (by weight fraction) of  $N_1$  of the neat polymers. At  $\omega = 0.46 \text{ rad/sec}$  the value of  $G'$  of the MB-25/75 blend is 6.5 times higher than  $G'$  based on the weighted average (by weight fraction) of  $G'$  of the neat polymers. These results indicate that the elastic contribution from the two phase morphology relative to the neat polymers decreases with orientation of the dispersed phase in the flow direction.

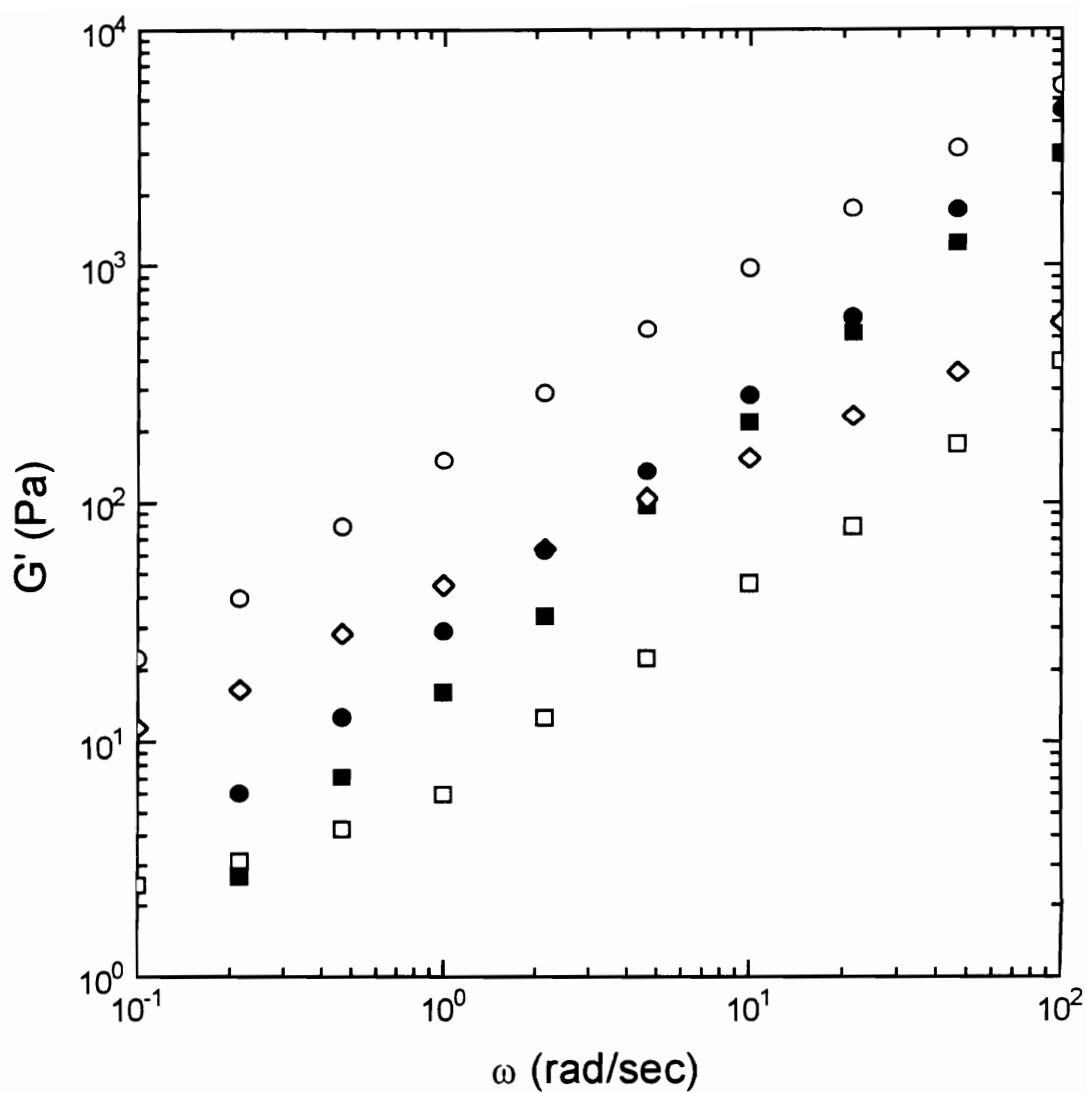


**Figure 4.10** Storage modulus as a function of frequency at 290 °C for melt blended PET/nylon 6,6 samples: (■) 100/0; (□) 75/25; (◇) 50/50; (○) 25/75; and (●) 0/100.

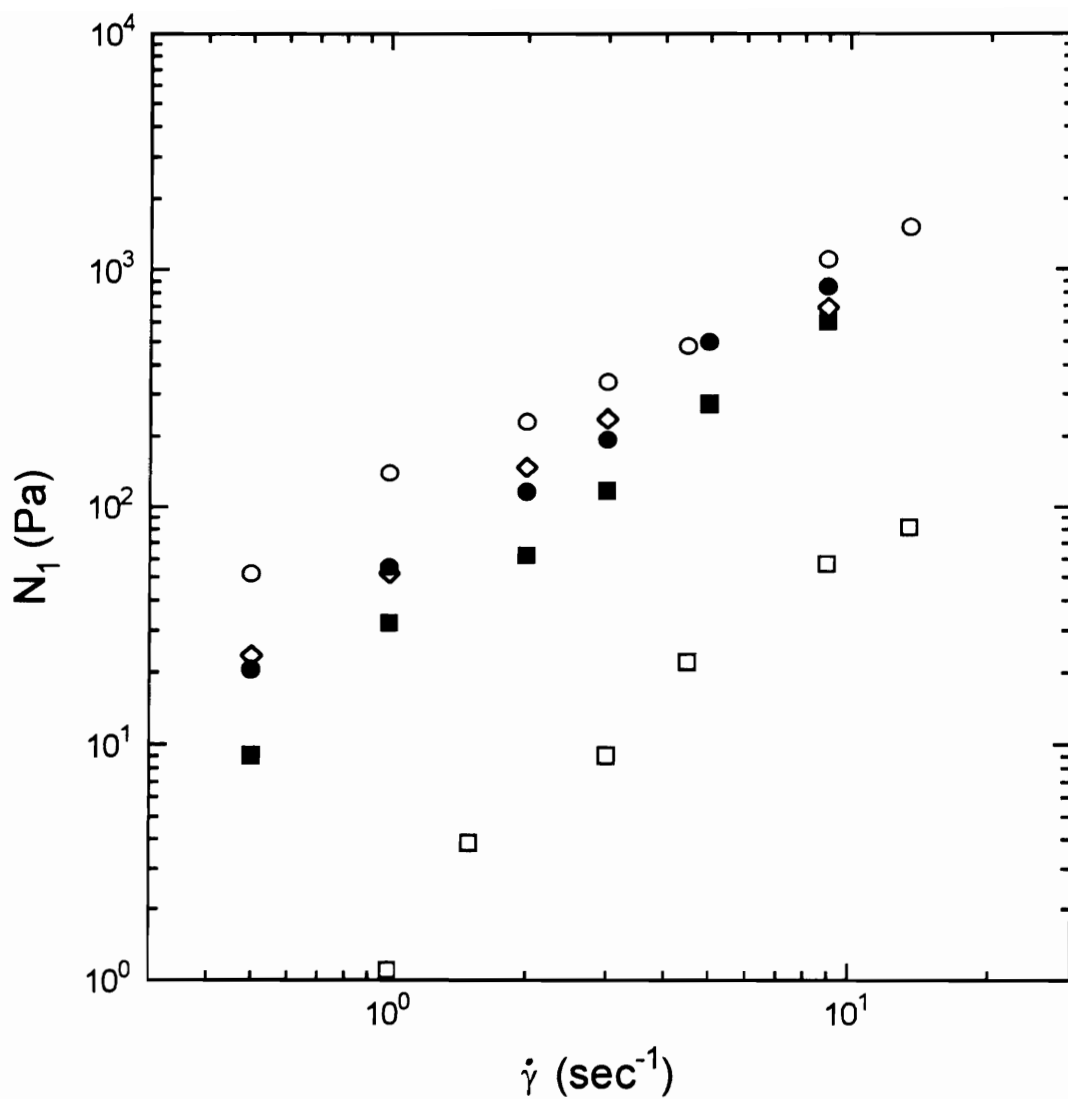


**Figure 4.11** Steady state first normal stress difference as a function of shear rate at 290 °C for melt blended PET/nylon 6,6 samples: (■) 100/0; (□) 75/25; (◇) 50/50; (○) 25/75; and (●) 0/100.



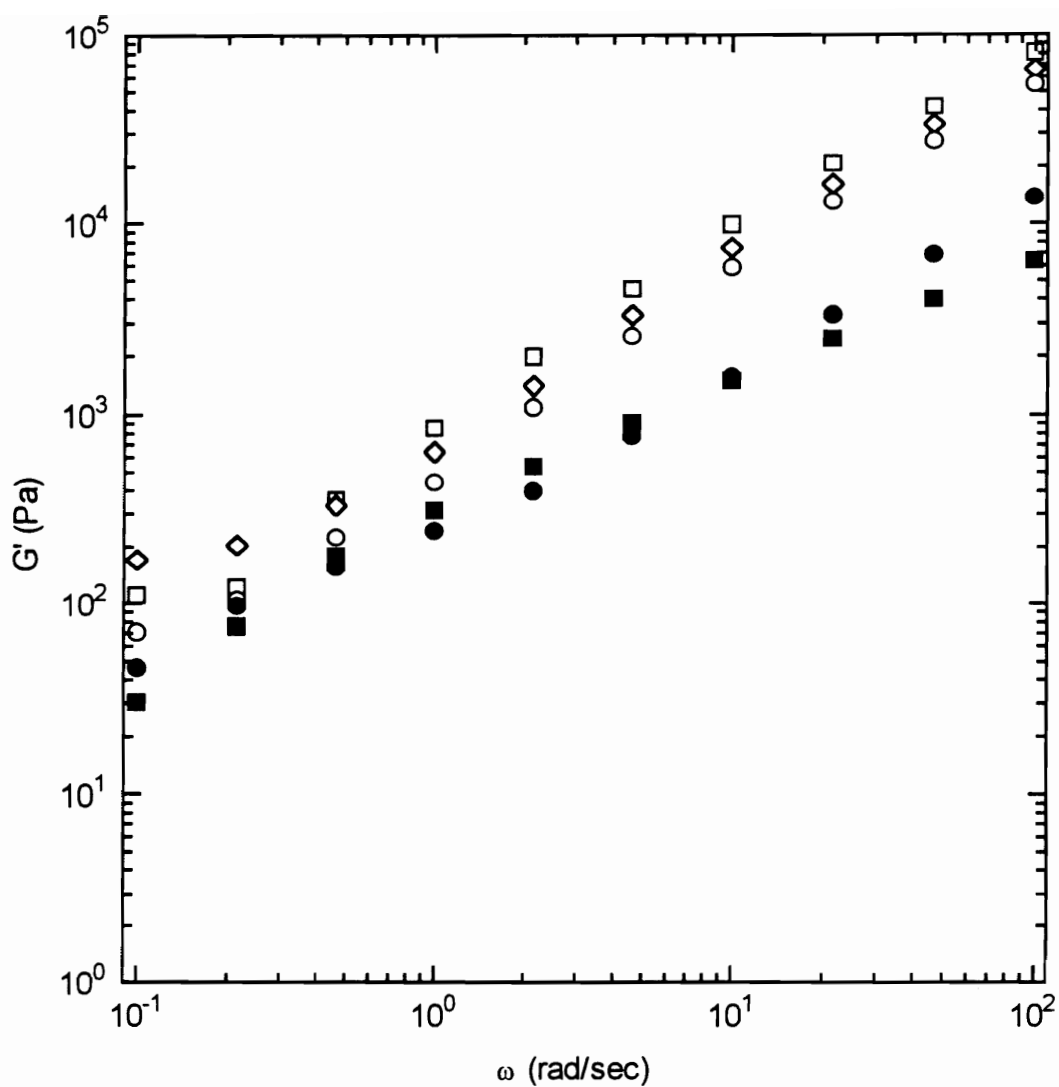


**Figure 4.12** Storage modulus as a function of frequency at 290 °C for dry blended PET/nylon 6,6 samples: (■) 100/0; (□) 75/25; (◇) 50/50; (○) 25/75; and (●) 0/100.

### 4.3.3 Transient Shear Stress and First Normal Stress Difference

The transient shear stress and first normal stress difference of the blends are discussed in this section. The transient experiments performed include start up of shear flow, stepwise changes of shear flow, and interrupted stress growth experiments. Using these experiments the role of interfacial tension and degradation on the transient rheology of the PET/nylon 6,6 blend was examined.

The transient shear stress at the start up of steady shear flow for the melt blended and dry blended samples at all three weight ratios are shown in Figures. 4.13 and 4.14, respectively. The shear stress at the start up of shear flow for the extruded neat polymers (see Fig. 4.13) is seen to increase monotonically to their steady state values. The MB-25/75 blend displays a large overshoot at the start up of shear flow followed by a monotonic decrease to a steady state value which is higher than that of the neat polymers. The presence of an overshoot may be associated with the two phase morphology of the blend, because this behavior is not observed in either neat polymer. While the MB-50/50 blend also displays an overshoot at start up of shear flow, the peak value of stress is small relative to the steady state value. In the case of the MB-75/25 blend no overshoot is observed at the start up of shear flow. The reduction in the magnitude of the overshoot relative to the steady state shear stress with an increase in PET content may be correlated to the increase in the extent of degradation occurring during extrusion. The enhancement of the overshoot is seen clearly in the dry blended samples at all weight ratios (see Fig. 4.14). Although the neat polymers which have not been degraded by extrusion show an overshoot, the overshoot for the dry blended samples is larger than that of the neat polymers, and much larger strains are required to reach steady state. The presence of the overshoot in the melt blended samples and enhancement of the overshoot in the dry blended samples may be associated

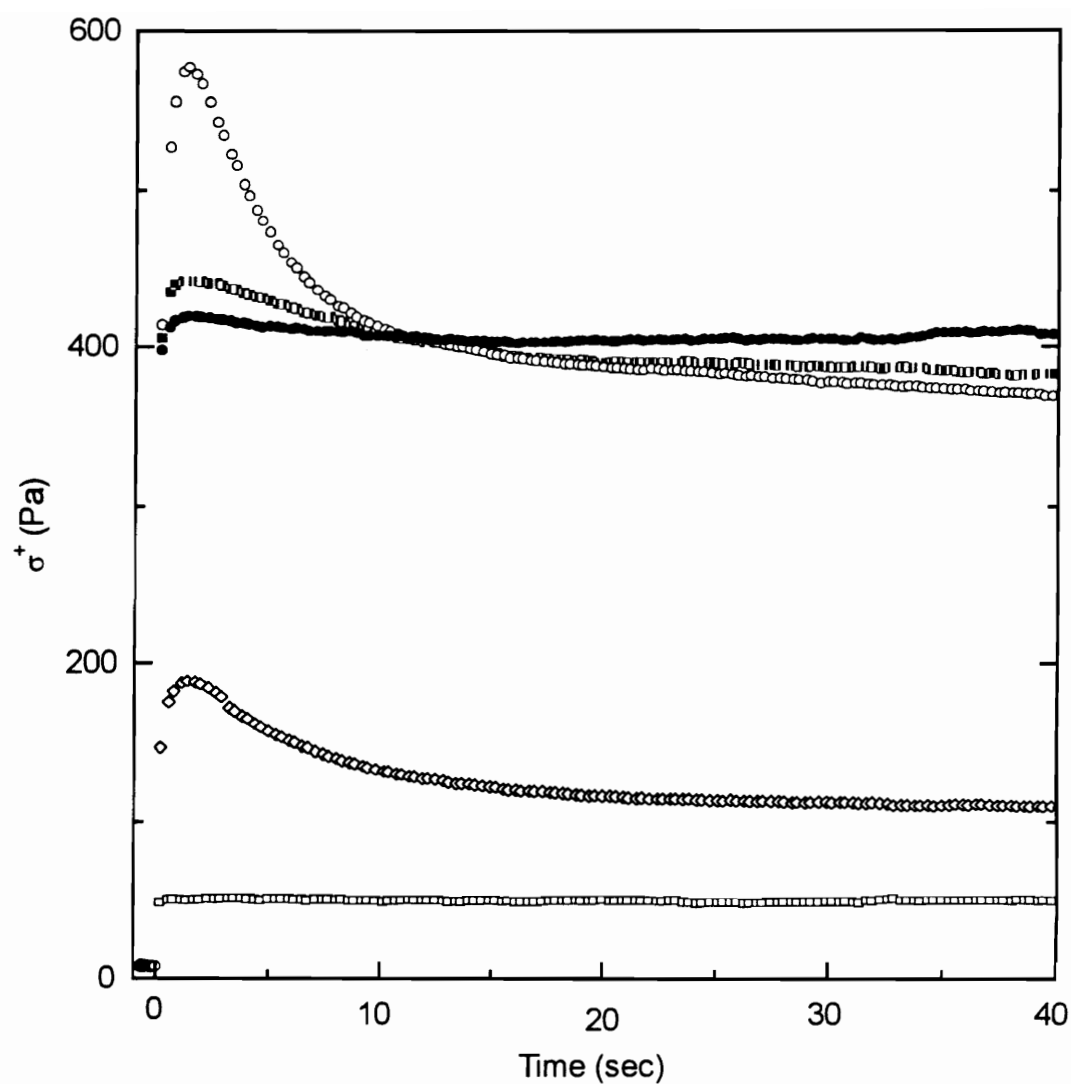


**Figure 4.13** Transient shear stress at the start up of shear flow at 290 °C and a shear rate of 1 sec<sup>-1</sup> for melt blended PET/nylon 6,6 samples: (■) 100/0; (□) 75/25; (◇) 50/50; (○) 25/75; and (●) 0/100.

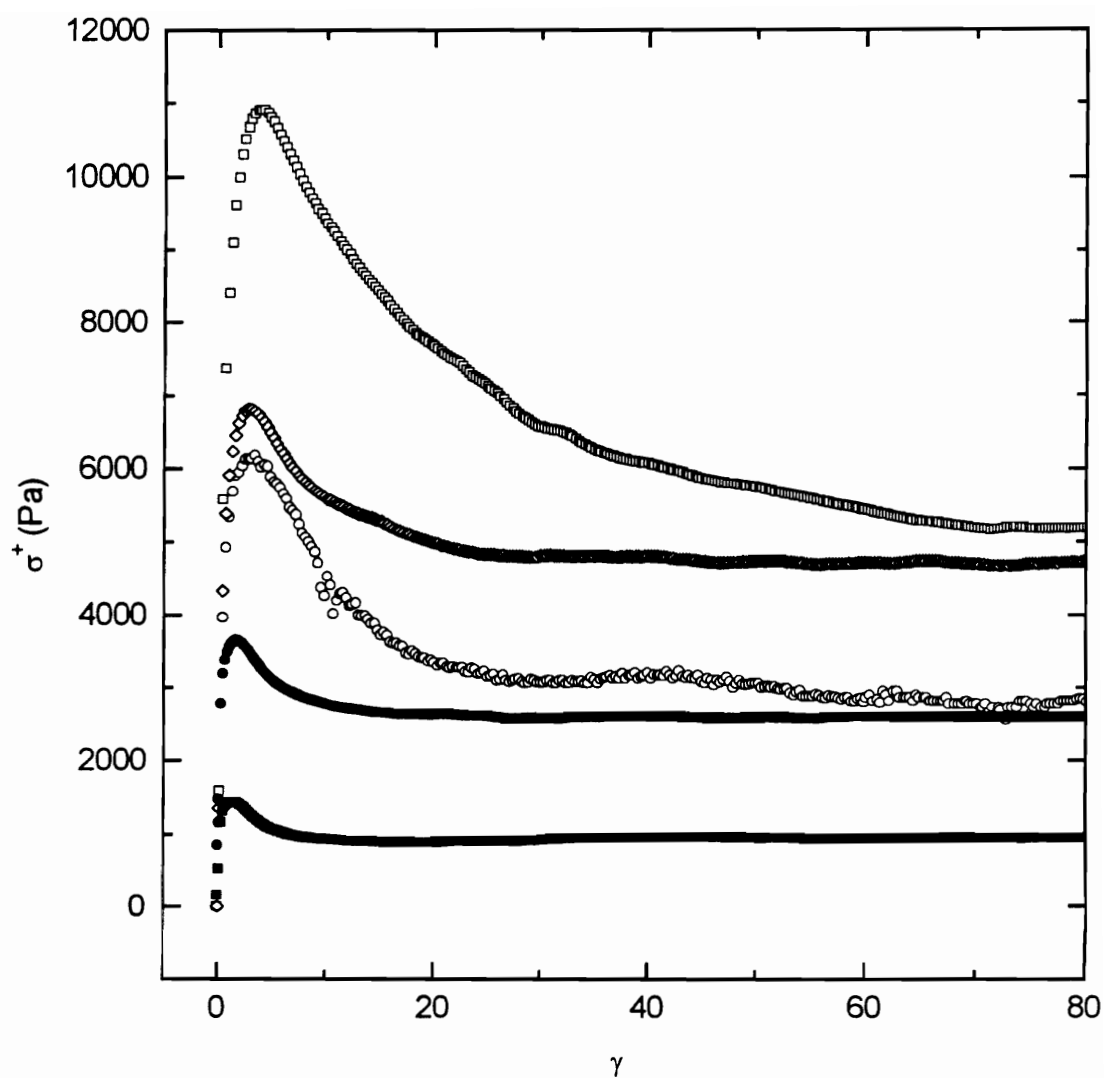


**Figure 4.14** Transient shear stress at the start up of shear flow at 290 °C and a shear rate of 1 sec<sup>-1</sup> for dry blended PET/nylon 6,6 samples: (■) 100/0; (□) 75/25; (◇) 50/50; (○) 25/75; and (●) 0/100.

with the two phase morphology because they are not seen in the neat polymers. The transient first normal stress difference for the MB-25/75 blend at the start up of shear flow displays enhanced behavior due to the two phase morphology when compared to data for the neat polymers (see Fig. 4.15). This behavior consists of an overshoot which is not seen in the neat polymers or the MB-75/25 and MB-50/50 blends.

The overshoot observed in the start up of shear flow experiments for the MB-25/75 blend was investigated further using interrupted stress growth experiments. Interrupted stress growth experiments were carried out by first shearing the samples at a shear rate of  $1 \text{ sec}^{-1}$  for 45 seconds and then the samples were allowed to recover for increasing amounts of time before start up of shear flow was performed again. The recovery of the overshoot associated with a recovery of the equilibrium texture can be seen in Figure 4.16 for the MB-25/75 blend where the shear stress is reduced by the steady state shear stress [e.g.,  $\sigma_r = \sigma^+(t, \dot{\gamma}_o) / \sigma(t)$ ]. In this figure it can be seen that 40 seconds are required to achieve approximately 90% recovery of the overshoot for the MB-25/75 blend.

The transient shear stress from step-up and step-down experiments for all three melt blended samples and the extruded neat polymers is shown in Figures 4.17 and 4.18. Step-up experiments were carried out using a constant step-up ratio ( $\dot{\gamma}_1 / \dot{\gamma}_0 = 3$ ), and the data is plotted as function of the scaled stress ( $\sigma_s$ )

$$\sigma_s = \frac{\sigma^+(t, \dot{\gamma}_1) - \sigma(\dot{\gamma}_0)}{\sigma(\dot{\gamma}_1) - \sigma(\dot{\gamma}_0)} \quad (4.3)$$

and strain ( $\gamma_1$ )

$$\gamma_1 = \dot{\gamma}_1 \cdot t \quad (4.4)$$

In the case of the neat polymers (Fig. 4.17a and 4.17e) and the MB-75/25 blend

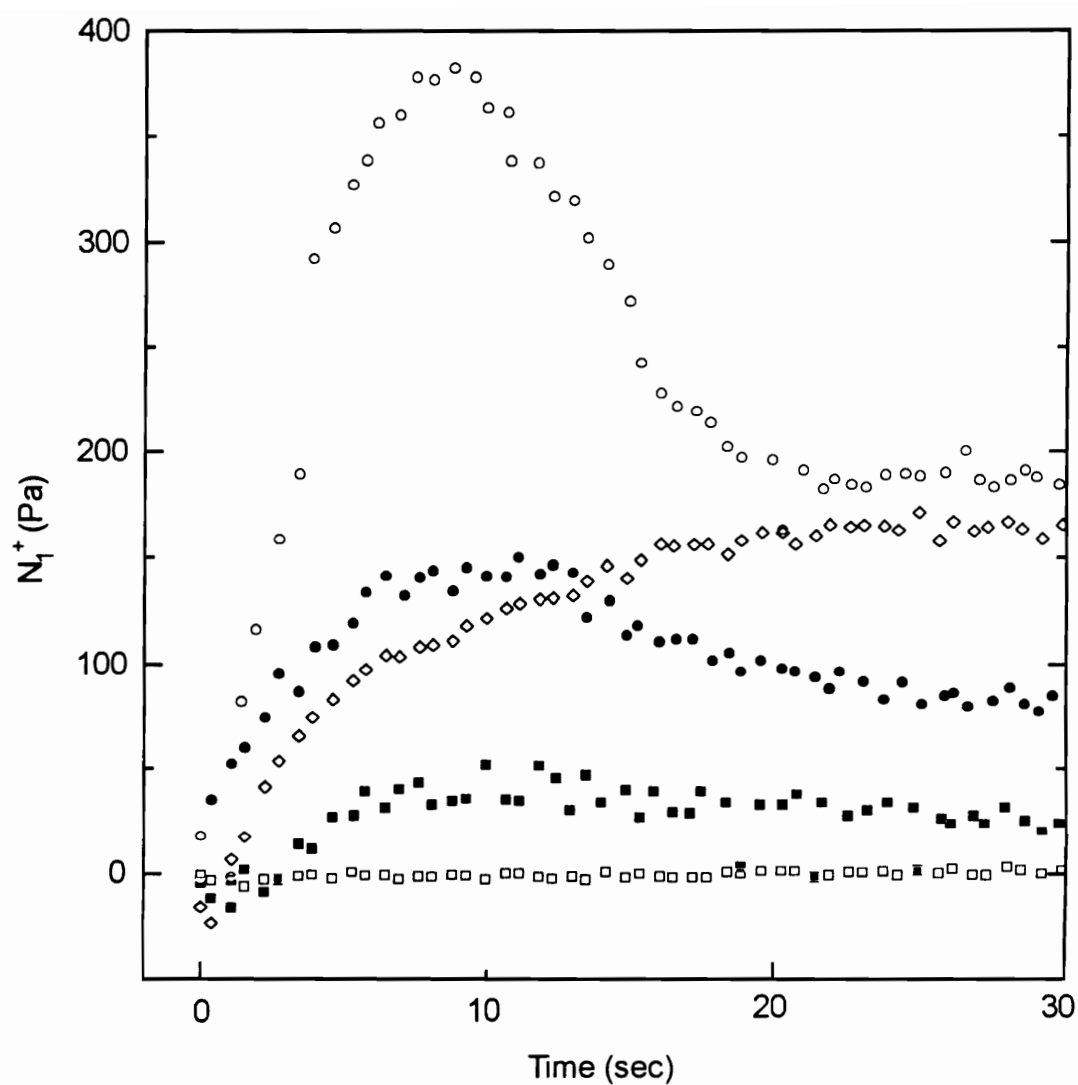


**Figure 4.15** Transient first normal stress difference at the start up of shear flow at 290 °C and a shear rate of 1 sec<sup>-1</sup> for melt blended PET/nylon 6,6 samples: (■) 100/0; (□) 75/25; (◇) 50/50; (○) 25/75; and (●) 0/100.

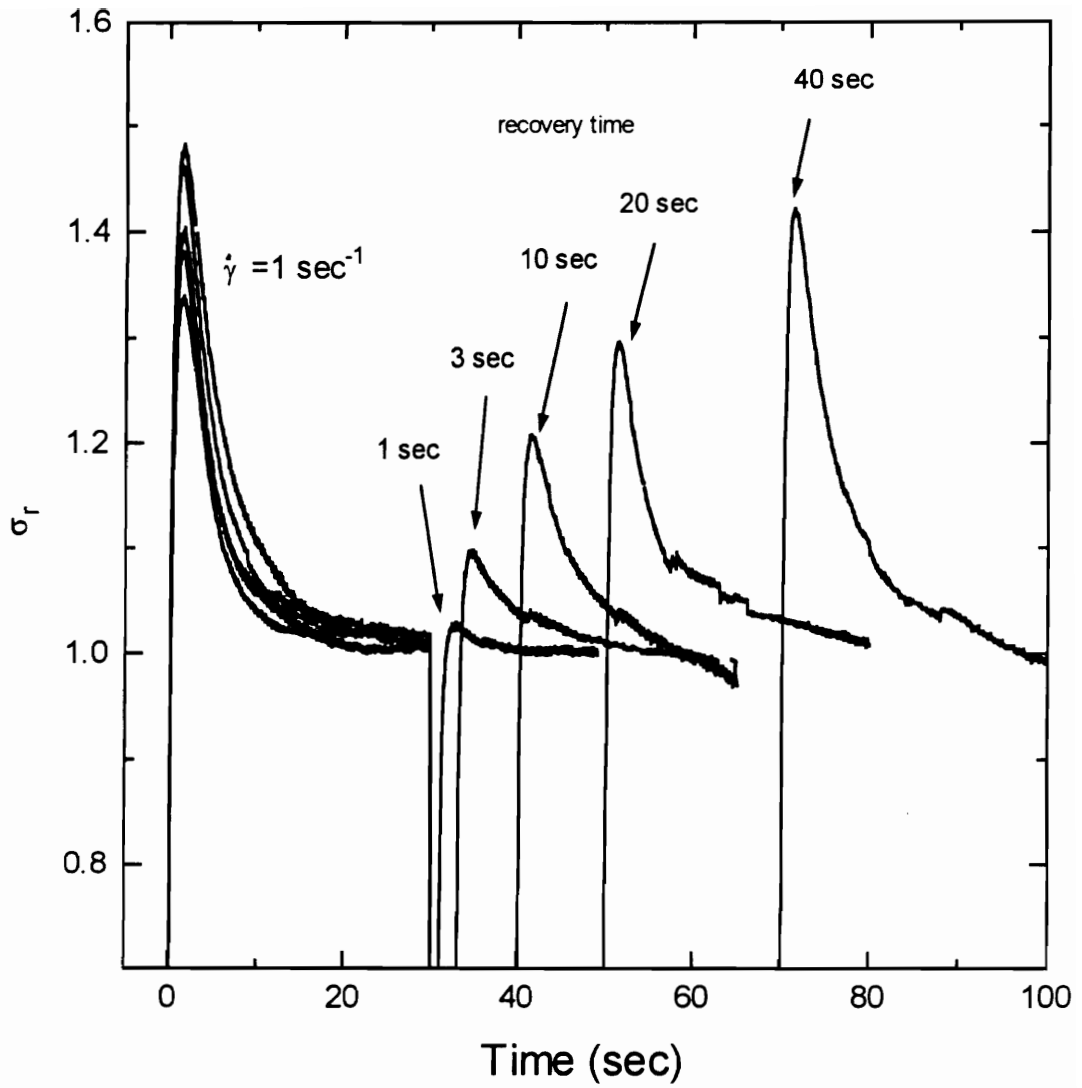


**Figure 4.16** Transient reduced shear stress  $\sigma_r = \sigma^+(t, \dot{\gamma}_o) / \sigma(t)$  versus time using interrupted stress growth experiments as function of recovery time for the melt blended 25/75 PET/nylon 6,6 sample at 290 °C.

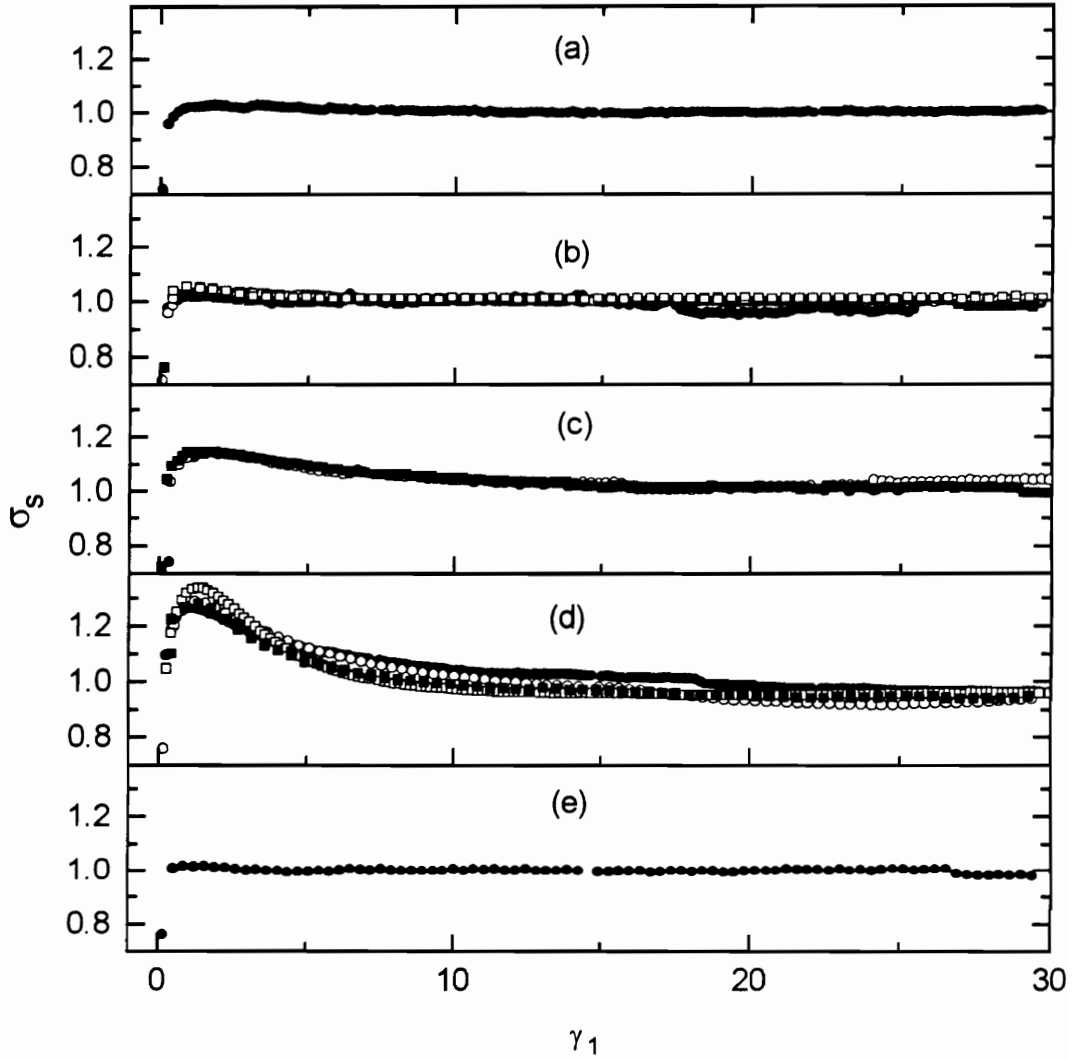


**Figure 4.17** Transient scaled shear stress  $\sigma_s = [\sigma^+(t, \dot{\gamma}_1) - \sigma(\dot{\gamma}_0)] / [\sigma(\dot{\gamma}_1) - \sigma(\dot{\gamma}_0)]$  versus  $\gamma_1$  where  $(\dot{\gamma}_1 / \dot{\gamma}_0 = 3)$  and where  $\dot{\gamma}_1$  is; (○)  $0.5 \text{ sec}^{-1}$ ; and (●)  $1.0 \text{ sec}^{-1}$ ; (■)  $1.5 \text{ sec}^{-1}$ ; and (□)  $3 \text{ sec}^{-1}$  for melt blended PET/nylon 6,6 samples: (a) 100/0; (b) 75/25; (c) 50/50; (d) 25/75; and (e) 0/100 at  $290^\circ\text{C}$



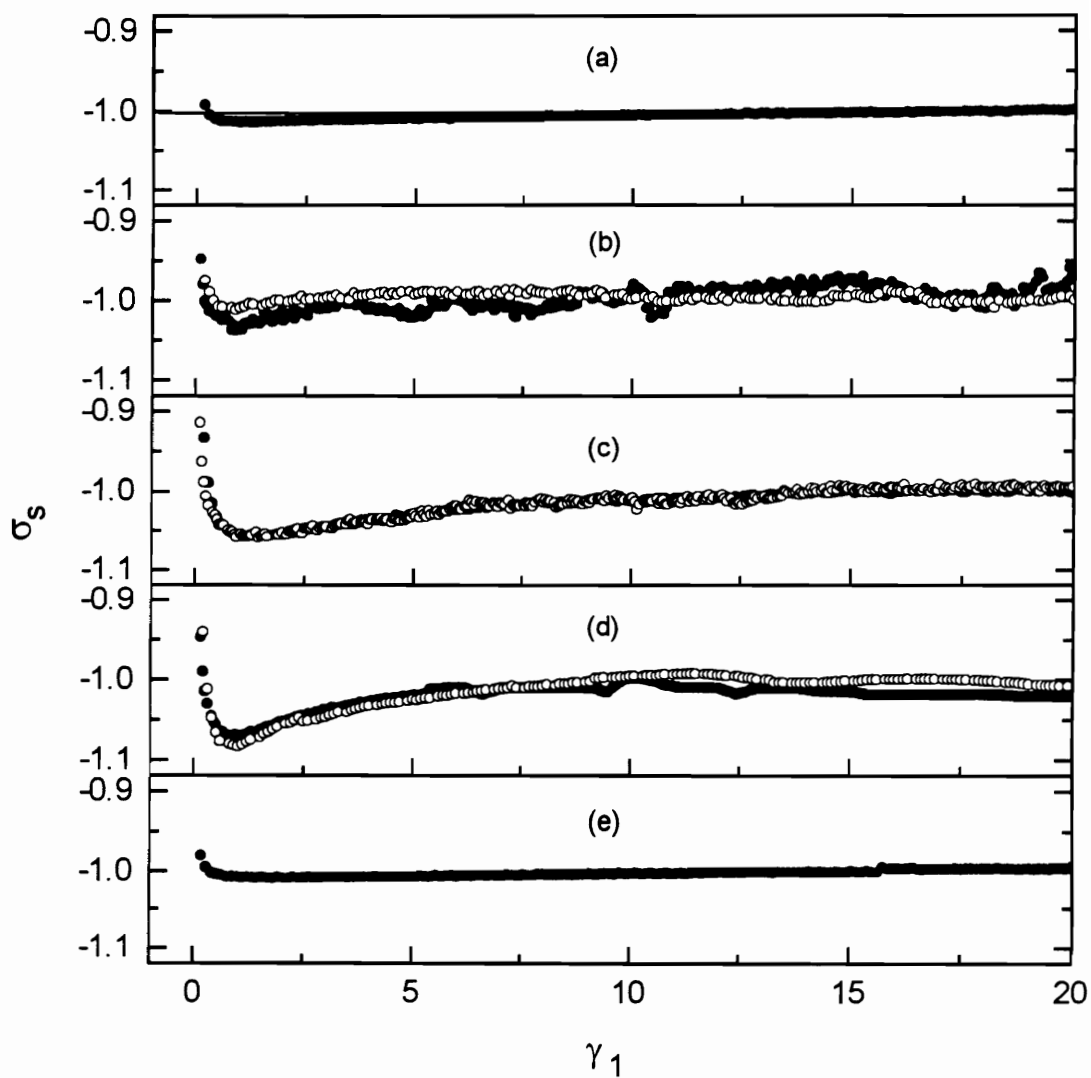


**Figure 4.18** Transient scaled shear stress  $\sigma_s = [\sigma^+(t, \dot{\gamma}_1) - \sigma(\dot{\gamma}_0)] / [\sigma(\dot{\gamma}_1) - \sigma(\dot{\gamma}_0)]$  versus  $\gamma_1$  where  $(\dot{\gamma}_0 / \dot{\gamma}_1 = 3)$  and where  $\dot{\gamma}_1$  is; (○)  $1 \text{ sec}^{-1}$ ; and (●)  $0.5 \text{ sec}^{-1}$  for melt blended PET/nylon 6,6 samples: (a) 100/0; (b) 75/25; (c) 50/50; (d) 25/75; and (e) 0/100 at  $290^\circ \text{C}$ .

(Fig. 4.17b) the stress is seen to increase monotonically to steady state values while an overshoot is observed in the MB-50/50 and MB-25/75 blends (Fig. 4.17c and 4.17d, respectively) with the overshoot of the MB-25/75 blend being higher. It can also be seen that the transients for the blends when plotted in the above mentioned manner superimpose to form a single curve regardless of the shear rate,  $\dot{\gamma}_1$ . The transient shear stress from step-down experiments for all three melt blended samples and the extruded neat polymers is shown in Figure 4.18. The step-down experiments were carried out at a constant step-down ratio ( $\dot{\gamma}_0 / \dot{\gamma}_1 = 3$ ), and the data is plotted in reduced form as described above in eqs. 4.3 and 4.4. In the case of the neat polymers (Figs. 4.18a and 4.18e) and the MB-75/25 blend (Fig. 4.18b) the shear stress is seen to decrease monotonically to the final steady state value while an undershoot is observed in the MB-50/50 and MB-25/75 blends (Fig. 4.18c and 4.18d, respectively) with the undershoot of the MB-25/75 blend being greater. It can also be seen that the transients from the step-down experiments for the blends when plotted in the above mentioned manner also superimpose to form a single curve regardless of the shear rate,  $\dot{\gamma}_1$ . This scaling relationship has been observed in some liquid crystalline polymers<sup>30,31</sup> with a polydomain texture and has recently been found to hold for immiscible mixtures of Newtonian fluids consisting of oils at all volume ratios tested.<sup>32</sup> These results indicate by removal of the time scale associated with the applied flow that there appears to be no intrinsic time constant for these blends. This result only holds when the shear rate used is below the longest relaxation time of the neat polymers. Similar scaling of the shear stress for the samples prepared by dry blending was not observed and may be due to incomplete mixing and the long relaxation times of the neat polymers which were not degraded by extrusion.

## 4.4 CONCLUSIONS

The rheological properties of PET/nylon 6,6 blends were found to be a strong function of polymer degradation during melt blending and while making rheological measurements. A high rate of degradation for PET, nylon 6,6 and PET/nylon 6,6 blends was found to occur during melt blending in an extruder due to the exposure of the materials to moisture. The rate of degradation for the blend at a weight ratio of 25/75 PET/nylon 6,6 was between that of the neat polymers and was higher than that of the neat polymers for the blends at weight ratios of 75/25 and 50/50 w/w PET/nylon 6,6. The lower values of  $|\eta^*|$ ,  $\eta$ ,  $G'$ , and  $N_1$  of the blends relative to those of the extruded neat polymers were found to be a consequence of the accelerated rate of degradation occurring for the 75/25 and 50/50 w/w PET/nylon 6,6 blends relative to the neat polymers during melt blending in an extruder.

The role played by the two phase nature on the rheological properties of 75/25, 50/50, and 25/75 w/w PET/nylon 6,6 blends was observed using samples prepared by dry blending and mixing in cone and plate fixtures under a nitrogen atmosphere and the melt blended 25/75 w/w PET/nylon 6,6 system. The blend at a weight ratio of 25/75 PET/nylon 6,6 prepared by mixing in an extruder was found to have rheological properties which were a function of the two phase nature of the blend because the rate of degradation of this blend and neat polymers was similar. The two phase nature of the dry blended samples and the extruded 25/75 w/w PET/nylon 6,6 resulted in values of  $|\eta^*|$ ,  $\eta$ ,  $G'$ , and  $N_1$  which were higher than those of the neat polymers. The effect of the two phase nature of the blends was also observed in enhanced transient shear and first normal stress difference behavior relative to that of the neat polymers. The enhanced transient behavior consisted of a large overshoot at the start up of shear flow which was found to recover upon cessation of shear

flow using interrupted stress growth experiments. In addition, an overshoot was observed using step-up experiments and an undershoot was observed using step-down experiments. The transients observed using stepwise changes of shear rate were found to superimpose when plotted in reduced form indicating that at rates lower than the longest relaxation time of the neat polymers there was no intrinsic time constant associated with the deformation of the interface in the blends.

## **4.5 ACKNOWLEDGMENTS**

The authors gratefully acknowledge the support of the Virginia Institute of Materials Systems for support of this work.

## 4.6 REFERENCES

1. D. R. Paul and S. Newman, *Polymer Blends*, Academic Press, New York 1978.
2. L. A. Utracki, *Polym. Eng. Sci.*, **28**, 1401 (1988).
3. M. Doi and T. Ohta, *J. Chem. Phys.*, **95**, 1242 (1991).
4. H. Gramespacher and J. Meissner, *J. Rheol.*, **36**, 1127 (1992).
5. P. Scholz, D. Froelich, and R. Muller, *J. Rheol.*, **33**, 481 (1989).
6. L. A. Utracki. and M. R. Kamal, *Polym. Engr. Sci.*, **22**, 96 (1982).
7. H. Chuang and C. D. Han, *J. Appl. Polym. Sci.*, **29**, 2205 (1984).
8. J. P. Montfort, G. Marin, J. Arman, and P. Monge, *Polymer*, **19**, 277 (1978).
9. C. Belaribi, G. Marin, and P. Monge, *Eur. Polym. J.*, **22**, 481, (1986).
10. C. Wisniewsky, G. Marin, and P. Monge, *Eur. Polym. J.*, **21**, 479 (1985).
11. J. P. Montfort, G. Marin, J. Arman, and P. Monge, *Polymer*, **19**, 277 (1978).
12. F. P. La Mantia, *Thermotropic Liquid Crystal Polymer Blends*, Ed. F. P. La Mantia, Technomic Publishing Co., Pennsylvania, 1993.
13. C. D. Han and Y. W. Kim, *Trans. Soc. Rheol.*, **19**, 245, 1975.
14. L. A. Utracki, A. M. Catani, G. L. Bata, M. R. Kamal, and V. Tan, *J. Appl. Polym. Sci.*, **27**, 1913 (1982).
15. M. R. Nobile, D. Arcieno, L. Incarnato, and D. Nicolais, *J. Rheol.*, **34**, 1181 (1990).
16. L. Z. Pillon and L. A. Utracki, *Polym. Engr. Sci.*, **24**, 1300 (1984).
17. J. A. Lefeler, *J. Polym. Sci.: Part B: Polym. Phys, Ed.*, **26**, 1469 (1988).
18. M. R. Kamal, M. A. Sahto, and L. A. Utracki, *Polym. Eng. Sci.*, **22**, 1127 (1982).
19. J. A. Lefeler, *J. Polym. Sci.: Part B: Polym. Phys, Ed.*, **26**, 1469 (1988).
20. M. Kimura, R. S. Porter and G. Salee, *J. Polym. Sci.: Polym. Phys. Ed.*, **21**, 367 (1983).

21. K. Dimov and M. Savov, *Vysokomol. Soed.*, **A22**, 65 (1980).
22. K. Okazaki and T. Nakagawa, Japan Pat. 6,911,669 (1969).
23. K. Inoshita, M. Terakawa, and T. Yasuda, Japan Pat. 7,228, 916 (1972).
24. Firestone Tire and Rubber Co., Neth. Pat. Appl. 6,410,530 (1965).
25. I. Marshall and A. Todd, *Trans. Faraday Soc.*, **49**, 67 (1953).
26. H. Zimmerman and N. T. Kim, *Polym. Engr. Sci.*, **20**, 680 (1980).
27. Z. Kumbloski, M. Michniewicz, and J. Torzecki, *Rheology, Proc. Intl. Congr. Rheol.*, G. Astarita, G. Marrucci, and L. Nicolais, Eds., Plenum, New York, 1980, Vol. 3, pp. 159.
28. S. Strauss and L. A. Wall, *J. Res. Nat. Bur. Std.*, **60**, 38, (1958).
29. E. P. Krasnov and L. B. Sokolov, *Vysokomol. Soed., Khim. Svoistva*, **19**, 275 (1964).
30. I. J. Goldfarb and A. C. Meeks, AFML-TR-68-347. Part I (1969).
31. Doppert, H. L. and S. J. Picken, *Mol. Cryst. Liq. Cryst.*, **153**, 109 (1987).
32. Moldenaers, P., H. Yanase, and J. Mewis, *ACS Symposium Series* (ACS, Washington, DC, 1990, Chap. 26, pp. 370-380).
33. Takahashi, Y. N. Kurashima, I. Noda, and M. Doi, *J. Rheol.*, **38**, 699 (1994).

## 5.0 An Evaluation of the Doi-Ohta Theory

### Preface

This chapter addresses the third objective of this thesis. Specifically, it is determined whether the Doi-Ohta theory can quantitatively or qualitatively predict the steady state viscosity and first normal stress difference as a function of shear rate, and the transient shear stress and first normal stress difference behavior of a textured material consisting of an immiscible polymer blend. This chapter is organized as a manuscript which will be submitted to the *Journal of Rheology* for publication.

## **An evaluation of the Doi-Ohta theory for an immiscible polymer blend**

by G. K. Guenther and D. G. Baird

*Virginia Polytechnic Institute & State University, Department of Chemical Engineering*

*Polymeric Materials and Interfaces Laboratory, Blacksburg, VA 24061-2011*

### **Synopsis**

The theory developed by Doi and Ohta was evaluated for its ability to predict the rheology of an immiscible polymer blend. The theory describes the additional stresses arising as a consequence of interfacial tension in two phase systems in which the constituents consist of Newtonian fluids and have equal viscosities. The blend considered in this paper consisted of an immiscible mixture of poly(ethylene terephthalate) (PET) and nylon 6,6 at a composition ratio of 25/75 w/w PET/nylon 6,6. The rheological properties of this blend were found to be stable for the time frame required for the rheological experiments used in this work (e.g., < 5 minutes). The Doi-Ohta theory was found to be capable of qualitatively predicting the extra stresses arising as a result of the interfacial tension as observed in the steady state viscosity and steady state first normal stress difference. The transient shear stress and first normal stress difference at the start up of steady shear flow were qualitatively predicted by the Doi-Ohta theory while the recovery of the initial overshoot observed experimentally was not. The overshoot observed experimentally during step-up experiments and the undershoot observed during step-down experiments were not predicted by the theory in which it was predicted that the stresses change monotonically with a stepwise change of the shear rate to the final steady state value. While the shear thinning behavior observed for this blend was not predicted by the theory, the scaling relation for the transient stresses predicted by the theory was found to hold for the blend using stepwise changes of shear rate at a constant step ratio.



## 5.1 INTRODUCTION

When two immiscible polymers are mixed a complex morphology is formed. In immiscible polymer blends, one of the phases may consist of drops which during flow undergo deformation, breakup and coalescence. Materials in which a two phase microstructure exists are referred to as "textured fluids" [Doi (1992)] Under an applied flow field textured fluids undergo complex structural changes and as a consequence may exhibit rheological properties which are a function of their texture and are not seen in the individual phases [Utracki (1988); Scholz *et al.* (1989); Doi and Ohta (1991); Gramespacher and Meissner (1992)].

Investigations of the rheological behavior of polymer blends have shown a number of peculiarities that are not well understood at this time [Utracki *et al.* (1982)]. These peculiarities include, but are not limited to, a significant degree of overshoot upon start up of simple shear flow [Nobile (1990)], apparent yield stresses [Utracki *et al.* (1982)], and a viscosity which relative to the log additivity of the viscosity of the neat polymers can be: 1) higher (positive deviation); 2) lower (negative deviation) and 3) higher and lower (positive-negative deviation) depending on shear stress or shear rate [Utracki (1982)].

In order to predict the rheology of immiscible polymer blends, the stresses arising as a consequence of the viscoelastic nature of the neat polymers as well as the extra stresses arising as a consequence of interfacial tension must be accounted for. During flow a complex texture is developed as a result of the mechanisms of drop deformation, breakup and coalescence. Each of these mechanisms must be accounted for in any suitable theory. The mechanisms of drop deformation, breakup, and coalescence, have each received considerable attention for purely viscous fluids by studying dilute systems [Elmendorp (1980); Utracki and Shi (1992)]. A single Newtonian drop in a Newtonian matrix was

studied in the pioneering work of Taylor (1934). The velocity and pressure fields inside and outside the droplet were calculated, and it was determined that the deformation of the droplet could be expressed by means of two dimensionless parameters: 1) the capillary number; and 2) the viscosity ratio. It was shown that for a given drop diameter the smaller the viscous stresses relative to the interfacial stresses (e.g., capillary number was small), the less the droplet deformed. As the viscous stresses became larger relative to the interfacial stress the droplet deformed more until at some critical ratio of these forces (e.g., the critical capillary number) the deformed droplet burst. While the work of Taylor has subsequently been continued for Newtonian fluids by a number of researchers [Utracki and Shi (1992)], little work has considered the deformation and breakup of drops in viscoelastic systems and even less work has been concerned with concentrated systems in which coalescence plays an important role.

A theory was developed by Doi and Ohta (1991) which attempted to predict the rheology of textured fluids. In the theory of Doi and Ohta it was predicted that viscoelastic behavior arises for two phase fluids in which the constituents are Newtonian and have equal viscosities as a consequence of the additional stresses generated during flow due to interfacial tension. The stresses arising as a consequence of interfacial tension were assumed in the theory to change with the deformation and relaxation of the interface during flow (drop deformation, coalescence and breakup). The relaxation of the size and shape of the interface due to interfacial tension was accounted for in the theory by two first order kinetic equations. It was predicted by the Doi-Ohta theory that the shear stress and first normal stress difference were proportional to the shear rate and transient stresses superimpose when the time scale associated with the flow were removed. This scaling phenomenon arises because the system was characterized by the viscosity and the interfacial tension from which a quantity with units of time could not be constructed. The scaling

relation for the system as described by Doi and Ohta indicated that there was no intrinsic time constant associated with the deformation and relaxation of the interface.

The scaling relation predicted by the Doi-Ohta theory was examined experimentally using mixtures of immiscible Newtonian fluids in an investigation by Takahashi *et al.* (1994). The textured fluids considered in their investigation included mixtures consisting of polydimethylsiloxanes (a silicone oil) and hydrocarbon-formaldehyde resins at several volume fractions. The shear stress and the first normal stress difference for the mixtures were found to be nearly proportional to the shear rate, and plots of scaled transient stresses after a stepwise change of the shear rate against strain were found to superimpose on a single curve. On the other hand, the overshoot observed upon stepping up the shear rate and the undershoot observed upon stepping down the shear rate are not predicted by the Doi-Ohta theory in which it is predicted that the stresses change monotonically to the final steady state value.

The ability of the Doi-Ohta theory in modified form to predict the rheology of a textured fluid consisting of an immiscible polymer blend was recently investigated [Lee and Park (1994)]. The system considered in the work by Lee and Park was an immiscible mixture of polystyrene (PS) and linear low-density polyethylene (LLDPE) at concentrations ranging from 10 to 90 wt. % PS. The original theory of Doi and Ohta (1991) was modified to account for a mismatch in the viscosities of the polymers. This modification consisted of the contribution to the stress tensor from the viscosity ratio of the polymers as described by the theories of Schowalter *et al.* (1968) and Willemse (1983) in which nearly spherical drops were considered. The theory was also modified with an additional kinetic equation associated with the relaxation of the interface due to droplet breakup (the original theory does not account for this mechanism explicitly). Their results showed good agreement between the experimental and predicted storage and loss moduli. Although good agreement

was observed between predicted and experimental small amplitude dynamic oscillatory properties, model predictions for steady shear and transient experiments in which the mechanisms of coalescence and breakup play a large role were not reported.

The objective of this paper is to determine whether the theory proposed by Doi-Ohta can model the steady shear viscosity, steady state first normal stress difference, and transient shear stress and first normal stress difference of a textured fluid consisting of an immiscible polymer blend. This is done by comparing the predicted and observed rheological behavior for blends of poly(ethylene terephthalate) (PET) and nylon 6,6 at shear rates lower than the longest relaxation time of the neat polymers ( $De < 1$ ). PET and nylon 6,6 were selected because they nearly meet several conditions of the system described by the Doi-Ohta theory (i.e., the PET and nylon 6,6 used have nearly equal viscosities which are Newtonian over a broad range of shear rates and each has a short relaxation time).

## **5.2 SUMMARY OF THE DOI-OHTA THEORY**

In order to provide a general understanding of the basis of the theory proposed by Doi and Ohta for mixtures of Newtonian fluids, a summary of the model is presented in this section. The kinetics and rheological properties of the system are discussed, and a semi-phenomenological kinetic equation is described. Specifically, an equation for the time evolution of the size and orientation of the interface as function of interfacial tension and the macroscopic flow field is presented. In addition, the important assumptions included in the derivation are presented, and the behavior predicted by the model is described.

The theory of Doi and Ohta was based on the observation that when two immiscible fluids are sheared, a rather complex interface is formed due to the coalescence, rupture, and deformation of the droplets. The system considered in the development of the theory was

that of two immiscible fluids having the same viscosity. The interface of the fluid was regarded as a mathematical surface with no thickness. The theory was then based on the following formulation for the stress tensor [Rosenkleid (1967); Onuki (1987); Doi (1987)] for emulsions of two immiscible liquids having the same viscosity,  $\eta_o$ ,

$$\pi_{\alpha\beta} = \eta_o(\kappa_{\alpha\beta} + \kappa_{\beta\alpha}) - \Gamma q_{\alpha\beta} - p\delta_{\alpha\beta} \quad (5.1)$$

where  $\kappa_{\alpha\beta} = \partial v_\alpha / \partial x_\beta$  is the macroscopic velocity gradient,  $\Gamma$  is the interfacial surface tension,  $q_{\alpha\beta}$  is the interface tensor, and  $p$  is the isotropic pressure, and  $\delta_{\alpha\beta}$  is the Kroenecker delta. The sign convention used was such that a tensile stress is taken as a positive stress. Eq. (1) indicates that the total stress consists of contributions from the viscous stress associated with the macroscopic flow (first term), the stress associated with the interfacial tension (second term), and the isotropic pressure (last term). Doi and Ohta used the formulation of the interface tensor as defined by Onuki (1987)

$$q_{\alpha\beta} = \frac{1}{V} \int (n_\alpha n_\beta - \frac{1}{3} \delta_{\alpha\beta}) dS, \quad (5.2)$$

where the integral is over the entire surface of the interface  $S$ ,  $n_\alpha$  are the components of the normal to the surface of the interface in the system of volume  $V$ . The interface tensor was assumed to be determined by two factors: 1) the flow field which enlarges and orients the interface; and 2) relaxation of the interface by interfacial tension which opposes these effects. The time evolution of the interface tensor was derived by accounting for the effects of the flow and relaxation by interfacial tension separately,

$$\frac{dq_{\alpha\beta}}{dt} = \left. \frac{dq_{\alpha\beta}}{dt} \right|_{\text{flow}} + \left. \frac{dq_{\alpha\beta}}{dt} \right|_{\text{relax}}. \quad (5.3)$$

The flow term in the time evolution of the interface tensor [Eq. (5.3)] was derived by considering the case where the expansion and orientation of the interface was driven by the macroscopic flow field and the interfacial tension was zero. The time evolution of the interface tensor due to macroscopic flow was

$$\left. \frac{dq_{\alpha\beta}}{dt} \right|_{\text{flow}} = -q_{\alpha\gamma}\kappa_{\gamma\beta} - q_{\beta\gamma}\kappa_{\gamma\alpha} + \frac{2}{3}\delta_{\alpha\beta}\kappa_{\mu\eta}q_{\mu\eta} - \frac{Q}{3}(\kappa_{\alpha\beta} + \kappa_{\beta\alpha}) + \frac{q_{\mu\nu}\kappa_{\mu\nu}}{Q}q_{\alpha\beta}, \quad (5.4)$$

where  $Q$  is the area of the interface per unit volume. The time evolution of the interfacial area per unit volume was

$$\left. \frac{dQ}{dt} \right|_{\text{flow}} = -q_{\alpha\beta}\kappa_{\alpha\beta}. \quad (5.5)$$

Next, the contribution to the time evolution of the interface tensor due to relaxation by interfacial tension was derived. The interfacial tension ( $\Gamma$ ) was assumed to drive the relaxation of the deformed interface by decreasing the area of the interface and making the system isotropic. Doi and Ohta assumed (for both lack of a better estimate and simplicity) that the relaxation process is described by first order kinetics. Specifically, a first order relaxation rate,  $r_1$ , was assumed for the interfacial area per unit volume, ( $Q$ ), and a first order relaxation rate,  $r_2$ , was assumed for the anisotropy ( $q_{\alpha\beta}/Q$ ). The relaxation rates  $r_1$  and  $r_2$  were assumed to be determined by the viscosity  $\eta_o$ , the interfacial tension,  $\Gamma$ , and the configuration of the interface. Although the configuration of the interface was characterized by  $q_{\alpha\beta}$  and  $Q$ , Doi and Ohta disregarded the dependence of the configuration

of the interface on  $q_{\alpha\beta}$  and assumed that relaxation rates  $r_1$  and  $r_2$  were determined by  $\eta_o$  ,  $\Gamma$  , and  $Q$  only. Then by dimensional analysis the kinetic equations for relaxation of interfacial area ( $Q$ ) and anisotropy ( $q_{\alpha\beta}/Q$ ) were given as

$$\left. \frac{d}{dt}(Q) \right|_{\text{relax}} = -r_1 Q \quad (5.6)$$

and

$$\left. \frac{d}{dt} \left( \frac{q_{\alpha\beta}}{Q} \right) \right|_{\text{relax}} = -r_2 \left( \frac{q_{\alpha\beta}}{Q} \right), \quad (5.7)$$

respectively, where

$$r_1 = c \frac{\Gamma Q}{\eta_o}, \quad (5.8)$$

$$r_2 = k \frac{\Gamma Q}{\eta_o}, \quad (5.9)$$

and  $c$  and  $k$  are unknown parameters. The possibility that these unknown parameters may be related to the volume fraction,  $\phi$  , is discussed later. Next, using Eqs. (5.6) and (5.7) the time evolution of the interface tensor due to relaxation by interfacial tension was

$$\left. \frac{d}{dt} (q_{\alpha\beta}) \right|_{\text{relax}} = -(r_1 + r_2) q_{\alpha\beta} \quad (5.10)$$

In the absence of flow Eq. (5.6) indicates that the system will form a macroscopically phase separated state ( $Q=0$ ). While a macroscopically phase separated state could occur in systems containing equal volume fractions (which would result in co-continuous phases), in systems where the volume fractions are not equal, the final state will

not reach  $Q=0$ . In order to account for this aphysical feature of Eq. (5.6), the theory was modified so that the relaxation of the interfacial area stops when all the drops become spherical. The modified form of the kinetic equation for the relaxation of the interfacial area per unit volume was

$$r_1 = c \frac{\Gamma}{\eta_o} \left( \sum q_{\alpha\beta}^2 \right)^{1/2}, \quad (5.11)$$

which assured that the relaxation stopped when the droplets of the minor phase became spherical (i.e., the summation goes to zero when  $q_{\alpha\beta} = 0$  and thus  $r_1$  goes to zero).

The time evolution of the interface tensor from the combined effects of enlargement and orientation of the interface due to macroscopic flow and relaxation of the interface due to interfacial tension were found by substituting Eqs. (5.4), (5.5), (5.6) and (5.8) into Eq. (5.3) to give

$$\begin{aligned} \frac{dq_{\alpha\beta}}{dt} = & -q_{\alpha\gamma}\kappa_{\gamma\beta} - q_{\beta\gamma}\kappa_{\gamma\alpha} + \frac{2}{3}\delta_{\alpha\beta}\kappa_{\mu\eta}q_{\mu\eta} - \frac{Q}{3}(\kappa_{\alpha\beta} + \kappa_{\beta\alpha}) \\ & + \frac{q_{\mu\nu}\kappa_{\mu\nu}}{Q}q_{\alpha\beta} - \lambda \left[ (1-\mu)Q + \mu \left( \sum q_{\alpha\beta}^2 \right)^{1/2} \right] q_{\alpha\beta} \end{aligned} \quad (5.12)$$

and the time evolution of the interfacial area was given by

$$\left. \frac{dQ}{dt} \right|_{\text{relax}} = -q_{\alpha\beta}\kappa_{\alpha\beta} - \lambda\mu \left( \sum q_{\alpha\beta}^2 \right)^{1/2} Q. \quad (5.13)$$

where



$$\lambda = (c + k)\Gamma/\eta_o \quad \text{and} \quad \mu = c/(c + k) \quad (5.14)$$

For a given macroscopic velocity gradient tensor  $\kappa(t)$  and initial values of the interfacial area per unit volume [ $Q(0) = Q_0$ ] and the interface tensor ( $q_{\alpha\beta}$ ) the stresses occurring in a textured system can be calculated using Eqs. (5.12), (5.13), and (5.1).

There is one dimensionless parameter ( $\mu$ ) found in the above equations. If the system is characterized by three parameters  $\eta_o$ ,  $\Gamma$ , and  $\phi$ , then  $\mu$  must be a function of the volume fraction  $\phi$ . The dimensionless parameter,  $\mu$ , represents the rate of the shape relaxation relative to the total relaxation rate. If  $\mu = 0$ , then the shape relaxation is rapid, and if  $\mu = 1$ , the shape relaxation is slow. In this case  $c$  can be considered to be a function of the volume fraction of the dispersed phase. At low volume fractions no coalescence takes place, the degree of anisotropy is low and the interfacial area per unit volume,  $Q$ , remains constant with  $\mu$  equal to zero ( $c$  is zero and  $r_1$  is zero). Doi and Ohta regarded  $\mu$  as a phenomenological parameter.

Several important assumptions were made in the derivation of the theory by Doi and Ohta. The assumptions contained in the above derivation included: 1) the viscosities of both phases were equal; 2) the relaxation of size and shape of the interface was characterized by first order kinetics; 3) the overall relaxation of the system during flow was assumed to be governed by only two kinetic equations when it is known that there are three mechanisms associated with the relaxation of the interface (e.g., shape relaxation, coalescence and breakup); 4) in Eq. (5.6) it was assumed that the relaxation of  $Q$  was controlled by a single relaxation rate, and no distinction was made between the relaxation caused by droplet coalescence (the interfacial area decreases when two droplets coalesce to form a larger droplet) and shape relaxation driven by interfacial tension (the interfacial area

of an elongated droplet decreases as the droplet becomes spherical). In dilute mixtures the shape relaxation occurs much faster than the size relaxation (the relaxation due to coalescence) which would be infinitely slow. In the case of concentrated mixtures these two mechanisms are expected to occur with similar speed.

It is predicted by the Doi-Ohta theory that viscoelastic rheological properties for textured fluids consisting of immiscible mixtures of Newtonian fluids arise as a consequence of the interfacial tension. The rheological properties which are predicted by the Doi-Ohta theory include a steady state viscosity which is independent of shear rate (Newtonian), a first normal stress difference which is proportional to the magnitude of the shear rate, a transient overshoot at the start up of shear flow, and a transient stress which scales in stress and strain. Scaling of transient shear stresses has been observed experimentally in textured fluids which include liquid crystalline polymers [Doppert and Picken (1987); Moldenaers *et al.* (1990)] and immiscible mixtures of Newtonian fluids [Takahashi *et al.* (1994)].

The scaling relationship predicted by the theory is based on the fact that the system is characterized by  $\eta_0$  and  $\Gamma$  from which a quantity with units of time can not be constructed. Doi and Ohta showed that for a given velocity gradient tensor,  $\kappa(t)$ , the solution of Eqs. (5.12), (5.13) and (5.14) was written as

$$\sigma = \sigma(t; [\kappa(t)]) \quad (5.15)$$

and then it was shown that for a new velocity gradient tensor  $c\kappa(ct)$  that

$$\sigma(t; [c\kappa(ct)]) = c\sigma(ct; [\kappa(t)]) \quad (5.16)$$

which states that the stress at time  $t$  under the velocity gradient  $c\kappa(ct)$  is  $c$  times larger

than the stress at time  $ct$  under the velocity gradient  $\kappa(t)$ . The consequences and significance of this scaling relationship are discussed in the results section as it applies to steady, transient and oscillatory shear flow.

### 5.3 EXPERIMENTAL

The materials and methods required to carry out the objective of this work are presented in this section. First, the polymers used and the blend preparation method are presented. Next, the methods used to determine the state of the texture (microscopy) and the rheological properties of the polymers are discussed.

#### 5.3.1 Materials and Sample Preparation

The polymers used in this investigation were poly(ethylene terephthalate) (PET) and nylon 6,6. The PET supplied by Dupont was PTX-267 ( $M_w = 25,000$ ) and was determined to have a melting temperature of 257 °C. The recommended drying conditions for PET were 120 to 125 °C for 3 to 4 hours in vacuum for a moisture content of 0.02 %. The nylon 6,6 supplied by Monsanto was Vydyne 66b ( $M_w = 30,000$ ) and was determined to have a melting temperature of 263 °C. The recommended drying conditions for nylon 6,6 were 75-80 °C for 3 to 4 hours in vacuum. These polymers were chosen because after extrusion, as a consequence of degradation, each neat polymer was characterized by a constant viscosity over a wide range of shear rates, and short relaxation times [Guenther and Baird (1995)]. In addition, these two polymers after extrusion had nearly equal zero shear viscosities as is required by the theory of Doi and Ohta.

A blend was prepared using the polymers described above at a composition ratio of 25/75 w/w PET/nylon 6,6 by mixing in an extruder. This composition ratio was chosen based on the results of a study by Guenther and Baird (1995) in which it was shown that the stability of the blend at a composition of 25/75 w/w PET/nylon 6,6 and the neat polymers was similar after extrusion. It was shown using rheological measurements (e.g., time sweeps) that within the time frame required for the rheological experiments used in this work (e.g., < 5 minutes), very little change due to degradation in the steady state and transient rheological properties of this blend occurred at 290 °C under a nitrogen atmosphere. Based on their observations the rheological properties of this blend relative to those of the neat extruded polymers were found to be a function of the morphology of the blend and not degradation.

Blending was carried out using dried polymers. PET was dried for 36 hours at 125 °C in a vacuum oven and nylon 6,6 was dried for 36 hours in a vacuum oven at 75 °C to insure a minimum moisture content in the samples. Weighed amounts of the dried polymers were dry blended and stored in a vacuum oven at 100 °C. Dry blended pellets in proportions of approximately 30 grams at a time were removed from the oven and immediately loaded into the hopper of a 2.54 cm Killion extruder. New pellets from the oven were added to the hopper only after the last pellets from the previous charge had reached the feed section of the extruder in order to minimize exposure time to moisture. Extrusion was carried out at 20 RPM with an attached capillary die with a diameter of 0.3175 cm and a L/D of 10. The barrel temperatures from the feed zone to the die were 260, 275, 290, 290 and 270 °C, respectively. The extrusion conditions described above correlate to a residence time in the metering section of the extruder of 4.5 minutes based on the flow rate and screw dimensions. The neat polymers were subjected to the same processing histories as the blends.

### 5.3.2 Rheological Measurements

Rheological experiments were carried out on the blends and neat polymers using a Rheometrics Mechanical Spectrometer (RMS-800) with a cone and plate fixture having a cone angle of 0.1 rad and a diameter of 12.5 mm. Steady shear viscosity ( $\eta$ ) and first normal stress difference ( $N_1$ ) data were obtained using start up of shear flow experiments after the sample was sheared long enough to reach steady state conditions. Time sweep experiments were carried out on all samples in which the magnitude of the complex viscosity,  $|\eta^*|$ , at a constant frequency of 1 rad/sec and a strain of 5% was measured. All experiments were carried out at a temperature of 290 °C under a nitrogen atmosphere.

### 5.3.3 Microscopy

The morphology of the blend was examined by scanning electron microscopy using a Cambridge Stereoscan S200 electron microscope. Samples were cryogenically fractured after immersion in liquid nitrogen for 5 minutes. The fractured samples were fixed to aluminum stubs and sputter coated.

### 5.3.4 Interfacial Tension

The value of interfacial tension,  $\Gamma$ , for the blend was obtained using contact angle measurements. Using two different solutions of known dispersive and polar components of surface tension, the dispersive and polar portions of the surface tension for both PET and nylon 6,6 were obtained. These values were then used to calculate the interfacial tension of the blend using the harmonic mean equation [Wu (1971)].

## 5.4 RESULTS

The rheological and numerical results of this work are presented in this section. First, the parameters and initial conditions required in evaluating the predictions of the theory are determined. Next, the steady state viscosity and first normal stress difference and the transient shear stress and first normal stress difference of the PET/nylon 6,6 blend are compared to predictions using the Doi-Ohta theory.

### 5.4.1 Parameters and Initial Conditions

In order to evaluate the Doi-Ohta theory values for the four parameters (e.g.,  $\eta_o$ ,  $\Gamma$ ,  $c$  and  $k$ ) and the initial values for  $Q$  and  $q_{\alpha\beta}$  had to be determined. Of the four parameters required by the theory only  $\eta_o$ ,  $\Gamma$  and  $k$  could be determined experimentally. The last unknown parameter,  $c$ , was determined by fitting the Doi-Ohta theory [Eqs. (5.12), (13), and (1)] to start up of shear flow data. The initial conditions required by the equations which included the initial values of the interfacial area per unit volume,  $Q(0) = Q_o$  and the interface tensor,  $q_{\alpha\beta}(0)$ , were determined using the results obtained from scanning electron microscopy. The values of the parameters and initial conditions used in this work are listed in Table 5.1.

The value of the system zero shear viscosity,  $\eta_o$ , was obtained in this work using the viscosity of the neat polymers after extrusion. The viscosity of the neat polymers before and after extrusion is shown in Figure 5.1. The neat polymers after extrusion have a viscosity which is both lower in magnitude and more Newtonian over the shear rates

**TABLE 5.1** Model parameters and initial conditions for the 25/75 PET/nylon 6,6 blend.

Parameter	Value
$\eta_o$ (Pa s)	205
$\eta (\dot{\gamma})$ (Pa s)	227 at $\dot{\gamma} = 0.3 \text{ sec}^{-1}$ 185 at $\dot{\gamma} = 9.0 \text{ sec}^{-1}$
$\Gamma$ (mN/m)	$.397 \pm .06$ $.513^{**}$
<b>k</b>	0.07
<b>c</b>	0.6
Initial Condition	Value
$Q_o$ (m <sup>2</sup> /m <sup>3</sup> )	300,000
$q_{\alpha\beta}(0)$	0

**\*\*Published [Smith (1969)]**

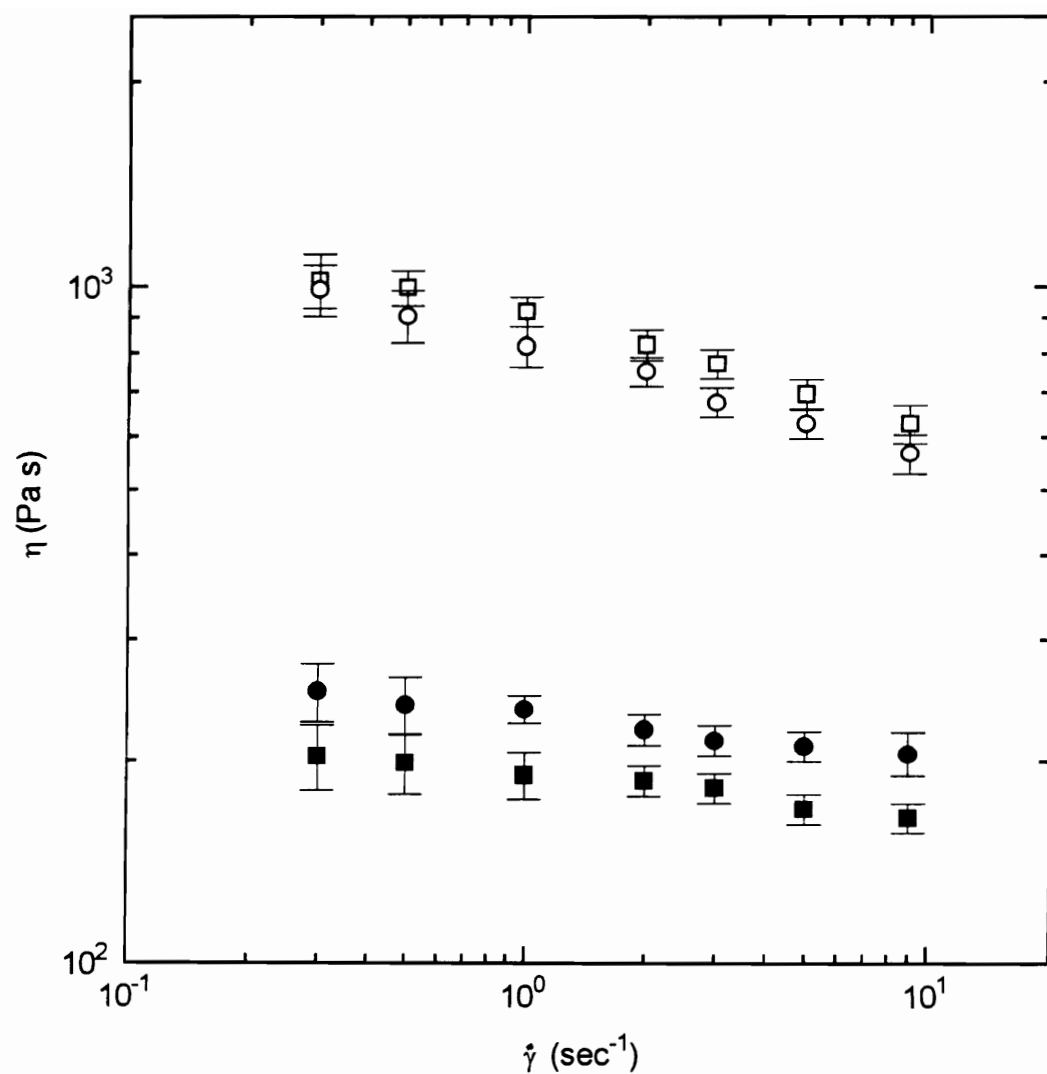


**Figure 5.1** Viscosity versus shear rate at 290 °C before and after extrusion: (□) PET; (○) nylon 6,6; (■) extruded PET; and (●) extruded nylon 6,6.



measured than the neat polymers which have not been subjected to extrusion. Although the magnitude of the viscosity and the degree of shear thinning observed in the neat polymers before extrusion are substantially reduced by extrusion, the neat extruded polymers are still slightly shear thinning, and a small mismatch in their magnitudes is observed. The value of the viscosity parameter  $\eta_o$  used in this work was calculated by taking the weighted average (based on the weight fractions of the neat polymers in the blend) of the mean viscosity of each polymer over shear rates ranging from 0.3 to 9.0  $\text{sec}^{-1}$ . In order to account for the shear thinning behavior of the neat polymers in the predictions of the Doi-Ohta theory, shear rate dependent values of the viscosity [e.g.,  $\eta(\dot{\gamma})$ ] were used in place of the constant viscosity parameter,  $\eta_o$  in Eqs. (5.1), (5.9), and (5.11). The values of  $\eta(\dot{\gamma})$  were calculated at shear rates ranging from 0.3 to 9  $\text{sec}^{-1}$  using the weighted average of the viscosities (based on the weight fraction of the neat polymers in the blend) of the neat polymers after extrusion.

In order to determine the stability of the samples during the rheological measurements used in this work, time sweeps were performed on the samples under a nitrogen atmosphere at 290 °C. The time frame for the rheological measurements used in this work was less than 3 minutes for the steady shear ( $\eta$  and  $N_1$  versus  $\dot{\gamma}$ ) and transient experiments [ $N_1^+(t)$  and  $\sigma^+(t)$ ]. The change in  $|\eta^*|$  with time at a frequency of 1 rad/sec for the blend and the neat polymers is shown in Fig. 5.2. The magnitude of the complex viscosity of the PET is seen to decrease by 7.5% in 3 minutes while that of the extruded nylon 6,6 remains essentially constant for 4 minutes. The decrease in  $|\eta^*|$  with time for the blend is seen to be between that of the neat polymers (e.g., 2.5% in 3 minutes). Based on these results, rheological data obtained for the blend and neat polymers will be assumed to be not significantly affected by the degradation occurring during the rheological experiments.

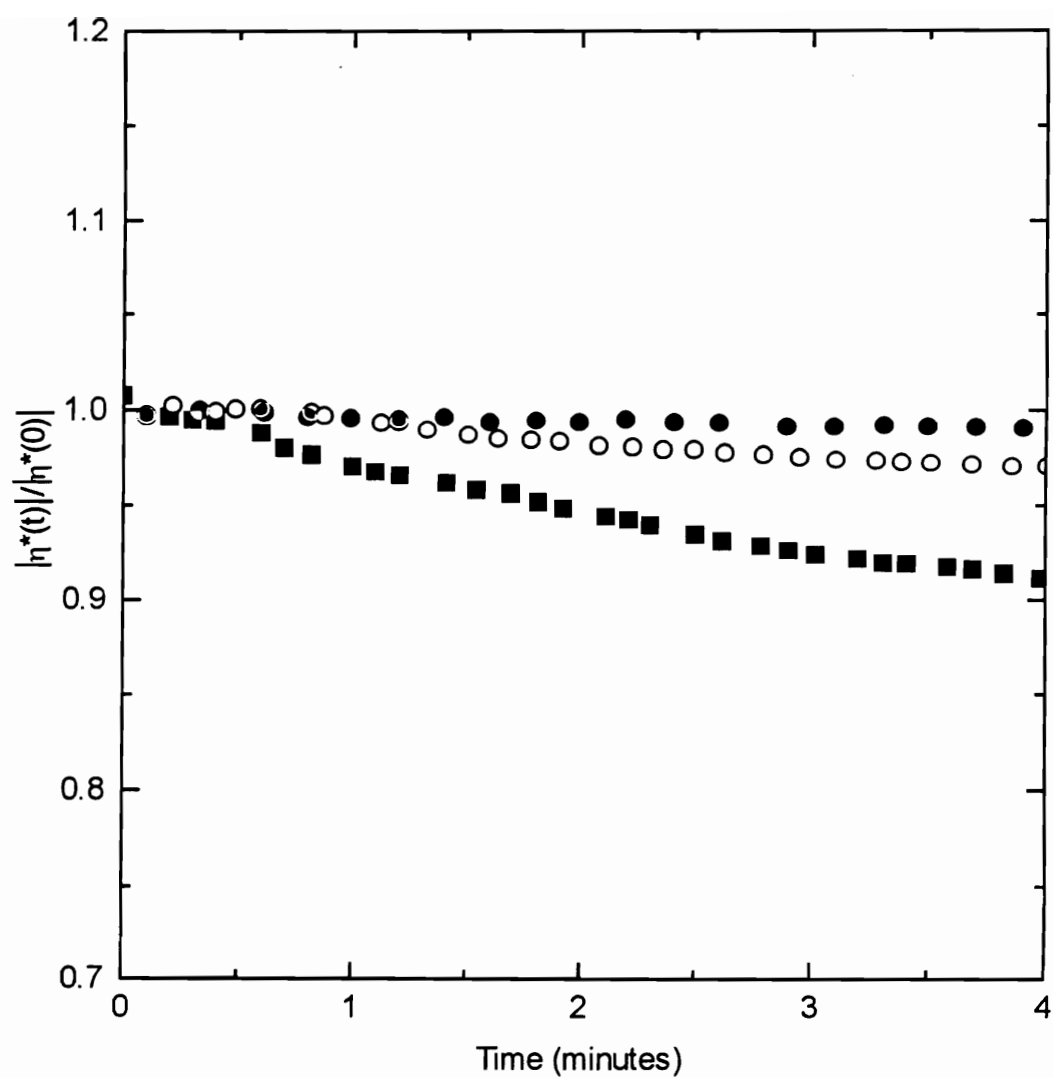


**Figure 5.2** Magnitude of the complex viscosity versus time at 290 °C for: (■) PET; (○) nylon; and (●) 25/75 PET/nylon 6,6 blend.

The initial values of  $Q$  and  $q_{\alpha\beta}$  required in the evaluation of the Doi-Ohta theory were determined using scanning electron micrographs of the blend. A micrograph of a sample which had been held at a temperature of 290 °C for 1 minute to allow for relaxation of the morphology and then quenched is shown in Fig. 5.3. It can be seen that the blend has a dispersed phase of PET in the form of unoriented drops with diameters on the order of 5  $\mu\text{m}$ . Based on an average drop diameter of 5  $\mu\text{m}$  obtained from the scanning electron micrograph shown in Fig. 5.3 and the volume fraction of the blend, the initial value  $Q_o$  was calculated to be 300,000  $\text{m}^2/\text{m}^3$ . The initial value of the interface tensor was assumed to be an isotropic condition of  $q_{\alpha\beta}(0) = 0$  based on the scanning electron micrograph shown in Fig. 5.3 in which the drops are observed to be spherical.

The last two parameters  $c$  and  $k$  required by the theory are the unknown constants in the kinetic equations for relaxation of the size [Eq. (5.11)] and shape [Eq. (5.9)] of the interface, respectively. The parameter,  $k$ , in Eq. (5.9) was obtained from the theory developed by Choi and Schowalter (1975) and later modified by Scholz (1989) which describes the role played by interfacial tension in concentrated emulsions of two Newtonian fluids on the storage and loss moduli as follows:

$$G'(\omega) = \frac{\eta}{\tau_1} \left( 1 - \frac{\tau_2}{\tau_1} \right) \frac{\omega^2 \tau_1^2}{1 + \omega^2 \tau_1^2} \quad (5.17)$$

$$G''(\omega) = \frac{\eta}{\tau_1} \left( 1 - \frac{\tau_2}{\tau_1} \right) \frac{\omega \tau_1}{1 + \omega^2 \tau_1^2} + \omega \eta \frac{\tau_2}{\tau_1} \quad (5.18)$$

where

$$\eta = \eta_{\text{mol/rx}} \left[ 1 + \phi \frac{(5h+2)}{2(h+1)} + \phi^2 \frac{5(5h+2)^2}{8(h+1)^2} \right] \quad (5.19)$$

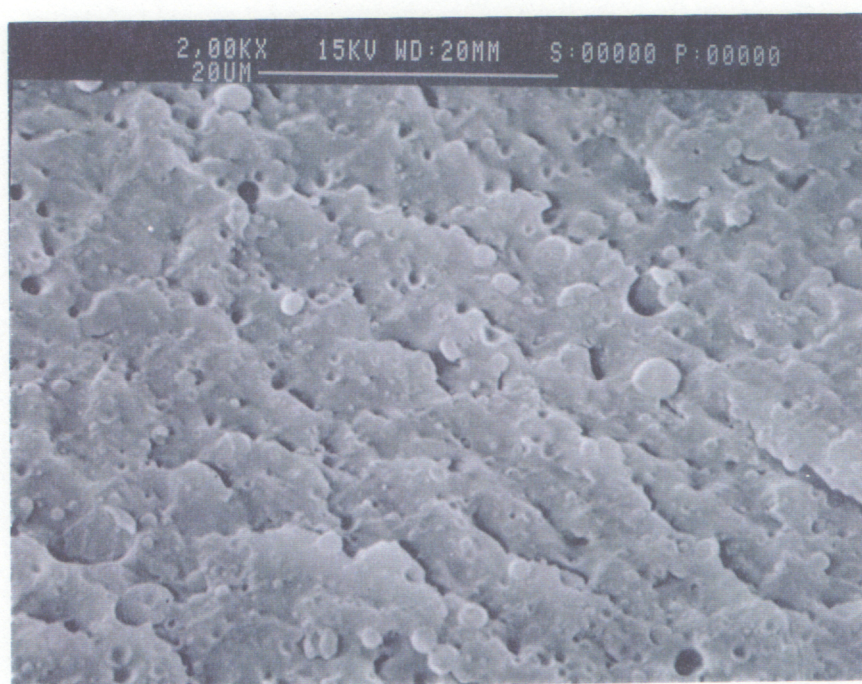


**Figure 5.3** Scanning electron micrograph of 25/75 PET/nylon 6,6 blend.

$$\tau_1 = \tau_o \left[ 1 + \phi \frac{5(19h + 16)}{4(h + 1)(2h + 3)} \right] \quad (5.20)$$

$$\tau_2 = \tau_o \left[ 1 + \phi \frac{3(19h + 16)}{4(h + 1)(2h + 3)} \right] \quad (5.21)$$

$$\tau_o = \frac{\eta_{matrix} D}{2\Gamma} \frac{(19h + 16)(2h + 3)}{40(h + 1)} \quad (5.22)$$

$$h = \frac{\eta_{dispersed\ phase}}{\eta_{matrix}} \quad (5.23)$$

and where  $\phi$  is the volume fraction of the dispersed phase and  $D$  is the diameter of the dispersed phase. The relaxation time  $\tau_1$  calculated using Eqs. (5.20) and (5.22) was found in the work by Gramespacher and Meissner (1992) to be equal to the relaxation time associated with the interface for immiscible polymer blends consisting of polystyrene and poly(methylmethacrylate). The relaxation time associated with the interface was obtained experimentally by Gramespacher and Meissner from the relaxation spectrum of the blend in which three peaks were observed. The relaxation times at which the first two peaks occurred were attributed to the relaxation times of the two neat polymers and the relaxation time at which the third peak occurred was attributed to the relaxation time associated with the interface. Hence, assuming that the relaxation time associated with the interface,  $\tau_1$  in Eq. (5.20), is equal to  $1/r_2$  in Eq. (5.9) in small deformations, the parameter,  $k$ , was calculated directly using Eqs. (5.20), (5.22) and (5.9). The value of  $\tau_1$  calculated using Eqs. (5.20) and (5.22) was 6 seconds. Using the relaxation time  $\tau_1$  determined in the manner described above, the parameter  $k$  was calculated to be 0.07. Justification for the use of this method to determine the parameter  $k$  is based on the assumption that in small deformations the change in the area of the interface is negligible ( $\Delta Q \cong 0$  and  $r_1 \cong 0$ ), and, therefore the only contribution from the interface is that from the anisotropy ( $Q/q_{\alpha\beta}$ ) of the

interface.

The value calculated above for the relaxation time associated with the interface,  $\tau_1$ , was correlated to that obtained from the relaxation spectrum of the blend. The relaxation spectrum was calculated by fitting the experimental storage ( $G'_j$ ) and loss ( $G''_j$ ) moduli as a function of angular frequency ( $\omega$ ) of the blend using the following truncated forms of the generalized Maxwell model

$$G'(\omega_j) = \sum_{k=1}^N \frac{\eta_k \tau_k \omega_j^2}{1 + (\tau_k \omega_j)^2} \quad \text{and} \quad G''(\omega_j) = \sum_{k=1}^N \frac{\eta_k \omega_j}{1 + (\tau_k \omega_j)^2} \quad (5.24)$$

where  $G'(\omega_j)$  and  $G''(\omega_j)$  are the predicted values of storage and loss moduli,  $\eta_k$  and  $\tau_k$  are the relaxation viscosities and times, respectively, and  $N$  is the number of constants to be used in the fit. The equation was fit by minimizing the error between predicted [ $G'(\omega_j)$  and  $G''(\omega_j)$ ] and measured [ $G'_j$  and loss ( $G''_j$ )] moduli. This was done using a nonlinear least squares method in which the following quantity was minimized [Bird et al. (1987; Papanastasiou *et al.* (1983)],

$$\sum_{j=1}^N \left\{ \left[ \frac{G'(\omega_j)}{G'_j} - 1 \right]^2 + \left[ \frac{G''(\omega_j)}{G''_j} - 1 \right]^2 \right\} \quad (5.25)$$

The relaxation spectrums for the blend and the neat blend constituents obtained using Eqs. (5.24) and (5.25) are shown in Fig. 5.4. From the plot shown in Fig. 5.4 the relaxation time associated with the interface,  $\tau_1$ , seen as the third peak in the spectrum was found to be approximately 5 seconds and agreed with that obtained above using Eq. (5.20).

The remaining parameter required by the model,  $c$ , was determined using start up of shear flow experiments. In this experiment the sample was presheared for 1 minute at a shear rate of  $1 \text{ sec}^{-1}$  and allowed to relax for 1 minute before the start up of shear flow was

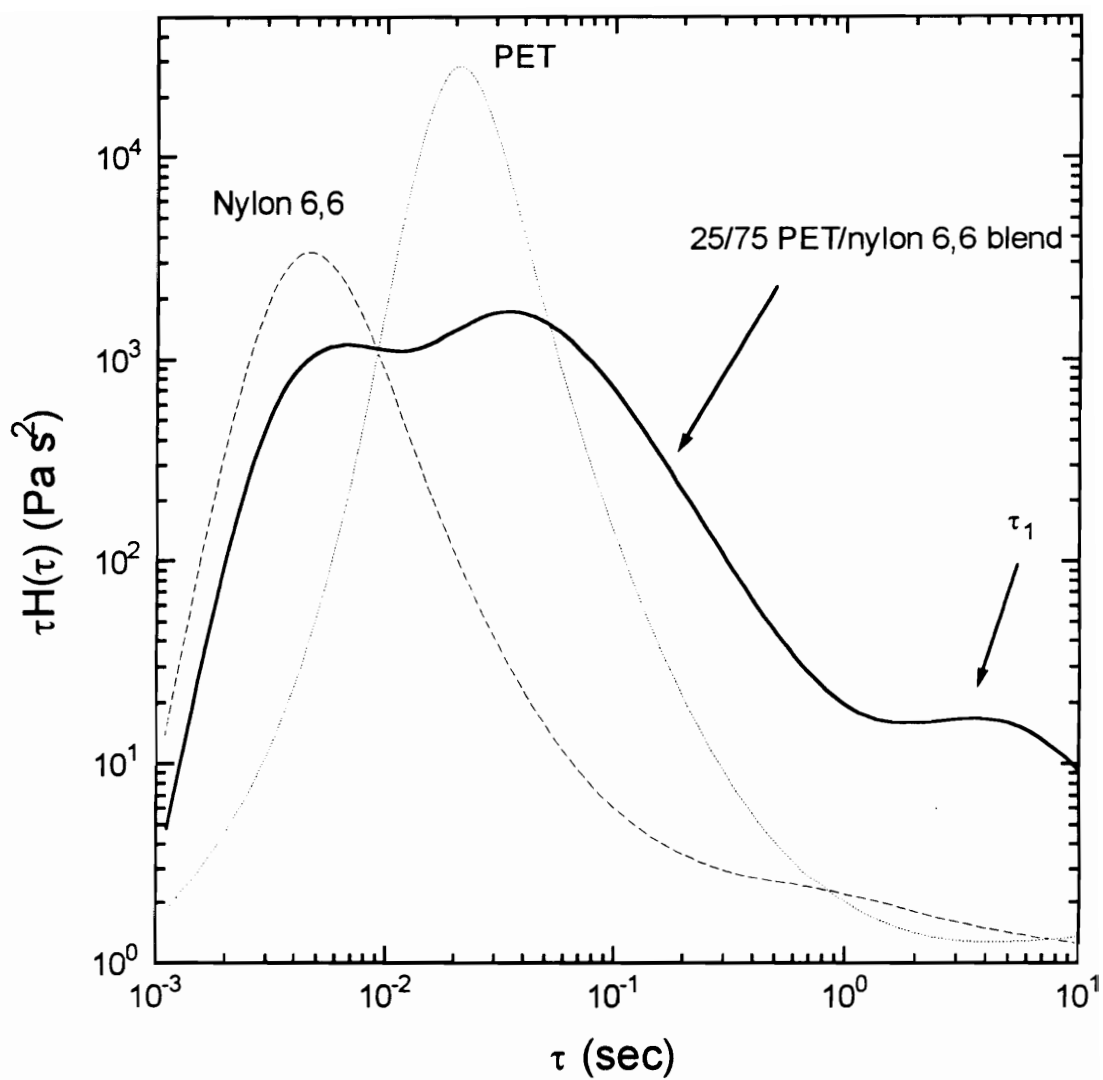


**Figure 5.4** Weighted relaxation time spectra for PET, nylon 6,6 and 25/75 PET/nylon 6,6 blend at 290 °C.

performed. This procedure provided for reproducible data with an error which was within a 5% range and was used to fit the parameter,  $c$ , in the theory. This procedure provided for reproducible data with an error which was within a 5% range and was used to fit the parameter,  $c$ , in the theory using the values of  $\eta_o$ ,  $\Gamma$ ,  $k$ ,  $Q$  and  $q_{\alpha\beta}$  determined above. The magnitude of the overshoot and steady state values of the transient shear stress and first normal stress difference at the start up of shear flow are seen to be predicted accurately (see Fig. 5.5 and 5.6). However, some error is seen in the transient first normal stress difference in which the strain at which the maximum in the overshoot occurs is underpredicted by the theory. This error may be related to presence of a substantial contribution to the transient first normal stress difference of the blend from those of the neat polymers.

#### 5.4.2 Steady Shear Flow Predictions

A comparison of the predicted and experimental steady shear rheology of the 25/75 PET/nylon 6,6 blend is presented here. Under steady state conditions the texture of the system is in a constant state of droplet deformation, breakup, and coalescence in which the droplets have a distribution of sizes and orientations of their interfaces which are constant. At steady state the area of the interface per unit volume and the components of the interface tensor are predicted to be constant in the theory of Doi and Ohta. The steady state viscosity is predicted to be independent of shear rate and the first normal stress difference is proportional to the shear rate. These results should hold because they are a result of dimensional analysis, and the steady-state viscosity should be determined by  $\Gamma$ ,  $\eta_o$  and  $\dot{\gamma}$ .



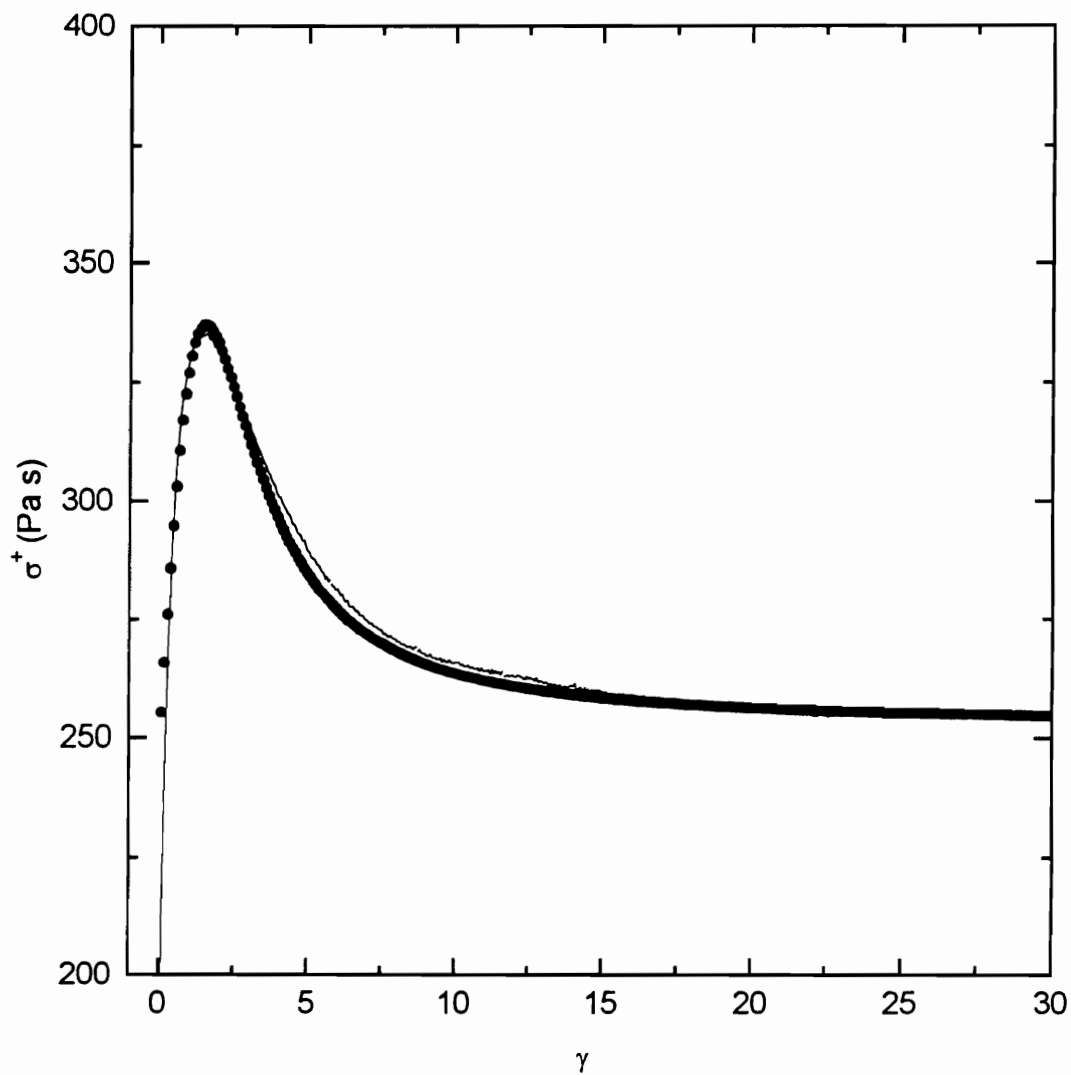


**Figure 5.5** Best fit for parameter  $c$  using transient shear stress at start up of shear flow at 290°C for 25/75 PET/nylon 6,6 blend: (●) experimental; and (—) model.

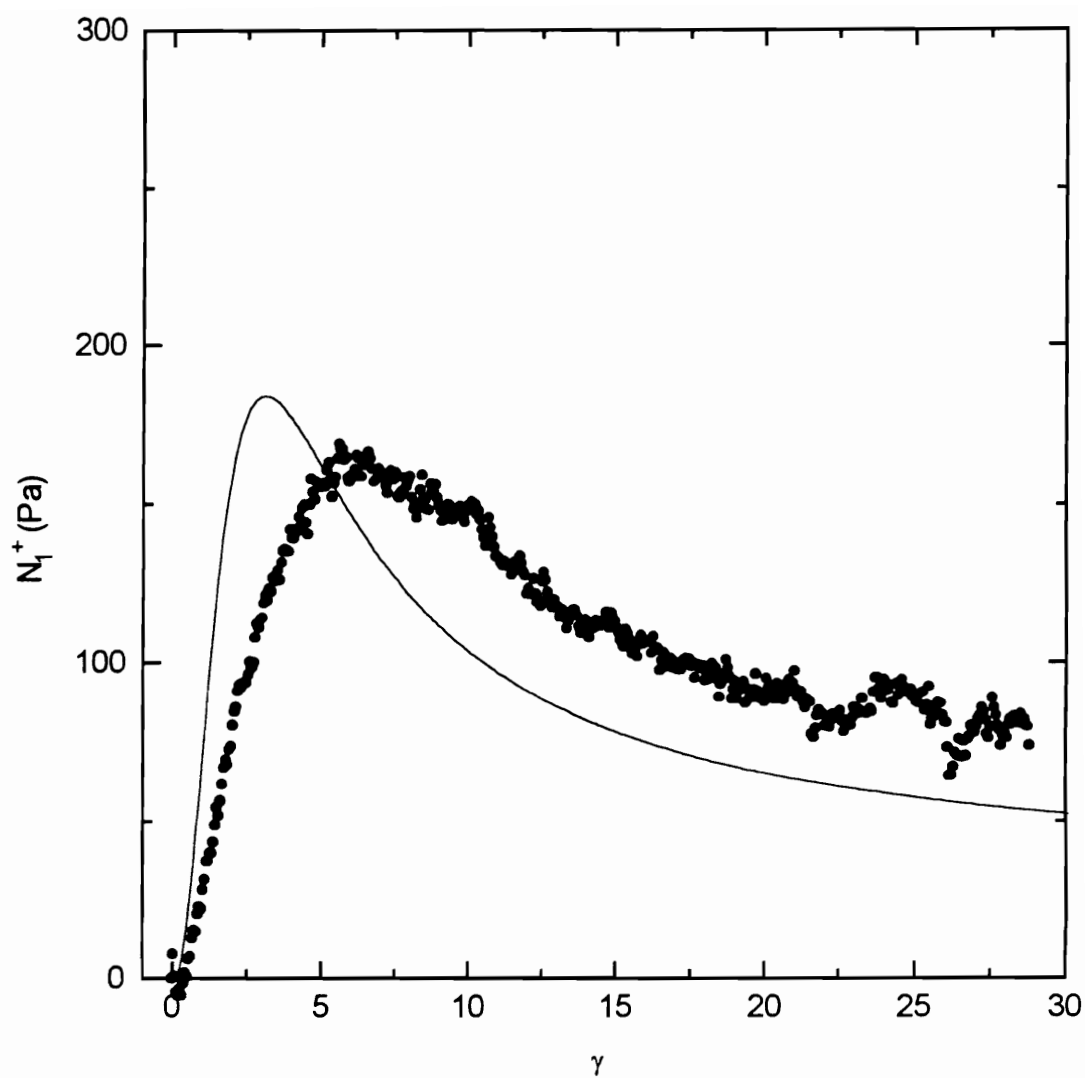


**Figure 5.6** Best fit for parameter  $c$  using transient first normal stress difference at start up of shear flow at 290°C for 25/75 PET/nylon 6,6 blend: (•) experimental; and (—) model.

A comparison of the predicted viscosity using the Doi-Ohta model to experimental values is shown in Fig. 5.7. In this figure the predicted blend viscosity using both a constant ( $\eta_0$ ) and a shear rate dependent [ $\eta(\dot{\gamma})$ ] viscosity parameter is shown. It can be seen that when a constant value for the viscosity parameter is used the predicted viscosity for the blend is Newtonian. The use of a shear thinning viscosity parameter  $\eta(\dot{\gamma})$  in place of the constant viscosity parameter  $\eta_0$  in Eqs. (5.1), (5.9), and (5.11) results in a predicted blend viscosity which is more shear thinning than observed experimentally for the neat polymers. Despite this correction, the degree of shear thinning observed experimentally for the blend is not predicted. It can be seen that the model only roughly approximates the magnitude of the viscosity of the blend observed experimentally and does not predict the shear thinning behavior the blend observed experimentally. The shear thinning behavior of the blend suggests that a characteristic time scale associated with the interface exists in the blend and therefore the inability of the Doi-Ohta theory to predict this behavior may be related to the form or order of the kinetic equations and the relaxation times associated with the neat polymers.

Although the viscosity is predicted to be independent of shear rate (if a constant  $\eta_0$  is used), the model predicts other interesting rheological behavior. It can be shown that the first normal stress difference is proportional to  $|\dot{\gamma}|$ . A finite stress is predicted because even at infinitesimally small shear rates the texture can change. A comparison of predicted and observed steady state first normal stress difference behavior as function of shear rate is shown in Fig. 5.8. In order to determine if the contribution to the first normal stress difference from the interface is accurately predicted by the theory, the contribution to  $N_1$  from the neat polymers was added to the normal stress predicted by the theory since in the theory the fluids are Newtonian. The  $N_1$  contribution of the blend constituents at each shear rate was calculated using the weighted average (based on the weight fractions of the

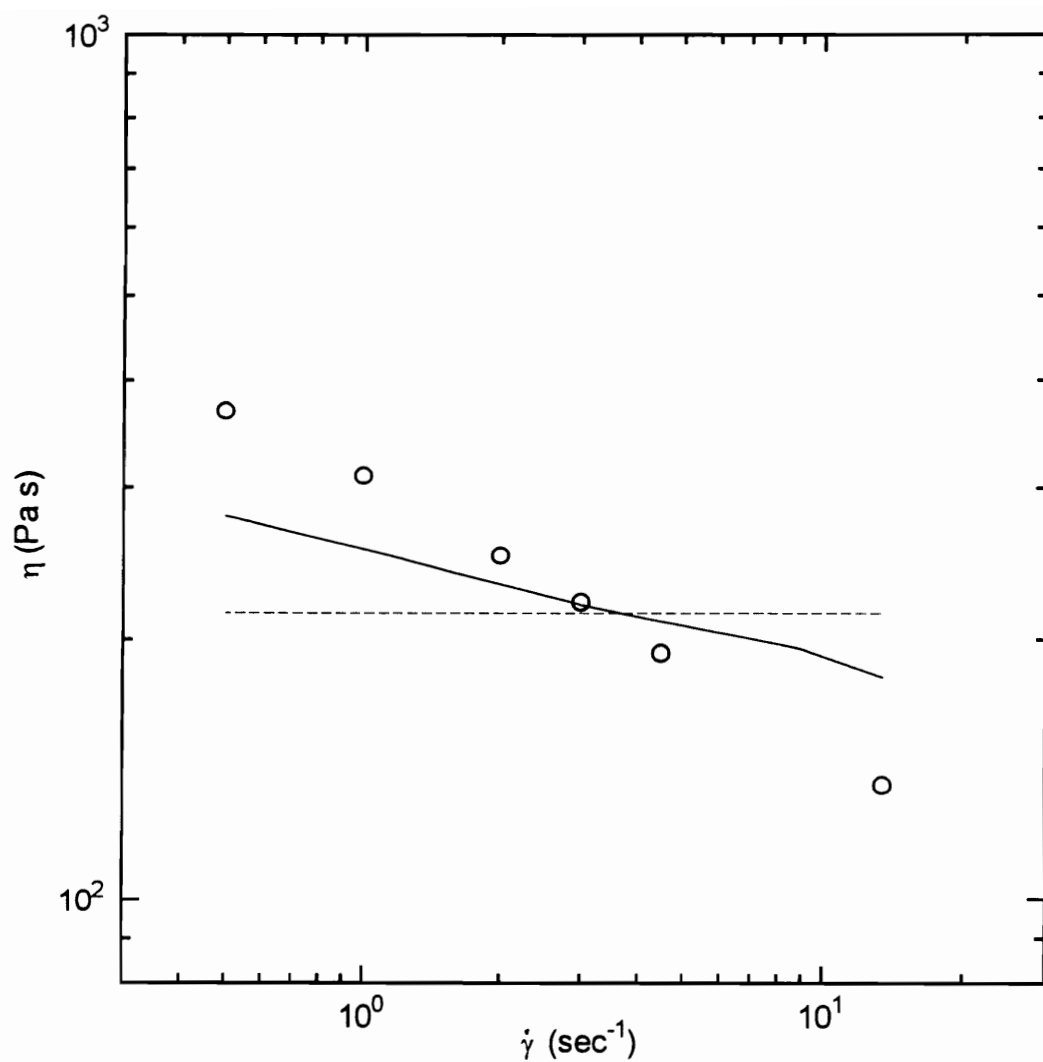


**Figure 5.7** viscosity as a function of shear rate at 290 °C for 25/75 PET/nylon 6,6 blend: (○) experimental; (----) predicted  $\eta_0$  (constant); and (—) predicted  $\eta_0(\dot{\gamma})$ .

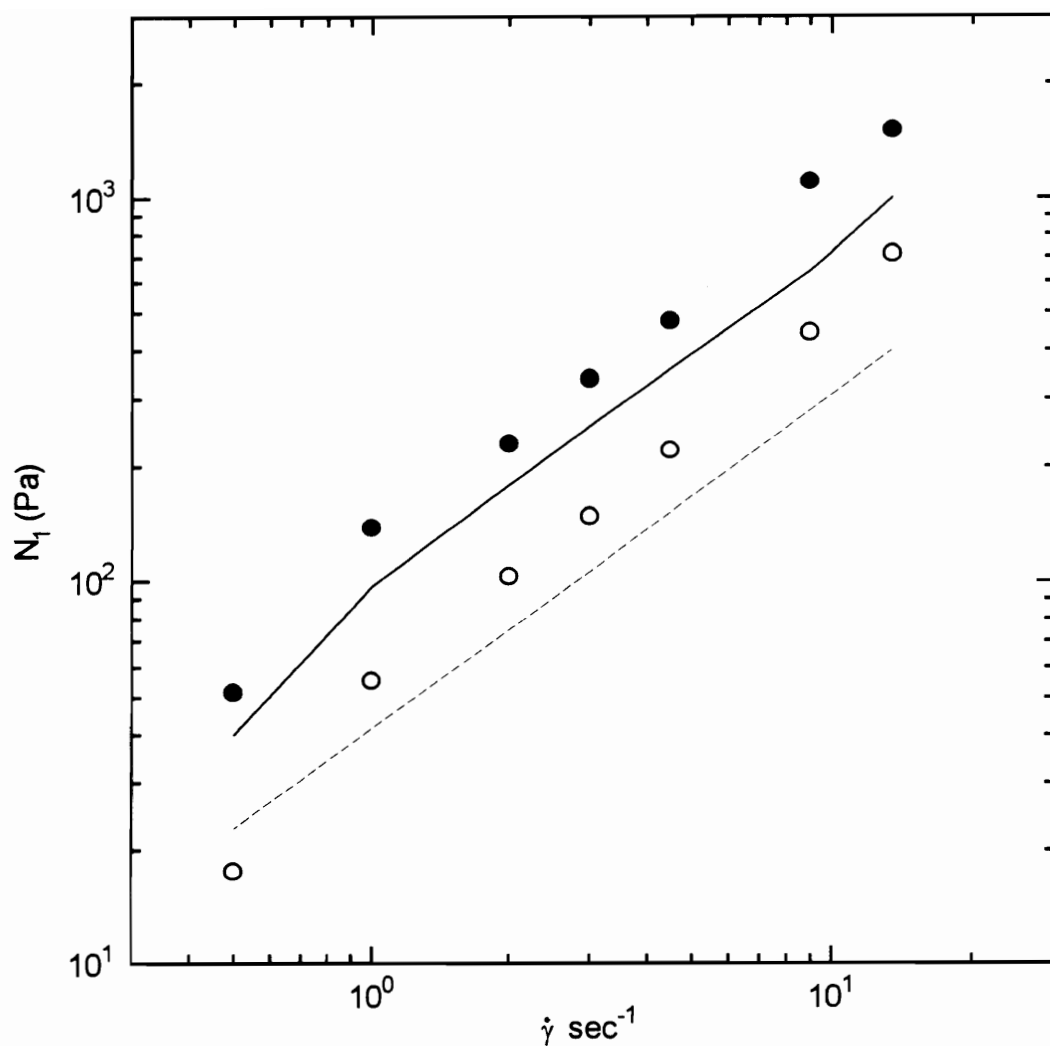


**Figure 5.8** First normal stress difference as a function of shear rate at 290 °C: (○) weighted average of PET and nylon 6,6; (●) experimental 25/75 PET/nylon 6,6 blend; (----) predicted by Doi-Ohta theory; and (—) predicted using weighted average of neat polymers plus Doi-Ohta theory.

neat polymers in the blend) of the measured first normal stress difference for the neat polymers. The contribution to  $N_1$  from the neat polymers was simply added to the extra stress calculated using the model at each shear rate. It can be seen in Fig. 5.8 that the first normal stress difference calculated in this manner very nearly approximates the first normal stress difference observed for the blend both in magnitude and rate dependence.

### 5.4.3 Transient Shear Flow Predictions

The transient shear stress and first normal stress difference predicted using the Doi-Ohta theory and the experimental results for the 25/75 PET/nylon 6,6 blend are shown in Fig. 5.9 and 5.10, respectively. These two figures show a transient experiment consisting of the start up of steady shear flow, a step-up of the shear rate, and a step-down of the shear rate. As a consequence of the short relaxation times of both neat polymers the transients for the shear stress and first normal stress difference for the neat polymers do not show the overshoot at the start up of shear flow and upon a stepwise increase of the shear rate or the undershoot upon a stepwise decrease of the shear rate which is observed for the blend. It can be seen that both the shear stress and first normal stress difference are qualitatively modeled by the theory at the start up of shear flow. As the shear rate is stepped up in the experiment, the overshoot in shear stress and first normal stress difference are not predicted by the theory. As the shear rate is stepped down in the last part of the experiment, the undershoot in both shear stress and first normal stress difference is not predicted by the theory. Failure of the theory to predict the overshoot and undershoot observed in step changes of shear rate indicate that the kinetic equations do not accurately model the relaxation behavior of both shape and size of the interface which may occur in this flow.

The scaling relationship predicted by the Doi-Ohta equations for transient shear

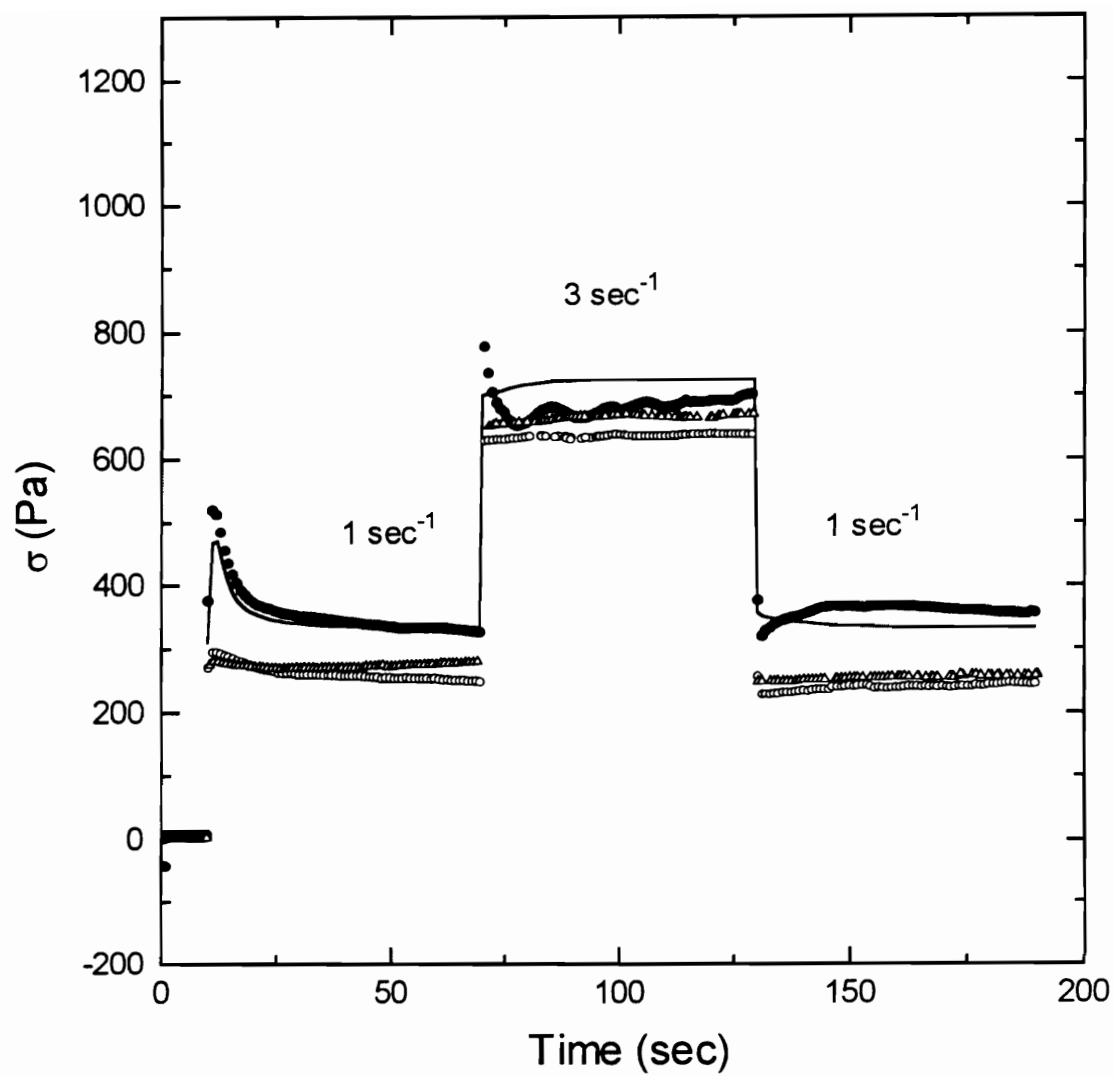


**Figure 5.9** Transient shear stress versus time for at 290 °C: (○) PET; (Δ) nylon 6,6; (●) 25/75 PET/nylon 6,6 blend; (—) predicted by Doi-Ohta theory.

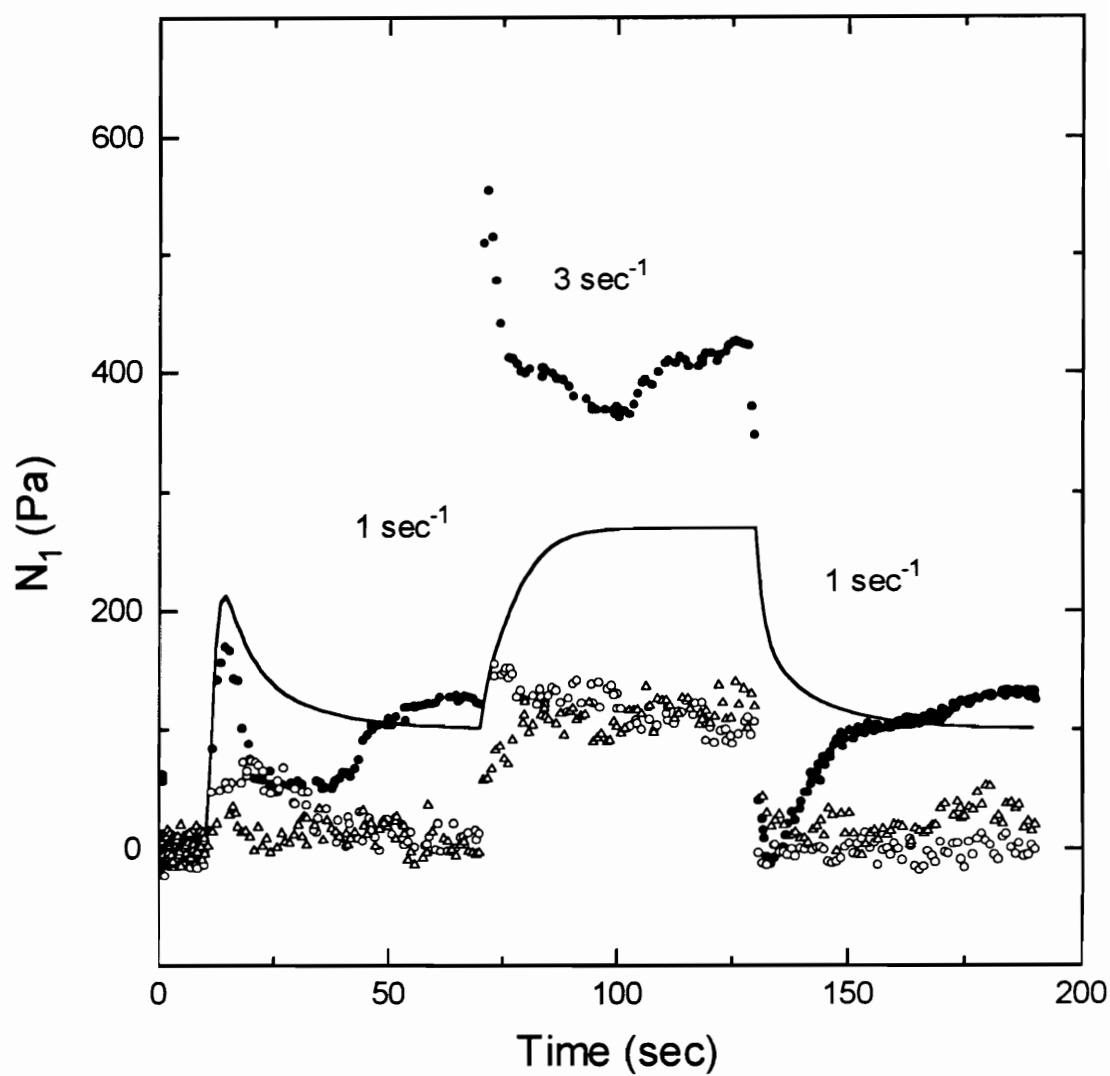


**Figure 5.10** Transient first normal stress difference versus time for at 290 °C: (○) PET; (Δ) nylon 6,6; (●) 25/75 PET/nylon 6,6 blend; (—) predicted by Doi-Ohta theory.



flows was investigated using the transient shear stress data obtained from stepwise changes of the shear rate. Consider the transient experiment where the shear rate is changed from  $\dot{\gamma}_1$  to  $\dot{\gamma}_2$  at time  $t = 0$ . The Doi-Ohta theory predicts that the stress growth or relaxation curve plotted in terms of scaled stress ( $\sigma_s$ )

$$\sigma_s = \frac{\sigma^+(t, \dot{\gamma}_1) - \sigma(\dot{\gamma}_0)}{\sigma(\dot{\gamma}_1) - \sigma(\dot{\gamma}_0)} \quad (5.26)$$

and strain ( $\gamma_1$ )

$$\gamma_1 = \dot{\gamma}_1 \cdot t \quad (5.27)$$

can be superimposed at constant step ratios  $\dot{\gamma}_0 / \dot{\gamma}_1$  regardless of the final shear rate,  $\dot{\gamma}_1$ . This scaling relationship can be observed using step-up and step-down experiments with a constant step-up and step-down ratio ( $\dot{\gamma}_0 / \dot{\gamma}_1 = \text{constant}$ ) and plotted as function of the scaled stress ( $\sigma_s$ ) for the blend as shown in Figs. 5.11 and 5.12. Although the overshoot and undershoot are not predicted by the theory the transient shear stress of this blend does in fact scale. This is a special case of the more general scaling relation described by Eqs. (5.15) and (5.16).

Additional evidence of the wrong form or order of the relaxation equations is revealed by the inability of the Doi-Ohta theory to predict a recovery of the initial overshoot observed experimentally for the blend using start up of shear flow experiments. The recovery of the overshoot associated with a recovery of the equilibrium texture can be seen in Figure 5.13 where the shear stress is reduced by the steady state shear stress [e.g.,  $\sigma_r = \sigma^+(t, \dot{\gamma}_0) / \sigma(t)$ ]. In this figure it can be seen that at a recovery time of 40 seconds approximately 90% of the overshoot is recovered. The inability of the Doi-Ohta theory to

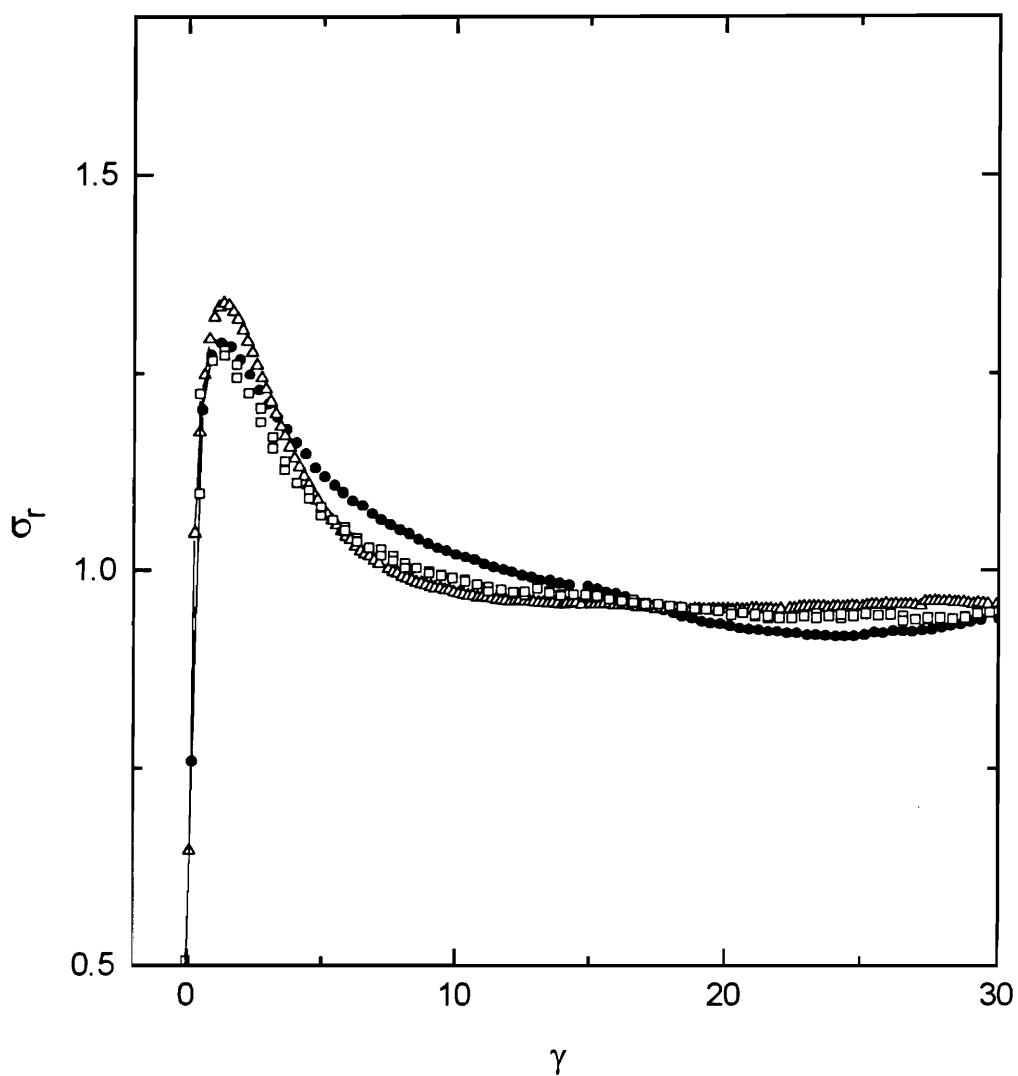


**Figure 5.11** Scaled transient shear stress versus strain after a step-up of shear rate from  $\dot{\gamma}_1$  to  $\dot{\gamma}_2$  where  $(\dot{\gamma}_2 / \dot{\gamma}_1 = 3)$  and where  $\dot{\gamma}_2$  is; ( $\Delta$ )  $1.5 \text{ sec}^{-1}$ ; ( $\bullet$ )  $3.0 \text{ sec}^{-1}$ ; and ( $\square$ )  $4.5 \text{ sec}^{-1}$  for 25/75 PET/nylon 6,6 blend at  $290^\circ\text{C}$

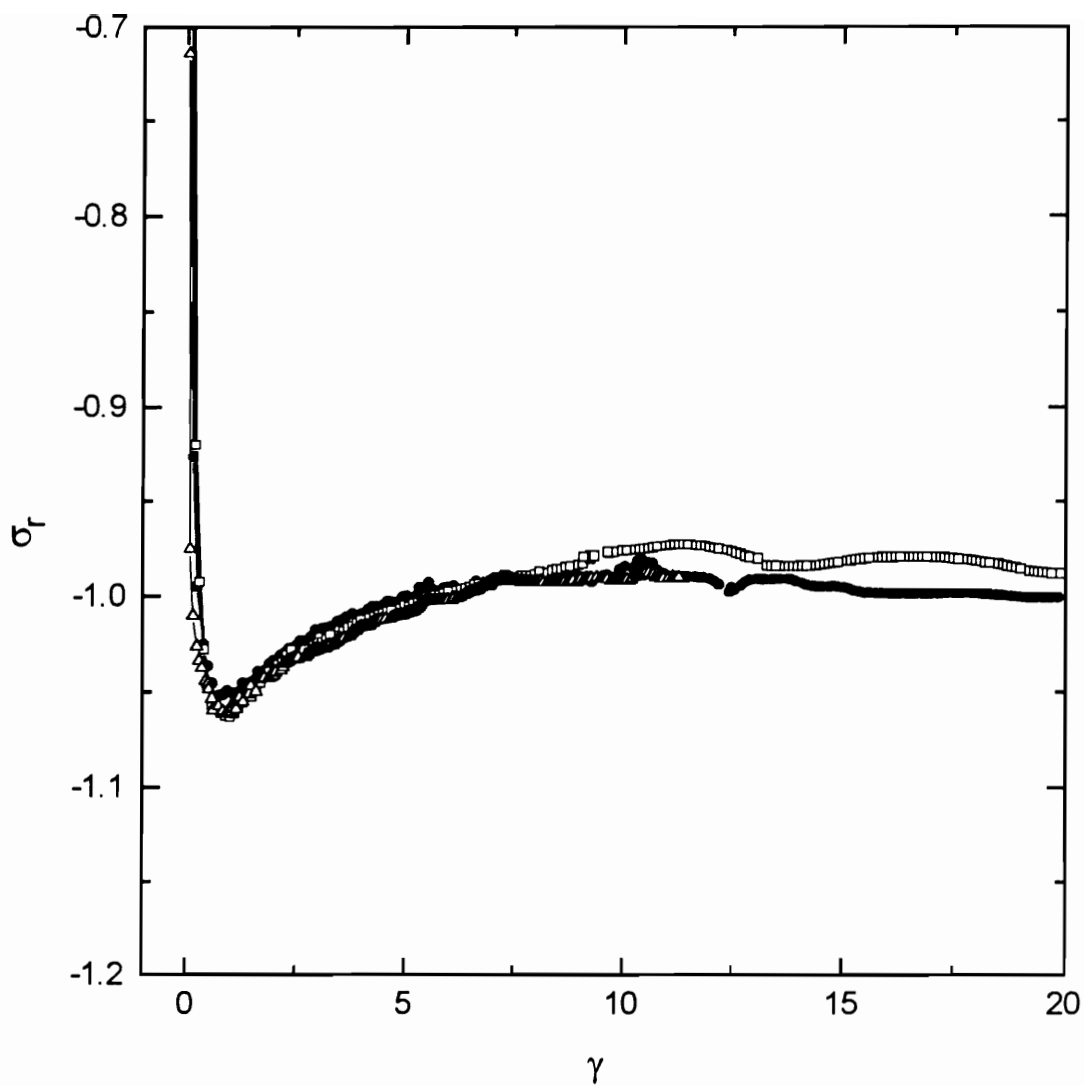


**Figure 5.12** Scaled transient shear stress versus strain after a step-down of shear rate from  $\dot{\gamma}_1$  to  $\dot{\gamma}_2$  where  $(\dot{\gamma}_1 / \dot{\gamma}_2 = 3)$  and where  $\dot{\gamma}_2$  is; ( $\Delta$ ) 0.5  $\text{sec}^{-1}$ ; ( $\bullet$ ) 1.0  $\text{sec}^{-1}$ ; and 1.5  $\text{sec}^{-1}$  for 25/75 PET/nylon 6,6 blend at 290 °C

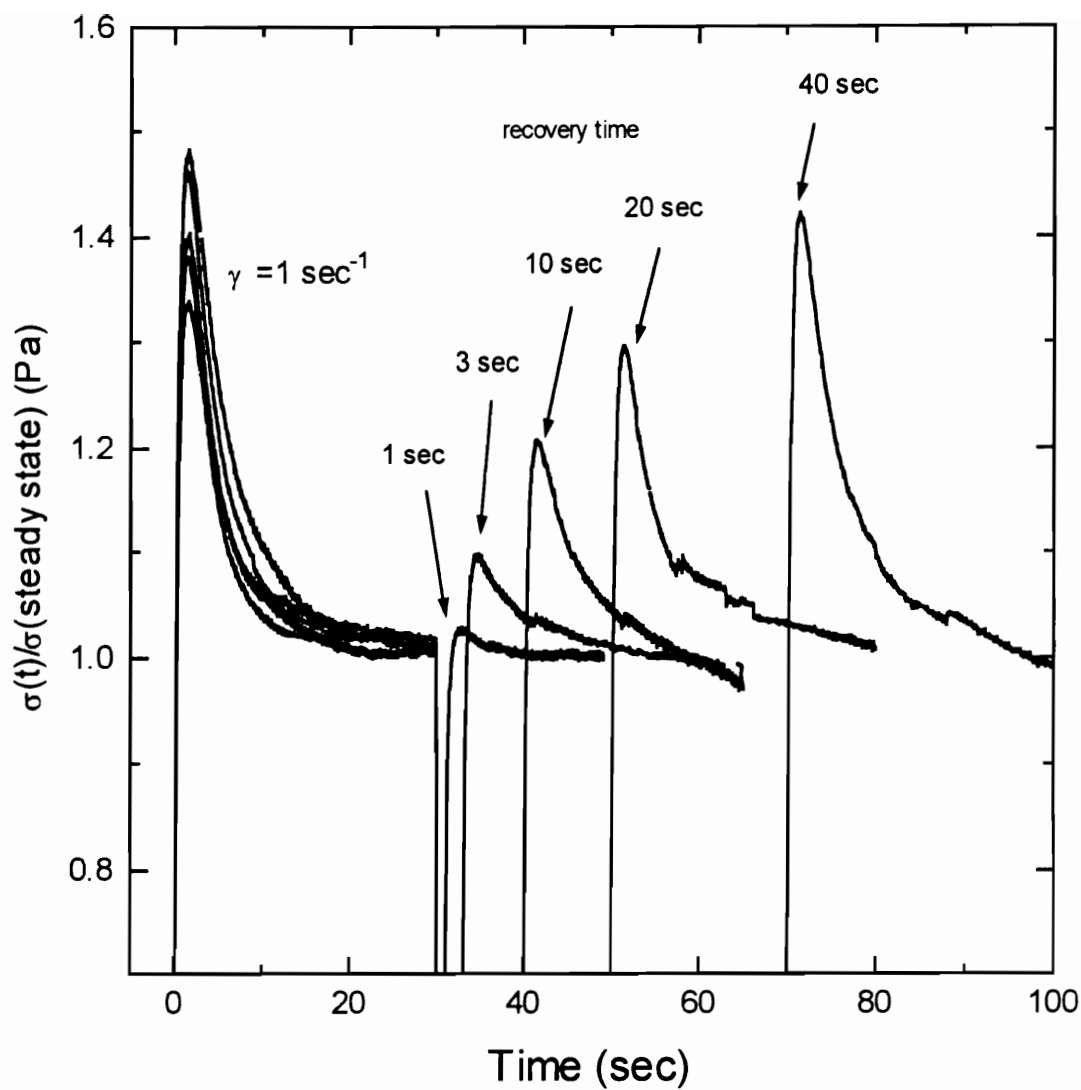


**Figure 5.13** Recovery of overshoot as a function of recovery time using interrupted stress growth experiments for the 25/75 PET/nylon 6,6 blend at 290 °C.

predict this recovery may be explained using a quantitative analysis of the predicted area of the interface per unit volume ( $Q$ ) which shows that the recovery of the texture observed experimentally is not predicted. This can be seen by the change in  $Q$  predicted for a transient shear flow consisting of a start up of shear flow, step-up of shear rate, and cessation of shear flow as shown in Fig. 5.14. It can be seen that the model predicts a decrease in the area of the interface at start up of shear flow and an increase in the area upon stepping up the shear rate. However, the model inaccurately predicts that upon cessation of shear flow the area of the interface will decrease. It was observed using scanning electron microscopy but not shown here that the dispersed phase size of a blend which had been subject to a shear flow between cone and plate fixtures for 1 minute at a shear rate of  $5 \text{ sec}^{-1}$  and then allowed to relax for 1 minute before quenching was the same as a sample which had not been sheared shown in Fig. 5.3. This result indicates that the kinetic equations should be of a form and order which would predict that the equilibrium texture prior to shear flow recovers upon cessation of shear flow.

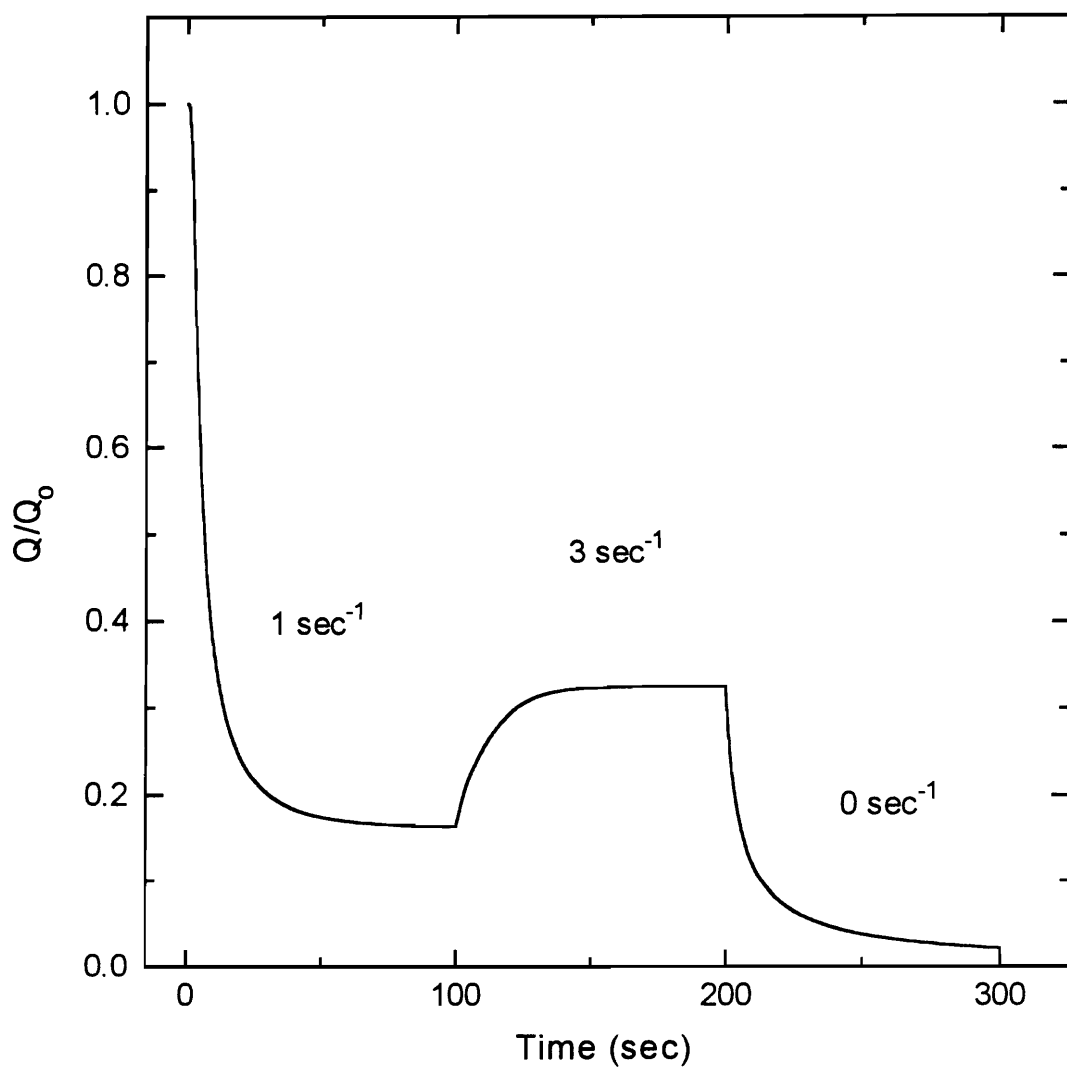


**Figure 5.14** Predicted normalized interfacial area per unit volume as a function of time at start up, step-up and cessation of shear flow.

## 5.5 Conclusions

At this time several limitations of the Doi-Ohta theory are apparent. Although the Doi-Ohta theory predicts an increase in blend viscosity over that of the blend constituents as is seen experimentally for the 25/75 PET/nylon 6,6, the theory does not predict the shear thinning behavior seen in this blend experimentally. The steady shear viscous and elastic properties of the 25/75 PET/nylon 6,6 blend system can be approximately estimated using the Doi-Ohta theory if the shear thinning and elastic properties of the blend constituents are taken into account. This represents a failure of the theory for systems which are made up of materials each with their own non-Newtonian properties. By definition the theory is not able to account for these contributions. On the other hand, the contributions or extra stresses which occur as a result of the texture or two phase nature of the system appear at least in magnitude to be predicted by the theory using parameters determined experimentally and by fitting the prediction of the model to start up of shear flow experiments from an isotropic system.

The shear stress and first normal stress difference are qualitatively modeled by the theory at the start up of shear flow. On the other hand, the inability of the theory to predict the overshoot and undershoot observed experimentally using stepwise changes of shear rate indicates that the kinetic equations do not accurately model the relaxation behavior of both the size and shape of the interface which may occur in this experiment and may also be consequence of the relaxation behavior of the neat polymers. While the shear thinning behavior of the 25/75 w/w PET/nylon 6,6 blend is not predicted by the Doi-Ohta theory (stress is predicted to be proportional to shear rate), the scaling relationship for the transient stresses does appear to hold for the blend using step-up and step-down experiments.

## **5.6 Acknowledgments**

The authors gratefully acknowledge the support of the Virginia Institute of Materials Systems for support of this work.



## 5.7 References

- Choi, S. J. and W. R. Schowalter, "Rheological properties of nondilute suspensions of deformable particles," *Phys. Fluids* **18**, 420-427 (1975).
- Doi, M. and T. Ohta, "Dynamics and rheology of complex interfaces. I," **95**, 1242-1248 (1991).
- Doppert, H. L. and S. J. Picken, "Rheological Properties of Aramid Solutions: Transient and Rheo-Optical Measurements," *Mol. Cryst. Liq. Cryst.* **153**, 109-116 (1987).
- Elmendorp, J. J., *Mixing in Polymer Processing* (Marcel Dekker, New York, 1980).
- Gramespacher, H. and J. Meissner, "Interfacial tension between polymer melts measured by shear oscillations of their blends," *J. Rheol.* **36**, 1127-1141 (1992).
- Guenther, G. K. and D. G. Baird, "Steady shear and transient rheology of an immiscible polymer blend," to be published *J. Rheol.* (1995).
- La Mantia, F. P., *Thermotropic Liquid Crystalline Polymer Blends* (Technomic, Pennsylvania, 1993).
- Lee M. L. and O. O. Park, "Blend structure and viscoelasticity," *J. Rheol.* **38**, 1405-1425 (1994).
- Mellema, J. and M. W. M. Willemse, "Effective viscosity of dispersions approached by a statistical continuum method," *Physica* **122**, 286-312 (1983).
- Moldenaers, P., H. Yanase, and J. Mewis, "Effect of the shear history on the rheological behavior of lyotropic liquid crystals," *ACS Symposium Series* (ACS, Washington, DC, 1990), Chap. 26, pp. 370-380.
- Nobile, M. R., D. Arciello, L. Incarnato and D. Nicolais, " " *J. Rheol.* **34**, 1181, (1990).
- Onuki, A., "Viscosity Enhancement by Domains in Phase-Separating Fluids near the Critical Point: Proposal of Critical Rheology," *Phys. Rev.* **35**, 5149-5155 (1987).

- Papanastasiou, A. C., L. E. Scriven, and C. W. Macosko, " , " J. Rheol. **27**, 387-410, (1983).
- Paul, D. R. and Newman S., Eds., *Polymer Blends* (Academic Press, New York, 1978).
- Scholz, P., D. Froelich, and R. Muller, "Viscoelastic Properties and Morphology of Two-Phase Polypropylene/Polyamide 6 Blends in the Melt. Interpretation of Results with Emulsion Model, " J. Rheol. **33**, 481-499 (1989).
- Schowalter, W. R., C. E. Chaffey, and H. Brenner, "Rheological behavior of a dilute emulsion," J. Colloid Interface Sci. **26**, 152-160 (1968).
- Smith, J., " , " **13**, 1741-1747 (1969).
- Sigillo, I. and N. Grizzuti, "The effect of molecular weight on the steady shear rheology of lyotropic solutions. A phenomenological study," J. Reol. **38**, 589-599 (1994).
- Takahashi, T., N. Kurashima, I. Noda, and M. Doi, "Experimental tests of the scaling relation for textured materials in mixtures of two immiscible fluids," J. Rheol. **38**, 699-712 (1994).
- Taylor, G. I., "The Formation of Emusions in Definable Fields of Flow," Proc. Roy. Soc. **A146**, 501-523 (1934).
- Utracki, L. A. and M. R. Kamal, "Melt Rheology of Polymer Blends," Polym. Engr. Sci. **22**, 96-114 (1982)
- Utracki, L. A. and Z. H. Shi, "Development of Polymer Blend Morphology During Compounding in a Twin-Screw Extruder. Part I: Droplet Dispersion and Coalescence-A Review," Polym. Engr. Sci. **32**, 1824-1833 (1992).
- Wu, S., "Calculation of Interfacial Tension in Polymer Systems," J. Polym. Sci. **34**, 19 (1971).

## 6.0 Recommendations

- It was found that anisotropic solutions of PPT in sulfuric acid display similar rheological properties to the solution in its isotropic state with small differences observed in the flow curves and transient first normal stress difference behavior. It was also shown that a biphasic condition exists over a large temperature range and therefore it is unclear at this time whether the differences observed are due to the anisotropic nature of the solution or due to the two phase texture which is present. In order to determine the rheological properties which arise as a consequence of the anisotropic nature of the solution the isotropic or solid phase present in the sample should be removed. This might be done by employing a centrifuging process by which the differences in density of each phase could be utilized to separate each of them out.
- Since the rheological properties of solution of PPT in sulfuric acid may be a function of both the anisotropic nature and polydomain texture found in the system, it would be interesting to isolate the relaxation behavior of each. This could be done using jump strain, stress relaxation, interrupted stress growth experiments as well as determining the relaxation spectrum of the solution using  $G'$  and  $G''$  data. The relaxation behavior determined using jump strain experiments from the relaxation spectrum could be related to molecular relaxations and in the case of stress relaxation from steady shear flow related to the relaxation of the texture. In addition, the use of interrupted stress growth experiments might be used to determine how much of the initial texture is recoverable and the time frame associated with this process. Since the time scale associated with the relaxation of the texture is most likely long this experiment would require careful exclusion of moisture throughout the experiment.
- The degradation behavior of PET/nylon 6,6 blends was found to be highly sensitive to moisture content of the samples. A correlation of moisture content of the blend components prior to mixing to the degradation rate of the blends might prove useful in optimizing the

blending process. Since any moisture in PET leads to degradation an equilibrium amount of water is necessary to avoid polymerization of nylon 6,6, an optimum moisture content for each neat polymer prior to blending might prove useful in optimizing the blend properties.

- In this work the conditions of blending were far from optimal. In the case of melt blending in an extruder inaccuracy in the temperature control, viscous heating and polymer exposure to moist air were all present. In the case of melt blending in cone and plate fixtures the lack of distributive mixing using simple shear flow resulted in large concentration gradients in the samples. Since the degradation rates of the neat PET and nylon 6,6 are different from those of blends of these two polymers, it would be interesting to determine the rheological properties of the blend in which no degradation occurred. This might be done using a carefully controlled blending process in which accurate control of the temperature and atmosphere throughout blending could be maintained..

- In order to accurately evaluate the ability of the Doi-Ohta theory to model the rheology of immiscible polymer blends, a more suitable polymer pair might prove useful. First, the polymers should be stable with respect to degradation and devoid of any reactions which might occur as the two polymers are mixed and tested at melt temperatures. Second, the role of interfacial tension on the rheology of the system would be much clearer if a polymer pair was chosen with a relatively high value of interfacial tension.

- Using a polymer blend which satisfies the condition described above the form and order of the kinetic equations in the Doi-Ohta theory could then be evaluated. This could be done by fitting the kinetic equation associated with the relaxation of anisotropy using step strain experiments where the relaxation associated with the interfacial area could be considered negligible and the associated kinetic equation would then be constant. Next, knowing the kinetic equation for the relaxation of the anisotropy, the kinetic equation for the relaxation of interfacial area could be evaluated using stress relaxation from steady shear experiments. This

method of evaluating the kinetic equation in the Doi-Ohta theory would require an assumption of the form of the kinetic equations.

## Vita

The author was born in Abington, Pennsylvania on January 13, 1966. His academic career at the college level began in May of 1984 at Texas A&M University in the Department of Mechanical Engineering. Interests in the area of polymer science and engineering in the last year as an undergraduate were pursued after receiving his B.S. in mechanical engineering in 1984 by immediately enrolling in the masters program at Texas A&M. After receiving his M.S. in mechanical engineering in August of 1991 he came to the Chemical Engineering Department at Virginia Polytechnic Institute and State University where he was granted a Ph.D. in Chemical Engineering in February of 1995. In December of 1994 he was offered and accepted a position in research and development with Phillips Petroleum Company in Bartlesville Oklahoma.

A handwritten signature in black ink, reading "Gerhard K. Grentz". The signature is written in a cursive style with a large, stylized 'G' and 'K'.